LIBRARY

TRANSLATION

NUMBER 111

THE STUTTGART SHEAR TESTS, 1961

Contributions to the treatment of the problems of shear in reinforced concrete construction

by

F. Leonhardt and R. Walther

A translation of the articles that appeared in "Beton- und Stahlbetonbau". Vol. 56, No. 12. 1961. Vol. 57, Nos. 2, 3, 6, 7 and 8. 1962.

(Translation made by C.V. Amerongen)

CEMENT AND CONCRETE ASSOCIATION
52 GROSVENOR GARDENS LONDON SW1

Price £3

Cj.111(12/64)

CONVERSION FACTORS

Length	1 cm	=	0·394 in.
	1 m	=	3·281 ft
Weight	1 kg	=	2·205 lb
	1 metric ton	=	0·984 long ton
Stress	1 kg/cm^2	=	14·22 lb/in^2
	1 kg/mm^2	=	0·635 ton/in^2
Bending moment	1 kg m	=	7·233 lb ft

PREFACE

With a view to making them more readily accessible to readers, the reports on shear tests and shear problems, which appeared in six instalments from December 1961 to August 1962, have been collected in the present special publication. The object of the research work was to make a thorough investigation of the factors affecting the shear strength of simply supported reinforced concrete beams under present-day conditions of high concrete strengths and high-tensile reinforcing steel. From the results it appears that the permissible shear stresses τ_o as hitherto laid down in German Standard DIN 1045 can be at least doubled and that for moderate values of τ_o the full safeguard against shear failure, as hitherto required, can be substantially reduced without involving any sacrifice of the specified safety against failure. The tests also showed that stirrups, when functioning at high stresses as shear reinforcement, are more suitable than bent-up inclined bars. It is possible to take advantage of this fact to simplify the reinforcement and thus effect savings in wages. Hence substantial advantages of economy can be effected in shear design when the rules embodying these test results have been incorporated into the new DIN 1045 regulations now in course of preparation.

In 1962 the shear tests were continued with a view to providing further support for the proposal for the design of the shear reinforcement in conjunction with reduced shear safeguard, as indicated in Section III of the present publication. The results of these tests were already available before Section III went into print and they showed that the proposal in question is on the safe side.

Tests on beams continuous over several spans are now in progress.

In addition, the tests served as a means of further developing the shear failure theory which was formulated in its essentials by R. Walther in 1957 (7), so as to enable us, after the intended adoption of the ultimate-load method of design for bending in the new DIN 1045, soon also to proceed similarly with regard to shear. This shear failure theory will moreover enable us to check the shear strength of slabs and beams with and without shear reinforcement.

The authors wish to express their indebtedness to the organizations whose financial support made these tests possible:

Ministry of Economic Affairs of the State of Baden-Württemberg

Fachverband Bau Württemberg e.V.

Verein Deutscher Zementwerke e.V.

Betonstahlgemeinschaft Deutscher Hüttenwerke

Deutscher Ausschuss für Stahlbeton

"Ludwig Bauer Stiftung" (Ludwig Bauer Foundation)
of the firm of Ludwig Bauer, Stuttgart
(for the large-scale tests II.1)

We furthermore wish to thank all our co-workers for the devotion and care with which they did their work.

Stuttgart, August 1962

F. Leonhardt and R. Walther

THE STUTTGART SHEAR TESTS, 1961

I. INTRODUCTION

1. The significance of shear stress in reinforced concrete

Shear problems in reinforced concrete construction have hitherto been considered in terms of the shear stress $\tau_o = Q/bz$, i.e. in terms of a quantity derived solely from the shear force. We must give this shear stress τ_o careful consideration in order to obtain a correct understanding of its real significance in reinforced concrete structures. To this end, we shall start from the bending theory for a beam made of the brittle material concrete in the uncracked condition and recapitulate some well-known facts.

Loads on a beam produce a system of principal tensile and principal compressive stresses (Figure 1) which change in magnitude and direction at various levels in the cross-section. For the theoretical determination of the stresses, a rectangular system of co-ordinates x-y is generally adopted, whereby we arrive at the usual stress formulae $\sigma_x = M\,y/J$ and $\tau_{xy} = QS/Jb$ (J is the moment of inertia). The magnitude and direction of the principal stresses are determined from σ_x and τ_{xy}. The shear stress τ_{xy} indicates that the principal stresses do not act in the directions of the co-ordinate axes and that they are therefore oblique stresses.

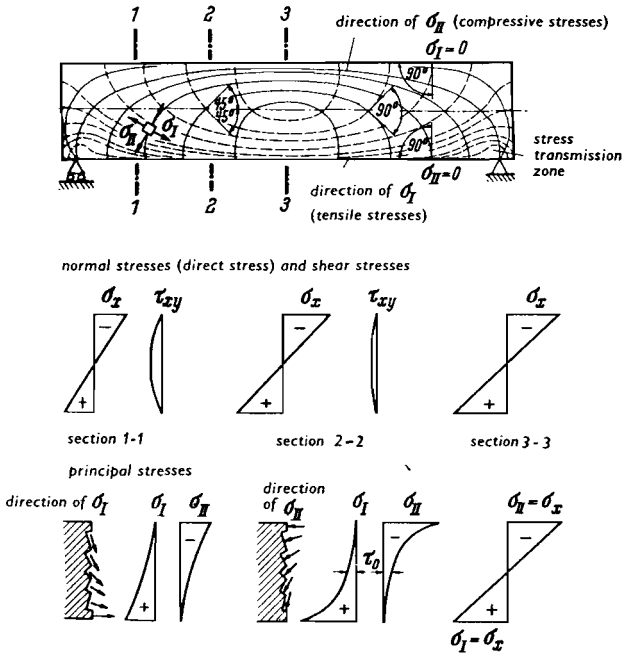

Figure 1: Magnitude and direction of the principal stresses in a beam subjected to uniformly distributed loading, in state I (uncracked).

The stress τ does not by itself provide a criterion for the failure of the concrete, inasmuch as the shear stress failure hypothesis - i.e. the assumption that the maximum shear stress is the cause of failure - is not applicable to brittle materials. On the other hand, the principal tensile stresses are of decisive importance with regard to the cracking of the brittle concrete. These principal tensile stresses σ_I are dependent upon both the moment and the shear force. Only the magnitude of the tensile stress at the extreme fibre (maximum tensile bending stress) is determined by the moment alone, since $\tau = 0$ at the extreme fibre. The neutral axis ($\sigma_x = 0$), on the other hand, is a fibre at which the principal stresses are dependent only

upon the shear force. Hence the magnitude of the shear stress τ_o at the neutral axis is equal to the principal stresses, which there have a slope of 45^o. The principal stresses at the level of the neutral axis, however, are usually not the maximum values of the principal stresses for the section concerned, so that τ_o is not of decisive significance with regard to cracking nor with regard to ultimate strength. The cracks generally start from the tensile face; this applies also to the oblique shear cracks. Only in exceptional cases (beams with very thin webs; cross-sections subject to large shear force and small moment) can it happen that the principal stresses σ_I in the vicinity of the neutral axis are critical with regard to cracking.

In the practical bending theory for beams the stress component σ_y is usually neglected. However, it is present wherever external loads and forces are acting approximately vertically in the plane of the beam, i.e. especially in the vicinity of the bearing reactions and of concentrated loads, where σ_y becomes a compressive stress. As a result of this, the principal tensile stresses are reduced and are directed at a flatter angle, whereas the principal compressive stresses become larger and steeper.

Now let us consider the composite material "reinforced concrete" and apply load to the beam until cracks develop in the tensile zone of the concrete (state II)*: the internal stress conditions will change significantly, and the stresses can then no longer be accurately analysed, since the internal stresses in state II depend upon the shape and extent of the cracks and upon the quantity, direction and distribution of the reinforcement provided. A theoretical determination of the stresses will be possible only as a rough approximation.

It is therefore usually assumed that the neutral axis is the same for shear and for bending and that no tensile stresses occur in the concrete below this neutral axis. This also means that the static moment S, and therefore the shear stresses below the neutral axis, must be constant and that the principal stresses down to the level of the longitudinal reinforcement must be at 45^o (Figure 2):

$$\sigma_I = -\sigma_{II} = \tau_o = \frac{Q\,S_o}{b\,J} = \frac{Q}{bz}$$

These conditions have long been known. E. Mörsch described them in detail and from them proceeded to derive his well-known design rules for the shear reinforcement of reinforced concrete beams, for which he provided confirmation by carrying out a large number of epoch-making tests. His rules are based on the "lattice" analogy which assumes that the forces associated with the principal tensile stresses are resisted by the sloping steel bars, while the principal compressive stresses are resisted by the concrete "struts" between the cracks.

Equilibrium of the internal forces calculated on the assumptions represented in Figure 2 is, however, possible only if closely spaced bars inclined at 45^o are provided and if furthermore the shear cracks are also sloped at 45^o. If the cracks deviate from the 45^o direction and become steeper - as occurs over substantial lengths of a beam in the region of large moments and small shear forces - then the compression struts sloped at 45^o will no longer be possible. The internal stress conditions in the struts between the cracks will have to be considerably modified. With sloping bars

* "State I" refers to the uncracked section; "state II" refers to the case where the section is cracked and the tension is resisted by the steel only. (Translator's note.)

and approximately vertical bending cracks, or with sloping cracks and vertical stirrups, "lattice" type structural action is nevertheless still possible. On the other hand, no such action can develop if the only shear reinforcement consists of stirrups in a region where nearly vertical bending cracks occur. We know that the beam will then function as an arch provided with a tie-rod, the greater part of the shear force being resisted in the compressive zone by the resultant D taking on a sloping position (Figure 3). In that region the stresses τ therefore become large, while τ below the neutral axis becomes almost zero. Load-carrying functions of this type even occur to some extent under the conditions of Figure 2. The carrying capacity of the flexural compressive zone is, however, weakened by a large stress component τ.

With regard to the "lattice" analogy it should furthermore be borne in mind that these are internally redundant lattice-works with multiple intersection of web members and flexurally rigid chords, while the tension members are much more flexible than the compression members and therefore exhibit larger deformations. On considering the compatibility conditions for these lattice girders we find that the stiffer compression members (struts) always have to trahsmit a greater amount of force than the more yielding tension members (ties), while the chords are stressed in bending. The struts will, under these circumstances, derive useful support from the stirrups which enclose the concrete section. The larger horizontal component of the strut forces has the result that the arch tie-rod action is still developed even in the region of oblique cracks and oblique bars if full shear reinforcement is provided. In this connexion the cross-section of the "tie-rod" (i.e. also the steel stress) is of importance. Obviously, it is essential to continue a large proportion of the bottom reinforcing bars to the bearings and properly anchor them there.

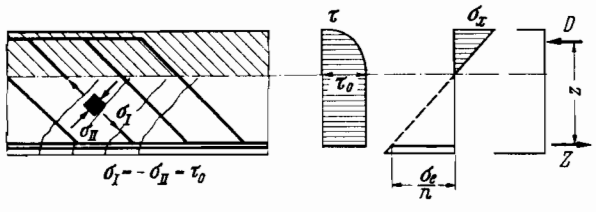

Figure 2: Idealized stress distribution in state II (cracked). $\sigma_I = -\sigma_{II} = \tau_o$ is possible only if the cracks as well as the shear reinforcement are inclined at 45^o.

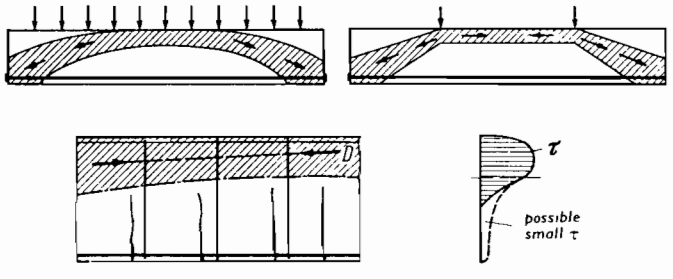

Figure 3: Arch or truss action: the shear stresses are confined to the compressive zone.

The arch tie-rod action will play a more important part with decreasing slenderness of the beam, because then the "arch" (or the "truss") will have a considerable load-carrying capacity of its own, without the assistance of the lattice system. Hence it follows that relatively short stout beams are less liable to be affected by shear than would be suggested by the lattice analogy and, therefore, by the magnitude of τ_o.

In shear tests performed at the Swiss Federal Materials Testing Laboratory (EMPA) at Zurich in 1955, R. Walther[1] demonstrated that this arch tie-rod action of the bottom reinforcing bars depended on the quality of

the bond - also in the case where the shear reinforcement is constituted by stirrups and inclined bars (Figure 4). In all beams, under the higher loads, considerable tensile stresses were found to occur in the bottom bars even only a short distance from the bearing. In tests with polished round bars the case of the pure trussed beam with tie-road was obtained, and the cracks were not appreciably sloped.

Even if shear is fully catered for by means of inclined bars and stirrups, the lattice action is not entirely developed: this is apparent from measurements of stress in the steel made on the inclined bars (Figure 5). Before cracking occurs, these stresses are approximately equal to n times σ_b^I (n being the modular ratio); but in state II, with good bond, they remain far below the values calculated with τ_o, even if the effect of σ_y over the bearing is taken into account.

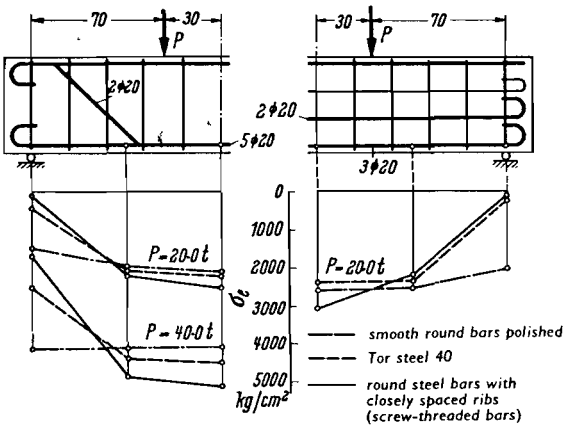

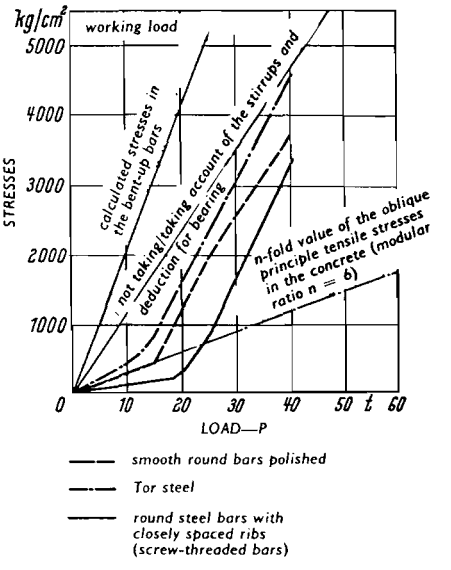

Figure 4 (left): The stresses in the main reinforcement do not decrease in accordance with the bending moment diagram; they depend on the bond quality (from tests by R. Walther).

Figure 5 (right): The stresses in bent-up inclined bars remain below the calculated stresses (from tests by R. Walther).

In reality, therefore, in state II the stress τ_o is neither equivalent to the principal tensile stress nor to the principal compressive stress. This fact must particularly be taken into consideration in investigating the safety against failure in shear. It must be said - and the following test reports will prove this - that τ_o does not constitute a suitable criterion for safety against shear failure. For a brittle material like concrete there is, in fact, no shear strength in the sense of a material property. Even under loading of a definitely shearing character, concrete does not develop shear fractures but brittle fractures at right angles to the principal tensile stresses. The compression trajectories in such cases are usually steep arches and the tensile trajectories in the region of the large tensile stresses are very flat.

The design and character of the shear reinforcement conforming to the rules given by E. Mörsch do, however, always provide adequate safety against shear failure. This fact, which is confirmed by practical experience, would therefore not have given any reason for considering the shear problems afresh, were it not that we know that the factor of safety against shear failure with

this kind of reinforcement varies considerably and is therefore often excessively large. Besides, as a result of the introduction of the high permissible steel stresses and deformed reinforcing bars with much improved bond properties, a new set of conditions has been created whose effect upon shear behaviour had to be re-checked by tests. The main reason for the fresh consideration of the problem, however, consists in the simplifications and savings that are possible in designing the shear reinforcement. These will be indicated at the end of this report.

2. Comments on the hitherto permissible limits for the shear stress τ_o

In the German Standards DIN 1045, 1075, 4227, etc. two limiting values for the permissible shear stress τ_o are stated for each quality (strength class) of concrete.

1. A lower limit, below which no check for shear reinforcement is required.

2. An upper limit which must on no account be exceeded and which therefore determines the minimum permissible cross-sectional dimensions.

Hence if the shear stress τ_o in a structure remains below the lower limit, the designer is free to provide nominal reinforcement without the need to produce a calculation to justify it. It has gradually become established practice not to install any shear reinforcement at all in slabs in this range of stress, while beams are provided merely with a very few stirrups.

No one had then conclusively shown that this sort of reinforcement provides adequate shear safety for all types of loading, especially in the case of members in which the main (bottom) reinforcing bars are not all continued as far as the end supports of the member. Investigations on the subject were therefore most essential. They showed that for concrete B 300 and reinforcing steel IIIb* the stresses τ_o may range between 14 and 94 kg/cm^2, whereas the permissible value of τ_o is 10 kg/cm^2.

The upper limit is a fairly low one - e.g. 20 kg/cm^2 for concrete B 300. In deciding this limit, the principal tensile stresses and the tensile strength, or the slightly higher so-called "shear strength", of the concrete were envisaged, and it was supposed that, as a result of this low limit for τ_o, the structures would remain uncracked in the shear region. It was overlooked that, for positive bending moment, the principal tensile stress is already considerably larger at only a short distance below the neutral axis and that, in any case, it exceeds the tensile strength of the concrete at the extreme fibre, so that cracks occur there.

It is not clear, however, why the permissible stress, particularly for the fibres at the level of the neutral axis, is limited on the basis of the tensile strength of the concrete, whereas for the fibres below the neutral axis this is not the case and the tensile zone of the concrete is simply assumed to be cracked. This assumption also underlies the design of the shear reinforcement. If we are prepared to allow cracks in the extreme fibres and ensure, by the provision of adequate reinforcement, that such cracks will remain very narrow under working load, then we should grant the same rights to the fibres situated somewhat higher up and allow the tensile stresses or forces in this zone also to be resisted by suitable reinforcement.

---

* B 300 denotes concrete with minimum specified 28-day cube strength of 300 kg/cm^2; similarly B 400, etc. Steel IIIb: for some typical properties see Table XIV. (Translator's note.)

We shall show that, with appropriate reinforcement, the shear cracks will then be narrower than the bending cracks. However, in thin webs provided with ample reinforcement for resisting the oblique tensile forces, it is not the tensile strength but the compressive strength of the concrete that is of decisive importance in that the concrete struts between the shear cracks are liable to fail in compression. In one of the tests described in the following, relating to beams made from concrete B 300, web failure in oblique compression was reached at a load corresponding to a value of 180 kg/cm^2 for τ_o - i.e. nine times the permissible value of this stress. The permissible values of τ_o can therefore be substantially increased above those hitherto adopted.

Structural considerations undoubtedly played a part in deciding the permissible upper limit of τ_o. As a result of low values for this stress, the webs of ordinary beams have to be made very thick so that the reinforcement can conveniently be accommodated and the concrete in the webs can be placed and compacted without difficulty. Nowadays these considerations have in a good many cases lost their significance. More particularly for factory-made precast beams there is a preference for thin webs in which the concrete is placed in steel moulds and vibrated by means of external vibrators. In France, where designers are not tied to an excessively low permissible value of τ_o, it has, for example, been proved that very thin webs of long-span beams can be concreted perfectly satisfactorily. In recent years the low permissible value of τ_o has frequently proved to be an obstacle to the sensible design of structures in which the shear forces are very large in relation to the bending moments - especially in the case of heavily loaded deep beams (girder walls) such as first-storey walls of multi-storey buildings with heavy column loads. In some cases, beam webs or wall diaphragms had to be made more than 1 m thick merely because of the permissible τ_o, whereas 30 or 40 cm would have been adequate and would not have caused any difficulties in fixing the reinforcement and placing the concrete.

As a prerequisite for increasing the permissible value of τ_o, however, it was necessary to investigate the effect of the nature and direction of the reinforcement upon the oblique compressive stresses, in order to ensure that the upper limit of τ_o - in so far as it is desired to continue to work with this particular stress concept - is so determined as to provide always an adequate margin of safety.

For this reason the tests described in the following also had to consider the question of the upper limit for τ_o.

3. Future design based on ultimate shear load

These considerations in themselves already show that the shear design of reinforced concrete structures, based on the calculated shear stress τ_o with two limits for the permissible value, as hitherto employed, cannot be considered a satisfactory method. This is made abundantly evident by the tests described in the following, inasmuch as the calculated τ_o under failure load was, for example, found to vary between 14 and 180 kg/cm^2 for concrete B 300. We now know that in the absence of shear reinforcement the safety against shear failure is in many cases inadequate, despite the low lower limit for τ_o, and that in other cases - with or without shear reinforcement - the safety against shear failure is actually much greater than is required.

The ultimate load for flexural failure can now be calculated in advance

with a fair degree of accuracy, and in many countries flexural design according to the ultimate load method - i.e. on the basis of the critical load P_{kr} in the event of critical deformation or on the basis of the ultimate load P_U, in conjunction with a certain factor of safety - has accordingly been adopted. It is intended to adopt this method in Germany also. Now it would be most unsatisfactory if two different methods of design had to be used for one and the same structure, i.e. ultimate load design for bending, and design based on permissible stresses for shear. For this reason it is urgently necessary to be able also to calculate the ultimate load for shear failure with some measure of accuracy. The shear failure of reinforced concrete and prestressed concrete beams has been the subject of a good many - mostly foreign - research projects in recent years[2-6]. Nearly all these investigations have indicated that the shear force Q alone is not the determining factor, but that the entire pattern of forces represented by N, M and Q - and, in the case of bending without direct force, more particularly the ratio M/Qh - is of decisive importance as the shear failure criterion. The load-carrying capacity with respect to shear is represented by a moment, the so-called "shear failure moment" M_{SU}.

This ratio M/Qh, which in the case of concentrated loads corresponds to the ratio a/h, has been designated the "shear span" by some authors. This is not a very appropriate term, however, as this is a dimensionless quantity. H. Rüsch chose the term "shear slenderness", which is rather more appropriate, In the present paper we shall simply call it the "moment-shear ratio" or the ratio M/Qh in order to obviate any misunderstanding.

By means of this ratio M/Qh the reduction of the strength of the bending compressive zone over the shear crack can be expressed when that zone is subject not only to the stress σ_x (direct stress) but also to τ (shear stress) - i.e. when there is a biaxial state of stress or, in other words, when the compression resultant (thrust) D due to the arch action acts obliquely and therefore comprises a vertical component D_v or ΔQ as was already envisaged by Mörsch.

In his thesis[7] R. Walther has incorporated these relations into a proposed shear failure theory. In particular, this theory is characterized by the fact that it establishes a deformation condition which takes account of the influence of the degree of reinforcement and the bond quality. The compatibility of the deformations plays a part in all structures and significantly affects the internal forces. For bending, the deformation condition yields the position of the neutral axis, and similar relations must be available for the case of bending in combination with shear force. Walther's shear failure theory is based also upon equilibrium and compatibility conditions by means of which the position of the neutral axis in the shear region (where it is significantly lower down than in the region where bending predominates) is determined.

The first-mentioned of the two present authors considered these views to be relevant and logical. Accordingly, in collaboration with R. Walther, he had tests carried out at the Otto Graf Institute of the Technological University of Stuttgart with a view to further developing this shear theory. For the most part these tests have been so arranged as to enable particular parameters for the shear failure theory to be determined.

The present test reports will be immediately followed by the publication of Walther's shear failure theory in its present form. This theory provides a basis for ultimate load design in respect of shear failure and therefore appropriately links up with flexural design.

4. The test programme

In the first place the test programme comprised several series of tests on simple rectangular beams without shear reinforcement. The main object of these was to elucidate the influence of the degree of reinforcement, the bond and the type of loading, which are important factors with regard to the shear failure theory. Beams without shear reinforcement are very suitable for the purpose, as they enable the various influencing factors to be investigated separately to some extent. In addition, such tests were urgently necessary with regard to the many varieties of concrete slab without shear reinforcement which have nowadays come into use. The determining influence of the moment-shear ratio was studied in a large number of tests with varying M/Qh.

One of the objects of the tests was also to investigate the influence of the absolute size of the beams. This influence is bound up with that of the bond quality.

E. Mörsch already investigated various kinds of shear reinforcement comprising stirrups and bent-up bars and came to the conclusion that the best solution for safeguarding against shear failure consisted in having about one-third of the force resisted by stirrups and about two-thirds by inclined bars. The tests dating from those days, however, include some which show that vertical stirrups by themselves can attain about the same ultimate loads as the above-mentioned distribution of the force over stirrups and inclined bars[8]. In the U.S.A. it has also been shown a number of times that stirrups are quite favourable when used alone. This can help to simplify the shear reinforcement. At the present time this possibility is of great importance, now that the ratio of wages to cost of materials has considerably increased. Accordingly, tests have been performed on rectangular beams and T-beams with varying amounts of shear reinforcement, the object being to ascertain whether better shear strength can be obtained with bent-up bars, vertical stirrups or inclined stirrups and to determine what contribution to shear strength is made by each of these types of shear reinforcement.

It is known that in many cases it is not necessary to provide the full amount of reinforcement for resisting the shear forces by means of stirrups and inclined bars, as recommended by Mörsch. By means of the shear failure theory it will be possible to determine the degree of shear reinforcement necessary for achieving any particular degree of safety against failure. To begin with, a large number of test results published in the literature were examined with a view to seeking confirmation of the theory.

From various tests by other investigators[9] it appears that the cross-sectional shape has a marked effect upon the ultimate shear strength. Walther's shear failure theory also states that the width of the compressive zone is more important than the web thickness. Some tests were also carried out with a view to elucidating this matter.

Having regard to the forthcoming revision of DIN 1045, the authors considered it particularly important to carry out tests with a view to determining the upper permissible limit of the shear stress τ_o (as explained in Section 2) in relation to the prism strength of the concrete. Because of the urgency of this matter, the report on these tests will be given first.

To begin with, only short-term tests under static loading have been carried out, since the effects of sustained loading or alternating loading (fatigue loading) are adequately known from numerous other tests, so that safety with regard to the adverse consequences of such effects can be achieved by the introduction of reduction factors of known approximate size.

The tests were carried out chiefly with ribbed Tor steel, as this type of reinforcing steel is predominantly used in concrete construction in Germany. In the case of stirrups some comparisons were made between ribbed Tor steel IIIb and plain round steel bars I or plain round steel bars IIIb, because plain bars are still frequently used for stirrup reinforcement.

Concrete of class B 300 and class B 225 was chiefly used in the tests, as these concretes are now very widely used. For tests it is sometimes considered essential to reduce the concrete strength to two-thirds of the nominal value. The present authors, however, regard this as inappropriate in this case, as it complicates the determination of the actual degree of safety. Such a reduction is justified in all cases where the failure of the steel is the determining factor and the concrete serves merely as the means of enabling the reinforcement to develop its behaviour. It is not justified in cases where the failure of the concrete itself determines the ultimate strength, as is usually found to occur in the following shear tests. In fact, the scatter of the concrete strength is taken into account in the design by the introduction of an increased safety factor in the form of the reduced concrete strength, by means of which the effects of sustained loading, fatigue, shape, etc. can also be allowed for. It must also not be overlooked that various concrete properties, such as shrinkage, deformability or the ratio of tensile to compressive strength, are sometimes improved by the reduction of the strength of the concrete of which the test specimens are made.

The following test reports confine themselves to the principal data, results and conclusions. The complete tests reports will be published in the Research Bulletins of the Deutscher Ausschuss für Stahlbeton (German Committee on Reinforced Concrete).

II. TEST REPORTS

1. Tests with high shear stresses

1.1 THE TEST SPECIMENS

1.11 Shape and design

It was assumed that the upper shear stress limit $\tau_o = Q/bz$ causing destruction of the concrete due to oblique compression would correspond approximately to the compressive strength of concrete walls, i.e. about $0.6\ \beta_p$ or in the region of 150 kg/cm^2 for concrete B 300 (β_p is prism strength). In order to obtain failure by oblique compression, the test specimens therefore had to be so contrived that very high shear stresses of around 65 kg/cm^2 would occur under working load. Values of this magnitude can be produced in deep beams (girder walls) but in these the stresses σ_y disturb the desired pattern of trajectories. For this reason "double T-beams" were chosen, having a wide compression flange and a densely reinforced tension flange in order to obviate premature failure due to bending. The web had to be made excessively thin in relation to these flanges, though not too thin to prevent the proper installation of two-leg stirrups. Thus the beams illustrated in Figure 6 were obtained. These beams of somewhat unusual cross-section are not to be regarded as prototypes of beams for practical purposes. Instead, the only 10 cm thick web should be regarded as an instance of a diaphragm highly stressed in shear or of a web of a long-span box-section girder.

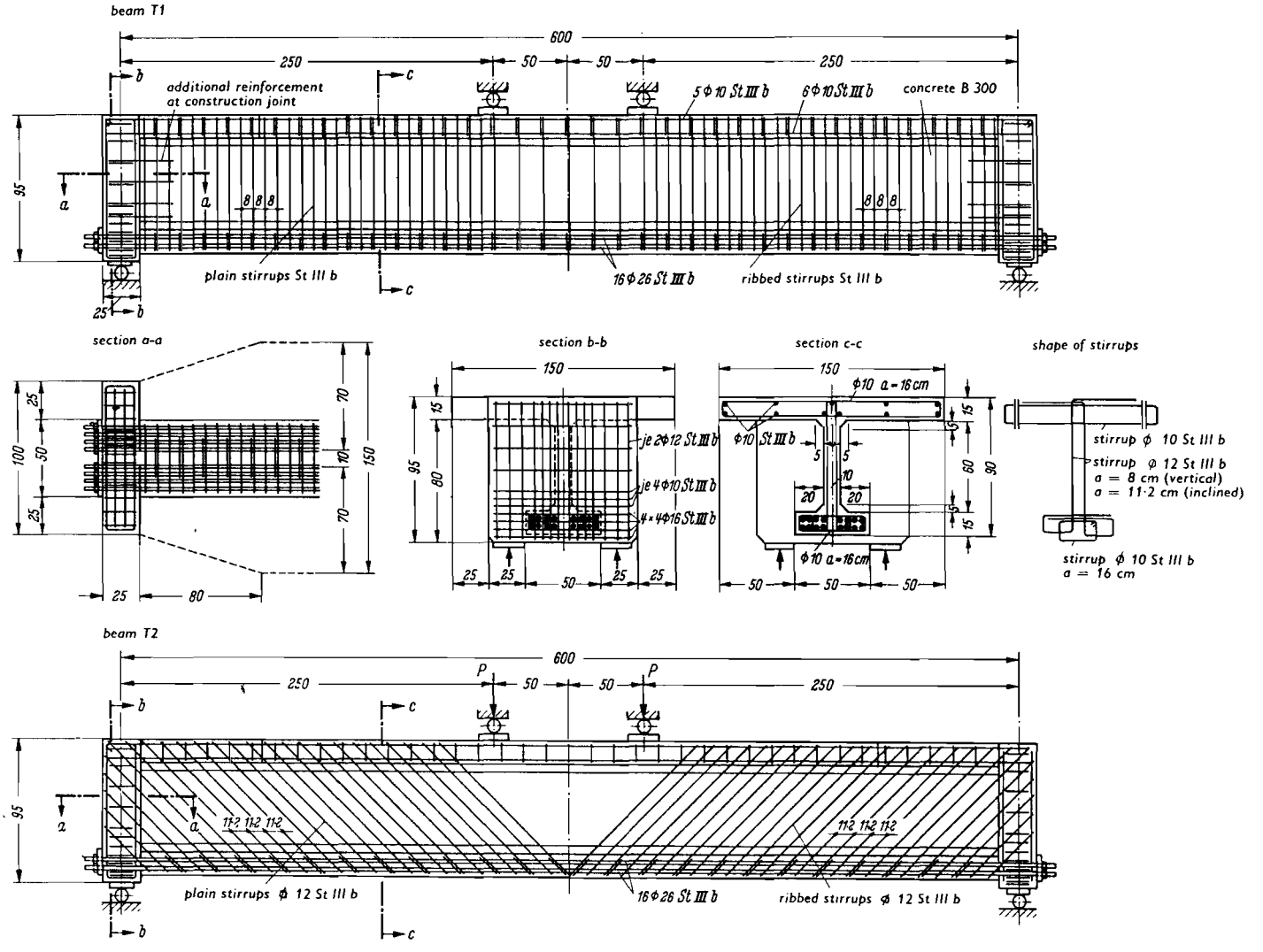

Figure 6: Test beams T1 and T2 for high shear stresses in order to determine the upper τ_o limit.

In addition, it was desirable to obtain principal stresses which would, as far as possible, be of constant magnitude over a fairly large distance and be inclined at 45° at the level of the neutral axis. This can most simply be achieved by means of two-point loading. In the present case the distance between bearing and load was equal to three times the effective depth in order to obtain a sufficiently long zone free from disturbance due to the transmission of load into the beam.

Two variants of these large beams - designated T_1 and T_2 - were constructed and tested. These differed only in the arrangement, not in the amount, of shear reinforcement provided.

1.12 Web reinforcement

The web of the beam T_1 was reinforced with vertical stirrups of 12 mm diameter spaced at 8 cm centres. The stirrups steel cross-sectional area corresponded to "full safeguard against shear", according to Mörsch, for a working load of about 100 tons. At the top the stirrup bars were bent round transversely into the slab, and at the bottom they were looped outwards around some of the longitudinal bars. In this way secure anchorage of the stirrups

at top and bottom was ensured. Ribbed Tor steel was used in the right-hand half and plain Tor steel was used in the left-hand half of the beam. The plain Tor steel was specially made for the purpose by the Rheinhausen Steelworks and was cold-worked in such a manner as to give it practically the same stress-strain diagram as the ribbed Tor steel. Hence the only difference in the stirrups in the two halves of the beam was in the quality of the bond that they could develop.

The web of beam T_2 was provided with inclined stirrups consisting of 12 mm diameter bars of reinforcing steel IIIb spaced at 11·2 cm and designed for "full safeguard against shear", as above; the slope of these stirrups was 45°, and their general shape was similar to that of the stirrups in beam T_1. Again ribbed bars were used in the right-hand and plain bars in the left-hand half of the beam; in the region between the two loads no additional web reinforcement was installed.

It should furthermore be noted that no extra longitudinal reinforcement was provided in the webs of these beams, though in actual practice such reinforcement would undoubtedly have to be installed. In the present case, however, it was considered desirable not to make the compaction of the concrete in the thin web by means of immersion vibrations unnecessarily difficult. Also, it was desired to investigate the action of the stirrups alone.

The inclined stirrups were secured to the longitudinal bars by means of tie wire only, i.e. they were not welded to them. With good bonding of the longitudinal bars and adequate transverse reinforcement the inclined stirrups evidently do not develop any slip.

1.13 Bearing conditions

At each end of the beam the unfavourable case of laterally installed bearings under cast-on diaphragms was adopted, so as to reduce the favourable effect of σ_y in the bearing zone and to test the anchorage of the main reinforcing bars under unfavourable conditions.

The 1 m wide and 25 cm thick transverse diaphragms at the bearings were likewise highly stressed in shear. In view of the short span of these diaphragms in relation to the depth, this could be described as a case of direct shearing load. Incidentally, these diagragms afforded fresh proof that, in order to resist such load, it is better to use several layers of horizontal bars, with a small number of stirrups, than bent-up bars inclined at 60° as is often recommended. In this connexion reference should be made to the tests on "fanwise" anchorages for "concentrated" prestressing cables by Leonhardt and Andrä [10].

1.14 Flange reinforcement

The bottom flange was provided with tensile reinforcement consisting of 16 ribbed Tor steel bars of 26 mm diameter, steel IIIb, all of which were continued straight to the ends of the beam. Bent-up bars would merely have been a nuisance in the thin web. The projecting ends of the bars were watched to see whether slip would occur, which was a definite possibility in view of the nature of the bearings and their location so close to the ends of the beam. In order to obviate the risk of failure due to destruction of the bond, the ends of the bars were provided with screw threads and anchor plates. However, the nuts were not screwed up tight against the plates: a small gap was left. The nuts would be tightened only in case of need. The

bottom reinforcement was laterally restrained by means of 10 mm diameter binders spaced at 16 cm or 22 cm centres. The 15 cm thick compression flange was provided with the same transverse reinforcement and a small amount of longitudinal reinforcement.

1.15 Permissible working load, flexural failure load, stresses, etc. *

Section properties: $F_e = 85{\cdot}0\ cm^2$ (16 bars 26 mm diameter, IIIb)

$z = 75{\cdot}1$ cm

$x = 34{\cdot}1$ cm

Dead weight: $g = 1{\cdot}05$ t/m (including loading attachments)

$M_g = 4{\cdot}7$ tm

Permissible working load:

$M_{g+p} = 122{\cdot}6$ tm (as based on DIN 1045 with permiss.$\sigma_b = 90\ kg/cm^2$)

$M_p = 117{\cdot}9$ tm

Permissible live load (or superimposed load): $\underline{2P = 94{\cdot}3\ t}$

$Q_p = 47{\cdot}15$ t

$Q_g = 3{\cdot}15$ t

$Q_{g+p} = 50{\cdot}3$ t

Total working load: $2\,P_{kr} + G \simeq 100$ t

Ultimate-load moment on reaching yield point in tension flange:

$M_{Bkr} = F_e\,\beta_{0.2}\,z = 85 \times 4{\cdot}0 \times 0{\cdot}75 = 255$ tm

for which condition $\sigma_b \simeq 160\ kg/cm^2$

Ultimate load corresponding to this condition: $2\,P \simeq 191$ t

Working-load stresses (calculated in accordance with DIN 4224):

Extreme fibre stresses due to bending:

σ_b = permiss. $\sigma_b = 90\ kg/cm^2$

$\sigma_e = 1916\ kg/cm^2$ (permiss.$\sigma_e = 2{,}400\ kg/cm^2$)

Shear stress at bearing:

$$\tau_o = \frac{Q_{g+p}}{b_o z} = 67\ kg/cm^2$$

permiss. $\tau_o = 20\ kg/cm^2$

Design of stirrups:

Shear force: $T = \tau_o\, b_o\, l = 67 \times 10 \times 100 = 67$ t/m

---

* Subscripts: e refers to steel, e.g. F_e = steel cross-sectional area; b refers to concrete; g denotes dead load; p denotes live load or superimposed load; kr denotes "critical" (presumably). (Translator's note.)

Beam T_1 : vertical stirrups

$F_{e(stirrups)} = T/permiss.\sigma_e = 67/2{\cdot}4 = 27{\cdot}9\ cm^2/m$

12 mm dia. bars, steel IIIb, e = 8 cm, provides $F_e = 27{\cdot}2\ cm^2$

Beam T_2 : inclined stirrups

required $F_{e(stirrups)} = 67 / 2{\cdot}4\sqrt{2} = 19{\cdot}8\ cm^2$

12 mm dia. bars, steel IIIb, e = 11·2 cm, provides $F_e = 20{\cdot}0\ cm^2$

1.16 Manufacture of the beams

The beams were concreted in the inverted position, i.e., with the tension flange upwards, the concrete for the web being poured in through the gap (provided for the insertion of vibrators) between the bars. The main reinforcement was therefore in the most unfavourable position from the point of view of concrete compaction, namely at the top of the beam.

In order to ensure the greatest possible dimensional accuracy of the webs, the formwork for these was constructed from 350 mm deep rolled steel channels. This did mean, however, that the transverse diaphragms at the bearings could only be concreted on afterwards and that the construction joints for this purpose were located in the region of the highest shear stresses. Thanks to the provision of suitable extra reinforcement, no damage occurred at these joints during testing.

1.2 MATERIALS

1.21 Steel

Figure 7 shows the stress-strain diagrams for the 26 mm ribbed Tor steel used as longitudinal reinforcement and for the 12 mm Tor steel (ribbed and plain) used for the stirrups.

The cross-sectional stirrup area, determined by weighing, was somewhat smaller for the plain bars than for the ribbed bars (see Table I).

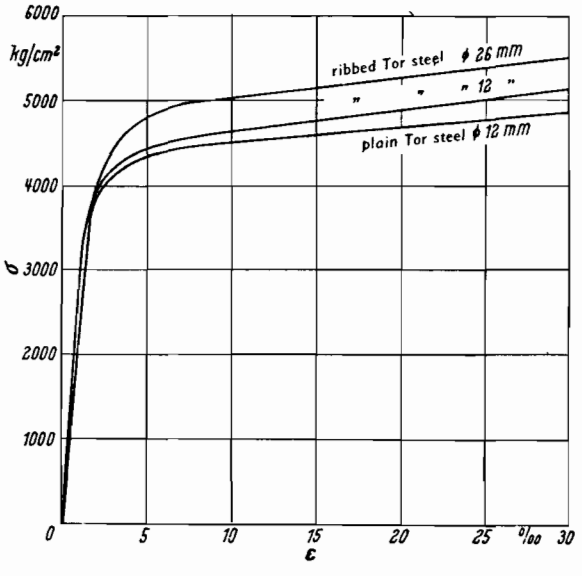

Figure 7: Stress-strain diagrams for the reinforcing bars in beams T.

TABLE I: Characteristics of the reinforcing steels.

Grade of steel	Nominal diameter (mm)	Measured cross-sectional area (mm^2)	$\beta_{0\cdot2}$ (kg/cm^2)	β_z (kg/cm^2)	Ultimate strain (%)	E (kg/cm^2)
Plain Tor steel	12	109	4270	5490	14·8	$2\cdot10 \times 10^6$
Ribbed Tor steel	12	116	4350	5470	17·0	$2\cdot10 \times 10^6$
Ribbed Tor steel	26	529	4740	5600	*	$2\cdot08 \times 10^6$

*Several fractures at gripping jaws.

TABLE II: Characteristics of the concrete.

Beam		T_1	T_2
Cement	(kg/m^3)	230	230
Water	(L/m^3)	199	207
Fine quartz	(kg/m^3)	118	118
Water/cement ratio (referred to cement and quartz)		0·57	0·59
Spread, by flow-table test	(cm)	35	40
Air voids content	(%)	3·0	2·6
Weight of 1 m^3 of compacted concrete	(kg)	2250	2250
Cube strength on day of testing (age 28 days)	(kg/cm^2)	298	269
Flexural strength	(kg/cm^2)	40	36

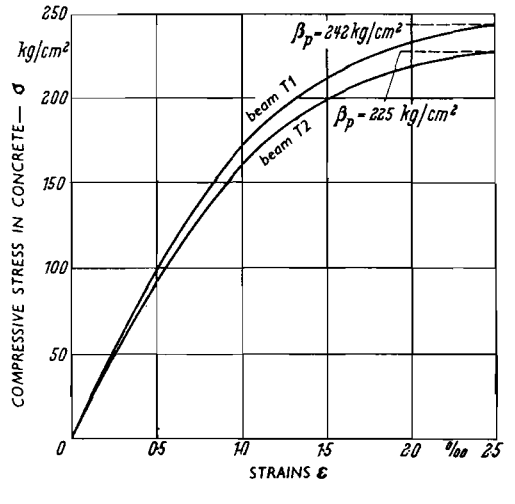

Figure 8: Stress-strain diagrams for the concrete in beams T, determined on axially compressed prisms.

1.22 Concrete

For both beams the specified concrete quality was B 300, i.e. a minimum compressive strength of 300 kg/cm^2 at 28 days. In order to minimize the increase of strength during the three-day testing period, a rapid-hardening Portland cement Z 475 was used.*

The aggregate consisted of washed Rhine gravel and was separated into four size fractions, namely 0-3 mm, 3-7 mm, 7-15 mm and 15-30 mm. The proportion of very fine particles was increased by the addition of 0-0.02 mm quartz powder. The mortar content (0 - 7 mm particle size) of the mix was 71 %. The composition of the concrete and significant technological data are summarized in Table II.

The cube strength β_w was in each case determined from twenty test cubes 20 cm in size, and the flexural strength β_{bz} was determined on prisms measuring 10 x 10 x 53 cm.

The stress-strain diagrams for the concrete, as shown in Figure 8, were each determined on two 10 x 10 x 53 cm prisms.

1.3 MEASURING POINTS AND MEASURING PROCEDURE

Because of the large size of the test specimens, it was possible to carry out extensive measurements for investigating the stress and strain behaviour. Arrangements were made for making measurements at some 350 points on each beam. In addition, the crack widths were measured at three levels at about 300 points during the loading of the beams. In order to limit the duration of each stage of loading, the readings were taken by twelve observers.

Detailed information on the positioning and identification of the individual measuring points will be subsequently published in the complete test report mentioned above. For reasons of space this information has been omitted from the present publication.

1.31 At the stirrups the strains were determined by means of demountable mechanical strain gauges and electrical resistance strain gauges. For the first-mentioned gauges (20 cm gauge length), ten stirrups in each half of beam T_1 were each provided with three measuring points. Similarly, eight stirrups in each half of beam T_2 were each provided with three measuring points. These measuring points had been formed in the stirrups by drilling before the latter were installed in position. These drilled holes were provided with small access tubes filled with paraffin wax and, after concreting, were made accessible (for insertion of the pin of the strain gauge) by scraping out the paraffin wax. Accuracy of measurement was approximately $\pm$ 0·002 %.

In beam T_1 six stirrups were each provided with four 1 mm wide slots milled into the bars themselves, and in beam T_2 six stirrups were each provided with five such slots. An electrical resistance strain gauge was

---

* Z 475 means that the cement has a minimum specified 28-day compressive strength of 475 kg/cm^2 (determined on standard mortar specimens). "PZ" means "Portland cement". (Translator's note.)

fixed in each slot and was sealed up and electrically insulated with Araldite. Accuracy of measurement was approximately ± 0·001 %.

1.32 Electrical resistance strain gauges were also inserted into slots in the flange reinforcement: two gauges at each quarter-span point and in the vicinity of each bearing, and four gauges at mid-span.

1.33 As for the concrete in the web zone, at each of six sections in each half, three four-armed rosettes were fixed, provided with stuck-on locating plates for demountable strain gauges. In view of the anticipated disturbance of the measurements by cracks, the minimum available gauge length of 5 cm was adopted. However, only the lower compression direction, inclined at 45°, yielded results that were serviceable for interpretation.

1.34 The strains of the concrete of the compression flange and tension flange were also measured by demountable strain gauges, over the entire length of both flanges, with gauge lengths of 20 cm and 50 cm. Between and directly beside the loads the transverse distribution of the longitudinal strains was also measured.

1.35 The deflexions were measured by a precision levelling instrument provided with a plane-parallel supplementary lens. Accuracy of measurement was approximately ± 0·1 mm.

1.36 Cracking was closely observed by means of magnifying glasses, the concrete surfaces having been whitewashed. The crack widths were determined at three levels with the aid of a measuring microscope (with readings to 0·01 mm), namely at the level of the main reinforcement, at the junction of the tension flange and the web, and half-way up the web. The cracks were numbered in the order in which they occurred (circled values in Figures 10 and 11) and the ends of the cracks were marked by a figure representing the corresponding load in tons.

1.37 With the aid of dial gauges, the protruding ends of the main reinforcing bars were checked for slip. It was found, however, that the anchorage of the bars in the concrete was fully preserved right up to failure of the beams.

1.4 LOADING

Because of the numerous measurements to be performed, it took three days to test a beam. The load was applied in increments of 20 tons, this being done twice in each case, with intermediate unloading. For each stage of loading, the measurements took about 45 min to perform, so that the influence of time upon the deformations of the concrete, especially at the higher loads, was unavoidable. During all intervals in testing (including overnight) the beams were unloaded.

Figure 9 shows a beam mounted under the MAN 1500-ton loading apparatus.

1.5 TEST RESULTS

We shall compare the test results of beams T_1 and T_2 as this yields some valuable information. The cracking patterns of the beams after failure are shown in Figures 10 and 11.

Figure 9: Beam T1 in the testing machine, with measuring instruments and team of observers.

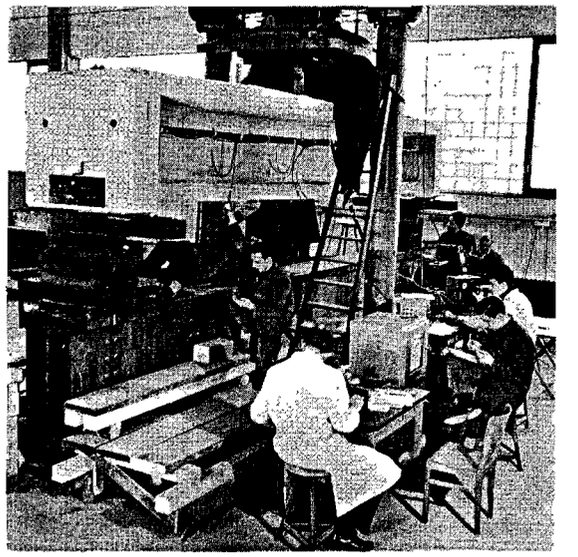

Figure 10: Cracking pattern of beam T1 after shear failure in web; ribbed stirrups on the left, plain ones on the right.

Figure 11: Cracking pattern of beam T2 after shear failure in web; ribbed stirrups on the left, plain ones on the right.

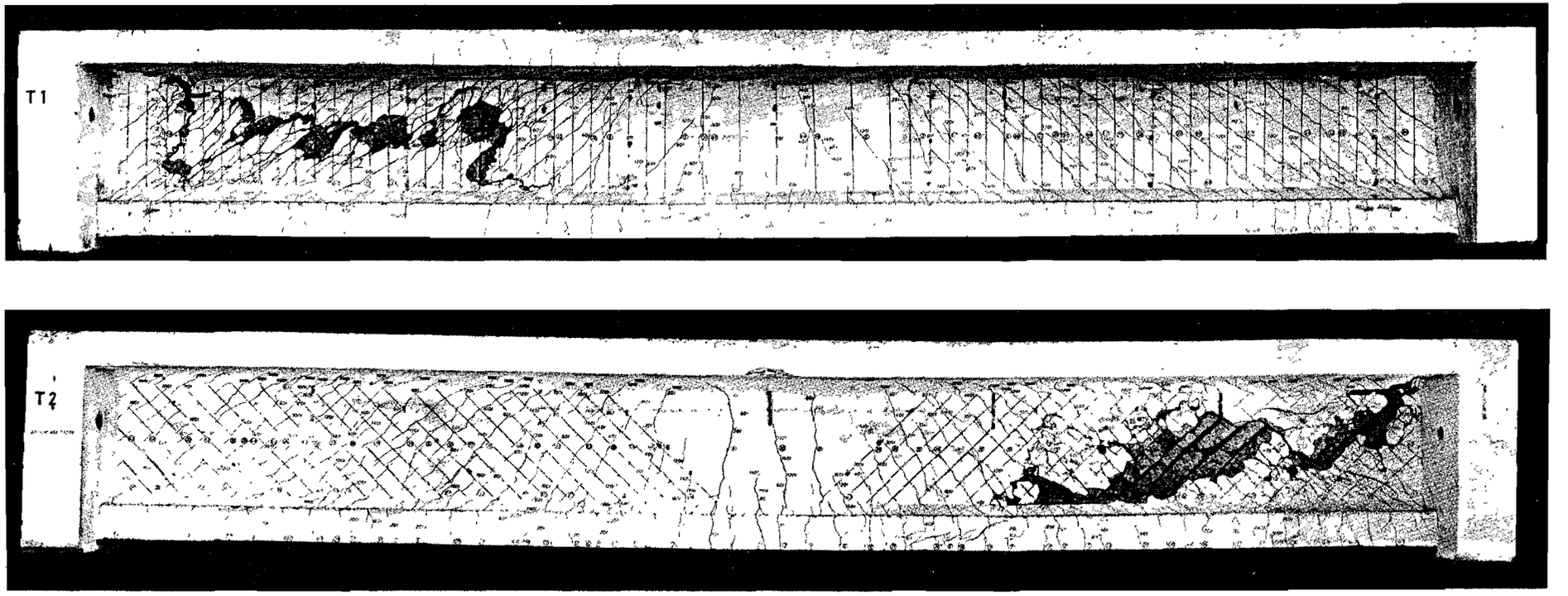

1.51 Ultimate load

Beam	Cube strength β_w (kg/cm^2)	Ult. load 2P (metric tons)	max. τ_o at failure (kg/cm^2)	
			test	converted to β_w=300
T_1	298	160	111	112
T_2	269	232	160	178·5

1.52 The cause of failure

In both beams the concrete in the web failed under oblique compression - as expected - by superficial spalling and disintegration into thin fragments (Figures 12 and 13). There were no signs of buckling of the concrete "struts", nor was this expected to occur, since the thin web was held in check by the stirrups functioning under high tensile stress.

Although the cause of failure was the same in both beams, the ultimate load of T_1 was substantially higher than that of T_2. This must mean that with vertical stirrups the web concrete is much more severely stressed than it is with inclined stirrups. This is confirmed by the following results.

1.53 The oblique compressive stresses in the web

The compressive stresses inclined at about 45° were determined from the numerous concrete strains measured on the web, with the aid of the stress-strain diagram (Figure 8). In Figure 14 the average values occurring outside the zones where external forces are transmitted into the beam have been plotted against the load applied. The measuring points whose readings were used for obtaining the averages and which were not affected by cracks are also shown in Figure 14.

The results confirm that with vertical stirrups the oblique compressive stresses (in beam T_1) are much higher (about 1·5 times) than they are with inclined stirrups. This ratio corresponds approximately to that of the ultimate loads.

In both beams at failure, oblique compressive stresses σ_{II} (as principal compressive stress) of about the same magnitude as the prism strength were attained:

for beam T_1 : $\beta_p = 0{\cdot}85\ \beta_w = 253$ kg/cm^2; $\sigma_{II} \simeq 220$ kg/cm^2

for beam T_2 : $\beta_p = 0{\cdot}85\ \beta_w = 228$ kg/cm^2; $\sigma_{II} \simeq 230$ kg/cm^2*

* For beam T_2, the value of σ_{II} was obtained by linear extrapolation from the last measured value.

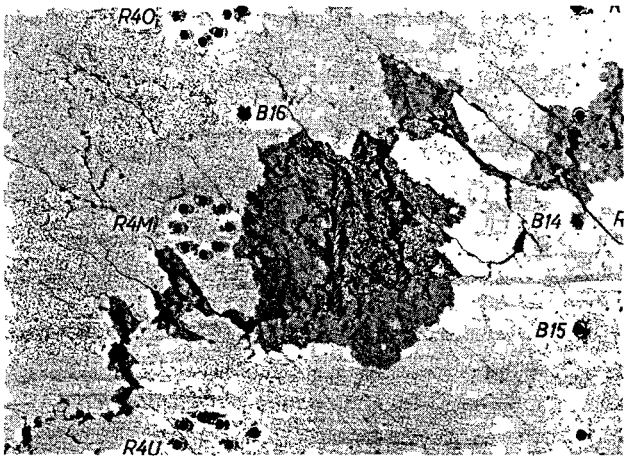

Figure 12: Close-up of part of the web zone of beam T1, destroyed by oblique compression.

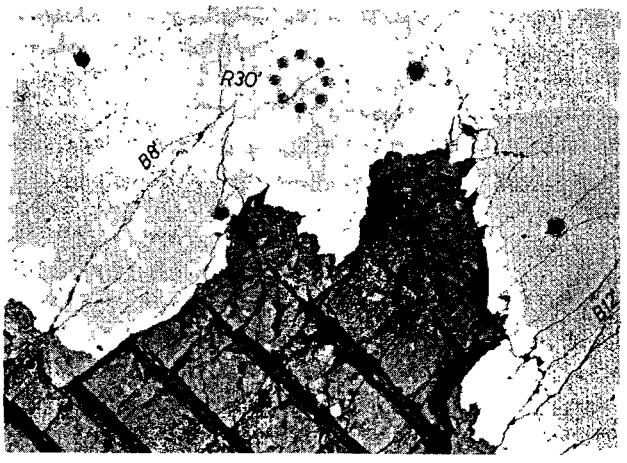

Figure 13: Close-up of part of the web zone of beam T2, destroyed by oblique compression.

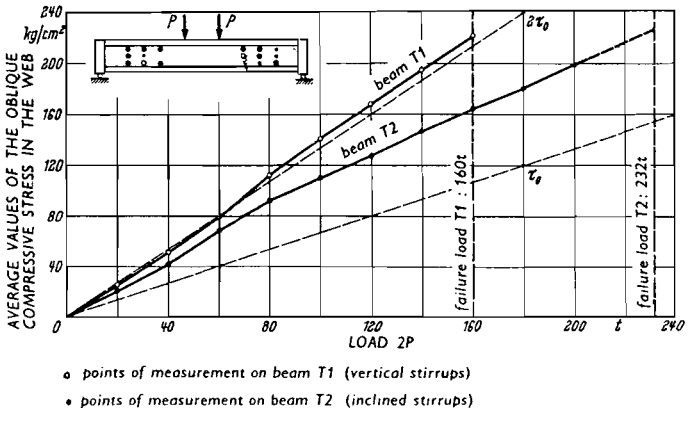

Figure 14: Average values of the oblique compressive stresses in the webs of beams T1 and T2, and comparison with the stresses τ_o (and 2 τ_o) obtained from the conditions of equilibrium (see Figure 15).

This proves that the inclined concrete struts are subjected more or less to pure compression and that stresses at failure, as determined from the strains, are in good agreement with the strengths. This inference is an important one because the magnitude of σ_{II} differs substantially from the values calculated from the lattice analogy.

Figure 15 gives the derivations of the stresses and internal forces determined by the equilibrium condition, on the assumption that the forces in the flanges are horizontal and that the shear force is therefore absorbed in the web only. On this basis the oblique compressive stresses for stirrups inclined at 45° would be equal to τ_o, whereas for vertical stirrups it would be equal to 2 τ_o, i.e. twice as large. These theoretical values have likewise been plotted in Figure 14.

It is noteworthy that oblique compressive stresses measured in the case of inclined stirrups are about 50 % higher that the stresses τ_o, whereas the stresses in the stirrups attain only about 80 % of the calculated values, as will be shown later. We thus find that - as already stated at the beginning of this report - the stiffer struts (compression members) are more highly stressed than the more flexible tension members.

These somewhat unexpected results call for an explanation, since they are, at first sight, apparently at variance with the conventional equilibrium

conditions. It must, in the first place, be borne in mind that though the oblique compressive stresses plotted in Figure 14 are averages of a whole range of values, each measuring point whose reading was used for calculating the average was situated in a zone locally unaffected by cracks. In between the ramifications of individual cracks, where it was not possible to make measurements, the oblique compressive stresses were undoubtedly lower. Hence the average of σ_{II} over the entire shear region would be smaller than the values actually plotted. For beam T_1, with vertical stirrups, this may well be the principal cause of the discrepancy (approximately 15 %) between the calculated and the measured values of σ_{II}. This influence also occurs in the case of T_2 and is even more pronounced because of the larger number of shear cracks; but here the stresses in the stirrups also play a significant part. From Figure 15 (bottom left) it appears that the vertical components of D_S and Z_S together must be equal to Q. Since the measured force Z_S is only 80 % of the theoretical value, however, the difference of 20 % must therefore be resisted by the inclined struts. The fact that the resultant of D_S and Z_S is then not vertical merely means that the tension flange is somewhat more highly loaded and the compression flange somewhat less highly loaded than corresponds to the theory. In the case of vertical stirrups (Figure 15, right-hand side) the stirrup stress has no effect on the oblique compressive stresses, and for this reason the differences between the calculated and the measured values for beam T_1 are smaller than for beam T_2.

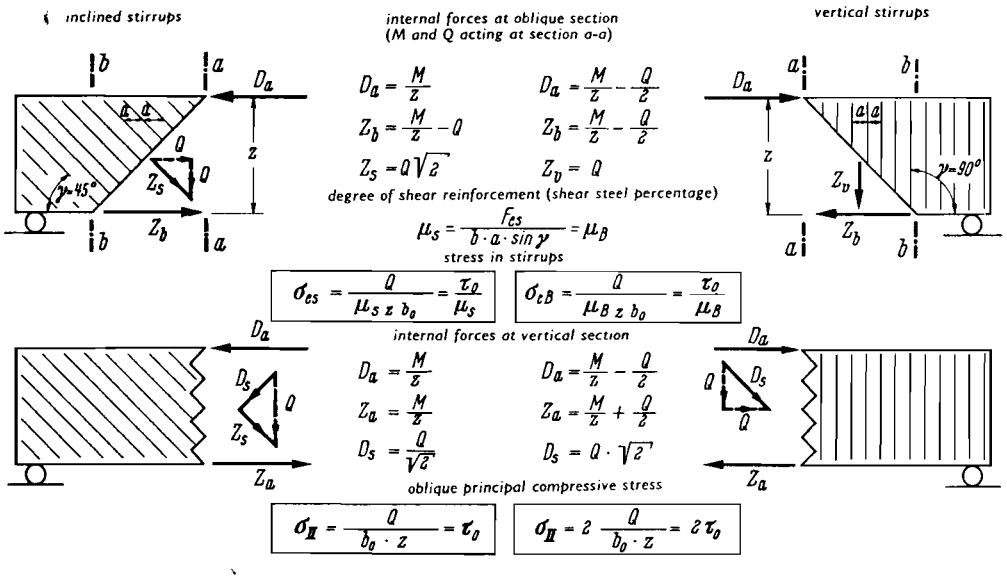

Figure 15: Internal forces and stresses derived from the equilibrium conditions, for beams with inclined or vertical stirrups, on the assumption that the forces in the flanges are horizontal.

1.54 Stresses in the stirrups

Let us first consider the average values of the stirrup stresses in the middle zone between the bearing and the load which were determined from the measured strains (Figure 16) and compare them with the stresses calculated on the basis of conventional shear theory.

$$\sigma_{eB} = \frac{\tau_o}{\mu_B} = \frac{\tau_o \, b_o \sin\gamma}{F_{eB}}$$

where F_{eB} = cross-sectional area of a stirrup

a = stirrup spacing along axis of beam

γ = slope of stirrups in relation to axis of beam

The stirrups, each provided with three demountable strain gauge measuring points, for which the results were used for calculating the average value are indicated in Figure 16.

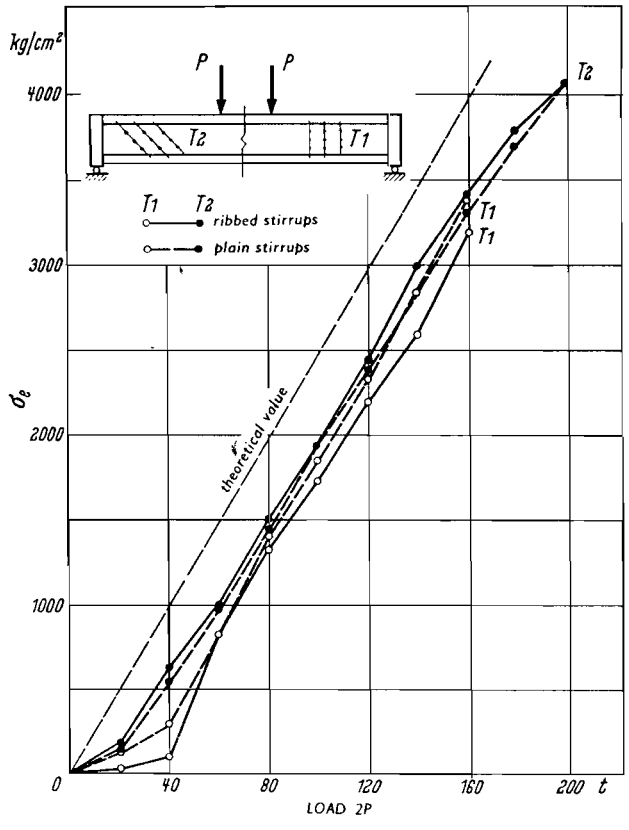

Figure 16: Comparison of the measured stresses in the stirrups with the calculated stress, plotted against the load (averages obtained from nine points of measurement in the medium shear region).

For both beams the stirrups stresses up to ultimate load remain definitely below the calculated values: by an amount of 750 kg/cm^2 in beam T_1 and of 600 kg/cm^2 in beam T_2. For live load this corresponds to a difference of about 30% and 25 % respectively, and for 1·7 times live load it corresponds to a difference of about 20 %. At ultimate load for beam T_1 the average stress in the vertical stirrups was 3,300 kg/cm^2. At ultimate load for beam T_2 the estimated stress in the inclined stirrups was 4,400 kg/cm^2, whereas the theoretical value was much higher, being 5,700 kg/cm^2. From the shape of the stress curve it appears that the stirrups were already to some extent in the plastic range.

The only possible explanation of the fact that the stresses in the stirrups remained below the calculated values is that, even with so considerable an amount of shear reinforcement, a proportion of the shear force is still being resisted by the "truss" with the tie-rod action, which is confirmed by the increased stresses in the tension flange and in the struts.

The inclined stirrups consisting of ribbed bars exhibited somewhat higher stresses than those consisting of plain bars, whereas with vertical stirrups the opposite tendency was observed. These differences may be attributed to random features of cracking, but it may also be that plain

stirrups slide a little and thus relieve themselves of some of the force acting upon them or that it was because these bars had a slightly smaller cross-sectional area than the ribbed ones. With the inclined stirrups it was presumably the bond, and with the vertical stirrups it was presumably the smaller cross-sectional area that decided the difference in behaviour.

Figure 17 shows the stress distribution in some of the stirrups. In plotting these curves, minor irregularities have been levelled out. The measuring points are designated by "o" (top), "m" (centre) and "u" (bottom). The full lines relate to ribbed stirrups and the dotted ones relate to plain stirrups. In the edge zones of the shear region the inclined stirrups are thus found to carry considerably more load than the vertical stirrups. As

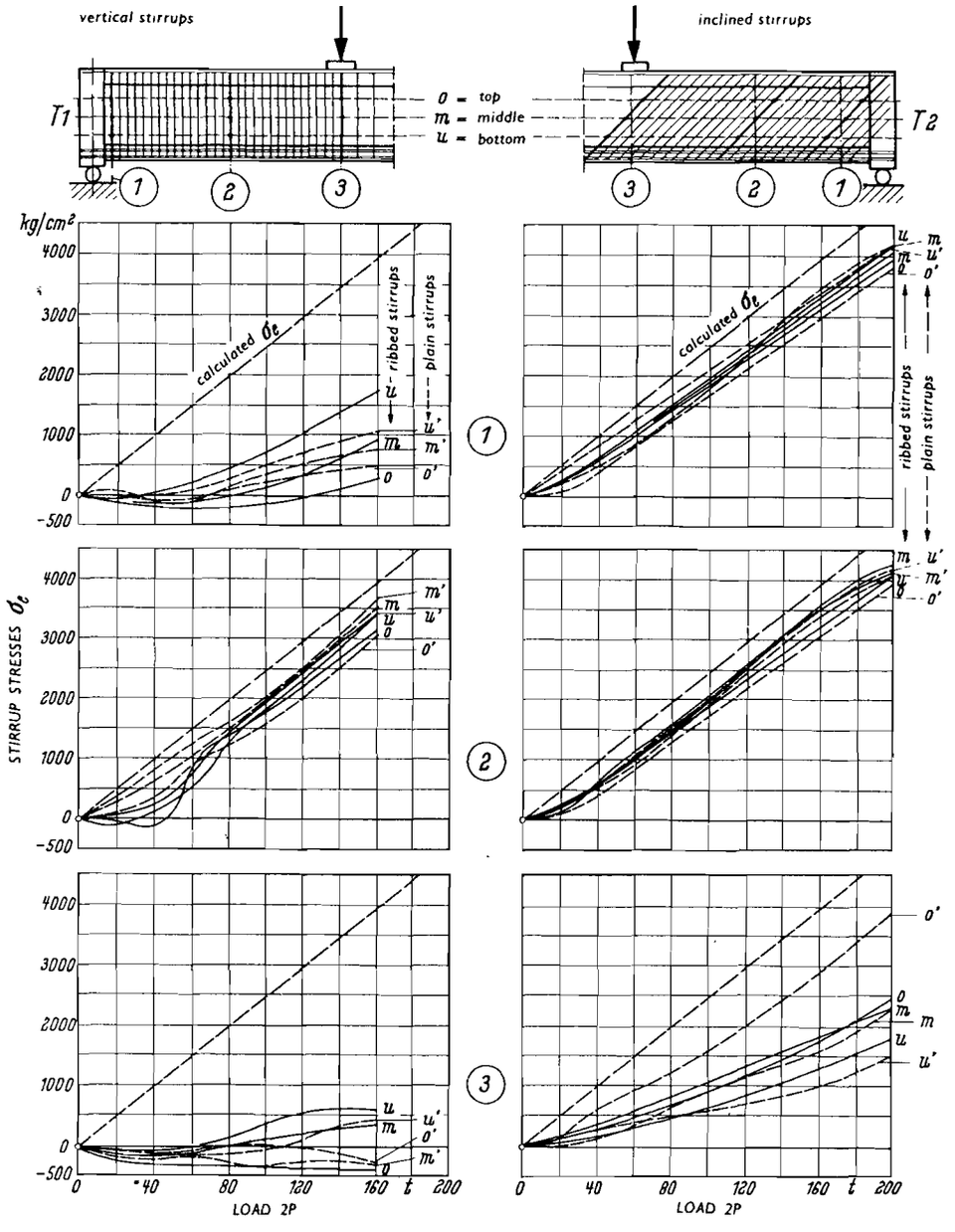

Figure 17: Summary of the steel stresses at various levels in the web (in each case compared with the calculated stress).

will be seen later, this also clearly manifests itself in the deflexion and cracking. In the lower stages of loading, vertical stirrups are stressed in compression. In the middle shear region all the stirrups exhibit a decrease in stress from bottom to top, but this decrease is slight, so that, also with ribbed bars, it is most essential to anchor the stirrups at the top as well as at the bottom by providing the ends of the bars with loops or hooks, as was in fact done in the test beams.

1.55 The stresses in the compression and tension flanges

In Figure 15 let us again consider the theoretical forces in the flanges of the two different lattice systems. We see that in the shear region (Q effective) the different diagonal forces also produce different flange forces for vertical sections. Only with stirrups inclined at 45° can we expect to obtain equal forces in the two flanges of the beam, namely $D = Z = M/z$. With vertical stirrups the flange forces D and Z differ by an amount Q. The horizontal tensile force in the web, which is mentioned in E. Rausch's book (11) and which would have to be resisted by horizontal web reinforcement, is merely the result of the arbitrary assumption that the flange forces are equal. Actually this is impossible, however, since the fibre at the neutral axis is not subjected to tensile strain and horizontal reinforcement will therefore not be stressed in tension. Instead, the equilibrium condition is satisfied by the difference between D and Z, as was clearly manifested in the case of beam T_1. In the pure bending zone ($Q = 0$), i.e. in the region between the loads P, the two flange forces must again be equal and of opposite sign.

The results of the measurements show that the extreme stresses at the compression flange (Figure 18) decrease more rapidly towards the ends of the beam than would be expected from the bending moment diagram. In the vicinity of the supports, considerable tensile stresses and cracks even occur in the compression flange, which is attributable to the "arch action". With vertical stirrups this action is more pronounced than with inclined ones. It is clearly apparent that in the undisturbed shear region the horizontal compressive force in the case of vertical stirrups falls short of M/z by an amount equal to about $Q/2$. The fact that the compressive stresses at midspan in T_1 are higher than in T_2 can be explained by the reduction of the compressive zone in T_1 by shear cracks extending beyond the flexural neutral axis (see Figure 10).

In Figure 18 the strains which have been measured across the cracks at the bottom of the tensile flange have also been plotted. In the shear region they are larger in beam T_1 than in beam T_2, which is in accordance with Figure 15. In the end regions of the beam, therefore, vertical stirrups relieve the load of the compression flange and increase the load of the tension flange.

According to 1.53, inclined stirrups are to be recommended for structural members which are subjected to shear and in which failure is caused by oblique compression, whereas for the many cases where shear failure results from destruction of the compressive zone it may be advantageous to provide vertical stirrups with their relieving effect upon the compression flange.

The pronounced strain peaks which occurred in the tension flange under the loads in the case of beam T_1 are also noteworthy. They are attributable to local flexural deformations due to the vertical compression of the web (negative σ_y, see Figure 17, stirrup 3), which effect is mitigated by the stirrup forces in that zone if the beam is provided with inclined stirrups.

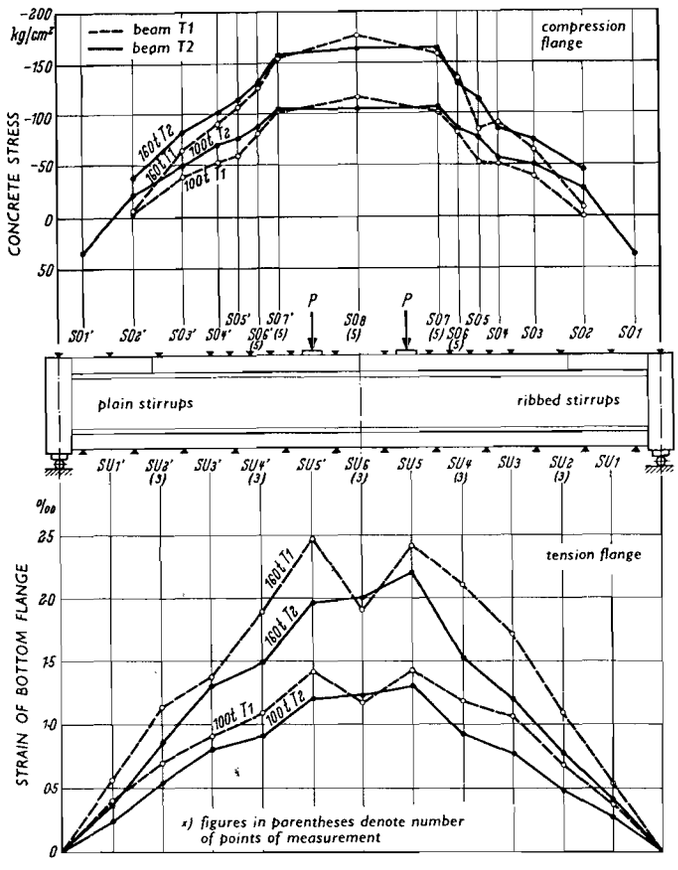

Figure 18: Extreme stresses in the concrete of the compression flange for two loading stages: P = 100 tons and 160 tons. Extreme fibre strains of the concrete in the tension flange were measured across cracks (gauge length 50 cm).

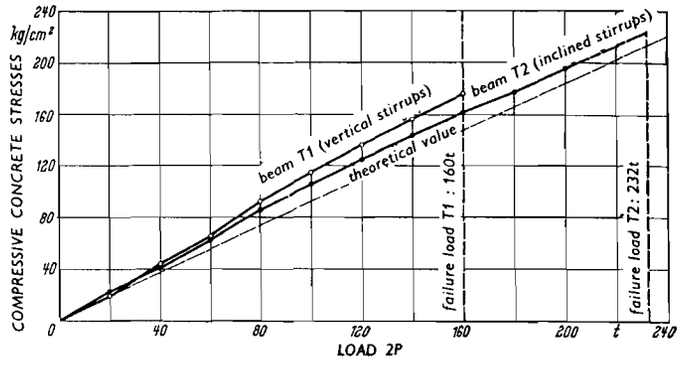

Figure 19: Extreme stresses in the concrete of the compression flange at mid-span.

Also, the presence of two struts, in opposite directions, must be conceived between the loads. These struts contribute towards this peak and then reduce the tensile force to the value M/z at mid-span, which value must be approximately the same for T_1 and T_2.

In Figure 19 the compressive stresses at mid-span have been plotted against the loading. The difference between T_1 and T_2 has already been explained. On the other hand, we must face the question why the measured values exceed the calculated values, the more so as statical considerations (e.g. with regard to the equilibrium of the internal forces for non-linear stress distribution above the neutral axis) would lead us to expect the opposite. In this connexion, time influences are hardly likely to be of decisive significance, since the permanent deformations in test prisms were about the same as those in the test beams. The strains occurring over the width of the compression flange were also approximately equal. We suspect the explanation to be that the stress-strain diagram for the prism axially loaded in compression - which diagram was used for converting the strains to stresses - does not correspond to the behaviour of the concrete at the compression face of a beam loaded in bending. Under axial compression the concrete strain at failure is only about 0·2 %, whereas in the case of a rectangular member loaded in bending the ultimate strain may be as much as 0·3 % or more. The stress-strain diagram of the extreme fibres of the flexural compressive zone may present a flatter shape than that obtained in the prism test. In that case the flexural stresses converted on the basis of the prism test would be rather too high. This surmise does, however, call for further investigation. In beam T_2 the highest compressive stress was about 225 kg/cm^2 and was close to the compressive strength, so that flexural failure was not very far behind shear failure.

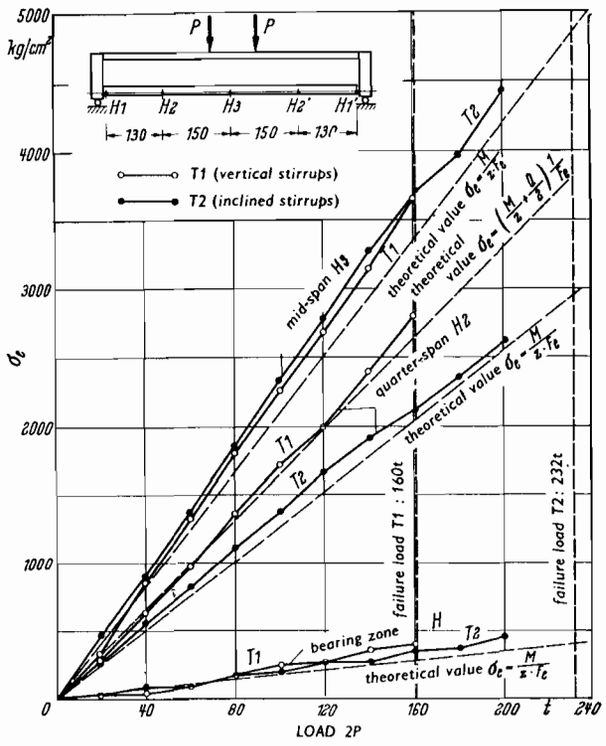

Figure 20: Average steel stresses in the bottom reinforcement at mid-span, quarter-span and close to the bearing.

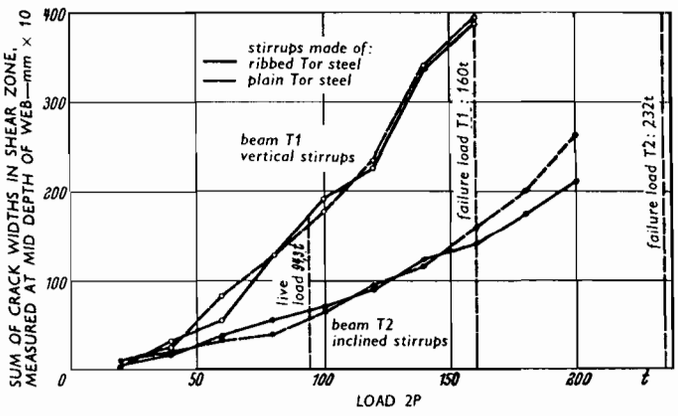

Figure 21: Sum of the crack widths in the shear zone, measured at mid-depth of web on beams T1 and T2.

The stresses in the longitudinal reinforcement at mid-span, at the quarter-span points and at the supports are represented in Figure 20. For both beams the mid-span values are in good agreement with the calculated values. At the quarter-span points, i.e. in the shear region, the difference which Figure 15 leads us to expect is clearly manifested: in the case of beam T_2 the measured stresses correspond to the values calculated from $Z = M/z$, whereas in the case of beam T_1 they correspond approximately to $Z = M/z - Q/2$. The difference vanishes directly beside the bearing. The struts of the "truss" thrust against the tie-rod already at some distance before the bearings, part of the shear forces being transmitted back into the compression flange by stirrups.

The steel stress attained at ultimate load was 3,600 kg/cm^2 in T_1 and had an estimated value of 4,900 kg/cm^2 in T_2 ; in the latter beam, therefore, a condition close to flexural failure had been reached.

1.56 Cracks

In both beams the cracks in the shear zone extended at almost exactly 45° over the full depth of the web and became vertical flexural cracks only in the tension flange (Figures 10 and 11). Because of the lateral location of the bearings (on either side of the beam), the oblique cracks extended as far as the transverse diaphragms at the supports, so that the compressive stress σ_y due to the transmission of the bearing reactions into the concrete therefore hardly affected the cracking pattern. Externally there was no noticeable difference between the cracks occurring with inclined and those occurring with vertical stirrups. However, when we come to consider the sums of the crack widths measured at mid-depth of the web (Figure 21), we perceive a considerable difference in effectiveness between the two stirrup directions: with vertical stirrups the crack widths at all stages of loading are almost three times as large as those occurring with inclined stirrups. Plain and ribbed stirrups exhibited hardly any difference with regard to the widths; not until very high loads were attained in the case of beam T_2 did the cracks associated with the plain stirrups become manifestly wider.

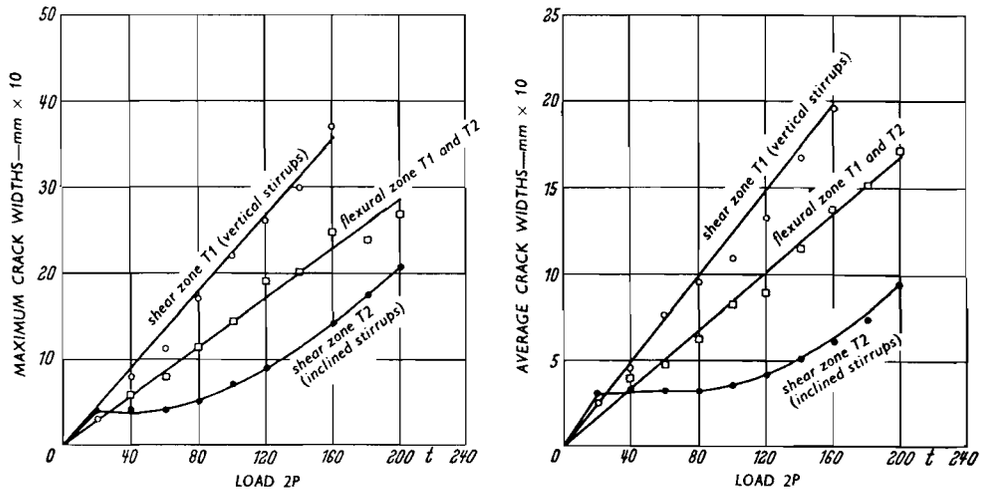

Figure 22: Comparison of the maximum and average crack widths in the shear region with the crack widths in the tensile flange.

In Figure 22 the maximum and the average widths of the shear cracks at mid-depth of the web are compared with the corresponding values for the flexural cracks in the tension flange between the loads. Accordingly, the shear cracks associated with inclined stirrups are always finer than the flexural cracks, whereas it is just the reverse with vertical stirrups. With inclined stirrups the measured average and maximum crack width under working load are 0·03 mm and 0·09 mm respectively - far below the value that is regarded as harmless in tensile zones. Even in the case of vertical stirrups the corresponding values, namely 0·10 mm and 0·24 mm respectively, are still within the "permissible" range. In both cases, therefore, we have only small crack widths in the web, so that, from the viewpoint of cracking, such high shear stresses in reinforced concrete beams are harmless. We shall see, however, that thick bent-up bars in thick webs are liable to be associated with wide shear cracks. The "distributed" reinforcement adopted in the present case is therefore a prerequisite for the observed favourable behaviour.

1.57 Deflexions

In view of the relations that have been indicated in the foregoing, it will hardly be surprising that larger deflexions were measured for vertical stirrups than for inclined ones. At mid-span the difference is about 35 %, and at the higher loading stages it is even as much as 45 % (Figure 23).

The deflexions δ_1 and δ'_1 at a distance of 1 mm from the supports, as plotted in Figure 23, show that ribbed stirrups give smaller deformations than do plain stirrups, the differences being more pronounced for inclined stirrups than for vertical ones.

1.58 Diaphragms and anchorage

Even at the highest loads the transverse diaphragms at the ends of the beams exhibited only some quite separate and very fine flexural cracks, but no inclined shear cracks, thanks to the suitable reinforcement consisting of

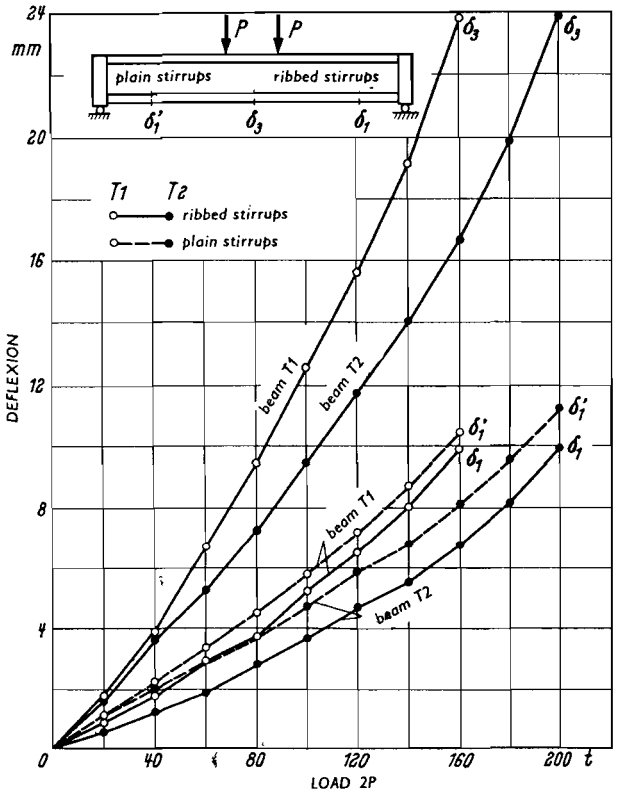

Figure 23: Comparison of the deflexions of beams T1 and T2. Effect of direction and surface condition (plain or ribbed) of the stirrups.

horizontal and vertical bars, as mentioned earlier. This is also the reason why the longitudinal reinforcement, despite the laterally placed bearings and the short anchorage length, exhibited no slip. The "emergency" nuts provided at the projecting ends of the bars therefore did not have to be tightened.

1.6 French tests by J.R. Robinson relating to high shear stresses

In 1960, J.R. Robinson [12] carried out tests on nine beams with a view to determining the upper shear stress limit. The beams had the dimensions shown in Figure 24, the webs being only 6 cm thick. The loading in each case consisted of a concentrated load applied at the left-hand quarter-span point. At the supports and at the point of load application the thin web was stiffened by 8 cm wide ribs, with the result that the compressive stresses σ_y due to the transmission of the forces into the concrete hardly affected the web itself. The load position adopted in the tests gave a low moment-shear ratio of 2 on the left-hand side, and a ratio of 6 on the right-hand side.

The reinforcement is shown in Figure 25. It was unusual in that the "stirrups" each consisted only of one bar placed centrally in the web and provided with hooked ends (hook diameter = 5 ϕ, straight protion of hook = 5 ϕ, where ϕ is bar diameter). These hooks were arranged longitudinally and partly overlapping. They passed around the transverse reinforcing bars which were provided at every second stirrup and which, in the tension flange of the beam, consisted of a closed ring of 8 mm diameter placed around the longitudinal bars and were therefore very strong. The results obtained with this unusual form of web reinforcement are very instructive.

In all the beams the longitudinal reinforcement consisted of two plain bars of steel I, 40 mm in diameter, provided with large end hooks and closely spaced transverse reinforcement in the anchorage zone.

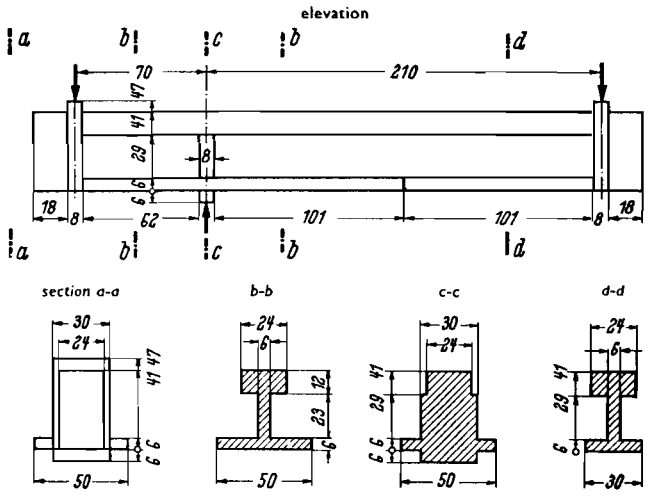

Figure 24: J.R. Robinson's test beam.

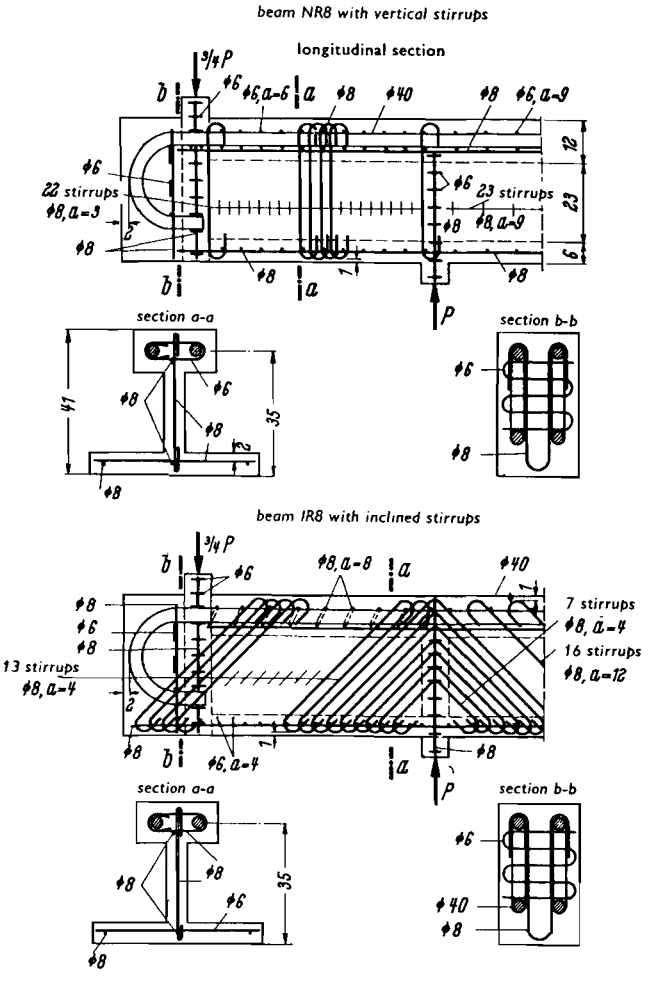

Figure 25: The reinforcement in J.R. Robinson's test beam.

The stirrups consisted in part of plain bars of steel III (designation R) and partly of Tor steel without transverse ribs (designation T). In beams N the stirrups were placed vertically, whereas in beams I they were inclined at 45°. In five beams the stirrups were of 8 mm diameter and in four beams they were of 10 mm diameter bars. The stirrup spacing was so chosen that an approximately equal degree of shear reinforcement was obtained in all cases, so as to produce a stress in the stirrups of the order of magnitude of the yield point (approximately 4,000 kg/cm^2) at the estimated ultimate load of 30 tons.

The conventional analysis based on a modular ratio n = 15 gave a neutral axis height x = 20 cm and an internal lever arm z = 31·4 cm, the steel stress in the tension flange being 2,000 kg/cm^2 for P = 30 tons. The tension flange reinforcement was therefore stressed only half as much as the stirrups.

The test results are summarized in Table III.

In the case of the first beam (NR 8) the concrete has a strength of only 182 kg/cm^2, so that a very low ultimate load was obtained. In the other beams with vertical stirrups, failure occurred in consequence of the oblique compression in the web. The oblique compressive stress approximately attained the value of the prism strength, on the assumption that with vertical stirrups this stress had the approximate value $\sigma_{II} = 2\tau_o$. With adequate concrete strength an ultimate load was reached at which the calculated stress in the short stirrups was 4,000 kg/cm^2.

TABLE III: Summary and evaluation of Robinson's tests.

Test No.	Shear reinforcement				Measured values			Type of failure	Shear stresses			Calculated stresses at failure		
		Steel and diameter	Spacing (cm)	μ_s (1) (%)	β_w (kg/cm^2)	P_R Crack (t)	P_u Failure (t)		$\tau_o = \frac{Q}{b_o z}$ (2) (kg/cm^2)	$\frac{2\tau_o}{\beta_p}$ (3)	$\tau_{o,R}$ at the first crack (kg/cm^2)	σ_e (kg/cm^2)	σ_b (kg/cm^2)	σ_e stirrups (kg/cm^2)
NR 8	Vertical stirrups	8 mm round bar	3	2·78	182	3·5	16	Crushing of web due to oblique compression	64	0·83	14	1060	95	2300
NR 10		10 mm round bar	4	3·29	290	6	30		120	0·98	24	2000	177	3700
NT 8-1		8 mm Tor steel	3	2·78	243	8	28		111	1·07	32	1870	165	4000
NT 8-2		8 mm Tor steel	3	2·78	248	7	28		111	1·05	28	1870	165	4000
NT 10		10 mm Tor steel	4	3·29	207	6·5	22		88	1·00	26	1470	130	2700
IR 8	Stirrups inclined at 45°	8 mm round bar	4	2·95	315	7	40	Shear failure in compression flange	159	Web not destroyed	28	2670	236	5400
IR 10		10 mm round bar	6	3·10	324	5	45		179		20	3000	266	5800
IT 8		8 mm Tor steel	4	2·95	242	7	29		156		28	2600	230	5300
IT 10		10 mm Tor steel	6	3·10	306	7	44		175		28	2940	260	5700

(1) Degree of shear reinforcement $\mu_s = \frac{F_e \, s}{b_o \, a \, \sin\gamma}$ γ = slope of stirrups

(2) $Q = \frac{3}{4} P_u$; $b_o = 6$ cm; $z = 31{\cdot}4$

(3) $\beta_p = 0{\cdot}85 \, \beta_w$

(4) Values calculated according to conventional theory from failure load, assuming n = 15 (modular ratio).

In the tests performed on the beams provided with inclined stirrups failure occurred not in the web but in the concrete of the compression flange, although shear stresses τ_o of the magnitude 156 to 179 kg/cm^2 were reached in the concrete (ranging in strength from B 240 to B 320) and the calculated steel stresses in the stirrups were 5,300 to 5,800 kg/cm^2 and were therefore above the nominal yield point.

Unfortunately, because of the considerable variation in the concrete strengths, it is not possible definitely to establish the effects of differences in diameter and sectional shape of the stirrup bars.

Robinson likewise found that the web cracks remained very fine up to ultimate load. He determined the development of the cracks (with the aid of highly sensitive extensometers) from discontinuities in the load-strain curves. The shear stresses τ_o associated with the cracking load are indicated in Table III. The cracks became visible only when a load corresponding to 1·4 to 2 times the cracking load has been reached. Shortly before ultimate load was attained, the maximum crack widths were 0·31 to 0·45 mm for vertical stirrups, and 0·06 to 0·37 mm for inclined stirrups. Nearly all the cracks to left and right of the load extended at an angle of 45° over the entire depth of the web.

From these French tests it is again evident how greatly the stress conditions in the web are affected by the direction of the reinforcement and they also confirm the test results reported in Section 1 of this report, although here the reinforcement conditions were much more unfavourable. It is therefore to be regarded as an unexpected result that it is apparently not even necessary to loop the stirrups around the tensile reinforcement and that, instead, it is sufficient to provide hooked anchorages (independent of the tensile reinforcement) for transmitting the diagonal tensile forces to the flange reinforcement. This conclusion will have an important bearing on possible types of reinforcement to be envisaged in new standard regulations. It should be borne in mind, however, that such reinforcement calls for good concrete as a prerequisite, as is apparent from the failure in the case of beam NR 8 in which the concrete was only of B 180 quality. In making conclusions from his tests, Robinson speaks of a rehabilitation of the "floating bars" which Mörsch, on the evidence of his tests, rightly considered to be unsuitable. In Mörsch's tests, however, the concrete was of low strength and the anchorage zone of the inclined bars was not provided with any special transverse reinforcement. In any case, Robinson's results now justify the use of "floating" shear reinforcing bars as a possible constructional solution, provided that they are well anchored in transversely reinforced concrete.

A further important consideration is that this transmission of force operates satisfactorily even with unfavourable bond conditions of the reinforcement in the tension flange: the plain bars of 40 mm diameter in these rather small beams are definitely unfavourable in this respect. In larger beams the bond conditions for this reinforcement are always likely to be much better.

1.7 INFERENCES FROM THE TESTS FOR HIGH SHEAR STRESSES

1. Summary of principal test results

For the same degree of shear reinforcement, vertical and inclined stirrups are approximately equally stressed - to about 80 % of the calculated value in the middle of the shear region.

The oblique principal compressive stresses σ_{II} are larger than the calculated shear stresses: with vertical stirrups the magnitude of σ_{II} is approximately $2{\cdot}1\ \tau_o$ and with inclined stirrups it is about $1{\cdot}5\ \tau_o$.

The web zone fails in consequence of oblique compression if the actual σ_{II} attains the prism strength of the concrete.

With inclined stirrups the compression flange is more heavily stressed than it is with vertical stirrups; for the tension flange it is the other way round.

With inclined as against vertical stirrups the shear crack widths are reduced to 1/3 and are smaller than the widths of flexural cracks.

Inclined stirrups give smaller deflexions than vertical stirrups. With plain stirrups the deflexions are somewhat greater than with ribbed stirrups.

2. Permissible shear stresses τ_o

Although the oblique compressive stresses σ_{II}, as we have seen, differ substantially from the shear stresses calculated by means of the conventional formula $\tau_o = Q/b_o z$ - depending on the direction of the shear reinforcement - we shall make use of this conventional value for determining the permissible stress conditions of structural members highly stressed in shear. Introducing a reduction factor of 0·85 in respect of the scatter of the concrete strength and a factor of the same magnitude in respect of the time influence associated with sustained loads, and specifying a factor of safety of 2·1 against failure, we obtain the following values.

Shear reinforcement approximately in the direction of σ_I:

$$\sigma_{II} \simeq 1{\cdot}5\ \tau_o \qquad \sigma_{II(\text{failure})} \simeq \beta_p$$

$$\text{permiss.}\tau_o = \frac{0{\cdot}85 \times 0{\cdot}85\beta_p}{1{\cdot}5 \times 2{\cdot}1} = 0{\cdot}23\ \beta_p$$

Shear reinforcement differing in direction from σ_I by up to 45° :

$$\sigma_{II} \simeq 2{\cdot}1\ \tau_o$$

$$\text{permiss. } \tau_o = \frac{0{\cdot}85 \times 0{\cdot}85\beta_p}{2{\cdot}1 \times 2{\cdot}1} = 0{\cdot}16\ \beta_p$$

As these values are very high in comparison with the hitherto permissible value of τ_o, it will be appropriate initially to adopt somewhat more conservative limits for permiss. τ_o until sufficient practical experience has been gained:

shear reinforcement in direction of σ_I (deviation $\pm$ 15°)	shear reinforcement differing 45° in direction from σ_I
permiss. $\tau_o = \beta_p/6$	permiss. $\tau_o = \beta_p/9$

In that case a factor of safety of at least 3 will be available even under fully sustained loading and even if the concrete strength is not quite attained. If the specified concrete strength is attained, the available factor of safety against shear failure due to oblique compression in the event of overloading of short duration will be about 4·2.

1.8 DESIGN AND NATURE OF THE SHEAR REINFORCEMENT

For severe shear conditions the shear reinforcement should be designed in the usual way according to the lattice analogy, i.e. so as to provide full safeguard against shear failure, even though permiss. $\sigma_{e(stirrups)}$ is not in fact fully utilized. It is recommended that the shear reinforcement be installed in the direction of the principal tensile stress (state I *, at level of neutral axis). Stirrups alone (i.e. not stirrups in conjunction with bent-up bars) can advantageously be employed, the stirrups being anchored by looping them around the flange reinforcement or by bending them at right angles and continuing them into the compressive flange or by providing them with hooks at the ends. For stirrups and flange reinforcement it is preferable to use ribbed bars.

The shear reinforcement can permissibly differ by up to 45° in direction from the principal tensile stress, provided that τ_o remains below the limit stated. Here again, stirrups alone are sufficient for the purpose, though these can advantageously be assembled into a trellis system by means of longitudinal bars.

In the case of shear reinforcement the principle of "distributed reinforcement" - i.e. closely spaced bars of small diameter - has a particularly favourable result with regard to crack widths in that the cracks remain very fine.

1.9 PRACTICAL SUGGESTIONS

It may be feared that the design of the concrete sections on the basis of the above-mentioned high permissible values of τ_o could give rise to constructional difficulties in that, for example, the fixing of the reinforcement or the concreting of the member would become more difficult. These practical problems must, of course, be given due consideration. The fact that a certain permissible value of τ_o is indicated does not necessarily mean that this value must be fully utilized in every case. The object of the high permissible values of τ_o is to allow of a more favourable dimensional design of the concrete of very long or very heavily loaded structural members than has hitherto been possible. In such cases these stresses provide much more favourable conditions - also with regard to the execution of the work - than the low stresses τ_o in conjunction with the type of shear reinforcement as hitherto employed. An example will help to explain this.

In practice, difficulties have often arisen with the diaphragm walls of the lower storeys of multi-storey buildings, which have to carry heavy column loads. Let us suppose that a wall of this kind is 90 cm thick and has to be reinforced for τ_o = 20 kg/cm^2, i.e. for a shear force of 180 tons/m.

---

* "State I" refers to the uncracked section; "state II" refers to the case where the section is cracked and the tension is resisted by the steel only. (Translator's note.)

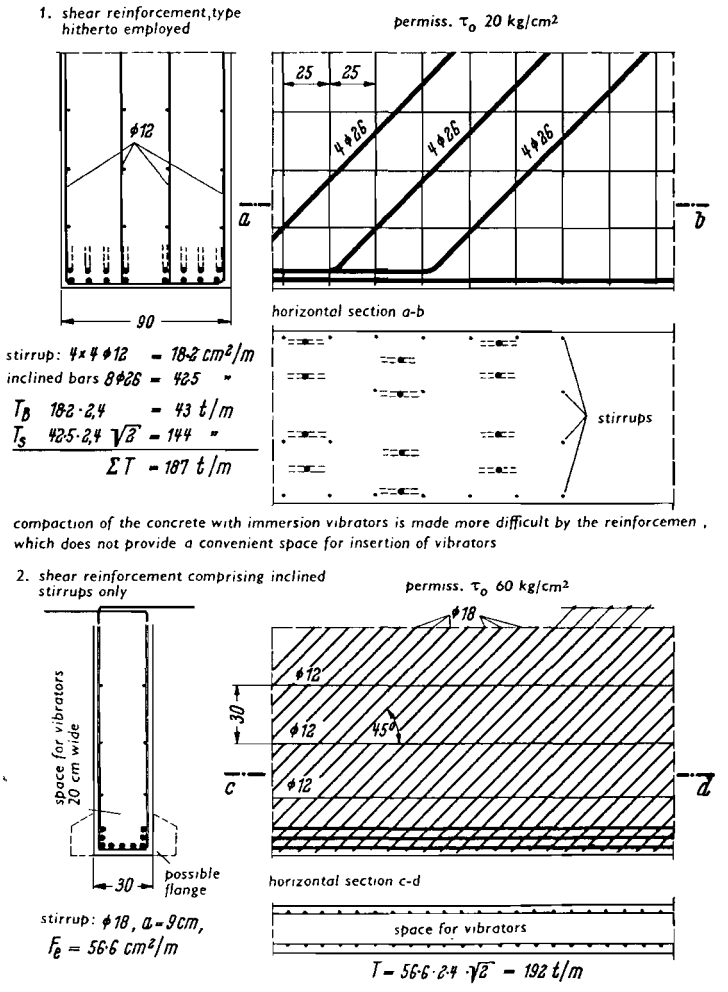

Figure 26: Comparison of two diaphragm walls for equal shear strength.

If we choose stirrup reinforcement consisting of four leg stirrups of 12 mm diameter spaced 25 cm apart, then it will be necessary to bend up eight 26 mm bars or add this amount of inclined bars (Figure 26). Usually these inclined bars cannot be disposed regularly one above the other and they constitute a serious hindrance to concreting.

Now let us design the same wall, with the same loading, for τ_o = 60 kg/cm². In that case the width becomes 30 cm. For this high value of τ_o the reinforcement must be installed in the direction of the tensile forces, i.e. we must use inclined stirrups. For this purpose we shall use two-leg stirrups of 18 mm diameter at 9 cm centres. These should preferably be laced with horizontal bars. The bottom longitudinal reinforcement consists of straight bars only. If need be, these can be distributed over a greater width by giving the beam a bottom flange. This shear reinforcement, which consists only of two "trellis" systems spaced a convenient distance apart and which comprises bars which are all equal, is undoubtedly easier to install than the four-leg stirrups and bent-up main bars. The quantity of reinforcement is the same as in the previous design, but the concrete quantity is reduced to a third. The concrete can be suitably placed and compacted with immersion vibrators. The high permissible values of τ_o - sensibly employed - in combination with closely spaced stirrup

reinforcement therefore lead to technically simpler and more convenient solutions than were provided by the earlier design methods. An important point to consider is the more favourable cracking behaviour that is obtained when the requisite reinforcement has smaller concrete sections to cope with. In addition, the smaller concrete dimensions give more favourable conditions with regard to stresses induced by temperature and shrinkage deformations.

The increased permissible values of τ_o are also of importance in the design of long-span box girders which are subjected also to torsion, so that the shear stresses arising from two different conditions of functioning are added together. There is now doubt that the laws governing that case are the same as those which have emerged from the present beam tests.

Concluding remarks on the tests I.1

The shear tests on the large beams subjected to high shear stresses were financed by the Ludwig Bauer Foundation of the firm of Ludwig Bauer, Stuttgart, by research funds made available by the Ministry for Economic Affairs of Baden-Wurtemberg, and by the German Committee on Reinforced Concrete (Deutscher Ausschuss für Stahlbeton). The tests were carried out in Prof. Dr-Ing. G. Weil's department at the Otto Graf Institute. The arrangement and interpretation of the tests were undertaken by the present authors in collaboration with Dipl.-Ing. W. Dilger. A number of co-workers associated with the Chair of Concrete Engineering gave their assistance in performing the measurements. We wish to express our indebtedness to all those who participated in the tests.

2. Influence of the moment-shear ratio upon the shear strength of rectangular beams, without shear reinforcement, subjected to concentrated loading and uniformly distributed loading

2.1 TEST ARRANGEMENT, TEST SPECIMENS AND LOADING

2.11 Arrangement

The influence of the moment-shear ratio M/Qh, which is an important criterion for shear strength (load-carrying capacity with regard to shear), was investigated for concentrated loads and uniformly distributed loads on rectangular beams which all had the same cross-sectional dimensions (19 x 32 cm) and were provided with longitudinal reinforcement consisting of two ribbed Tor steel bars of 26 mm diameter, steel IIIb. In order to obviate anchorage failure, amply projecting beam ends containing stirrups were provided, but no shear reinforcement was installed in the actual span of the beam.

In the beams subjected to concentrated loads the ratio M/Qh was varied by adopting different values for the distance from the bearings to the two symmetrically placed points of load application (Figure 27). In that case M/Qh is equal to the so-called shear span a/h. The distance a' between the two concentrated loads was quite small and was equal for all the beams. Thus, beams varying in span length and in slenderness were obtained. It must be emphasized, however, that with this type of loading (apart from the dead load) the spacing of the two loads, and therefore the slenderness of the beam, has no effect on the shear strength. The left-hand load-spreading plate, measuring 7.5 x 19 cm, was narrower than the right-hand one, which measured 13 x 19 cm, in order to ascertain whether differences in local bearing pressure under the loads have any effect.

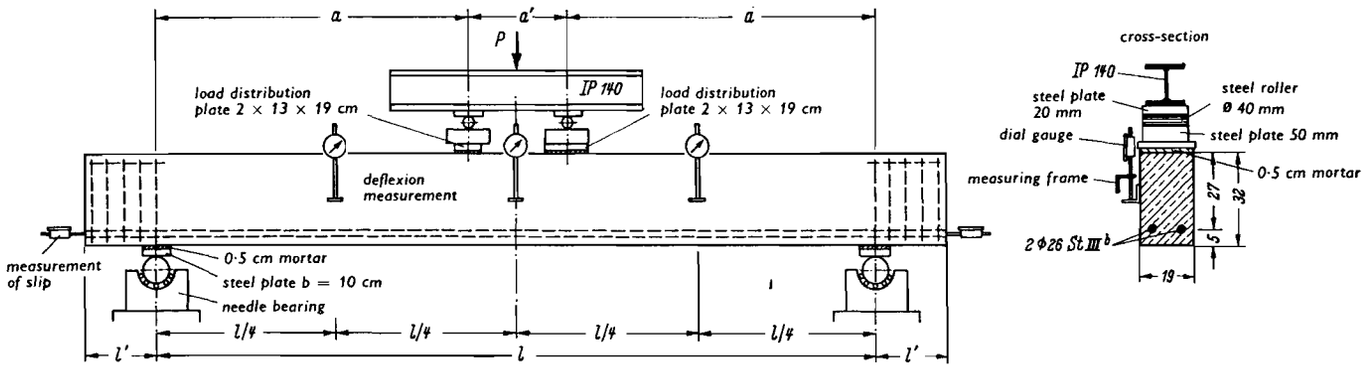

Figure 27: Tests on rectangular beams with concentrated loads.

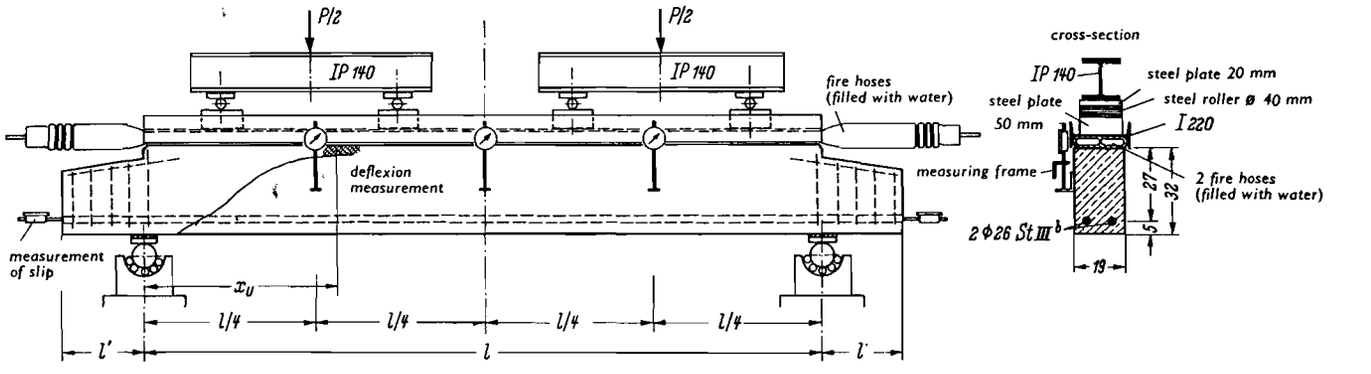

Figure 28: Tests on rectangular beams with uniformly distributed loading.

With uniformly distributed loading, the span length was simply altered. The loading was uniformly distributed over the entire beam surface by means of water-filled fire-hoses which were laterally held by means of a rolled steel joist. By this method, disturbing effects due to local high pressures or pressure differences were obviated (Figure 28). The hoses had a high degree of shear deformability in the longitudinal direction, so that the steel joist did not co-operate longitudinally in compression. To terminate the loaded area over the supports, a step was formed at the top of the beam over each bearing.

Most of the beams were manufactured in two identical specimens or the beam was "bandaged" on the fractured side and was then loaded to failure on the other side also.

2.12 Data on the test specimens

The material properties and the precise dimensions of the specimens and their age at testing are stated in Tables IV and V. The concrete had a high content of sand (60 % aggregate between 0 and 7 mm) with a cement content of 290 kg per m^3 of concrete (Portland cement PZ 475) and a water/cement ratio of 0·68. The beams were stored under moist conditions and were tested without having time to dry. This was done in order to eliminate shrinkage effects.

TABLE IV: Tests on rectangular beams with two concentrated loads.

1	2	3	4	5	6	7	8	9	10	11	12	13	14	15	16	17	18	19	20	21	22
										Failure				Conversion of the test results to the reference strength β_w = 350 kg/cm² and determination of averages in the case of duplicated tests							
Designation	l	a	a'	h	b	μ	β_w	$\frac{M}{Q\,h} = \frac{a}{h}$	Flexural cracking moments M_R (1)	P_U	Q_U (1)	τ_o (1)	M_{SU} (1)	Reduction (3) coefficient	P_U	M_{SU} (1)	Q_U (1)	τ_o (1)	s (4)	Type of failure (5)	Remarks
	(m)	(m)	(m)	(cm)	(cm)	(%)	(kg/cm²)		(tm)	(t)		(kg/cm²)	(tm)		(t)	(tm)	(t)	(kg/cm²)			
1	0·90	0·27	0·36	27	19	2·07	355	1·0	1·78	79·2	39·60	94·2	10·75	1·00	79·2	10·75	39·60	94·2	3·01	S	
2	1·15	0·40	0·35	27	19	2·07	355	1·5	2·50	53·0	26·50	62·8	10·60	1·00	53·0	10·60	26·50	62·8	2·96	S	
3	1·45	0·54	0·37	27	19	2·07	355	2·0	1·88	30·0	15·00	35·5	8·10	1·00	30·0	8·10	15·00	35·5	2·26	S	
4	1·70	0·67	0·36	27	19	2·07	355	2·5	2·48	l: 16·4 (2) r: 17·5	8·32 8·87	19·8 21·0	5·58 5·90	1·00	16·95	5·74	8·59	20·3	1·60	S	
5	1·95	0·81	0·33	27	19	2·07	355	3·0	2·18	l: 12·0 (2) r: 15·3	6·15 7·80	14·6 18·6	4·93 6·27	1·00	13·65	5·55	6·98	16·5	1·56	S	
6	2·35	1·10	0·35	27	19	2·07	355	4·0	2·44	l: 12·0 (2) r: 13·5	6·20 6·95	14·7 16·4	6·72 7·42	1·00	12·75	7·07	6·58	15·6	1·98	S	
7-1	3·10	1·35	0·40	27·8	19	2·01	372	5·0	1·55	12·2	6·35	14·8	8·42	0·92	11·80	8·08	6·11	14·5	2·26	S	Sudden failure
7-2	3·10	1·35	0·40	27·8	19	2·01	372	5·0	1·48	13·4	6·95	16·0	9·22								
8-1	3·60	1·62	0·36	27·8	19	2·01	373	6·0	1·57	12·8	6·70	15·4	10·61	0·93	11·90	9·86	6·24	14·8	2·77	S	Sudden failure
8-2	3·60	1·62	0·36	27·4	19	2·04	373	6·0	1·40	12·8	6·70	15·5	10·61								
9-1	5·80	1·89	2·02	27·3	19	2·04	382	7·0	2·16	11·1	6·00	14·0	11·14	0·94	10·50	10·48	5·64	13·4	2·94	B	
9-2	5·80	1·89	2·02	27·3	19	2·04	394	7·0	1·88	11·1	6·00	14·0	11·14								
10-1	4·70	2·16	0·40	27·2	19	2·05	361	8·0	2·17	9·6	5·15	12·1	10·79	0·97	9·75	11·00	5·22	12·4	3·08	B	
10-2	4·70	2·16	0·40	27·2	19	2·05	361	8·0	2·06	10·5	5·60	13·2	11·76								

(1) Self-weight of beam taken as 0·15 t/m.

(2) Beam bandaged on one side after occurrence of shear failure and further loaded to failure on other side.

(3) The reduction coefficient takes account of the excessive concrete strength and the deviations in the depth.

(4) s = shear failure load divided by permissible working load (bending).

(5) S = shear failure; B = flexural failure.

TABLE V: Tests on rectangular beams with uniformly distributed loading.

1	2	3	4	5	6	7	8	9	10	11	12	13	14	15	16	17	18	19	20	21	22	23	24	25	26	27	28	29	30
									Failure										Conversion of the test results to the reference strength β_w = 350 kg/cm² and determination of averages in the case of duplicated tests.										
														At failure section τ_o (2)															
Designation	l (m)	h (cm)	b (cm)	$\frac{l}{h}$	μ (%)	β_w (kg/cm²)	p (1) (t)	Cracking moment M_R (2) (t/m)	P_U (t)	p_U (2) (t/m)	Q_U (2) (t)	τ_o (2) x = 0 (kg/cm²)	M_U (2) x = l/2 (tm)	x_u (cm)	$\frac{M}{Q\,h}$	M_{SU} (tm)	$Q_{x'u}$ (t)	τ_o x = x_U (kg/cm²)	Reduction coefficient (3)	P_U (2) (t/m)	M_{SU} (2) x = x_U (tm)	Q_U (2) x = x_u (t)	Q_U (2) x = 0 (t)	τ_o (2) x = 0 (kg/cm²)	τ_o (2) x = h/2 (kg/cm²)	M (2) x = l/2 (tm)	s (4)	Type of failure (5)	Remarks
11/1	1·50	29·0	19·0	5·17	1·87	418	0·5	1·41	54·6	36·73	27·55	60·6	10·34	60	6·21	9·91	5·51	12·1	0·80	30·65	8·35	3·80	22·95	54·4	44·6	8·62	2·42	S	
11/2	1·50	29·6	19·0	5·06	1·88	418	0·5	1·30	59·1	39·75	29·80	64·0	11·18	65	9·33	10·98	3·98	8·6										S	
12/1	2·00	27·3	19·0	7·32	2·04	403	0·5	1·13	40·0	20·25	20·25	46·5	10·12	67	4·94	9·03	6·69	15·6	0·94	17·00	7·79	4·75	17·00	40·3	34·8	8·50	2·38	S	
12/2	2·00	27·2	18·9	7·35	2·06	403	0·5	1·38	31·6	16·05	16·05	37·7	8·03	77	7·57	7·60	3·69	8·7										S	
13/1	2·50	27·3	19·0	9·15	2·04	409	0·8	1·19	27·0	11·12	13·90	32·5	8·69	90	7·55	8·03	3·90	9·1	0·93	10·35	7·24	4·14	12·93	30·6	27·3	8·10	2·26	S	
13/2	2·50	27·2	18·9	9·18	2·06	409	0·8	-	27·0	11·12	13·90	32·6	8·69	80	5·55	7·56	5·00	11·7										S	
14/1	3·00	27·3	19·0	11·00	2·04	397	0·9	1·91	20·5	7·13	10·70	25·0	8·02	95	6·49	6·95	3·92	9·1	0·94	6·74	6·47	3·88	10·10	23·9	21·8	7·58	2·12	S	
14/2	3·00	27·3	19·0	11·00	2·04	397	0·9	1·91	20·6	7·16	10·75	25·1	8·06	90	5·77	6·77	4·30	10·0										S	
15/1	4·00	27·2	19·0	14·71	2·05	420	1·1	2·85	18·0	4·77	9·55	22·5	9·55	85	4·28	6·39	5·49	12·9	0·92	4·52	6·43	4·85	9·04	21·4	20·0	9·04	2·54	S	Sudden failure
15/2	4·00	27·3	18·9	14·65	2·05	420	1·1	1·95	19·2	5·08	10·15	23·8	10·16	100	5·50	7·62	5·08	11·9										S	
16/1	5·00	27·3	19·0	18·32	2·04	414	1·25	2·60	18·0	3·85	9·63	22·6	12·04	85	3·92	6·78	6·35	14·9	0·93	3·55	6·26	5·85	8·87	21·0	19·9	10·95	3·07	S	
16/2	5·00	27·4	18·9	18·25	2·05	414	1·25	1·91	18·0	3·83	9·58	22·5	11·97	85	3·90	6·75	6·32	14·8										S	
17/1	6·00	27·3	18·9	22·00	2·05	389	1·4	2·18	16·1	2·92	8·75	20·6	13·12	l/2					0·95	2·77	5·25	6·30	8·31	19·7	18·8	12·49	3·50	B	Sudden failure
17/2	6·00	27·4	18·9	21·90	2·04	389	1·4	1·40	16·0	2·90	8·70	20·5	13·05	72	3·04	5·51	6·62	15·5										S	

(1) Self-weight of beams + weight of loading device.

(2) Self-weight + loading device included.

(3) The reduction coefficient takes account of the excessive concrete strength and the deviations in the depth.

(4) s = shear failure load divided by permissible working load (bending).

(5) S = shear failure; B = flexural failure.

2.13 Duration of loading

The beams were loaded in incremental stages of about 1/10 of the anticipated ultimate load. At the end of each stage, which lasted only about 30 min, the beam was briefly unloaded and then reloaded up to the next stage. On an average, it took only six hours to produce failure, i.e. these were short-term tests. The rate of load application was approximately 5 tons per minute.

2.2 MEASUREMENTS

In these tests, interest centred chiefly upon the ultimate load and the fracture pattern obtained. For this reason the time-consuming operations of measuring the crack widths were omitted, the pattern of cracking merely being noted at each stage. The deflexions were measured at mid-span and at various intermediate points, depending on the length of the beam concerned.

2.3 TEST RESULTS

2.31 Type of failure and location of failure section

2.311 Concentrated loads. The series of photographs in Figure 29 shows the various cracking patterns obtained at failure due to concentrated loads. In the case of the shortest beam (beam 1) the shear fracture is steeply sloped because there the stress components σ_y between the load and the bearing (i.e. in the zones of transmission of force into the concrete) cause the principal tensile stress to be inclined at a flatter angle than 45°. In beams 2 and 3 the shear crack resulting in failure extended under the load into the zone of pure bending because the flexural compressive strength directly under the load is increased by the pressure exerted by the load. Although the concrete was destroyed in the zone of pure bending, the failure was produced by shear, inasmuch as the depth of the flexural compressive zone was reduced much more by the shear crack than by the flexural cracks.

In beams 1 to 5 the shear cracks outside the flexural cracks did not develop until a relatively high load was attained. In beams 5 to 8 the shear cracks in some cases developed from flexural cracks and in some cases they developed independently, running obliquely above flexural cracks that had already formed. In the upper part of the beam they have a very flat slope because, in slender beams, the struts of the "truss" slope very little and the cracks can develop only under these struts.

When the shear crack opens out a higher load, a portion of the shear force is transmitted to the bottom reinforcing bars, with the result that the concrete along or under this reinforcement spalls off as far as the bearing. This effect is intensified at the instant of failure.

The failure section is always located close to the point of load application, where M/Qh attains its maximum. For $M/Qh \geq 7$ the two beam pairs 9 and 10 failed in bending, owing to crushing of the concrete before the yield point was reached in the reinforcement. For these beams the limit of M/Qh, below which shear failure can be expected to occur, had therefore been reached.

In the case of beams 1 - 6 the critical cracks slowly went on spreading under successive increments of load until the compressive zone was destroyed. On the other hand, beams 7 and 8 failed suddenly and violently as a result of the sudden occurrence of a flatly sloped shear crack. Slender beams without shear reinforcement, which are subjected to concentrated loads acting

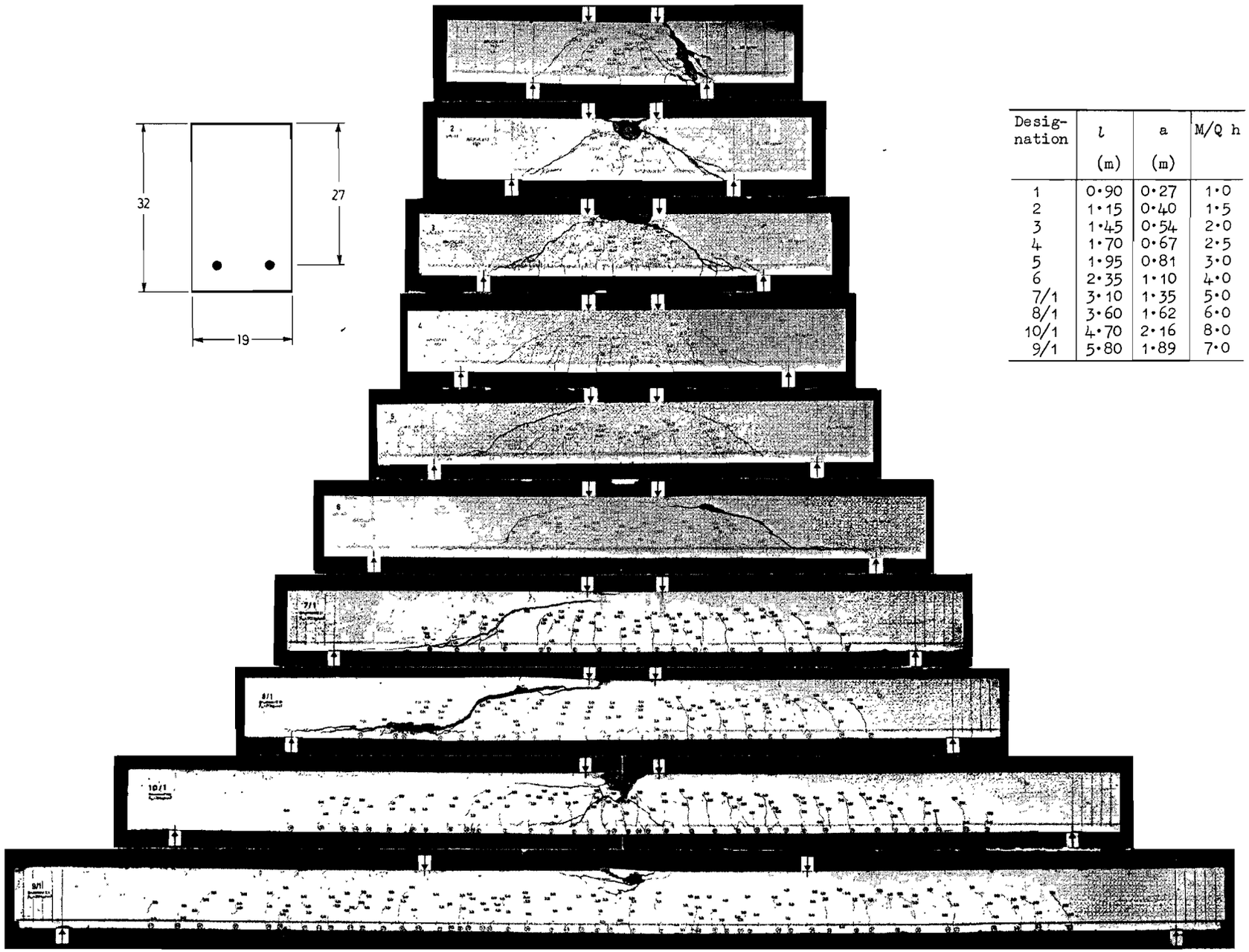

Designation	l (m)	a (m)	M/Q h
1	0·90	0·27	1·0
2	1·15	0·40	1·5
3	1·45	0·54	2·0
4	1·70	0·67	2·5
5	1·95	0·81	3·0
6	2·35	1·10	4·0
7/1	3·10	1·35	5·0
8/1	3·60	1·62	6·0
10/1	4·70	2·16	8·0
9/1	5·80	1·89	7·0

Figure 29: Cracking and fracture patterns of the beams subjected to concentrated loads. (The figures indicate the load in tons at which a crack had penetrated as far as the point indicated. Beams 4 and 6 were "bandaged" on the damaged side after failure had occurred and were then loaded further until failure occurred on the other side also.)

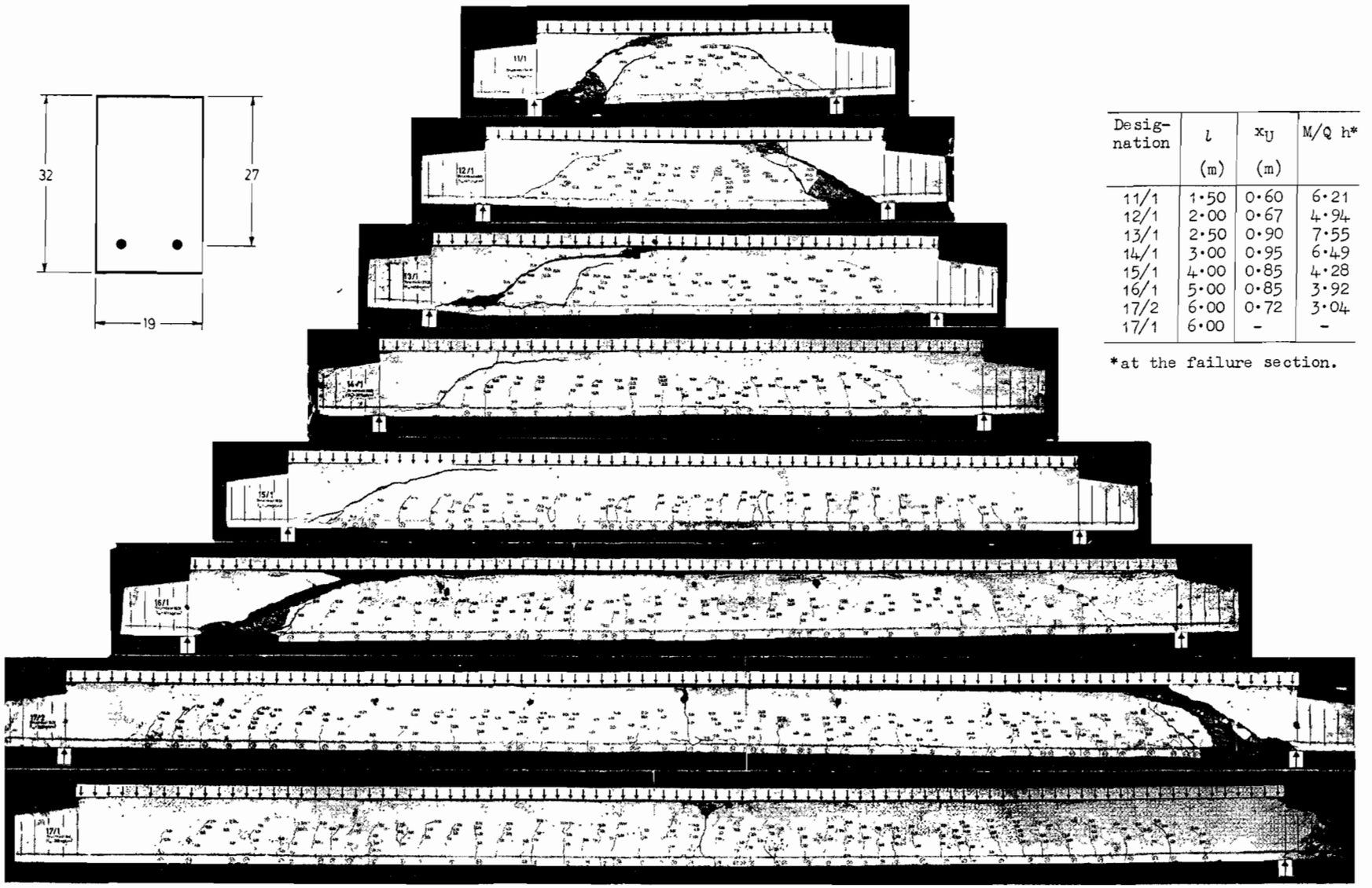

Designation	l (m)	x_U (m)	M/Q h*
11/1	1·50	0·60	6·21
12/1	2·00	0·67	4·94
13/1	2·50	0·90	7·55
14/1	3·00	0·95	6·49
15/1	4·00	0·85	4·28
16/1	5·00	0·85	3·92
17/2	6·00	0·72	3·04
17/1	6·00	-	-

*at the failure section.

Figure 30: Cracking and fracture patterns of the beams subject to uniformly distributed loading. (The figures indicate the load in tons at which a crack had penetrated as far as the point indicated. The encircled figures at the beam soffits indicate the sequence in which the cracks occurred.)

far away from the bearings, therefore behave more unfavourably than such beams with loads acting close to the bearings or than stout beams. We shall see in due course that, on the other hand, slender beams require less shear reinforcement to obviate failure than stout beams do. In the latter the ratio of ultimate shear load to ultimate flexural load, in the absence of shear reinforcement, is lower than in slender beams.

In these tests no effect of the difference in width between the two load-spreading plates (7·5 cm as compared with 13 cm) on the cracking and failure behaviour was detected.

2.312 Uniformly distributed loading. The series of photographs in Figure 30 shows the various cracking patterns at failure due to uniformly distributed loading. Here the critical cracks occur close to the bearing zone and, depending upon the slenderness of the beam concerned, extend for varying distances into the span. They rise to a considerable height * and thus have a substantially greater effect than the flexural cracks in reducing the depth of the compressive zone — i.e. for shear cracks the neutral axis depth x must be calculated from deformation assumptions different from those applicable to predominantly flexural conditions. In general, failure occurred when the compressive zone, reduced in height by the shear cracks, failed.

In the case of the beams with a span length of 6 m (slenderness l/d approximately 20), shear failure occurred in the first and flexural failure occurred in the second beam. Hence, for the conditions adopted, the limit between shear failure and flexural failure under uniformly distributed loading had been reached at this span of 6 m. In Figure 31 the position of the failure section in the compression flange had been plotted for various spans: it is situated at a distance of between 2 h and 3·5 h from the bearing. The following approximate value was determined provisionally:

$$\text{crit. } M/Qh = 9 - 0{\cdot}27\, l/h$$

We shall revert to this value later.

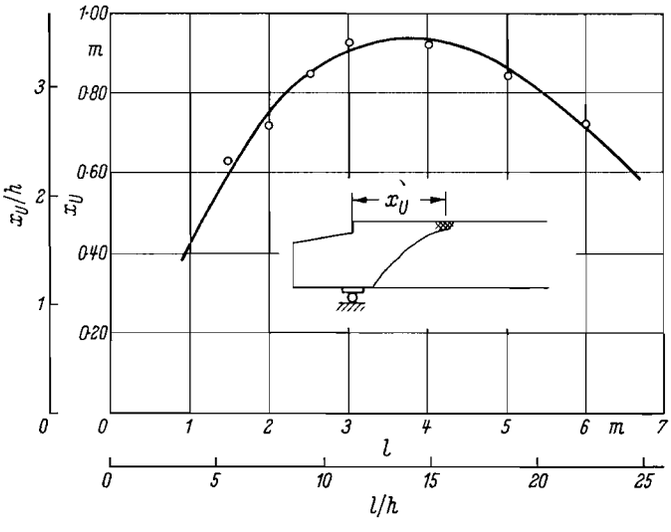

Figure 31: Beam with uniformly distributed loading. Position of the failure section x_U plotted against span l or slenderness ratio l/h.

* The fact that shear cracks rise higher than flexural cracks has been described by E. Mörsch in his book "Der Einsenbeton", Vol. I, Part 2. 6th edition. p. 7. on the basis of the numerous tests of the German Committee on Reinforced Concrete.

2.32 Anchorage -- slip

In none of the tests was it possible to detect any measurable slip at the ends of the reinforcing bars. Only in the case of the very short beams 11/1 and 11/2 was an average displacement of 0·18 mm in relation to the end of the beam, but this is to be regarded as a result and not a cause of failure.

2.33 The shear strength and the shear stress τ_o

The ultimate strengths of the beams are given in Tables IV and V. In columns 15 - 20 and 20 - 27 the measured ultimate loads and the stress resultants calculated from them have been converted to the "standard" concrete strength $\beta_w = 350$ kg/cm^2 and averaged in order to make them comparable with one another.

It follows from these results that the shear attained at shear failure is anything but constant. On the contrary, Q_U varies between the wide limits 5·22 - 39·60 tons, and τ_o correspondingly varies from 12·4 to 94·2 kg/cm^2. The values of the shear failure moment M_{SU} (moment at upper end of shear crack, at point with abscissa x_U) are not equal either, although they do not vary so greatly as the values of Q_U. If we leave the very short beams with $a/h \leq 1{\cdot}5$ out of account because in those beams the favourable effect of σ_y (due to the transmission of vertical forces into the concrete) would lead us to expect a higher τ_o, the values of τ_o are found to be within the limits 12·4 - 54·4 kg/cm^2. The favourable effect of the formation of an "arch" or "truss" with "tie-rod" extends up to the slenderness ratios 8 - 10; it is only above these ratios that the values of τ_o approximately become uniformly low.

2.331 Concentrated loads. These differences are particularly pronounced for concentrated loads. The shear forces, and therefore the shear stresses τ_o, are largest for stout beams and rapidly decrease with increasing slenderness. From $M/Qh = 4$ onwards Q_U is approximately constant and corresponds to $\tau_o = 14$ kg/cm^2 (state II) or 14·8 kg/cm^2 (state I). These values are still considerably below the tensile strength of the concrete, which can be taken as being around 30 kg/cm^2. Even for beams without shear reinforcement, therefore, there is no direct relationship between the calculated values of τ_o attained at shear failure and the tensile strength of the concrete.

In other tests, which will be reported later, it was established that the values of τ_o calculated for the ultimate load were also dependent upon the cross-sectional shape, the absolute size of the cross-section, the degree of reinforcement and the quality of the bond. Because of the many influencing factors involved, it is therefore very difficult to determine the actual principal tensile stresses and their direction.

In ultimate-load analysis methods for shear failure the shear failure moments M_{SU} are generally considered. These have been plotted against M/Qh in Figure 32. The high values associated with short load distance or short beams are due to the "truss" action and the favourable effect on the strength of the flexural compressive zone exercised by σ_y under the load. The minimum of the shear failure moments is situated between $M/Qh = 2{\cdot}5$ and 3. With increasing M/Qh the moments M_{SU} increase steadily until the flexural failure moment is attained at $M/Qh > 6$ and becomes decisive. The shear force that can be resisted is no longer perceptibly affected by the bending moment from values of $M/Qh = 4$ onwards.

that the "arch" loses its bearing. A few shear bars close to the bearing should suffice to obviate these sudden and therefore dangerous shear cracks at such low values of the shear stress.

As is well known, the tied arch is sensitive to half-span loading, and in those circumstances even lower values of τ_o are liable to be associated with failure. Tests relating to this aspect have not yet been carried out, however.

It is noteworthy that the lower values of τ_o for uniformly distributed loading are about 40 % higher than those for concentrated loads. This difference is in part attributable to the influence of the bending moment: with concentrated loads, shear failure occurs in the vicinity of the point of load application, i.e. in the region where large moments are produced in the beam; on the other hand, with distributed loading the failure section is near the bearing, i.e. at low values of the bending moment. In addition, the constant stress σ_y under the distributed load has a favourable effect on the compressive strength of the concrete at the compression face of the beam.

The mutual effect of bending moment and shear is also apparent from Figure 34, where these two quantities at the failure section have been plotted against the moment-shear ratio. Low values of M are associated with high values of Q, and vice versa: the moments exhibit an approximately linear increase with M/Qh, whereas the shear forces decrease in approximately the same ratio. As distinct from the beams subjected to symmetrically applied concentrated loads, the critical values of M/Qh in the case under present consideration were not predetermined by the load positions but had to be subsequently determined from the distance x_U to the failure section. Because of the extent of the crushed compressive zone, this gave rise to a certain amount of scatter in the results obtained.

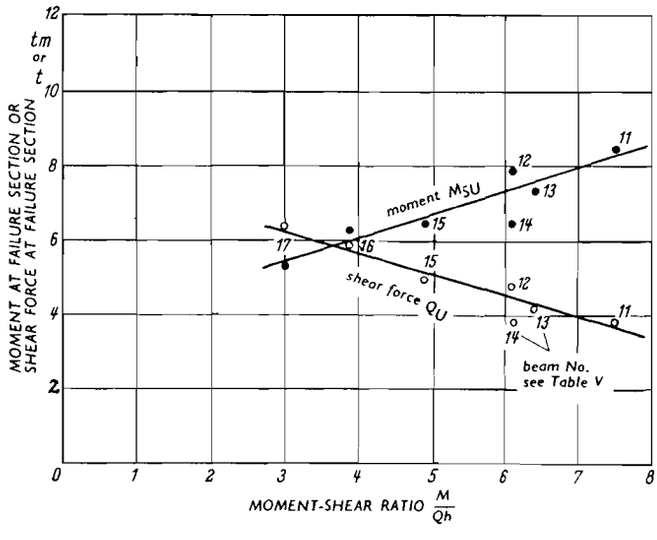

Figure 34: Beam with uniformly distributed loading. Moment and shear force at failure section, plotted against M/Qh.

2.34 Shear cracking load

The question arises as to whether the shear cracking load is essentially governed by τ_o (or the oblique principal tensile stresses in state I) or whether the bending moment also affects it. It is, of course, difficult to

ascertain the shear cracking load quite definitely, since the shear cracks often only develop gradually from flexural cracks. We shall therefore arbitrarily define it as that load (and the stress τ_o associated with it) at which the main shear crack has extended half-way up the effective depth of the beam. These stresses $\tau_{o(crack)}$ are found to vary between wide limits. For example, in the case of the slender beams 7 and 8 subjected to concentrated loads they are of the order of 10 kg/cm^2, whereas they increase to 27 kg/cm^2 in the stouter beams.

Hence it must be inferred that shear cracking is also affected by the magnitude of the bending moment and therefore by the steel strain that occurs in the cracked section. This is also apparent from the order of magnitude of $\tau_{o(crack)}$: the tensile strength of the concrete is approximately 30 kg/cm^2, which is considerably more than the minimum values of 9 kg/cm^2 as determined for $\tau_{o(crack)}$ in these tests. Indeed, in state II (cracked state) the principal stresses cannot be calculated without taking the deformation into consideration.

2.35 Safety obtained

2.351 Safety related to the permissible flexural load according to DIN 1045. In Tables IV and V the values of the quotient:

$$s = \frac{\text{shear failure load}}{\text{permiss. working load (flexural, according to DIN 1045)}}$$

have also been included. In arriving at these values the actual concrete strength has been taken into account in the denominator. The lowest value occurs in beam 5 (subjected to concentrated loads and with M/Qh = 3), namely s = 1·56, which is therefore far below the value 3 which has hitherto been required in short-term tests and which approximately corresponds to the factor of about 2·9 available with respect to bending (cf. beams 9 and 10). *

From the summarized results it also appears that for uniformly distributed loading the flexural failure moments are, on an average, 15 % higher than for concentrated loads, because with the former type of loading the flexural compressive zone is restrained and strengthened by the vertical pressure exerted by the loading. Besides, in the case of two concentrated loads, the maximum bending moment extends over a greater distance than it does in the case of distributed loading, so that the likelihood of max.M_B coinciding with a local flaw is greater with concentrated loads.

With ultimate-load design, however, it is not permissible to take advantage of the favourable effect of the distributed loading, inasmuch as such loading in this "pure" form is hardly likely to occur in actual practice.

2.352 Safety related to permissible τ_o according to DIN 1045. According to DIN 1045 the highest permissible value of τ_o for beams of concrete B 300 is 8 kg/cm^2 if no special check for shear reinforcement is made; for concrete B 350 the corresponding value for permiss. τ_o is 8·3 kg/cm^2. To ensure a factor of safety of 3, no value of τ_o must therefore exceed 24·9 kg/cm^2 at failure. In the case of concentrated loads, from M/Qh ≥ 2·5 onwards, we

* Latterly the adoption of ν = 2·1 for sudden failure (i.e. without previous warning) is being considered, but subject to adopting only 0·7β_p as the strength of the concrete in the calculations, so that for tests the requirement would still be approximately s = 2·1:0·7 = 3.

have lower values down to 12·4 kg/cm^2; and in the case of uniformly distributed loading, from $l/h \geq 10$ onwards, we have values down to 19·7 kg/cm^2. Especially for concentrated loads, therefore, the rule regarding permissible τ_o, as laid down in DIN 1045, fails to ensure that the requisite safety is obtained.

For $M/Qh < 2$ or (for uniformly distributed loading) for $l/h < 8$ - i.e. in the case of so-called "stout" beams or loads situated close to the bearings - a safe range clearly manifests itself. For this range the permissible value of τ_o can be increased without checking the shear reinforcement, whereas above these limits the permissible value of τ_o should be reduced until reliable means of analysis for shear failure become available. These stout beams are, however, substantially longer than the sum of the St. Venant regions where force transmission into the beam occurs and where τ_o also theoretically becomes smaller.

2.36 Deflexions

The load-deflexion diagrams exhibit lower values in the lower stages of loading than was theoretically to be expected (e.g. according to reference 13). In the upper loading stages they exceed the values calculated from bending alone - more particularly in the case of short beams - because considerable shear deformations additionally occur, which shortly before failure may attain the magnitude of the flexural deformations. The shear deformations, however, do not assert their influence until loads in excess of the working load are reached. Figure 35 shows some typical load-deflexion curves (beams 3, 5, 7/1 and 10/1).

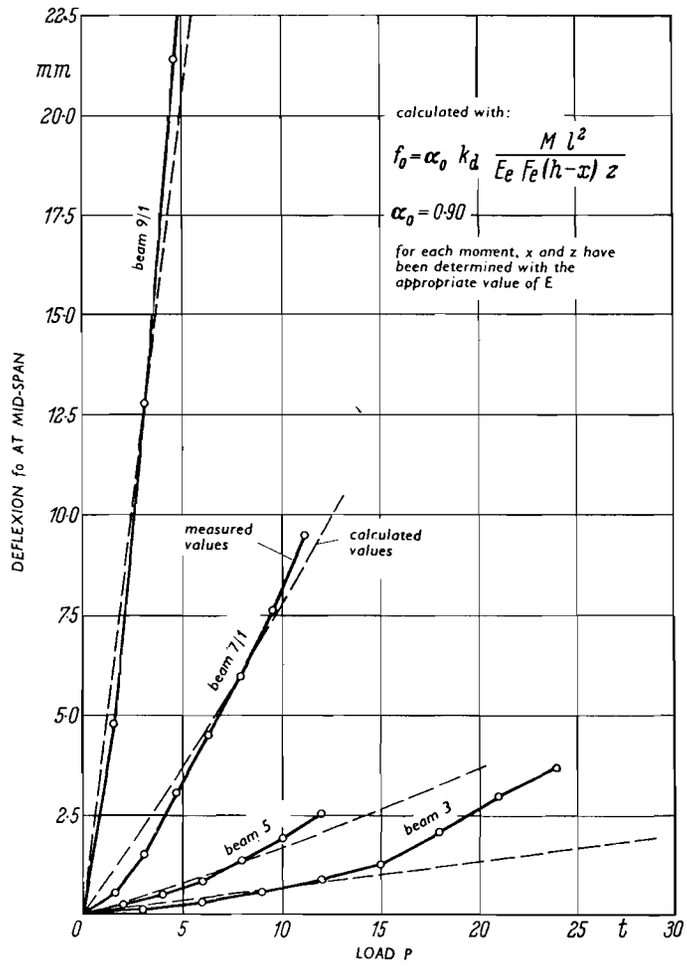

Figure 35: Deflexion at mid-span for characteristic beams with concentrated loads. Comparison of calculated values (according to reference 13) with measured values.

3. The effect of the bond of the longitudinal reinforcement upon the shear strength of rectangular beams without shear reinforcement

3.1 TEST ARRANGEMENT, TEST SPECIMENS AND LOADING

In eight beams - which were all identical in respect of span, cross-section, concrete strength β_w (cube strength) and degree of reinforcement μ - only the quality of the bond of the longitudinal reinforcement and the nature of the loading were varied. The beams were not provided with shear reinforcement, but their ends did project a considerable distance beyond the bearings in order to obviate failure due to defective bar anchorage. The anchorage zone had no stirrup reinforcement, however.

The bond quality was varied, on the one hand, by varying the number and diameter of the bars and, on the other hand, by varying the surface condition of the bars. We know that the bond is better according as the bars are thinner because of the higher ratio of perimetral surface area to cross-sectional area. Accordingly, the beams designated by the figure 1 were each provided with a small number of thick bars (e.g. two bars of 25 mm diameter), referred to as "concentrated" reinforcement, whereas the beams designated by the figure 2 were each provided with a larger number of thin bars (e.g. two bars of 14 mm plus three bars of 16 mm diameter), referred to as "distributed" reinforcement, (see Table VI).

The beams with the designation A contained bars with a ribbed surface pattern (ribbed Tor steel IIIb). On the other hand, the beams with the designation B were reinforced with smooth round bars with a brightly polished surface (grade St 37 K steel as used in mechanical engineering) (see Figure 36).

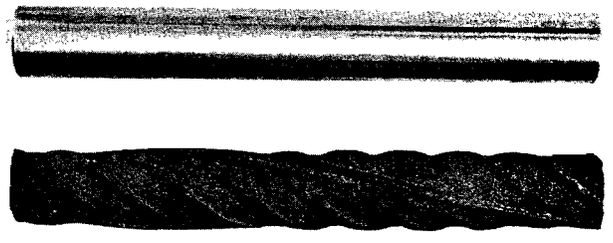

Figure 36: Surface condition of the reinforcing bars employed: ribbed Tor steel St IIIb and bright drawn engineering steel St 37 K.

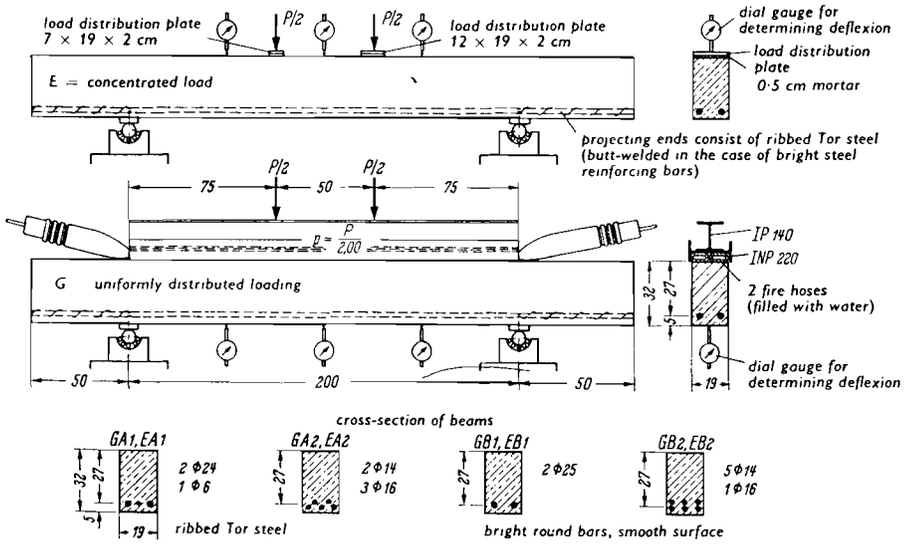

Figure 37: Test arrangement and dimensions of beams with varying bond of longitudinal reinforcement.

TABLE VI: Results of beam tests with varying conditions of bond.

1	2	3	4	5	6	7	8	9	10	11	12	13	14
	Designation	Grade of steel	Steel: No. of bars and diameter Ø in mm	Equivalent diameter(1)	μ	Concrete β_w	M_{crack} (bending)	Failure					Cause of failure*
								P_U	x_U	M_{SU}	τ_o max	σ_e	
				(mm)	(%)	(kg/cm²)	(tm)	(t)	(m)	(tm)	(kg/cm²)	(kg/cm²)	
Concentrated loads	EA 1	Ribbed Tor steel	2 Ø 24+1 Ø 6	22·1	1·89	251	1·74	11·9	0·75	4·46	14·0	2020	S
	EA 2		2 Ø 14+3 Ø 16	15·1	1·88	251	2·21	15·2	0·75	5·70	17·9	2590	S
	EB 1	Bright steel bar St 37 K	2 Ø 25	25·0	1·91	251	1·63	23·1	-	-	27·2	4080	B
	EB 2		5 Ø 14+1 Ø 16	14·4	1·88	251	1·40	20·2	0·75	7·58	23·8	3460	S
Uniformly distributed loading	GA 1	Ribbed Tor steel	2 Ø 24+1 Ø 6	22·1	1·89	253	1·40	25·0	0·67	5·57	29·5	2860	S
	GA 2		2 Ø 14+3 Ø 16	15·1	1·88	253	2·17	29·6	0·72	6·83	34·9	3450	S
	GB 1	Bright steel bar St 37 K	2 Ø 25	25·0	1·91	253	1·44	34·4	-	-	40·5	4010	B
	GB 2		5 Ø 14+1 Ø 16	14·4	1·88	253	1·47	38·8	-	-	45·8	4590	B

(1) Equivalent diameter: $\emptyset_A = \Sigma\emptyset^2/\Sigma\emptyset$ where Ø is the diameter in mm

* S = shear; B = flexural

To ensure proper anchorage of these smooth bars, lengths of ribbed bar were butt-welded to their ends.

Half the beams were loaded with two concentrated loads, as shown in Figure 37. Here again, load-spreading plates of different widths were used. These beams were designated by the letter E. For these beams the moment-shear ratio M/Qh was 2·78 and is therefore in the range particularly susceptible to shear. The other beams were tested with uniformly distributed loading and were given the designation G.

The data relating to the test specimens are summarized in Table VI, columns 1 - 7.

The four beams of each test series were cast simultaneously in steel moulds in order to obviate differences in concrete strength as far as possible. During concreting, the reinforcement was at the bottom of the mould. The concrete was compacted with internal vibrators. The specimens were stored for seven days under moist cloths and were then kept in the laboratory at about 60 % relative humidity. They were tested at an age of 28 - 30 days. By this means, it was possible to obtain similar shrinkage effects in the various specimens.

The concrete was of ordinary composition, containing 251 kg of Portland cement (PZ 375) per m^3, and had a water/cement ratio of 0·75.

The strengths, which were determined on 24 cubes and 24 prisms in all, exhibited a small amount of scatter. On the day of testing the average cube strength β_w was 252 kg/cm^2 (maximum 269 and minimum 231 kg/cm^2). The average flexural strength β_{bZ} was 41·4 kg/cm^2.

In the steel stress range associated with the shear failure the stress-strain diagrams of the two types of steel did not yet exhibit any appreciable differences. The steel St 37 K, however, had a significantly higher 0·2 % proof stress than the Tor steel IIIb (Figure 38).

3.2 MEASUREMENTS AND TESTING PROCEDURE

The following measurements and observations were performed:

behaviour and pattern of cracks at all stages of loading;

crack widths at the level of the reinforcement and (for the shear cracks) half-way up the effective depth;

deflexion at mid-span and quarter-span points (measured with dial gauges).

For beams E, each loading stage was 2P = 1·55 tons; for beams G the value $p\ell$ was 3·10 tons per loading stage. The period of load application lasted about 30 min at each stage. After each stage, the beam was unloaded and then reloaded (starting from zero load) for the next stage. The rate of load application was about 5 tons/min.

3.3 RESULTS OF THE TESTS TO FAILURE

The loads at which the first cracks developed, and the ultimate loads, are given in Table VI, which also states the abscissa x_U of the upper end of the shear crack, together with the shear failure moment about this upper end. Furthermore, the steel stress σ_e and the calculated shear stress τ_o, obtained from the ultimate load on the basis of the conventional theory, were

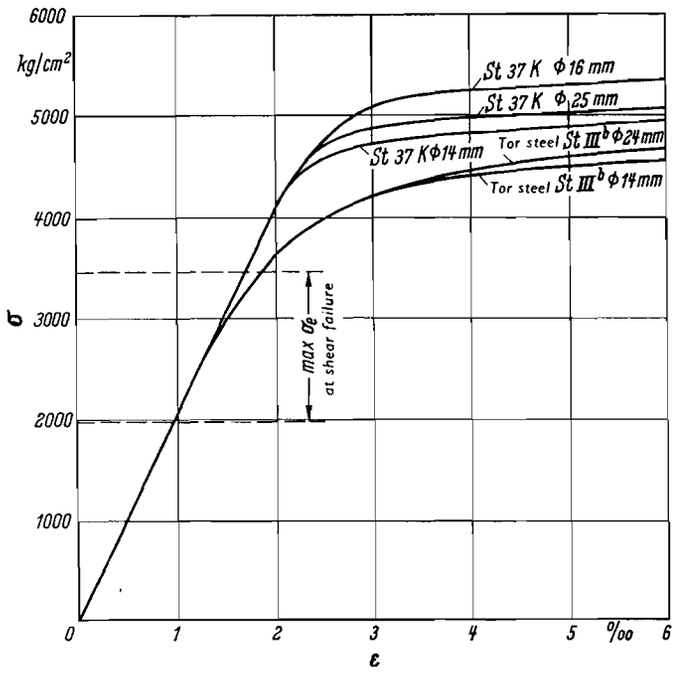

Figure 38: Stress-strain diagrams of the steels used in the test series with varying bond.

also determined. Three of the beams exhibited flexural failure; the five others developed definite shear failure.

The cracking patterns for the beams subjected to concentrated loads are given in Figure 39; those for the beams subjected to uniformly distributed loading are given in Figure 40. The figures in the circles indicate the sequence in which the cracks occurred, while the other figures indicate the loading stage at which the crack in question had extended as far as that particular point.

Figures 41 and 42 give information on the crack widths, the crack widths observed at each loading stage being given in 0·01 mm. In each case the diagram on the right shows the sum of the widths for the individual stages.

3.4 ASSESSMENT OF THE TEST RESULTS

Let us first consider the beams reinforced with ribbed Tor steel. We find that the "distributed" reinforcement consisting of thin bars gave definitely higher shear failure loads than did the "concentrated" reinforcement comprising only a few thick bars. With concentrated loads the ultimate load was 28 % and with distributed loading it was 18 % higher. This result is significant, as the bond quality was not modified by varying the surface constitution of the bars, but merely by varying their diameter and number - and not even in any extreme sense. Hence, with ribbed Tor steel, an increase in shear failure load can already be obtained by distributing the reinforcement (i.e. using a larger number of bars of smaller diameter) and thereby improving the bond.

However, the beams reinforced with smooth bright round steel bars exhibited significantly higher failure loads than the corresponding beams containing ribbed bars. At first sight this is a surprising and rather incredible result. On closer examination it nevertheless becomes understandable: the cracking patterns at failure show that the beams with smooth thick bars (EBI and GBI) did not fail in consequence of shear but in consequence of bending, notwithstanding that no shear reinforcement had been provided.

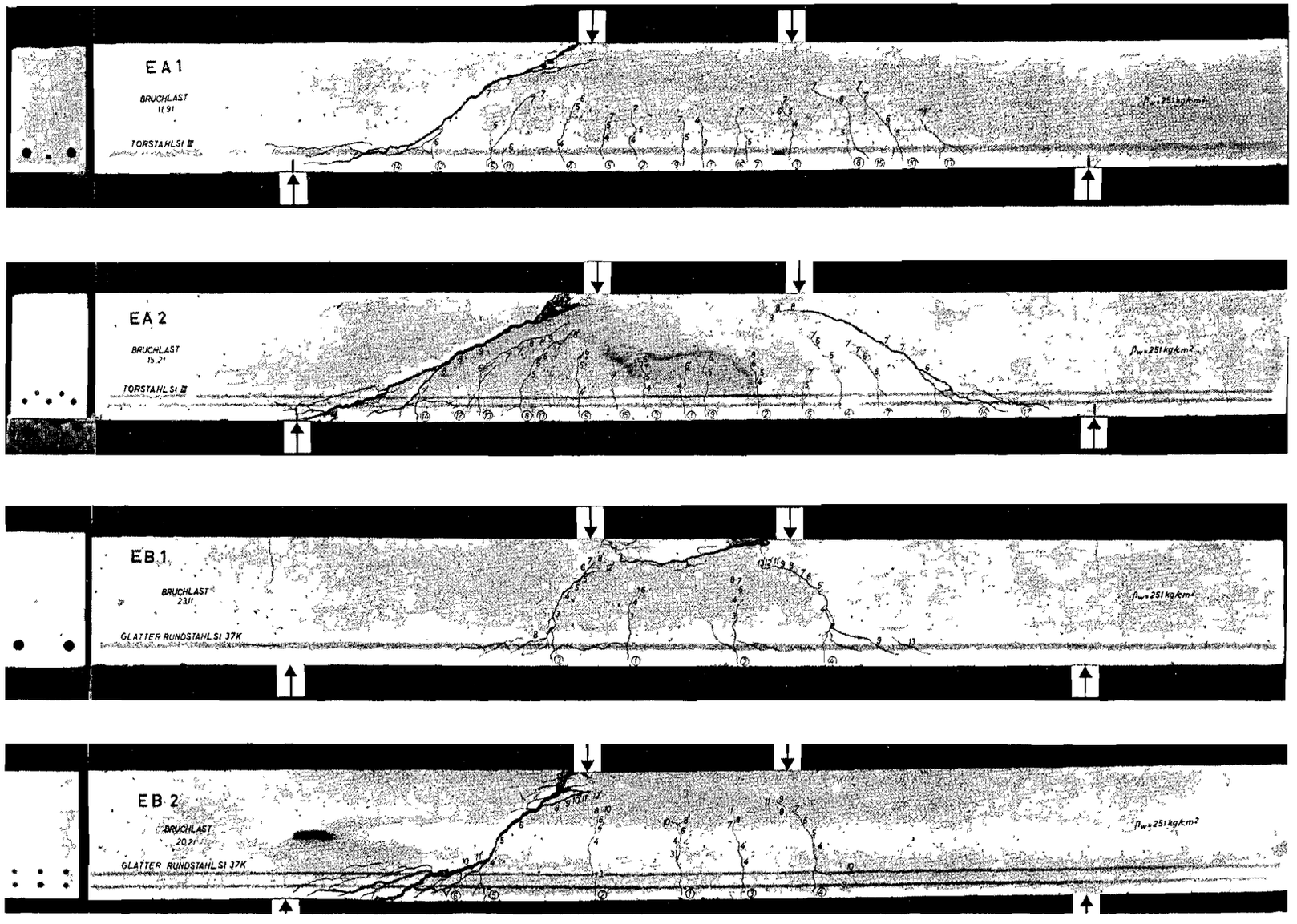

Figure 39: Cracking and fracture patterns for the concentrated-load beams with varying bond conditions. (Figures in circles denote serial numbers of the cracks in the order of their occurrence; the other figures denote the loading stage at which a crack had penetrated as far as the point indicated; each loading stage P = 1·55 tons.)

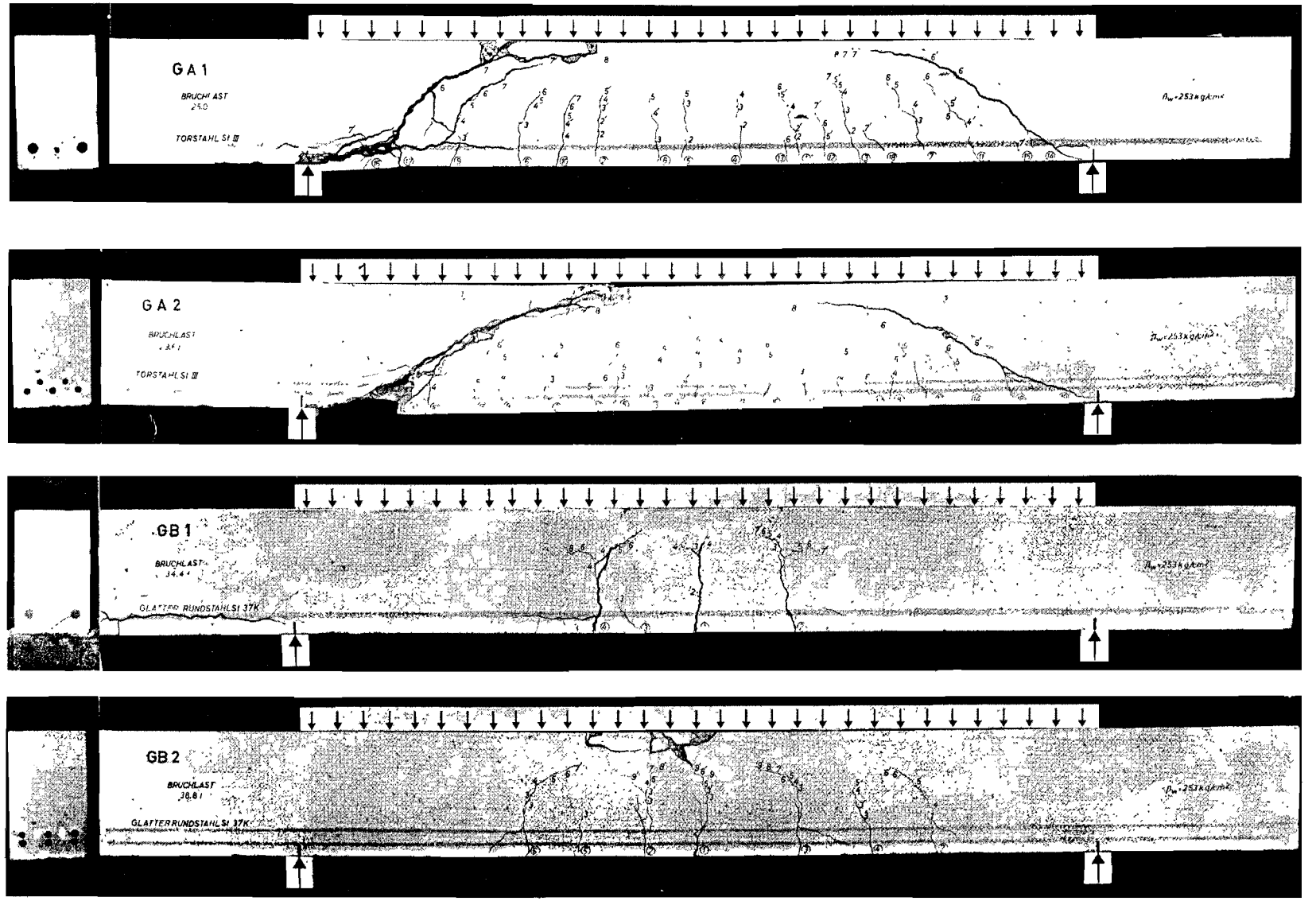

Figure 40: Cracking and fracture patterns for the uniformly load beams. (Details generally similar to Figure 39, but loading stage pl = 3·1 tons.)

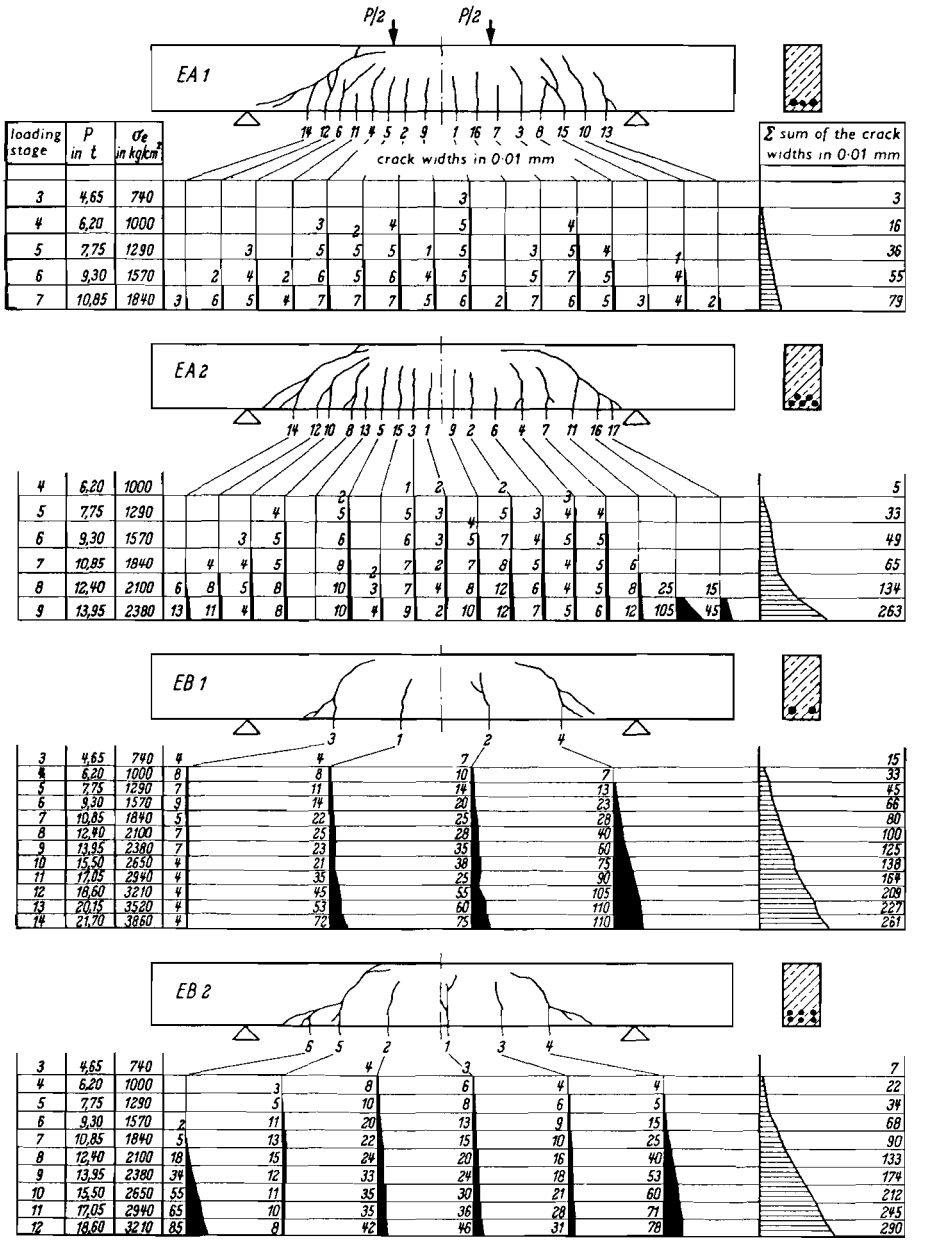

Figure 41: Crack widths for the concentrated-load beams with varying conditions of bond (compare equal loading stages!).

At the bottom the cracks had hardly any slope at all and forked approximately at the level of the neutral axis, in the manner familiar from other tests with deficient bond[14]. In the shear region these cracks are entirely absent. This is a clear indication that no appreciable shear stresses occurred, so that no critical oblique principal tensile stresses developed either. Hence the beam action, corresponding to the bending theory of beams, did not develop at all in this case, because the shear force transmission from the concrete to the bars was almost entirely lacking on account of the deficient bond. Under the uniformly distributed loading a tied arch and under the point loads a truss action was produced, in which the steel stress in the "tie-road" undergoes hardly any decrease up to the bearings, so that a large tensile force has to be taken up by the end anchorages. In the case of beam GBI this resulted in premature anchorage failure, which explains why the ultimate load for this beam was lower than for beam GB2. In the latter a tensile crack developed at the top of the beam in consequence of the large eccentricity of the tie-rod force over the bearing.

In the case of the beams containing a number of thin smooth bars, uniformly distributed loading (beam GB2) produced the same flexural failure pattern with only very few cracks. Under concentrated loads (beam GB2), on the other hand, the last flexural crack that occurred developed in the shear zone into a shear crack which eventually resulted in failure of the beam. This is because, with the six thin bars provided, the low bond strength of the concrete to the smooth steel already develops so much bond that the bond forces transmitted from the concrete to the steel result in a partial beam action and thus give rise to shear stresses and oblique principal tensile stresses. If bond had been entirely obviated, then flexural failure would certainly have occurred in this case also.

With deficient bond the cracks produced were, indeed, fewer but they were, of course, much wider than the cracks in the other beams (Figures 41 and 42). On comparing the crack widths for similar loading stages, the

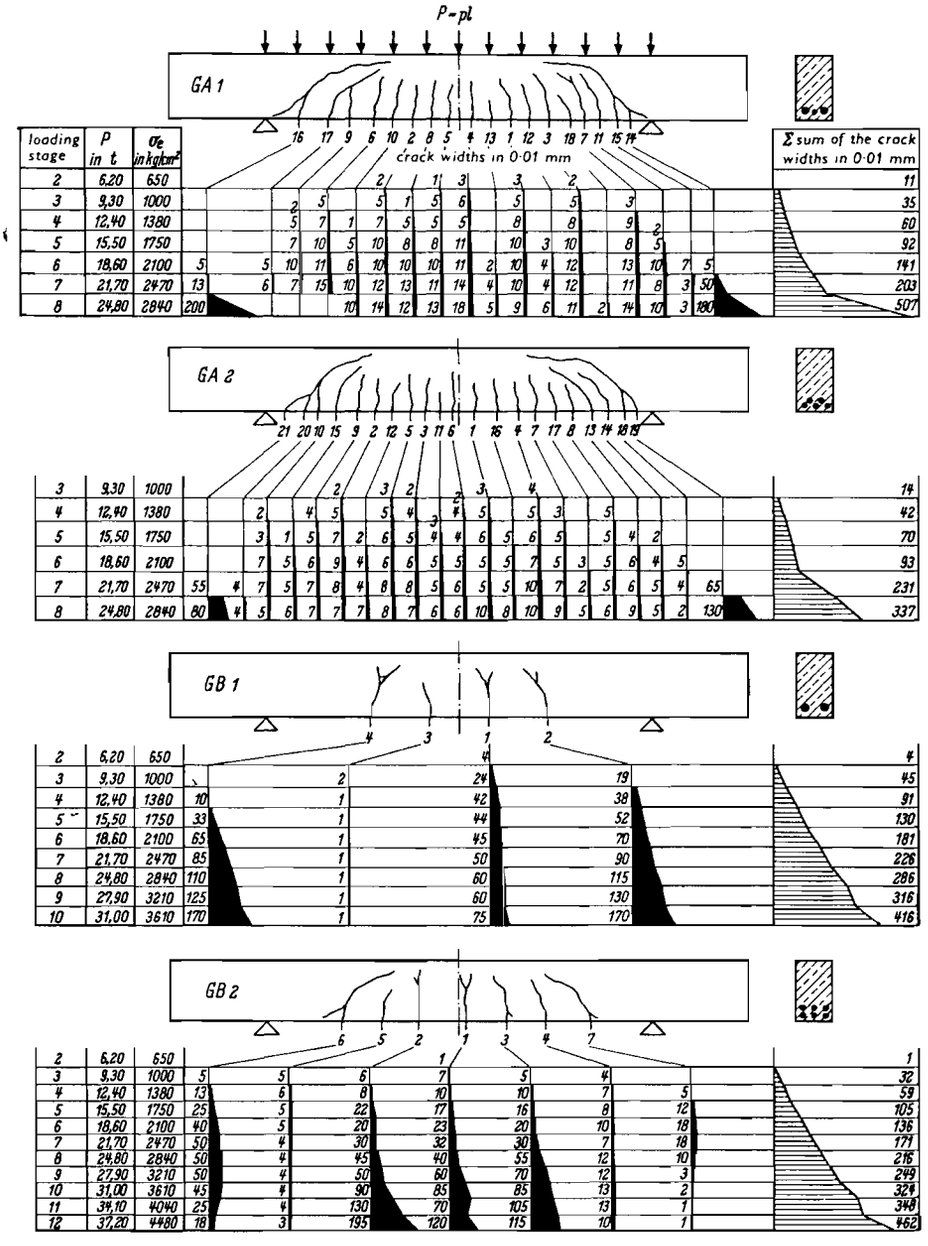

Figure 42: Crack widths for the uniformly loaded beams with varying conditions of bond (compare equal loading stages!)

widths are found to be 8 to 10 times larger, which means that, if only for this reason, deficient bond is an unsatisfactory condition, as is well known.

How is it, then, that beams reinforced with smooth round bars are less liable to fail in shear and are able to carry more load than beams with well-bonded reinforcement?

To account for this it must again be pointed out that in beams the position of the neutral axis associated with shear cracking is significantly higher than that associated with flexural cracking, as is also clearly manifested in the present case (see Figures 39 and 40). The height of the shear crack is very largely dependent upon the width that this crack develops at the reinforcement (Figure 43). At the reinforcement the bond is destroyed over short lengths and the crack widths developed are sometimes quite considerable (cf. the final loading stages of beams GA1, GA2 and EA2). The deformation that occurs there can therefore no longer be regarded as mere "strain" but is, rather, a quite significant extension which can be designated as Δs_u. It results in rotation of the two parts of the beam about the upper end of the shear crack. This will be termed "shear rotation" [14]. This deformation of the tensile zone is associated with a deformation of a certain length of the compressive zone, which latter deformation is usually already in the plastic range. As a result of the shear crack opening out at the reinforcement, the crack spreads upwards into the beam and greatly reduces the depth of the compressive zone, so that the beam fails sooner in shear than in bending.

The extension Δs_u at the tensile face of the beam depends on the steel strain ε_e and therefore also on the bending moment at that point and, more particularly, it depends on the quality of the bond. The poorer the bond, the more widely will the shear crack open. This in turn explains why, with efficient bond, increased ultimate strength in shear is obtained. It also follows that, in this type of shear failure, the calculated shear stresses τ_o and the resulting principal stresses σ_I are not by themselves the determining factor, but that the shear strength of the beam is to a significant extent dependent upon the strength and size of the shear compressive zone, and these in turn are governed by M and Q and by the shear deformations, i.e. by the degree of reinforcement and the bond quality. It is therefore important to introduce, for the ultimate shear load, a deformation condition which takes account of the bond quality.

3.5 DEFLEXIONS

The difference in structural action as a result of varying the quality of the bond is also manifested in the deflexions (Figures 44 and 45). In the lower stages of loading, the deflexions of the beams containing ribbed Tor steel are smaller than those of the beams containing smooth reinforcing bars. At higher loads, it is the other way round. This is because, with ribbed bars, shear cracks and therefore marked shear deformations occur, whereas these additional deformations do not occur in the beams which develop

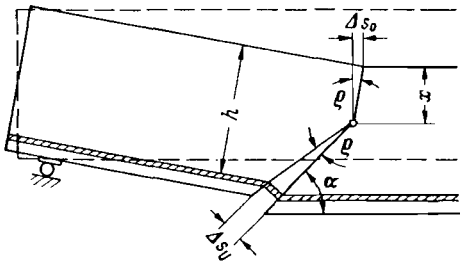

Figure 43: Deformations in the shear failure zone (shear rotation).

pure "arch" or "truss" action. Also, in the latter case the compressive zone will not become as small as when shear cracks are formed.

The "concentrated" reinforcement comprising a small number of bars was, with both types of steel and loading, associated with larger deflexions than was the "distributed" reinforcement consisting of a larger number of thinner bars.

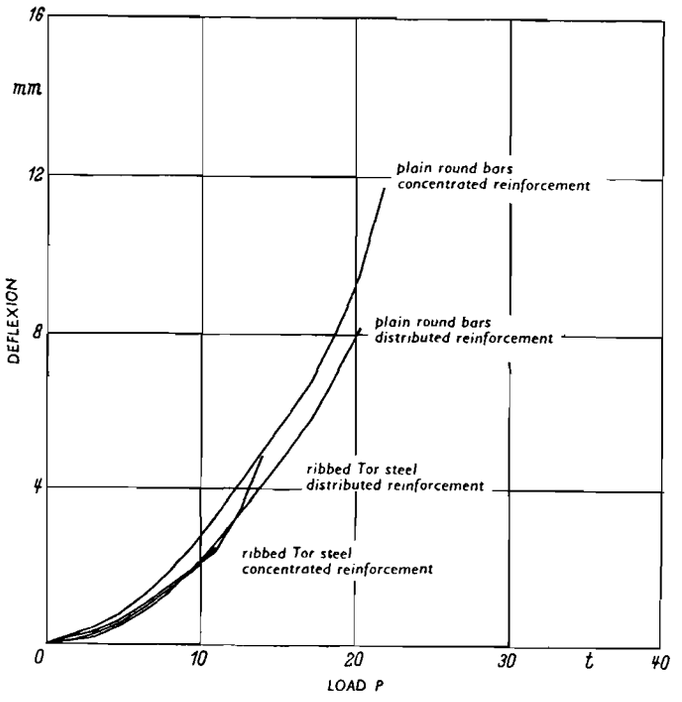

Figure 44: Deflexions of the concentrated-load beams with varying conditions of bond.

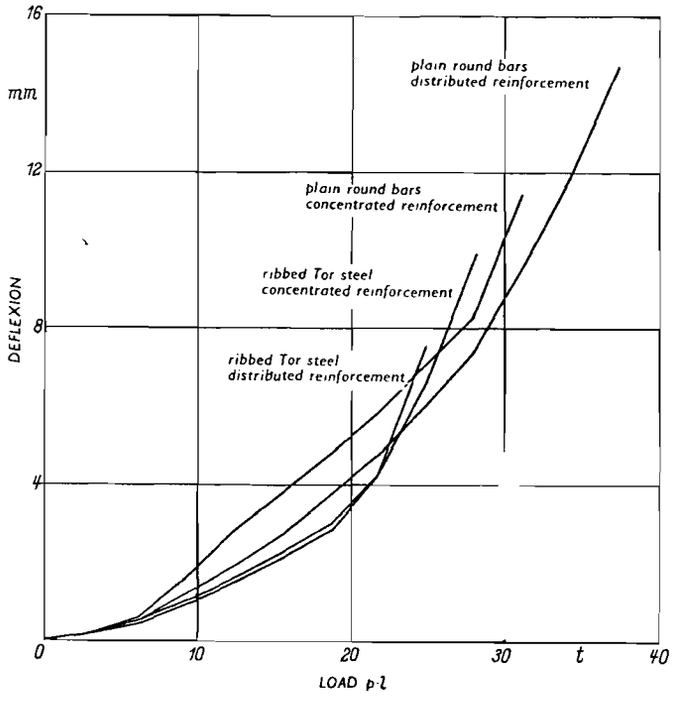

Figure 45: Deflexions of the uniformly loaded beams with varying conditions of bond.

3.6 CONCLUSIONS

The following conclusions can be drawn from the results.

1. The shear strength (ultimate strength of the beam in shear) is increased by improving the bond. In this connexion, dividing the reinforcement into a larger number of correspondingly thinner bars has a favourable effect similar to that obtained with predominantly flexural loading, more particularly with regard to the widths of the cracks.

2. If bond is almost entirely lacking (smooth bright bars), wide bending cracks, but no shear cracks, are formed. The beam acts as a "truss" or "tied arch". This type of load-carrying action, however, will be fully effective only in symmetrically loaded beams of low slenderness and if additional anchorage of the reinforcement is provided. For this reason, the favourable effect of smooth reinforcing bars upon the ultimate strength is not utilisable for practical purposes.

3. The bond quality affects the shear deformations and thus affects the depth of the shear compressive zone. In calculating the shear failure load it is therefore advisable to take an appropriate deformation condition into account

It is desirable to carry out further tests in this direction, e.g. with plain round bars in the as-rolled condition or with ribbed fabric mesh reinforcement and the like.

4. Influence of absolute beam depth on shear strength; checking the similarity laws in shear tests (rectangular beams without shear reinforcement)

4.1 INTRODUCTION

With regard to the many shear tests which have been carried out in recent years, more particularly in the United States, it is a striking feature that the beams investigated nearly always had an effective depth of about 30 cm and were 2 - 3 m in length. The question arises as to whether the results of these laboratory tests are valid also for larger structures. This question is all the more important because in some countries empirical design formulae have been based on these tests. It is therefore necessary to check whether the laws of similarity are validly applicable to shear failure tests.

For bending, the similarity laws state that the relative (or "specific") ultimate moment $m_U = M_U/bh^2$ or $m_U = M_U/\beta_p bh^2$ must be constant for beams which are made of the same materials and exhibit complete geometric similarity. It must therefore be investigated whether the "specific" shear failure moment M_{SU}, and consequently the shear stress τ_o, also conforms to this condition.

4.2 TEST ARRANGEMENT AND TEST SPECIMENS

Two test series were carried out, as follows (Figures 46 and 47).

Series D: Completely similar beams having the same degree of reinforcement but differing in size; bar diameter proportional to the external dimensions; number of bars constant.

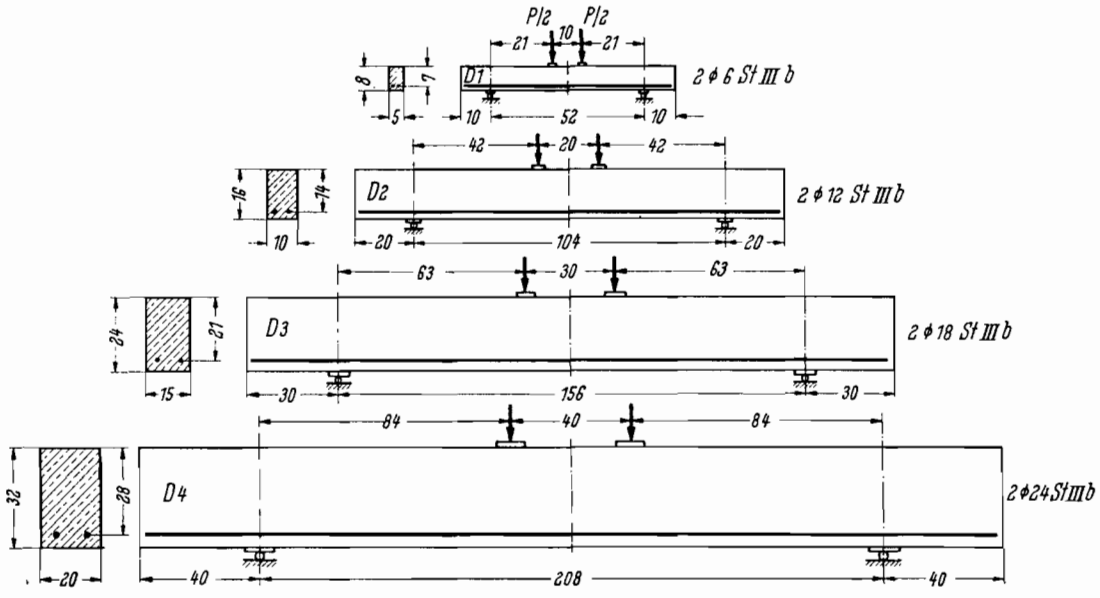

Figure 46: Dimensions of the test beams of series D: complete similarity (ratios 1:2:3:4); same construction materials.

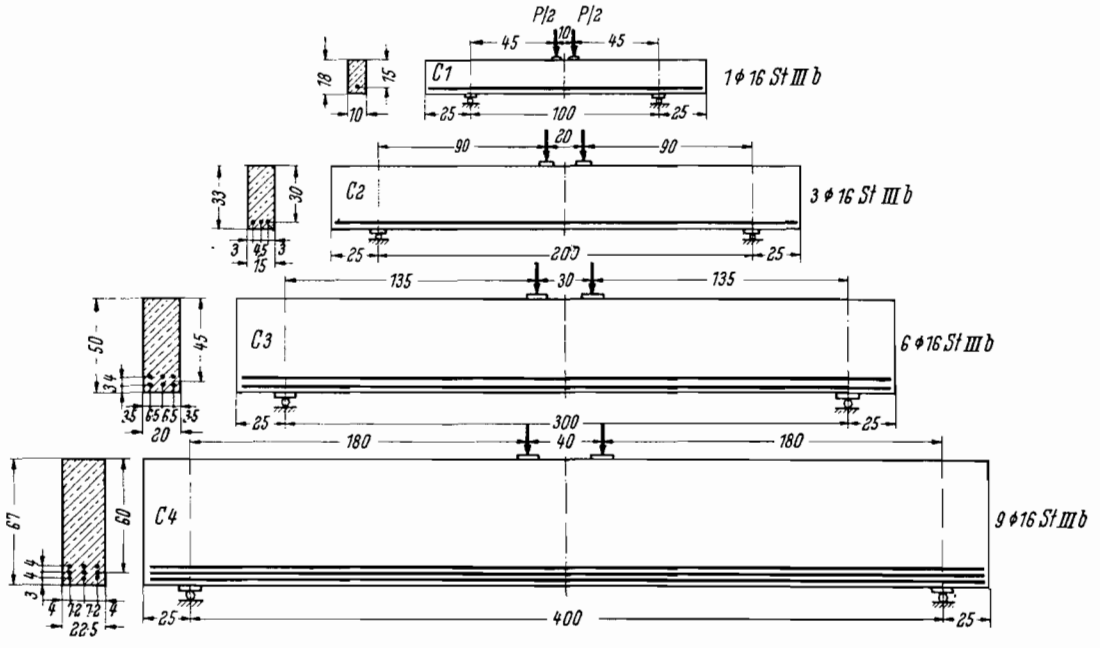

Figure 47: Dimensions of the test beams of series C: constant bar diameter (16 mm) and constant μ = 1·33%; number of bars varies; similarity ratios 1:2:3:4 (widths 1:1:5:2:2·5); same construction materials.

Series C: Completely similar beams having the same degree of reinforcement but differing in size; bar diameter constant, i.e. the number of bars was varied.

The beams had a slenderness ratio $l/h = 100/15 = 6{\cdot}7$. They were reinforced with straight continuous ribbed Tor steel bars and had no shear reinforcement or anchorage reinforcement. The loading was applied at two symmetrically situated points so positioned that $M/Qh = a/h = 3$; the dimensions are indicated in Table VII. For series D the geometric dimensions were in the ratios: D1:D2:D3:D4 = 1:2:3:4. The longitudinal reinforcement in each beam accordingly consisted of two bars of ribbed Tor steel (steel IIIb) with diameters of 6, 12, 18 and 24 mm respectively, thus providing a degree of reinforcement (reinforcement percentage) of $\mu \simeq 1{\cdot}65$ % in all cases. The anchorage length beyond the bearings was approximately equal to 16 bar diameters. The steel plates (affixed with mortar) under the loads and over the roller bearings were varied in size to conform to dimensional similarity. Two beams of each size were made and tested.

Larger dimensions were adopted for the beams of series C. As in the case of series D, the significant external dimensions - i.e. effective depth, span, and load spacing - were in the ratios: C1:C2:C3:C4 = 1:2:3:4. To effect a saving in the quantities of material, the widths were graded in the ratios of 1:1·5:2:2·25, this being merely of secondary importance with regard to considerations of similarity. In all the beams of series C the longitudinal reinforcement consisted of 16 mm diameter ribbed Tor steel bars, the ratios of the numbers of bars being 1:3:6:9 for a constant value $\mu = 1{\cdot}33$ % for the degree of reinforcement. In order to achieve as far as possible equal (but not similar!) bond and anchorage conditions, the longitudinal reinforcing bars were in all cases made to project a distance of 25 cm (about 16 bar diameters) beyond the bearings and the concrete cover at the bottom was in all cases made about 2 cm. Because of the varying numbers of bars installed, the beam depths d differ somewhat from the precise value according to the similarity scale.

All the beams of a series were manufactured at the same time from the same concrete.

The beams and cubes were demoulded after one day, cured for 7 days under damp cloths, and then stored at about 18° C and 60 % relative humidity until they were tested at 28 days of age. The beams were loaded with two symmetrically arranged concentrated loads in six to nine incremental stages with, in all cases, intermediate unloading. For each main and intermediate loading stage the deflexion at $l/2$ and $l/4$ and the spreading of the cracks were determined.

Testing a beam took about four hours.

4.3 MATERIALS

Steel

The characteristics of the ribbed Tor steel employed are summarized in Table VIII. The stress-strain diagrams are not given here because the stresses in the steel which were attained at failure were invariably below the 0·2 % proof stress ($\beta_{0.2}$).

TABLE VII: Results of the similarity tests. (All beams failed in shear.)

1	2	3	4	5	6	7	8	9	10	11	12	13	14	15	16	17	18	19
									Cracked state(3)			Failure						
Designation	l (m)	a (m)	h (cm)	b (cm)	F_e St IIIb (Ø = dia. in mm)	μ (%)	β_w (kg/cm²)	$\frac{M}{Qh}$	M_R Flexural cracking moment (tm)	β_{bz} Beam (with n = 7·5) (kg/cm²)	σ_e State I (uncracked) n = 7·5	P_U (t)	Q_U (t)	τ_o (kg/cm²)	M_{SU} (tm)	σ_{eU}(4) (kg/cm²)	$\frac{M_{SU}}{bh^2}$ (kg/cm²)	Average
D 1/1	0·52	0·21	7·0	5·0	2 Ø 6	1·71	447	3·00	0·051	80·2	450	1·49	0·74	24·8	0·156	4340	63·4	63·1
D 1/2	0·52	0·21	7·0	5·0	2 Ø 6	1·71	447	3·00	0·047	74·1	416	1·47	0·73	24·4	0·154	4280	62·8	
D 2/1	1·04	0·42	14·0	10·0	2 Ø 12	1·66	449	3·00	0·252	50·0	281	4·32	2·16	18·2	0·91	3230	46·5	48·5
D 2/2	1·04	0·42	14·0	10·0	2 Ø 12	1·66	449	3·00	0·235	46·5	262	4·74	2·37	19·9	0·99	3520	50·5	
D 3/1	1·56	0·63	21·0	15·0	2 Ø 18	1·62	464	3·00	0·756	44·6	251	9·46	4·73	17·7	2·98	3190	45·0	43·3
D 3/2	1·56	0·63	21·0	15·0	2 Ø 18	1·62	464	3·00	0·693	40·8	230	r. 9·08 l. 8·40	4·37	16·3	2·75	2940	41·6	
D 4/1	2·08	0·84	28·0	20·0	2 Ø 24	1·67	425	3·00	1·55	38·2	215	15·10	7·55	15·9	6·34	2780	40·4	39·6
D 4/2	2·08	0·84	28·0	20·0	2 Ø 24	1·67	425	3·00	1·30	32·2	181	r. 14·0 l. 15·1	7·27	15·3	6·10	2680	38·9	
C 1	1·00	0·45	15	10	1 Ø 16 (one layer)	1·33	471	3·00	0·13	(21·7)(5)	109	4·40	2·20	17·5	0·99	3740	44·0	
C 2	2·00	0·90	30	15	3 Ø 16 (one layer)	1·33	471	3·00	1·76	54·6	335	13·20	6·60	17·5	5·94	3760	44·0	
C 3(1)	3·00	1·35	45	20	6 Ø 16 (two layers)	1·33	471	3·00	3·98	44·0	264(4)	20·2	10·35	13·7	13·97	2940	34·5	
C 4(2)	4·00	1·80	60	22·5	9 Ø 16 (three layers)	1·33	471	3·00	9·90	50·2	298(4)	30·0	15·50	13·7	27·90	2960	34·5	

(1) Loading device + self-weight taken as 0·5 t

(2) Loading device + self-weight taken as 1·0 t

(3) First visible crack

(4) At centroid of reinforcement

(5) Lower value probably due to damage on removal of formwork

r. = right l. = left

TABLE VIII: Characteristics of the ribbed Tor steel St IIIb.

Nominal diameter (mm)	Cross-sectional area (mm^2)	$\beta_{0.2}$ (kg/cm^2)	β_z (kg/cm^2)
6	30	4600	5640
12	116	4350	5470
16	199	4330	5400
18	255	4210	5370
24	469	4480	5660

Concrete

The composition and strength properties of the concrete are indicated in Table IX. For series D, which comprised beams having very small dimensions, the maximum aggregate size was limited to 15 mm. Accordingly, more cement was used in the mix, as compared with the mix with higher sand content used for series C, in order to obtain approximately equal concrete strengths. Graduation of the maximum aggregate size in the same ratios as the dimensions of the beams would be unrealistic because in actual practice large and smaller structural members are made with concrete containing the same large aggregate. Besides, it was desired to use the same materials for the various beams.

For series D the test cubes were adjusted to suit the test beam sizes. The cube strength was found to vary only slightly with the size of the cube tested; the individual values do exhibit a considerable scatter, however.

4.4 TEST RESULTS

4.41 Cracks

Figure 48 shows the cracks which occurred in the beams of series D (Figure 46). It appears that with geometrically similar beams made with the same materials, the cracking patterns produced are also approximately similar.

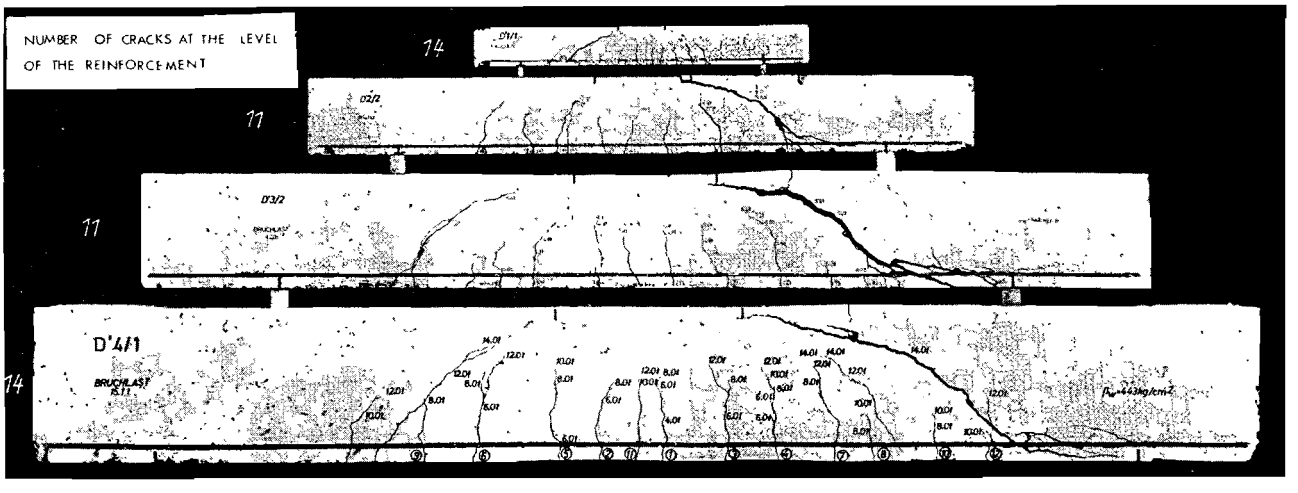

Figure 48: Cracking patterns of series D (complete similarity). Loading stages: D1 = 0·25 tons; D2 = 0·75 tons; D3 = 1·2 tons; D4 = 2·0 tons.

TABLE IX: Composition and strength of the concrete.

	Series D		Series C	
Aggregates (%) 0-3 mm	34		43	
3-7 mm	26		17	
7-15 mm	40		22	
15-30 mm	-		18	
Cement (kg/m^3)	373		297	
Water/cement ratio	0·49		0·62	
Age at testing (days)	28		28	
Cube strength (kg/cm^2)		average		average
for D1 : 7 x 7 x 7 cm	403, 462, 561, 406	447*	-	-
for D2 : 10 x 10 x 10 cm	435, 483, 447, 480, 421, 430	449	-	-
for D3 : 12 x 12 x 12 cm	466, 485, 459, 447, 461	464	-	-
for D4 and Series C : 20 x 20 x 20 cm	425, 395, 417, 440, 448	425	458, 442, 480, 473, 450, 475, 465, 497, 517, 468, 455	471
Flexural strength (kg/cm^2)	49·4, 51·4, 51·9, 49·8, 51·2	50·7	48·4, 47·8, 46·4, 51·3, 47·9	48·4

*This is not the average of the figures given. Presumably 561 should read 516. (Editor's note.)

In all the beams, 11 - 14 cracks developed at the level of the reinforcement, i.e. the average distance between consecutive cracks was about 5 bar diameters and thus roughly proportional to the external dimensions. The same is true of the lengths of the cracks at corresponding stages of loading, a striking feature being that here again the shear cracks spread much farther upwards than the flexural cracks.

Conditions are quite different in the beams of series C (Figures 47 and 49), in which bars of constant diameter were provided in numbers which varied to suit the constant degree of reinforcement. According to H. Rüsch[15] the spacing of the cracks is essentially governed by the so-called perimetral

percentage $\gamma = \Sigma u/F_b = \pi\Sigma\phi/F_b$ (where F_b denoted cross-sectional area of concrete). This γ is constant for all the beams of series C, i.e. approximately equal crack spacing could be expected for all these beams, so that the number of cracks would be proportional to the beam span; from the results summarized in Table X, it appears that this is not quite the case.

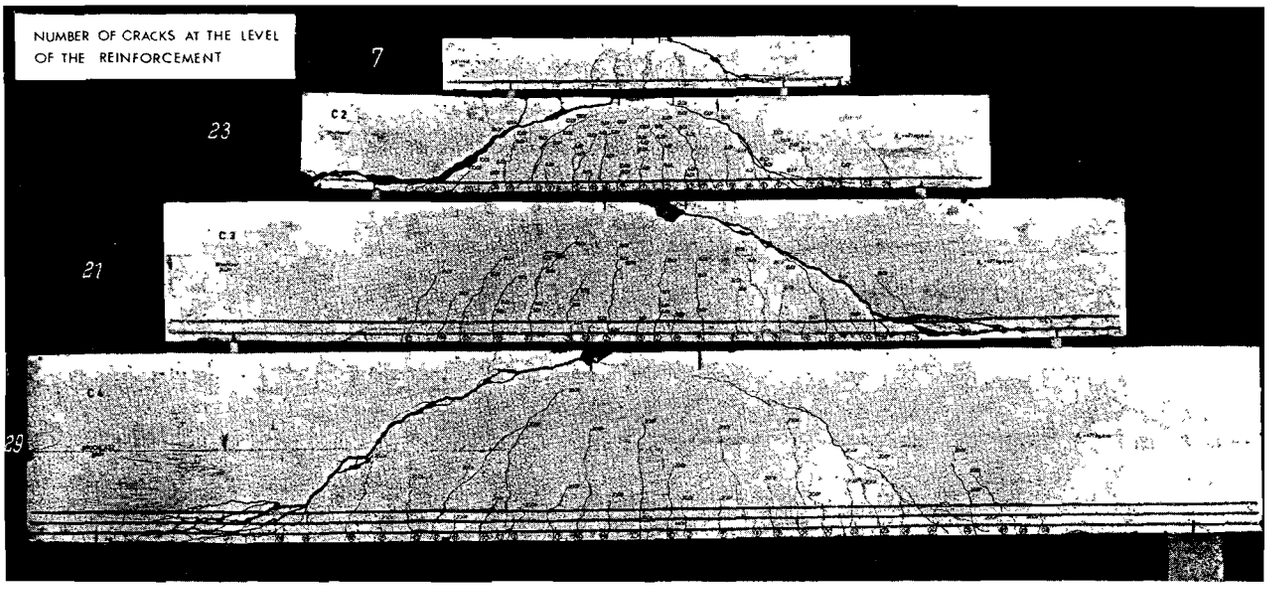

Figure 49: Cracking patterns of series C (similar specimens, but with constant bar diameter for constant steel percentage μ).

TABLE X

Beam	Span	Cracks			
		at $\frac{M}{bh^2} = 34{\cdot}5$ kg/cm^2		at failure	
		number	average spacing* (cm)	number	average spacing* (cm)
C1	1	7	12	6	12
C2	2	23	8	18	8
C3	3	21	10	21	10
C4	4	29	10	29	10

*At the higher stages of loading, the spacing of cracks remain constant, despite the larger number of cracks, inasmuch as fresh cracks formed only in regions closer to the bearings.

Hence it follows that, despite equal bar diameters and equal concrete cover at the beam soffits, the quality of the bond was not quite constant, and this also affects the ultimate strength (see 4.42). In beam C1 the lateral concrete width b_c was 8·4 cm and the tensile area of concrete associated with the solitary bar in this beam was greater than in the other beams, where b_c was 3·3, 5·0 and 5·8 cm for C2, C3 and C4 respectively. The tensile force which has to be transmitted by bond from the individual bar to the concrete and which is necessary for producing the next crack - and therefore the requisite transmission length - was therefore larger in beam C1 than in beam C2. The reason why this trend diminishes in the case of beams C3 and C4 is that with the reinforcement arranged in two or three layers the crack area per bar is greatly reduced. In the largest beam (beam C4) the first visible crack penetrated only as far as the middle layer of reinforcement, i.e. up to d/10, whereas in beam C1 it penetrated up to about d/3. On the other hand, with reinforcement arranged in several layers, the quality of the bond becomes poorer, and this counteracts the decrease in crack spacing. Despite the differences in the spacing of the cracks, it is clear that with bond quality which is not varied in scale but is kept approximately constant (series C) the spacing of consecutive cracks is not proportional to the beam dimensions. The difference in comparison with series D is quite apparent.

The interrelation between bond quality and cracking is also manifest from the calculated tensile stresses in the steel and at the soffit of the beam under cracking load (assumptions: state I, modular ratio n = 7 5). In this connexion it should be clearly realized that the cracking loads or cracking stresses mentioned in test reports relate, not to the actual occurrence of cracks, but to their first visible appearance. The actual cracking loads are often considerably lower and are difficult to determine or to define.

In the case of series D, therefore, the flexural tensile stresses corresponding to the cracking load probably undergo only an apparent decrease of such magnitude with increasing size of test specimen (Table VII, column 11). Since the crack spacing and the size of the crack area were roughly proportional to the external dimensions, the crack widths will also be approximately in the same ratio. Hence in small beams the cracks will become visible later than in larger beams. Besides, in large beams the absolute size of the specimen is liable to give rise to larger shrinkage stresses which also contribute towards reducing the flexural strength (β_{bz}) of larger beams.

That the quality of the bond and the distribution of the reinforcement (by "neighbourly help" in so far as the latter aspect is concerned) do, however, evidently affect the development of the first crack is apparent from the β_{bz} values for series C* which, despite the considerable change in dimensions, undergo only little decrease with increasing size for equal numbers of layers.⁄

4.42 The shear strength

As expected, all the beams failed by crushing of the shear compressive

---

* The improbably low value for C1 is perhaps due to damage sustained on demoulding; this suspicion is borne out by the fact that no further cracking occurred at the next two stages of loading.

⁄ The purport of the latter part of this sentence ("despite the considerable.. ..") is not clear and the translation is conjectural. (Translator's note.)

zone. This was associated with destruction of the bond - by horizontal cracks extending along the reinforcement from the shear crack to the bearing - shortly before failure.

The results of the tests to failure are summarized in Table VII, columns 13 - 18.

As distinct from what is found to occur in bending tests, the specific failure moment $m_{SU} = M_{SU}/bh^2$ (column 18), which here has the dimension of a stress, is not constant in the present case.

In the case of series D (complete similarity of test beams) the value of m_{SU} decreases from 63.1 to 39.6 kg/cm^2, i.e. a 37 % decrease, with increasing size of specimen. Hence the ususl laws of similarity are not valid for shear failure.

In the case of beams containing bars of constant diameter (series C) m_{SU} also decreases with increasing beam size, but here the difference between the values associated with the smallest and the largest beam is 21 % and is therefore considerably less than in series D.

How to account for these phenomena? An analogy with cracking (4.41) is not helpful, because in that case it was essentially a question of flexural cracks, whereas here the main shear cracks are decisive and exhibit few external differences. Instead, we must make use of the information on the effect of bond (Section 3) in order to arrive at an explanation.

In Section 3 it was found that a shear crack will spread farther upwards according as the bond is poorer (differences between beams with "distributed" and "concentrated" steel). This has been further clarified by the concept of shear rotation (Figure 43). The deformation Δs_u at the base of the shear crack is governed by the steel strain and the bond quality, i.e. by the quantities:

$$\Delta s_u = f(\varepsilon_e, \phi, \varkappa, \beta_p, \mu)$$

where ε_e = steel strain; ϕ = bar diameter; $\varkappa$ = surface coefficient of the bars; β_p = prism strength of the concrete as a criterion of bond strength, especially with regard to shearing bond; μ = degree of reinforcement (percentage of steel installed).

On the other hand, the beam size itself is bound to play a part, because with large beams and good bond more cracks undoubtedly will contribute to shear deformation than in the case of small beams. Hence Δs_u must increase with the actual size - or, as may primarily be assumed, with the length l_d of the inclined crack.

For otherwise equal conditions we must therefore take two influencing factors into account, namely the size of the region disturbed by shear cracks and the quality of the bond which, in these tests, depends mainly on the bar diameters. The relationship between these two factors is, to begin with, unknown.

On the basis of these and many foreign tests, R. Walther has established the empirical relationship:

$$\Delta s_u = k_1 \, l_d \sqrt{\phi}$$

where k_1 is a coefficient catering for the influence of the other parameters.

The following inferences can be drawn.

Series D: l_d and ϕ both increase proportionally to the beam dimensions, i.e. Δs_u increases more than proportionally. In large beams the shear cracks therefore penetrate relatively farther than they do in small beams, and the specific shear moment m_{SU} becomes smaller.

Series C: Since all the bars in these beams were of the same diameter, l_d and therefore also Δs_u would have to increase about proportionally to the beam size, i.e. the values m_{SU} would have to be constant. However, this is found to be the case only for the two smaller and for the two larger beams, the difference between these two sub-groups being 21 %. This is in part attributable to the difference in bond quality, which is affected by the number of layers of reinforcement.

A comparison of the analogous beams of series C and D:

$$\frac{D2}{D4} \text{ with } \frac{h = 14 \text{ cm}}{h = 28 \text{ cm}} \longrightarrow \frac{m_{SU} = 48{\cdot}5 \text{ kg/cm}^2}{m_{SU} = 39{\cdot}6 \text{ kg/cm}^2} = 1{\cdot}22$$

$$\frac{C1}{C2} \text{ with } \frac{h = 15 \text{ cm}}{h = 30 \text{ cm}} \longrightarrow \frac{m_{SU} = 44 \text{ kg/cm}^2}{m_{SU} = 44 \text{ kg/cm}^2} = 1$$

indicates that the difference in shear strength is determined only in part by the size of the beam and chiefly by the bond quality.

For the range of behaviour with which the present tests were concerned we arrive at the following conclusion:

> With complete similarity and therefore varying bond quality, the shear strength decreases with increasing beam size.
>
> With external similarity but constant bond quality, the shear strength is fairly independent of beam size.

With complete similarity, however, the decrease in shear strength is not proportional to the absolute sizes of the beams. Instead, it corresponds to a curve (Figure 50) from which it can be inferred that from approximately h = 40 cm onwards the decrease ceases to be significant. This knowledge is important from the point of view transferring the test results to practical cases, and it is also reassuring.

As the reinforcing bar diameters for structural members stressed in tension are now mostly limited to about 26 or 30 mm, the decrease in shear strength in large beams is thereby further kept within bounds.* Hence the results of shear tests on beams exceeding 25 cm in depth can be transferred to larger members. On the other hand, empirical formulae, such as those obtained by G. Brock [16] from tests on small reinforced gypsum plaster models, are unlikely to be quite so straightforward.

---

* This is confirmed by (unpublished) tests of H. Rüsch.

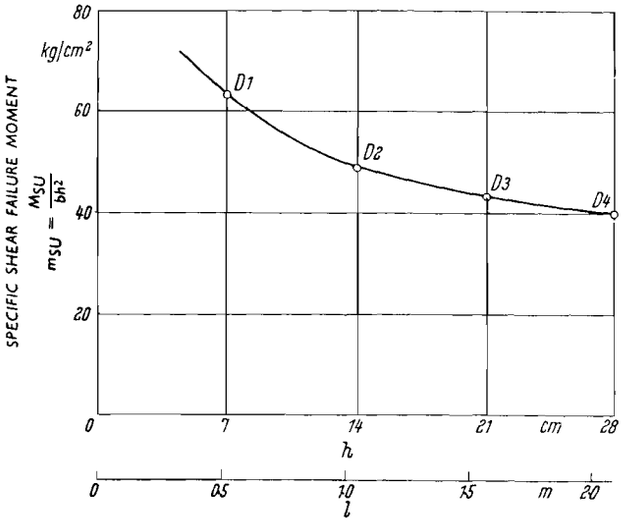

Figure 50: Reduction of the specified shear failure moment m_{SU}/bh^2 with increasing beam dimensions. (Series D with complete similarity.)

4.43 Shear stress τ_o

The shear stress τ_o is here proportional to m_{SU} because the loads were in all cases similarly positioned. However, we shall also consider the actual magnitude of τ_o. For B 425 concrete this is in some cases quite low. For D4 the value of τ_o is 15·3 kg/cm^2. For the comparable beam 5 in Section 2 (Table IV) we found τ_o = 14·6 kg/cm^2 for B 355, i.e. τ_o is not found to increase to an extent corresponding to the strength of the concrete.

For beams C3 and C4 the shear stress τ_o has an even lower value (13·7 kg/cm^2) although the distributed reinforcement is favourable to the bond quality and the concrete has a high strength (cube strength β_w = 471 kg/cm^2).

Hence, particularly with good concrete, we must reckon with τ_o values at failure which are even lower than those envisaged in Sections 2 and 3 of this report, if no shear reinforcement is installed and M/Qh is unfavourable. This provides a further indication that a design based on the usual permissible τ_o may result in an inadequate factor of safety, e.g. in the present case ν = 1·2 instead of 2·1.

5. Tests on slab strips without shear reinforcement (Beams of shallow rectangular section)

5.1 GENERAL CONSIDERATIONS

In practice, slabs are often constructed without shear reinforcement. Their thickness d is often much smaller than the depths of the beams tested according to Sections 2, 3 and 4. For this reason 14 "slab strips" were also tested. The object was to determine to what extent the shear failure behaviour, as determined from the beam tests, is also valid for "slabs" and whether there is a similar dependence upon the major influencing factors involved.

The following quantities were appropriately modified:

moment/shear ratio M/Qh;

degree of main reinforcement μ ;

bond, various bar diameters in conjunction with constant μ ;

effective depth h.

5.2 TEST SPECIMENS AND LOADS

The nature of the test specimens and the load arrangement are shown in Figure 51. The dimensions of the slab strips and the reinforcement provided in them are indicated in Table XI. The strength of the concrete was near the lower limit for concrete used in structural engineering and was β_w = 152 - 164 kg/cm^2 (cube strength). For purposes of comparison, two slabs (P8 and P9) of B 300 concrete were also made.

All the slabs were reinforced with straight continuous ribbed Tor steel bars (steel IIIb) without hooks and without any inclined bars or stirrups either in the longitudinal or in the transverse direction. The bars extended 20 cm beyond the bearings for anchorage. All the slabs were provided with transverse reinforcement consisting of 8 mm bars spaced at distances a = 20 cm. The bearings (movable rollers) extended over the entire slab width of 50 cm (Figure 51). The loading was applied on one side as a concentrated load (through a bearing plate measuring 8 cm square by 2 cm thick or 6 cm square by 2 cm thick affixed by means of a 5 mm thick cement mortar bed) and on the other side as a linear load (through a bearing plate 50 cm long, 4·5 cm wide and 1 cm thick). Both loads were at a distance a from the corresponding bearing. The loading was applied in eight incremental stages, the specimen being unloaded before each increment was applied. The loading rate was about 5 tons per minute.

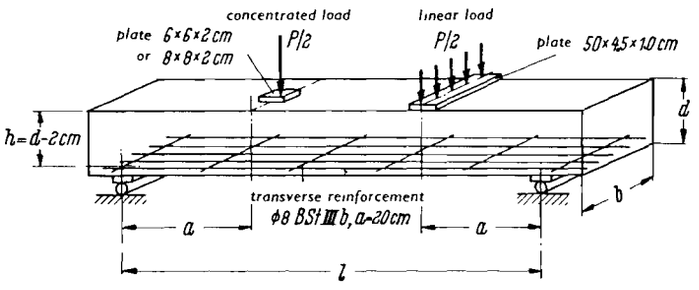

Figure 51: Dimensions and loading of slab strips.

Measurements

In addition to the determination of the cracking loads and failure loads, the following measurements were performed:

deflexions at $l/2$ and $l/4$ (by means of dial gauges);

pattern of cracks;

widths of cracks (only for the slabs P4, P6 and P7 with varying bond quality, containing bars of 12, 18 and 26 mm diameter).

TABLE XI: Dimensions and results of shear tests on slabs.

1	2	3	4	5	6	7	8	9	10	11	12	13	14	15	16	17	18	19	20	21	22	23				
											Failure												Variable of the individual test series			
Designation	l	b(1)	h(1)	a	Steel: no. of bars and diameter in mm	μ	β_w	Cracking moment M_R(2)	σ_{bz} Crack (State I-uncracked)	$\frac{M}{Q\,h}$	P_U	Q_U(2)	τ_o(3)	M_{SU}(2)	Type of failure(4)	Failure on side(9)	Permiss. M_B(6)	s(5)	σ_{eU}(7)	Calculated M_U(8) (bending)	Age at testing	$\frac{M}{Q\,h}$	μ	bond	h	β_w
	(m)	(cm)	(cm)	(cm)		(%)	(kg/cm²)	(tm)	(kg/cm²)		(t)	(t)	(kg/cm²)	(tm)			(tm)		(kg/cm²)	(tm)	(days)					
P 1	1·50	50·2	14·3	49	3 x 12	0·47	152	1·24	48·9	3·5	9·65	5·10	(7·9)	2·50	B	-	0·86	2·91	5780	2·1	26		0			
P 2	1·50	50·3	14·2	49	6 x 12	0·95	152	1·54	54·8	3·5	15·00	7·77	12·6	3·81	S	L	1·08	3·54	4860	3·5	25	0	0			0
P 3	1·50	50·2	14·2	49	7 x 12	1·11	152	1·64	56·5	3·5	16·00	8·27	13·6	4·06	S	E	1·13	3·60	4530	3·8	26		0		0	
P 4	1·50	50·0	14·5	49	9 x 12	1·40	164	1·49	47·0	3·5	20·00	10·28	16·8	5·04	S	L	1·25	4·03	4480	4·8	32		0	0		
P 5	1·50	50·3	14·5	49	12 x 12	1·86	152	2·48	70·8	3·5	20·00	10·28	17·0	5·04	S	E	1·36	3·71	3460	5·0	27		0			+
P 6	1·50	49·9	14·2	49	4 x 18	1·43	164	1·34	43·4	3·5	17·40	8·97	15·1	4·40	V	E	1·20	3·65	3850	4·5	32			0		
P 7	1·50	50·3	14·3	49	2 x 26	1·48	164	1·49	46·7	3·5	15·00	7·78	12·9	3·81	V	E	1·24	3·06	3010	5·0	33			0		
P 8	1·50	50·2	14·8	49	6 x 12	0·91	306	2·12	78·8	3·5	18·00	9·28	14·4	4·55	S	E	1·92	2·37	4980	4·3	21					0
P 9	1·50	50·0	14·6	49	12 x 12	1·86	306	3·11	105·9	3·5	21·00	10·78	17·9	5·28	S	E	2·29	2·31	3010	7·3	22					+
P 10	0·95	50·3	10·2	35	5 x 12	1·10	140	1·00	54·9	3·5	11·70	6·04	13·8	2·12	S	E	0·58	3·64	4780	1·9	27				0	
P 11	2·00	49·8	18·3	63	9 x 12	1·11	155	3·50	74·7	3·5	19·90	10·32	13·3	6·51	S	E	1·86	3·50	4320	6·4	29				0	
P 12	1·20	50·1	14·2	35	6 x 12	0·95	155	1·85	66·0	2·5	20·00	10·24	16·7	3·58	S	E	1·07	3·34	4460	3·5	28	0				
P 13	1·70	50·2	14·3	63	6 x 12	0·94	155	2·07	73·0	4·5	12·60	6·59	(10·6)	4·15	B	-	1·09	3·82	5350	3·5	28	0				
P 14	2·00	49·9	14·4	56	6 x 12	0·94	155	1·72	60·0	4·0	14·00	7·34	(11·8)	4·11	B	-	1·10	3·75	5200*	3·5	28	0				

(1) Dimensions at failure section.

(2) Taking account of the self-weight of the slabs and of weight of the loading device.

(3) According to DIN 1045: calculated as $\tau_o = Q_U/bz$, assuming $n = 15$.

(4) B = flexural failure; S = shear failure; V = anchorage failure.

(5) s = shear failure load divided by permissible working load according to DIN 1045 (bending).

(6) Calculated according to DIN 1045 with permissible σ_b = 60 (100) kg/cm².

(7) Determined for failure at failure section.

(8) Determined by Mörsch's graphical method with max ε_b = 0·3‰.

(9) L = linear load; E = concentrated load.

*Approximate value only: the original has 52, presumably a misprint. (Editor's note.)

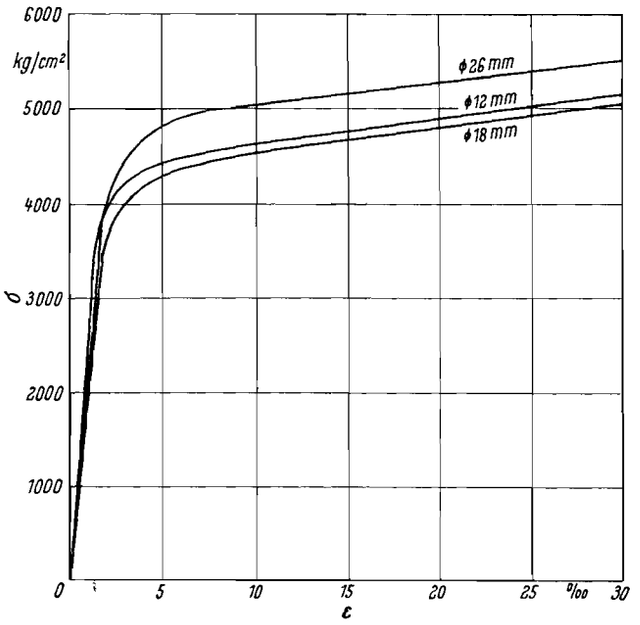

Figure 52: Stress-strain diagrams of the ribbed Tor steel employed (test series P, slab strips).

5.3 MATERIALS

Steel

The stress-strain diagrams were determined on specimens taken from the grade IIIb steel employed and are indicated in Figure 52 for the bar diameters used in the tests.

Concrete

The concrete was at the same time used for a mixer test which, according to the relevant directives *, had to be performed with a stiff concrete mix "S" and a high-water-content mix "W". For the former mix, rounded aggregates and a cement content of 300 kg per m^3 of concrete were specified; for the latter mix, the cement content was 200 kg per m^3, in conjunction with crushed stone aggregate for the 7 - 30 mm particle size range. Mixes as indicated in Table XII were accordingly prepared.

For both types of concrete the grading curves for the combined aggregates were approximately equal (Figure 53).

The reinforcing bars were at the bottom of the slabs during concreting. The concrete was compacted by means of internal vibrators. The test specimens were kept covered with damp cloths for 8 days and then stored dry until they were tested at between 21 and 33 days of age (Table XI, column 22), except the prisms for testing the flexural strength, which were kept in moist storage until testing (in accordance with DIN 1048).

Eighteen cubes and 9 prisms were made from mix "W", and 6 cubes but no prisms were made from mix "S". The cubes were 20 cm in size; the prisms were 53 cm long and of 10 cm square cross-sectional area. The strength tests were made on the same days as the slabs were tested. The average values are summarized in Table XI. The scatter exhibited by the results obtained from specimens tested on any particular day was slight.

---

* "Directives for efficiency of concrete mixers". Forschungsgesellschaft für das Strassenwesen, April 1953.

TABLE XII: Characteristics of the concrete for the slab strip tests.

	Concrete S	Concrete W
Number of batches	1	5
Used for slabs	P 8 and P 9	alternate slabs
Cement	300 kg/m^3 PZ 275	200 kg/m^3 PZ 275
Aggregates (fine fractions separated)	Washed Rhine gravel sand	Rhine sand 0-7 mm, Basalt chippings 7-30 mm
Fine quartz (referred to weight of aggregates)	4%	4%
Water/cement ratio (taking quartz into account)	0·72	0·78
Mixing time	50s	50s
Workability	Penetration e = 4·5 cm	Spread (German flow-table test) a = 48 ... 51 cm

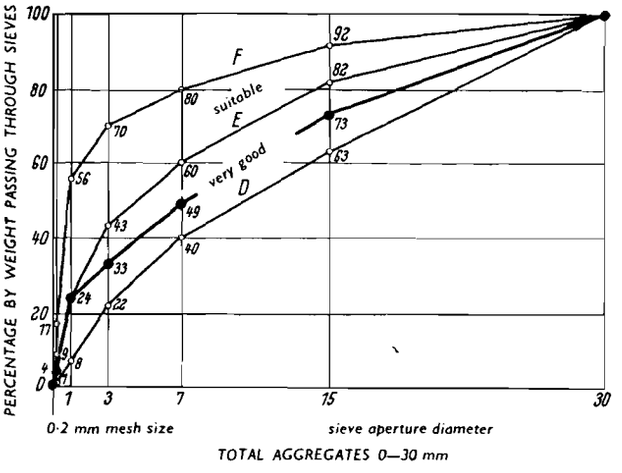

Figure 53: Grading curves for the aggregates used for the slab strip test specimens.

5.4 WORKING LOAD AND FLEXURAL FAILURE LOAD

5.41 Permissible working load according to DIN 1045 (bending)

The permissible bending moments are stated in Table XI, column 18.

In all the slabs the permissible concrete compressive stress is a determining factor - permiss. σ_b = 60 kg/cm^2 for concrete B 160 and 100 kg/cm^2 for B 300. Just as for the beams, the quotients s were determined in these tests also (Table XI, column 19), i.e.

$$s = \frac{\text{shear failure load}}{\text{permiss. working load (bending) according to DIN 1045}}$$

5.42 Flexural failure load (calculated)

The flexural failure loads (ultimate loads in bending) were determined by means of Mohr's graphical method [17], for which purpose the stress-strain diagrams of the steels employed in the tests were used. The compressive strain of the concrete was taken as 0·3 % and the stress distribution in the concrete compressive zone was assumed to conform to the test results obtained by Rüsch [18].

5.5 TEST RESULTS

The principal test results are summarized in Table XI, columns 9, 10, 12, 13, 14 and 15. Figure 54 illustrates some of the fracture patterns obtained.

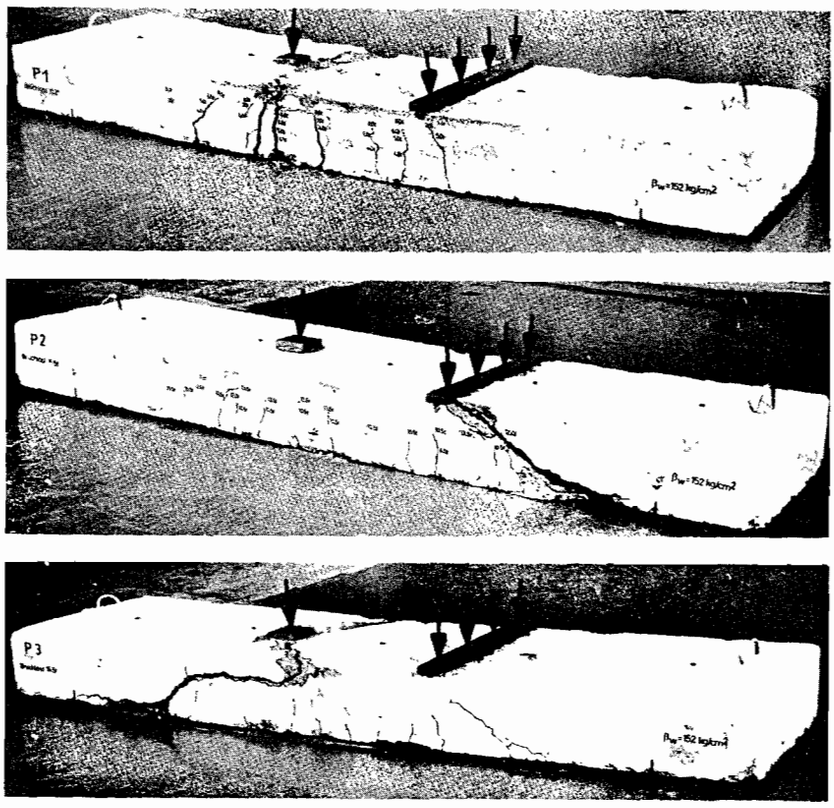

Figure 54: Characteristic fracture patterns obtained in the tests on slab strips.

5.51 Types of fracture

Most of the slabs failed in shear - usually (and rather surprisingly) on the side where the concentrated load was applied. On each side of the concentrated load the shear crack extended from the load application area towards the mid-span region * (Figure 54), i.e. into a zone in which the vertical stresses σ_y produced by vertical transmission of the load into the slab no longer acted. Directly under the load itself the concrete was held

* i.e. as viewed from above. (Translator's note).

together by the pressure exerted by the load, so that at this particular point the fracture line is situated to one side of the load. In these tests, too, the inclined shear cracks had, prior to failure, extended much higher than the flexural cracks. It was again apparent that the shear failure of rectangular-section members is often allied to flexural failure: in both cases the member fails when the extreme concrete stress attains the compressive strength, though the effective remaining compressive zone of the concrete is more reduced by the shear crack than by the flexural crack, so that shear failure occurs before the flexural failure load is reached. The magnitude of the bending moment will, of course, play an important part in this connexion.

In the case of slabs P2 and P4 the shear failure occurred at the linear load, directly beside the load-spreading plate. Since there appears to be no special reason for this different failure behaviour as compared with the other test slabs, it must be assumed that the shear strength does not differ much for the two types of loading and that the occurrence of failure on the one or other side is probably decided by minor local differences in the quality of the concrete.

Because of the higher bond stresses and the small amount of concrete cover, anchorage failures occurred in the slabs reinforced with thicker bars (P6 containing four 18 mm bars and P7 containing two 26 mm bars), which was associated with spalling of the concrete on the soffit of the slab along the reinforcing bars (Figure 55).

The slabs having moment-shear ratios larger than 4 (P13 and P14) and slab P1 with a low degree of reinforcement (μ = 0·47 %) failed in bending (Figure 54), the yield point of the steel being exceeded.

5.52 Effect of the moment-shear ratio

The tests on slabs P2, P12, P13 and P14 show the effect of the moment-shear ratio. In Figure 56 the values of τ_o and M_{SU} (shear failure moment) have been plotted against M/Qh. The trend of these curves corresponds to that of the narrow beams (cf. Figure 33), i.e. τ_o decreases with increasing M/Qh, whereas M_{SU} increases, the change in magnitude of τ_o being somewhat greater than in that of the moments.

The transition from shear failure to flexural failure occurs at M/Qh = 4. In the beam tests described in Section II.2 this limiting value was M/Qh = 7. The reasons for this difference was that in the slab strips the degree of reinforcement μ and the bar diameters were smaller than in the beams (μ = 0·94 % and 12 mm diameter as against μ = 2·07 % and 26 mm). We have already established that the higher the degree of reinforcement and the poorer the bond, i.e. according as the bar diameters are larger, the sooner will shear failures occur. With higher values we could therefore have expected shear failures to occur also in the slab strips for values of M/Qh in excess of 4.

The lowest value of τ_o attained at shear failure, namely 12·6 kg/cm^2, provides an inadequate factor of safety of only 1·58 with respect to the lower shear stress limit of 8 kg/cm^2 (for actual cube strength β_w = 152 kg/cm^2) which, according to DIN 1045, is permissible for a concrete B 160 without analysis of the safety against shear. The same is true of slabs made of concrete B 300 (P8 and P9) which, at failure, attained values of 14·4 and 17·9 kg/cm^2 for τ_o, as compared with a permissible value of 10 kg/cm^2 for this stress.

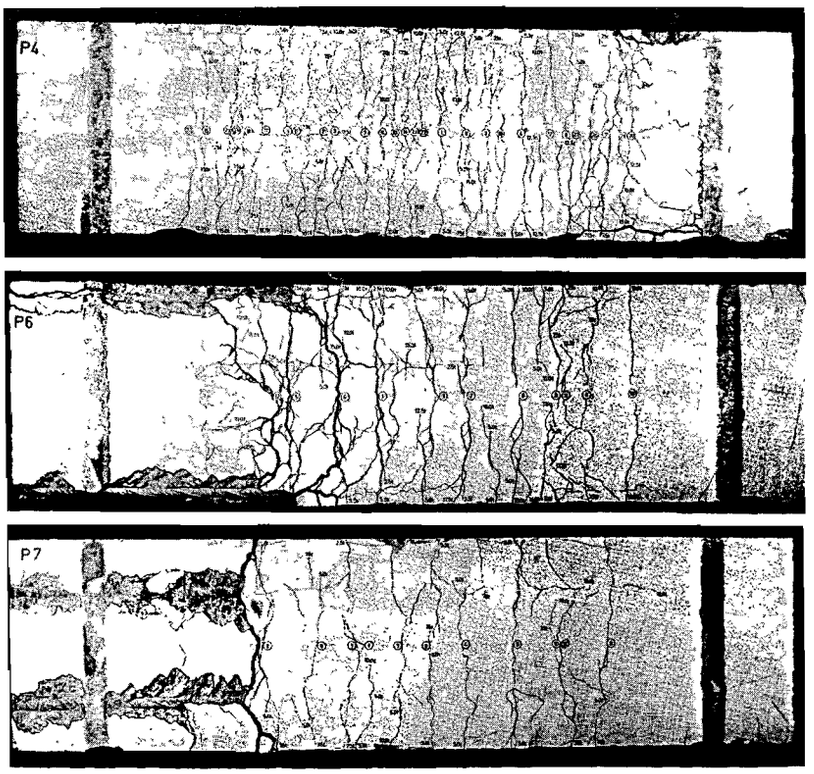

Figure 55: Cracking pattern on underside of slab strips with varying bond conditions: different bar diameters for μ = constant: P4 containing nine 12 mm bars, P6 containing four 18 mm bars, P7 containing two 26 mm bars.

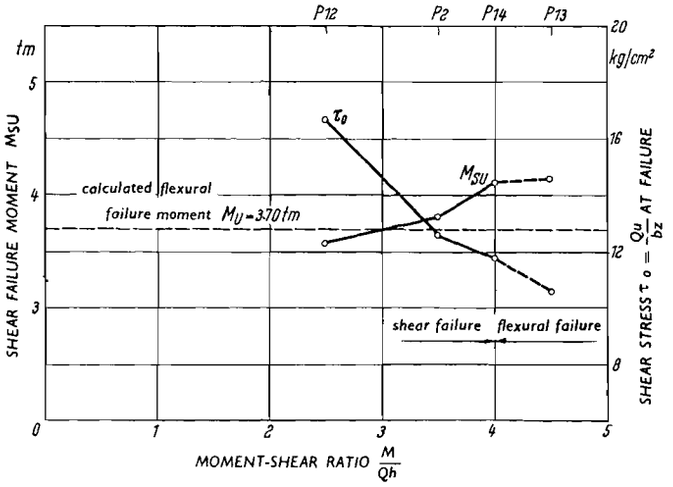

Figure 56: Moments and shear stresses at failure, plotted against M/Qh.

5.53 Effect of the degree of reinforcement

The slabs 1 - 5 with M/Qh = 3·5 and β_w = 155 kg/cm^2 were provided with 3, 6, 7, 9 and 12 ribbed Tor steel bars (12 mm diameter) respectively, corresponding to degrees of reinforcement (steel percentages) of 0·47, 0·95, 1·11, 1·40 and 1·86 %.

Apart from slab P1 with μ = 0·47 %, which failed in bending, shear failures occurred: up to μ = 1·40 %, the shear failure load, and therefore the shear failure moment M_{SU} and the values of τ_o reached at failure, increased steadily. The further increase of μ to 1·86 % did not produce any further increase of shear strength (Figure 57).

It is again apparent that, in addition to Q, the bending moment M also affects the shear failure, the latter being allied to flexural failure so long as final failure is the result of crushing of the compressive zone of the concrete. Here again the shear cracks penetrated more rapidly and farther up towards the compression face of the member than did the cracks in the purely flexural region. Q or ΔM produces high bond stresses along the main reinforcement, which at and after cracking give rise to a certain amount of slip between the steel and the concrete. Eventually this slip becomes greater than in the purely flexural region and causes a distinct "shear rotation". The opening-out of the cracks is, in part, determined by the steel strain, i.e. by the moment.

The steel stresses calculated from the ultimate load are summarized in column 20 of Table XI and in Figure 57. They decrease steadily with increasing μ ; the deformations therefore diminish, so that M_{SU} can increase, since the shear crack does not spread upwards so quickly.

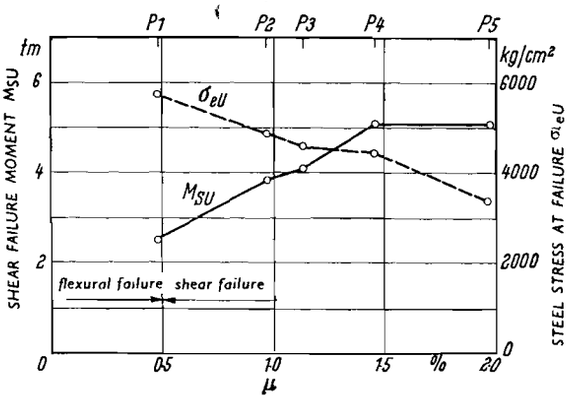

Figure 57: Shear failure moments and steel stresses plotted against the degree of reinforcement (steel percentage μ).

5.54 Effect of bond

In the case of slabs P4, P6 and P7 the bond was varied by using bars differing in diameter, while μ was kept approximately constant at 1·5 % (nine 12 mm bars, steel area F_e = 10·17 cm^2 in P4; four 18 mm bars, F_e = 10·16 cm^2 in P6; two 26 mm bars, F_e = 10·62 cm^2 in P7). The ultimate moments were found to decrease with increasing bar diameter and were 5·04 tm, 4·40 tm and 3·81 tm respectively. Hence the bond quality affects the shear failure load to a significantly higher degree than it affects the flexural failure load. The comparison of the failure loads is not quite conclusive, however, inasmuch as anchorage failures occurred in conjunction with the larger bar diameters (Figure 55). On the other hand, the tendency revealed in these tests is confirmed by the results indicated in Section II.3 and by a comparison of the deflexions and the crack widths.

5.55 Cracking behaviour

In Figures 58 and 59 the maximum crack widths and the total crack widths are shown plotted against the load. As was to be expected, both diagrams reveal a marked increase of the crack widths with increasing bar

diameters for constant μ. The neutral axis must accordingly have moved towards the compression face of the member, which explains the differences in the failure loads.

5.56 Effect of the actual slab thickness or beam depth (similarity investigation)

To supplement the tests for ascertaining the validity of the laws of similarity, as reported in Section II.4, three geometrically similar slabs

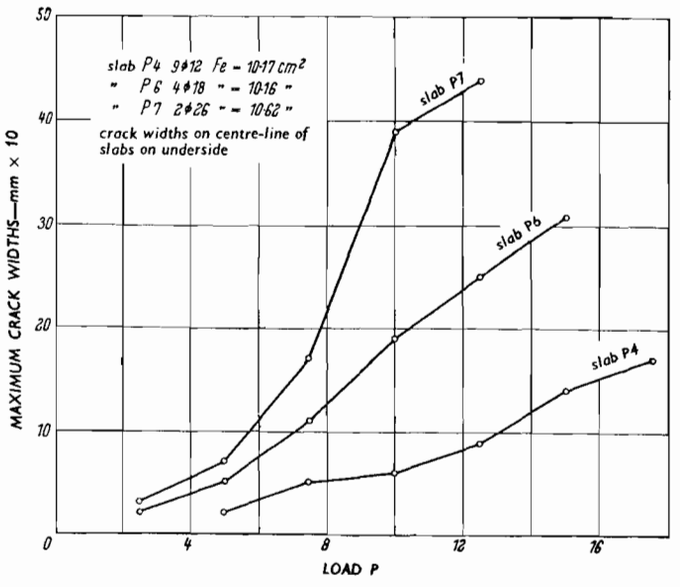

Figure 58: Maximum crack width plotted against load (slab strips with varying bond conditions: different bar diameters with μ constant).

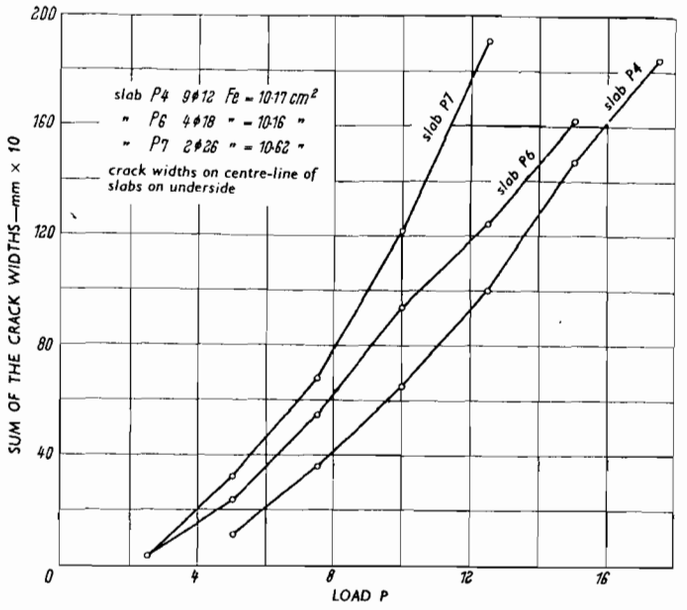

Figure 59: Sum of the crack widths plotted against load (slab strips with varying bond conditions: different bar diameters with μ constant).

P10, P3 and P11, with ratios 5:7:9, were made from the same materials. The slab width was kept constant at 50 cm in all cases, however. The number of bars was varied to suit the similarity ratio, namely five 12 mm bars, seven 12 mm bars and nine 12 mm bars respectively, whereby in all cases a degree of reinforcement of 1·11 % was obtained. Since b is constant, the quality of the bond diminishes with the number of bars, i.e. with the closer spacing of the bars, but with bars of constant diameter this effect is hardly likely to be significant.

According to the laws of similarity (see Section II.4) the stresses (and more particularly τ_o) producing failure should be constant for slabs with equal bond properties (constant bar diameter). This was indeed found to be approximately the case. However, the ratios of the values of τ_o for P10, P3 and P11 are 13·8:13·6:13·3 kg/cm^2, which corresponds also to the shear failure moments as related to bh^2, and thus exhibit a slight decrease with increasing effective depth.

5.57 Effect of concrete quality

For slabs P2 and P5, made of class B 150 concrete, comparison tests with slabs made of B 300 concrete were carried out (slabs P8 and P9 respectively). The failure loads (Table XI) clearly indicate how little the shear strength (ultimate strength of the member in shear) increased as a result of using concrete with twice as high a strength (Figure 60): in the case of the slabs with μ = 0·93 % (P2 and P8) the increase in shear strength was only 20 %, and in the case of the slabs with μ = 1·86 % (P5 and P9) the increase was as little as 5 %. From theoretical considerations and also on the evidence of other tests (19), however, we should expect to have obtained an increase in shear strength proportional to about $\sqrt{\beta_w}$ (where β_w denotes the cube strength of the concrete). Comparison with the results of the beam tests reported in II.2 and II.3 shows that the failure loads obtained with B 300 concrete are by no means too low, but that, on the contrary, the slabs made of B 150 concrete had unusually high shear strengths: according to Figure 32 of Section II.2 a shear stress τ_o = 16·1 kg/cm^2 at failure could be expected for a beam with μ = 2·07 %, 26 mm diameter bar, β_w = 350 kg/cm^2 and M/Qh = 3·5; slab P9 with μ = 1·86 %, 12 mm diameter bar, β_w = 306 kg/cm^2 and M/Qh = 3·5 is comparable to that beam, but exhibits a stress τ_o = 17·9 kg/cm^2 at failure, despite the lower concrete strength. The corresponding slab P5 with β_w = 152 kg/cm^2 attained a stress τ_o = 17·0 kg/cm^2 which, in comparison with the other slab tests, is even rather on the low side.

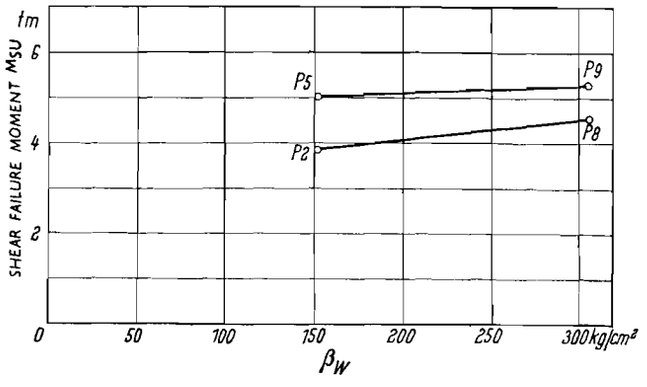

Figure 60: Shear failure moments plotted against cube strength of the concrete.

From this it must be inferred that the usual ratio of the cube strength to the strength of the flexural compressive zone with shear is not borne out for the concrete B 150 made with basalt chippings, as used in these tests. This is probably due to the greater plastic deformability of this concrete. It is also confirmed by the results obtained with the slab strips that failed in bending: for these the measured failure loads were approximately 20 % higher than the values calculated with max. $\varepsilon_b = 0{\cdot}3$ % and $\beta_p = 0{\cdot}85\ \beta_w$. Also, the bond action may have been increased as a result of interlocking of the sharp basalt chippings with the ribs of the steel.

It also appears from these tests that the shear strength of slab strips, even under concentrated load, is greater than that of beams. Notwithstanding this higher strength, the slabs P8 and P9 with $\tau_o = 14{\cdot}4$ and $17{\cdot}9$ kg/cm^2 provide too low a factor of shear safety in relation to the permissible value of 10 kg/cm^2 for B 300 according to DIN 1045.

5.58 Deflexions

The results of the deflexion measurements - in each case for one particular variable - are indicated in Figures 61, 62 and 63. The values calculated from M alone, according to reference 13, are shown as broken lines. Again the measured deflexion fails to attain the calculated value in the lower stages of loading, whereas with increasing load the measured values far exceed the calculated ones, owing to shear deformation.

Figure 61 shows that the deflexion increases with decreasing degree of reinforcement (as expected), this effect being particularly pronounced in this case since the degree of reinforcement was varied only by varying the number of bars but not by varying the bar diameters, so that the bond properties were hardly altered.

The deflexions for varying qualities of bond are plotted in Figure 62. They clearly increase for decreasing bond quality associated with increasing bar diameter, the degree of reinforcement being kept unchanged. This corresponds to the observed crack widths (Figures 58 and 59). The slabs containing a small number of relatively large diameter bars exhibited few and wide cracks, which caused the larger deformations.

In Figure 63 the deflexions of slabs of various concrete strengths are compared with one another, viz. the two slab pairs P2 and P8 with $\mu \simeq 0{\cdot}9$ % and P5 and P9 with $\mu = 1{\cdot}86$ %. In both cases the deflexions for concrete B 150 are much greater than for B 300, which is attributable to differences in the stress-strain diagram and flexural strength of the concrete and to differences in the bond quality.

5.59 Safety related to permissible bending moment

From column 19 of Table XI it is seen that, despite the sometimes lower τ_o, the shear failure load is invariably above 2·1 times the permissible working load associated with flexural design according to DIN 1045. On comparing the shear failure moment (column 15) with the calculated ultimate moment (column 21), we find that only two of the former values - for P6 and P7 - are below the latter, and these correspond to the anchorage failures. Despite the low τ_o, therefore, the safety against shear failure is not far below the safety against flexural failure. The actual flexural failure moments were in this case, however, substantially higher than the calculated ones (up to about 20 % higher), this being due to the above-mentioned properties of the concrete made with basalt chippings.

It must be pointed out, however, that the safety against shear failure proves to be considerably lower if the reinforcement is not fully continued up to the bearings but is, instead, curtailed so as to correspond to the bending moment diagram.

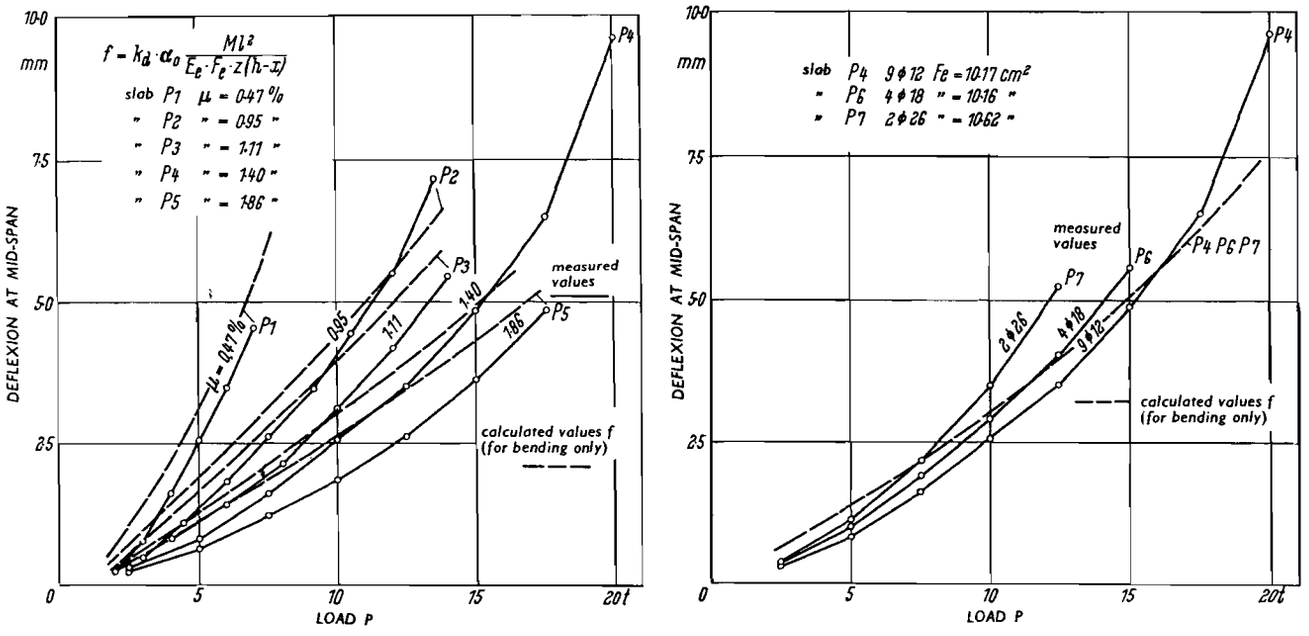

Figure 61 (left): Measured and calculated deflexions of slab strips with different steel percentages μ.

Figure 62 (right): Measured and calculated deflexions of slab strips with varying bond conditions (different bar diameters and μ constant).

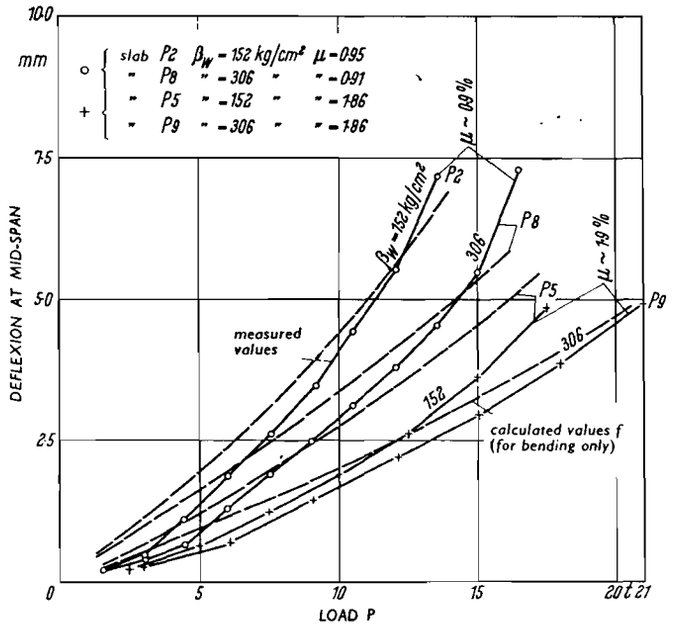

Figure 63: Measured and calculated deflexions of slab strips with varying concrete strengths.

6. Tests on rectangular beams with various types of shear reinforcement

6.1 INTRODUCTION

The shear tests described in Section II.1 showed the considerable effect of the slope of the stirrups on the shear failure load and shear deformations of thin-webbed T-beams. By means of the following series of tests this effect was investigated for rectangular beams. In these tests vertical stirrups and stirrups inclined at 45° with two different spacings were compared, as were also bent-up bars (which in each case were designed for the same shear force as the stirrups). The tests in question were of a tentative character.

6.2 TEST SPECIMENS

The series comprised seven beams subjected to concentrated loads and four beams with uniformly distributed load, the ratio l/h being approximately 7·4 (see the accompanying Table).

Type of loading	Designation	Shear Reinforcement
Concentrated	E 1	Bent-up bars inclined at 45°
	E 2	Inclined stirrups 45° widely spaced
	E 3	Inclined stirrups 45° closely spaced
	E 4	Vertical stirrups widely spaced
	E 5/1	Vertical stirrups closely spaced
	E 5/2	Vertical stirrups closely spaced
	E 6	Without shear reinforcement (for comparison)
Uniformly distributed load	G 1	Bent-up bars inclined at 45°
	G 3	Inclined stirrups 45° closely spaced
	G 5	Vertical stirrups closely spaced
	G 6	Without shear reinforcement

The beams designated "E" and "G" and bearing the same numbers were provided with exactly the same reinforcement, with constant spacing of the stirrups or bent-up bars. For uniformly loaded beams the shear reinforcement was therefore not progressively varied along the beam so as to correspond to the magnitude of the shear force.

6.21 Dimensions and reinforcement

All the beams were equal in respect of their dimensions and of the

longitudinal reinforcement (Figure 64 and Table XIII). In view of the degree of reinforcement (percentage of steel) provided (2·47 %), failure of the compressive zone could be expected to occur before the tensile bars reached their yield point. The bars had been given the ample anchorage length of 50 cm to obviate anchorage failure.

All the beams were intended to have the same degree of shear reinforcement: $\mu_s = F_{es}/b\ a \sin \gamma$. The differences presented by μ_s in Table XIII, columns 5 and 6, are due to the fact that the actual measured section properties differed considerably from the nominal values. In all cases the stirrups consist of ribbed Tor steel (steel IIIb) on one side of mid-span, and of plain round steel bars (steel I) on the other side. Hence the load-carrying capacities of the stirrups on the two sides were approximately in proportion to the yield point values of the types of steel employed, namely 2·6/4·3 = 0·6.

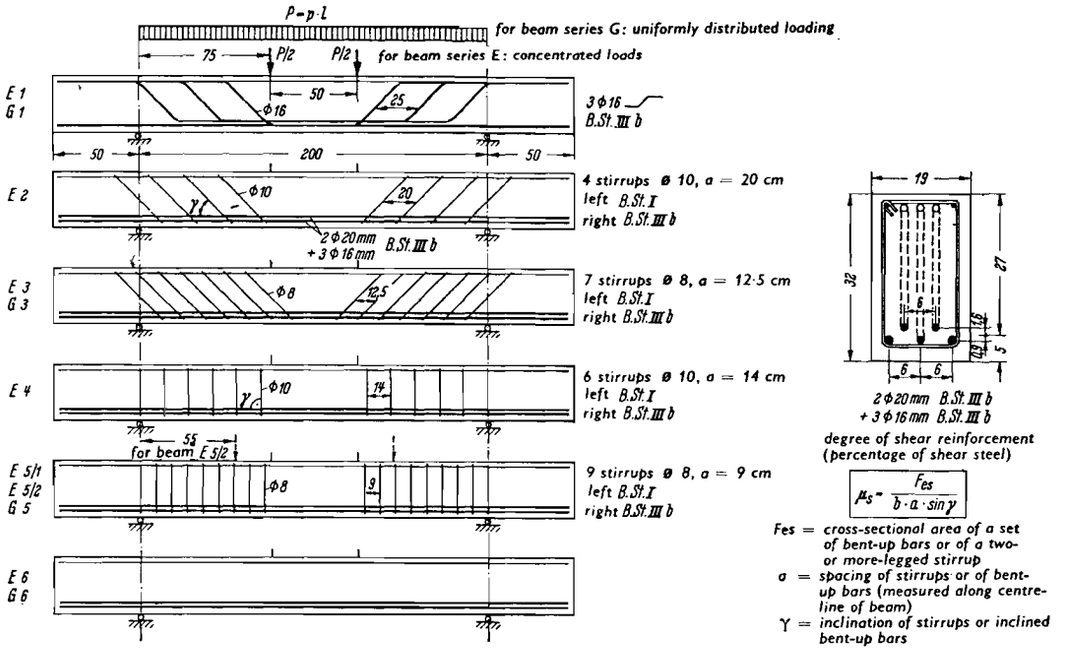

Figure 64: Dimensions and reinforcement of the beams with varying shear reinforcement.

In beams E1 and G1 the shear reinforcement on each side consisted of three bent-up bars of 16 mm diameter (steel IIIb), producing a double system of struts. No stirrups were provided, although the codes of practice insist that they be present in beams; the object was to investigate the effects of bent-up bars and stirrups separately.

Beam E2 was reinforced with 10 mm diameter stirrups inclined at 45° and spaced at 20 cm centres. The stirrups were closed at the top and tied to two auxiliary bars (steel IIIb) of 10 mm diameter. At the bottom the stirrups enclosed the 20 mm diameter main reinforcing bars, to which they were likewise connected only by tying with wire. Beams E3 and G3 were provided with 8 mm diameter stirrups spaced 12·5 cm apart and inclined at 45°.

Beam E4 had vertical stirrups of 10 mm diameter spaced at 14 cm centres (= approx. 20 cm/ $\sqrt{2}$), while beams E5 and G5 had vertical stirrups of 8 mm diameter at 9 cm centres (= approx. 12·5 cm/ $\sqrt{2}$).

The "control" beams E6 and G6 had no shear reinforcement.

TABLE XIII: Summary of shear tests with various types of shear reinforcement.

Dimensions: l = 2·00 m; b = 19 cm; d = 32 cm; h = 27 cm Tensile reinforcement: 2 x 20 mm + 3 x 16 mm Grade IIIb; μ = 2·47% Compressive reinforcement: 2 x 10 mm Grade IIIb; μ' = 0·33%

1	2	3	4	5	6	7	8	9	10	11	12	13	14	15	16	17	18	19	20	21	22	23	24	25
								Working load conditions								Cracking load					Failure conditions				
Designation	Load	Shear reinforcement left Grade I	Shear reinforcement right Grade IIIb	Proportion of shear reinforcement $\mu_s = \frac{F_{es}}{b\ a\ \sin\gamma}$ left (%)	Proportion of shear reinforcement right (%)	Quality of concrete β_w (kg/cm^2)	Permiss. σ_b (extrapolated) in accordance with β_w (kg/cm^2)	M_{g+p} (1) (tm)	P_{g+p} (t)	σ_e under g + p (kg/cm^2)	max τ_o (kg/cm^2)	calculated σ_{es} (Shear reinforcement) left (kg/cm^2)	calculated σ_{es} (Shear reinforcement) right (kg/cm^2)	permiss. σ_{es} / calculated σ_{es} left (kg/cm^2)	permiss. σ_{es} / calculated σ_{es} right (kg/cm^2)	M_{crack} (bending) (tm)	σ_{bz} of the beam (kg/cm^2)	P_U (t)	M_U (tm)	τ_o (kg/cm^2)	calculated σ_{es} left (kg/cm^2)	calculated σ_{es} right (kg/cm^2)	$s = \frac{M_U}{M_{g+p}}$	Type and cause of failure
E 1	Concentrated load $\frac{a}{h} = \frac{75}{27} = 2{\cdot}78$	3 x 16 mm Grade IIIb inclined at 45°		0·59	0·59	336	109	3·96	10·56	1415	12·6	2140		1·12		1·90	45·5	34·1	12·79	40·5	6860		3·23	Shear failure Crushing of compressive zone beside load.
E 2		45° stirrups 10 mm diameter a = 20 cm	a = 20 cm	0·60	0·63	380	120	4·35	11·60	1555	13·8	2300	2190	0·61	1·10	1·48	36·4	39·0 (37·2)(3)	14·62	46·5	– (6750)(4)	7380	F 3·37 (S 3·22)	Shear failure on side with stirrups Grade I at 34·1 tons; after "bandaging", flexural failure at mid-span.
E 3		45° stirrups 8 mm diameter a = 12·5 cm	a = 12·5 cm	0·54	0·72	352	112	4·06	10·80	1450	12·9	2400	1800	0·58	1·33	1·55	37·0	37·7 (37·2)(3)	14·12	44·9	– (8250)(4)	5160	F 3·48 (S 3·44)	Shear failure on side with stirrups Grade I at 37·2 tons; after "bandaging", flexural failure at mid-span.
E 4		Vertical stirrups 10 mm diameter a = 14 cm	a = 14 cm	0·60	0·64	380	120	4·35	11·60	1555	13·8	2300	2160	0·61	1·34	2·10	50·1	37·5	14·06	44·6	7430	6960	3·23	Flexural failure
E 5/1		Vertical stirrups 8 mm diameter a = 9 cm	a = 9 cm	0·53	0·71	380	120	4·35	11·60	1555	13·8	2600	1950	0·54	1·23	1·55	37·0	37·8	14·18	45·0	8490	6340	3·26	Flexural failure
E 6				–	–	352	112	4·06	10·80	1450	12·9	–	–	–	–	1·55	37·0	18·6	6·98	22·1	–	–	1·72	Shear failure (no shear reinforcement)
E 5/2	$\frac{a}{h}$ = 2·04	Vertical stirrups 8 mm diameter a = 9 cm	a = 9 cm	0·53	0·71	352	112	4·06	14·76	1450	17·6	3320	2480	0·42	0·97	2·01	48·0	52·8 (34·1)(3)(5)	14·25	62·8	– (7650)(4)	8840	F 3·51 (S 2·31)(5)	Shear failure on side with stirrups Grade I at 34·1 tons; after "bandaging", flexural failure at mid-span.
G 1	Uniformly distributed load $\frac{l}{h} = \frac{200}{27} = 7{\cdot}4$	3 x 16 mm Grade IIIb inclined at 45°		0·59	0·59	380	120	4·35	17·40	1555	20·7	3040(2) (1750)(3)		0·79(2)		2·01	48·0	61·5	15·38	73·2	10700(2)		3·53	Flexural failure
G 3		45° stirrups 8 mm diameter a = 12·5 cm	a = 12·5 cm	0·54	0·72	332	108	3·92	15·68	1400	18·7	3000(2) (1730)(3)	2250(2) (1300)(3)	0·47	1·06	1·53	36·5	60·2	15·05	71·6	11450(2)	8600(2)	3·84	Flexural failure
G 5		Vertical stirrups 8 mm diameter a = 9 cm	a = 9 cm	0·53	0·71	332	108	3·92	15·68	1400	18·7	3050(2) (1760)(3)	2280(2) (1320)(3)	0·46	1·05	1·55	37·0	59·3	14·83	70·5	11500(2)	8580(2)	3·79	Flexural failure
G 6		–		–	–	332	108	3·92	15·68	1400	18·7	–	–	–	–	2·62	62·6	40·1	10·03	47·8	–	–	2·56	Shear failure (no shear reinforcement)

(1) Compressive reinforcement taken into account.

(2) Calculated at distance $\frac{1}{4}h$ from bearing.

(3) Average stirrup stress.

(4) After yielding of the stirrups had occurred on the side with Grade I (wide shear cracks), the beam was "bandaged" on this side.

(5) "Bandaged" too early. Shear failure load would probably have been substantially higher.

*F = flexural failure; S = shear failure.

6.22 Working load and associated stresses

The working load P_{g+p} and the moment M_{g+p} associated with it (Table XIII, columns 9 and 10) were determined by means of the conventional theory of reinforced concrete (modular ratio n = 15) for the condition that the permissible concrete stress (permiss. σ_b) due to bending would be attained. As the concrete strength of the beams was higher than the value β_w = 300 kg/cm^2 (cube strength) envisaged in DIN 1045, the values adopted for permiss. σ_b were obtained by linear extrapolation in proportion to the actual cube strength. The auxiliary bars installed at the top of the beam (two 10 mm diameter bars, steel IIIb) were taken into account in the stress analysis. The stresses calculated with this working load are indicated in columns 11 - 14 of Table XIII.

The theoretical stirrup stresses are obtained from the relation:

$$\sigma_{es} = \tau_o / \mu_s$$

For beams subjected to concentrated load the theoretical stresses σ_{es} in the stirrup steel are constant over the entire shear zone (τ_o = constant; μ_s = constant), whereas with uniformly distributed load the stress in the shear reinforcement varies from section to section (τ_o = variable; μ_s = constant). The σ_{es} values in Table XIII (columns 13 and 14) relate to the section at a distance h/2 from the bearing. For comparison the average values over the whole shear region are given in parentheses. On comparing with the permissible stirrup stresses, viz. permiss.σ_{es} /calcul. σ_{es}(columns 15 and 16), we see that the Tor steel stirrups (steel IIIb) can be rated as providing full safeguard for shear in accordance with the requirements of DIN 1045, whereas with the stirrups of steel I only 40 - 60 % of the full shear safeguard is obtained.

6.23 Manufacture of the beams

The beams were cast in steel moulds and their external dimensions were consequently accurate to within ± 1 mm. They were concreted four at a time, the batches from the 150-litre pan-type mixer being equally distributed over the four beams. At the same time, sixteen 20 cm cubes and sixteen 10 x 10 x 53 prisms were cast. The concrete was compacted by means of an internal vibrator of 5 cm diameter. The tensile reinforcement was at the bottom of the mould during concreting.

The beams, cubes and prisms were demoulded after 2 days and kept moist under wet cloths at about 18° C for 7 days. The beams were then stored at about 18° and 60 % relative humidity and were tested at between 27 and 30 days of age.

6.24 Materials

Steel. The properties of the steel employed are indicated in Table XIV. In some cases the cross-sections differ significantly from the nominal value (up to 22 %), which has been taken into account in the calculated values stated in Table XIII.

TABLE XIV: Characteristics of the steels employed.

Designation	Nominal diameter (mm)	Theoretical cross-sectional area (mm^2)	Cross-sectional area	Yield point β_S (kg/mm^2)	0·2% Proof stress $\beta_{0·2}$ (kg/mm^2)	Tensile strength β_Z (kg/mm^2)	Ultimate strain β_{10} (%)
Round steel bars	8	50·3	45·4	27·3		38·0	24
(BSt I)	10	78·5	80·1	26·1		36·5	36
Ribbed Tor steel	8	50·3	61·0(1)	-	46·5	57·8	15·6
(BSt IIIb)	10	78·5	85·3(1)	-	43·0	52·6	15·4
	16	201	199(1)	-	43·3	54·0	13·6
	20	314	334(1)	-	43·4	52·2	-(2)

(1) Determined from the weights of the test bars with assumed specific gravity of 7·80.

(2) Repeated fracture at gripping jaws.

Concrete

Composition of the concrete

Aggregates: grading (grading curve E, DIN 1054)	0 - 3 mm	43 %
	3 - 7 mm	17 %
	7 - 15 mm	22 %
	15 - 30 mm	18 %
Cement: Portland cement (PZ 475)		289 kg/m^3
Water:		216 litres/m^3
Water/cement ratio:		0·75
Bulk density:		2310 kg/m^3

28-day concrete strengths (each value is an average of 12 to 16 individual values)

(β_w = cube strength; β_{bz} = flexural strength)

	Strength (kg/cm^2)	Coefficient of* variation (%)
Beams E 1, E 3, E 5/2, E 6	β_w = 348	4·8
	β_{bz} = 46·3	6·9

* ($V = \frac{1}{\beta_m}\sqrt{\frac{(\beta - \beta_m)^2}{n - 1}}$)

Beams E 2, E 4, E 5/1, G 1	β_w = 380	3·0
	β_{bz} 41·5	6·8
Beams G 3, G 5, G 6	β_w = 332	4·6
	β_{bz} 41·1	8·4

6.3 TESTING PROCEDURE

The loading and bearing conditions for the beams were the same as those adopted in the beam tests described in Section II.2 or II.3.

The beams "E", which exhibited imminent shear failure on the side reinforced with stirrups of steel I in consequence of excessive widening of the shear cracks, were unloaded and locally "bandaged" by means of tensioned vertical rods (Figure 65). These beams were then subjected to further loading up to failure, which - because of the "full safeguard against shear failure" provided by stirrups on the other side - invariably took the form of flexural failure.

The incremental stages of loading adopted were P = 3·1 tons for concentrated load and p_l = 6.2 tons for uniformly distributed load.

The following were measured: cracking loads, failure loads, crack widths at the level of the centroid of the tensile reinforcement, crack widths at mid-depth of the beam in the shear region, and deflexions at the mid-span and quarter-span points.

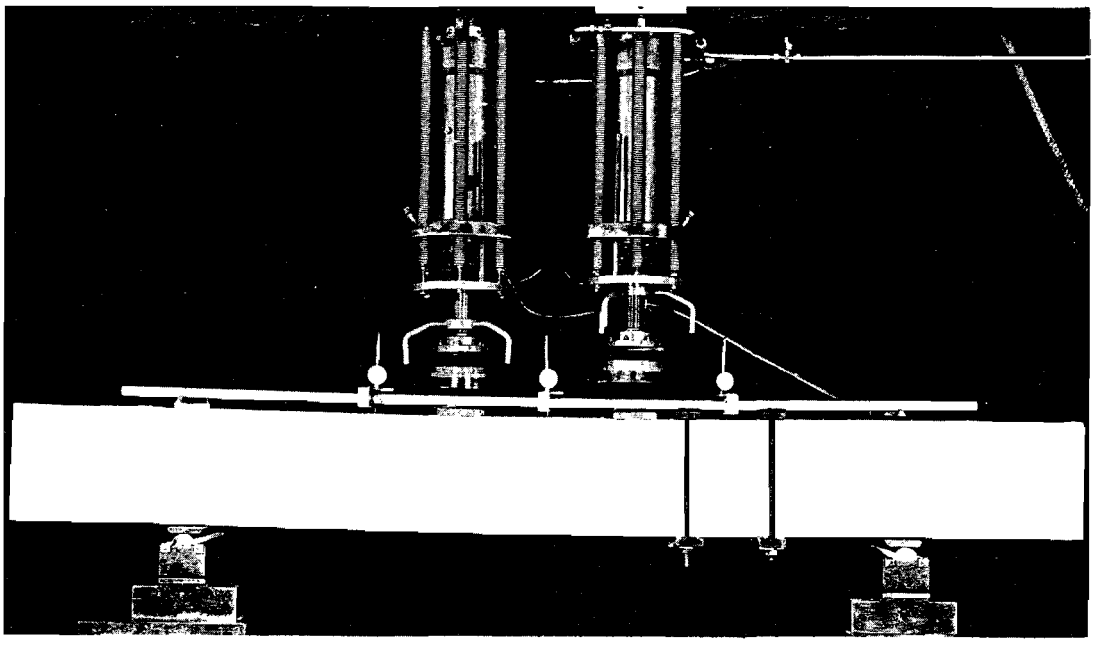

Figure 65: Testing arrangement. When the main shear crack had opened wide on the side of the beam provided with stirrups of steel St I, the beam was "bandaged" and further loaded up to failure.

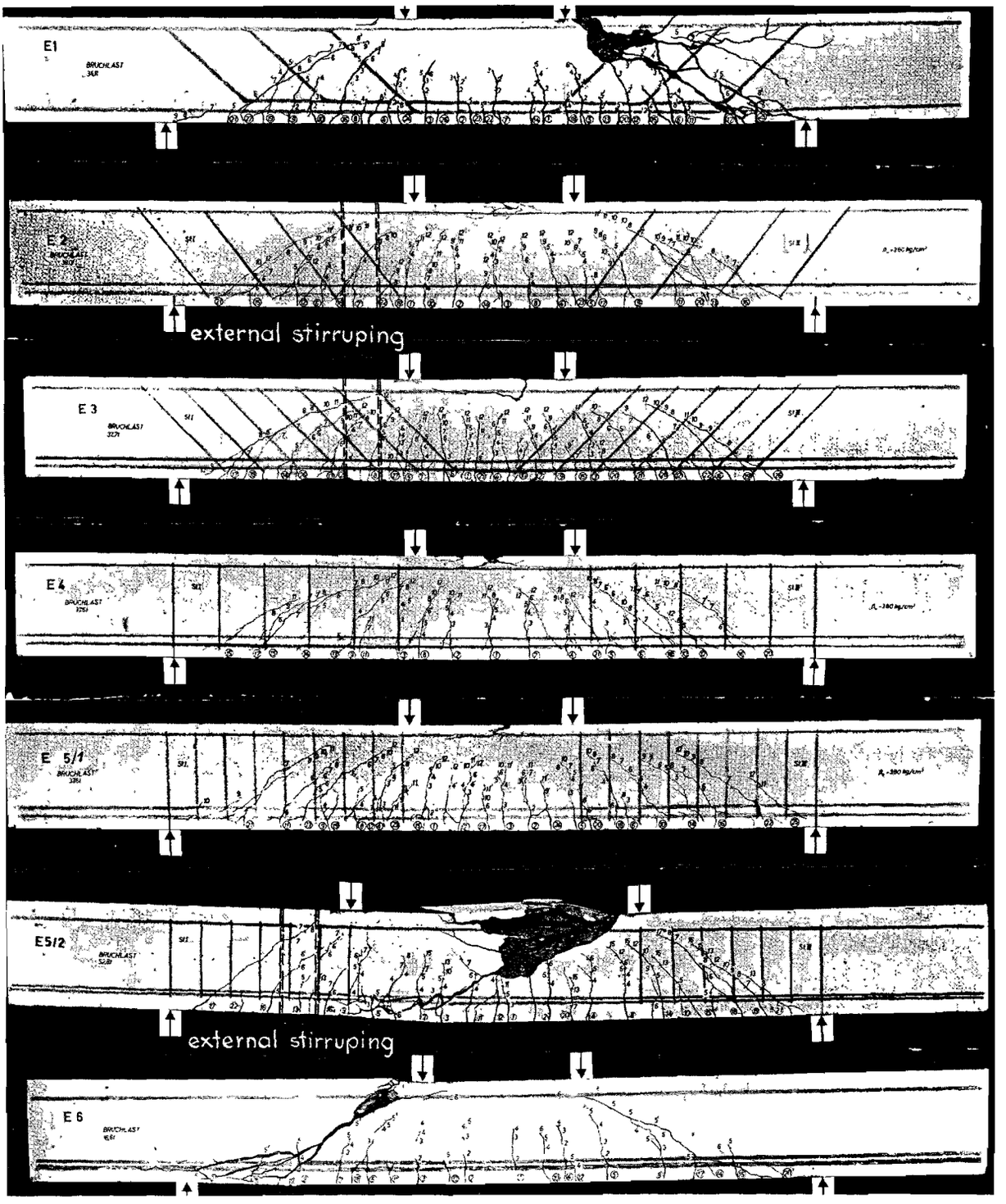

Figure 66: Cracking and fracture patterns of the concentrated-load beams with different shear reinforcements. (Figures in circles are serial numbers of cracks; other figures denote loading state at which a crack penetrated up to the point indicated: loading stage P = 3·1 tons.)

6.4 RESULTS

6.41 Failure load and cause of failure for beams subjected to concentrated loads

The failure patterns for the beams subjected to concentrated loads (Figure 66) - except beams E1 and E6 - exhibit flexural failure, though in the case of beams E2, E3 and E5/2 shear failure was prevented only by bandaging the beams on the side reinforced with stirrups of steel I.

In the case of beam E1 (bent-up bars) shear failure occurred: the compressive concrete zone crushed beside the load, over the principal shear crack, although the shear reinforcement had been adequately designed in compliance with DIN 1045 (cf. Table XIII, column 15/16, row 1). The failure of the beam is attributable to the unfavourable distribution of the inclined bars in the cross-section (in the case of bent-up bars), to the absence of stirrups with their lateral restraining action, and to the weakening of the tensile side of the beam due to the bending-up of main bars.

In beam E2 the side reinforced with inclined stirrups of steel I developed wide shear cracks at a load P = 37·2 tons, so that this value can be taken as approximately representing the shear failure load. After the beam had been bandaged, flexural failure occurred at P = 39·0 tons.

In beam E3, yielding of the inclined stirrups of steel I began to occur at P = 37·2 tons. After the beam had been bandaged, failure occurred at 37·7 tons. Hence the more closely spaced stirrups of steel I in this beam were almost adequate to ensure flexural failure, even though they provided only 0·58 of the "safeguard against shear failure" required by DIN 1045.

The fact that beam E3, despite its lower concrete strength and smaller μ_s, was able to develop a somewhat higher shear strength than beam E2, emphasizes the favourable effect of closer stirrup spacing. The stirrups, with their lateral restraining action, extended somewhat closer to the zone endangered by the load.

In the case of beams E4 and E5/1 with vertical stirrups the flexural failure load was reached without having to bandage the beam. Hence the vertical stirrups of steel I produced a higher shear strength than the corresponding inclined stirrups were able to do. This is because the shear compressive zone, which here determines failure, is more effectively restrained by vertical stirrups than by inclined ones. Furthermore, it appears from the equilibrium conditions (Section II.1, Figure 15) that the resultant thrust for vertical stirrups is smaller than for inclined stirrups (by an amount Q/2), so that the shear compressive zone is less severely stressed.

In the testing of beam E5/2 the load was applied at a distance a = 0·55 m from the bearing, i.e. a/h = 2. The left-hand side of the beam (containing stirrups of steel I) was bandaged at a load P = 34·1 tons. This was obviously somewhat premature, since - on account of the lower a/h = M/Qh - a shear failure load higher than that for E5/1 was to be expected. The deformations and cracks also show that shear failure was not yet imminent at 34·1 tons. The failure load P_U = 52·8 tons produced approximately the same flexural failure moment as in the other beams. After the flexural compressive zone had failed, an additional diagonal crack developed in the stirrupless region between the loads.

Beam E6, which contained no shear reinforcement, failed at a load of 18·6 tons. This was a case of shear failure by crushing of the compressive zone beside one of the loads.

Beams subjected to uniformly distributed loading

The failure patterns for these beams are shown in Figure 67. The beams provided with shear reinforcement all failed at about the same load $p\ell$ = 60 tons (flexural failure). In the case of beam G5 - just as in E5/2 - an oblique crack developed in the stirrupless region after flexural failure had occurred. In beam G6, shear failure took place at $p\ell$ = 40·1 tons as a result of crushing of the compressive zone at a distance of between 2 h and 2·5 h from the bearing.

Whereas in the case of the concentrated-load beams which failed in bending an average value of 3·37 was obtained for the quotient s = flexural failure load / permissible working load, this quotient attained a value of 3·72 in the case of the beams with uniformly distributed loading. Here again we thus observe the strengthening effect exercised by the pressure applied along the top of the beam with regard to the compressive strength of the concrete in bending.

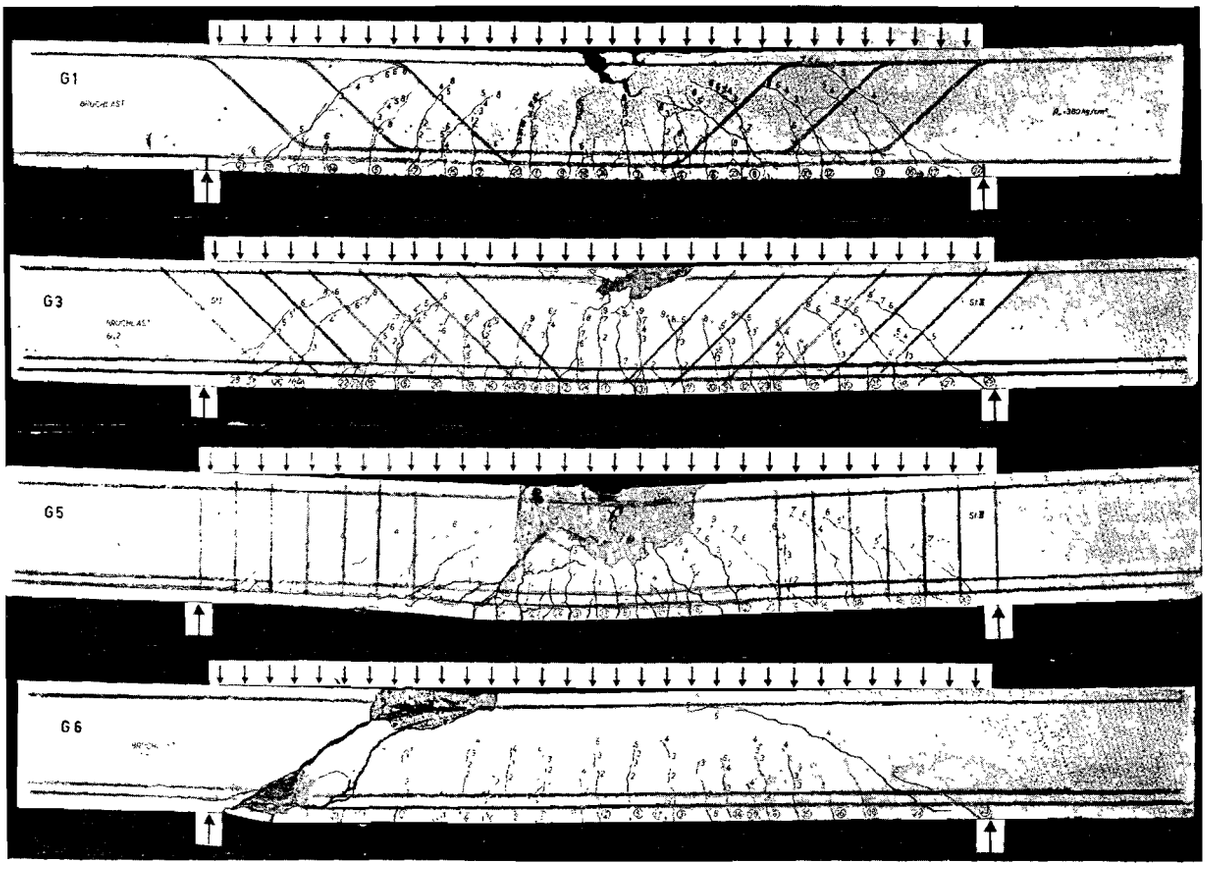

Figure 67: Cracking and fracture patterns of the uniformly loaded beams with different shear reinforcement. (Figures in circles are serial numbers of cracks; other figures denote loading stage at which a crack penetrated to the point indicated; loading stage $p\ell$ = 6·2 tons.)

6.42 Cracking behaviour of the beams

The first flexural crack occurred at approximately the same value of the load in all the beams, from which an average value of 43·2 kg/cm^2 is

calculated for the flexural (tensile) strength of the concrete (the effect of the tensile and the compressive reinforcement being taken into account by the adoption of a modular ratio n = 7·5): see Table XIII, column 18. The test prisms loaded in bending gave the same value, namely β_{bz} = 43·0 kg/cm^2.

All the beams exhibited almost the same behaviour of the flexural cracks up to failure. There were, however, differences in cracking behaviour in the shear zone for the different types of shear reinforcement.

The different grades of steel used for the stirrups result in differences in the total crack widths only at stresses beyond the yield point of steel I (Figure 68). The direction and spacing of the stirrups already affect the crack widths at working load, viz. both at the level of the tensile reinforcement and also at mid-depth of the beam (at h/2) (Figure 69).

The most favourable cracking behaviour was exhibited by beams E3 and G3 with closely spaced stirrups at 45° (Figure 69). Of the concentrated-load beams, E2 (inclined stirrups, widely spaced), E5/2 (vertical stirrups, closely spaced) and E4 (vertical stirrups, widely spaced) showed approximately the same crack widths (at the bottom of the beam).

Beam E1, with three bent-up bars, exhibited the largest total crack width. This is attributable to the unfavourable distribution of the shear reinforcement in the cross-section and also to the weakening of the tensile zone and the consequently greater amount of strain at the beginning of the shear cracks.

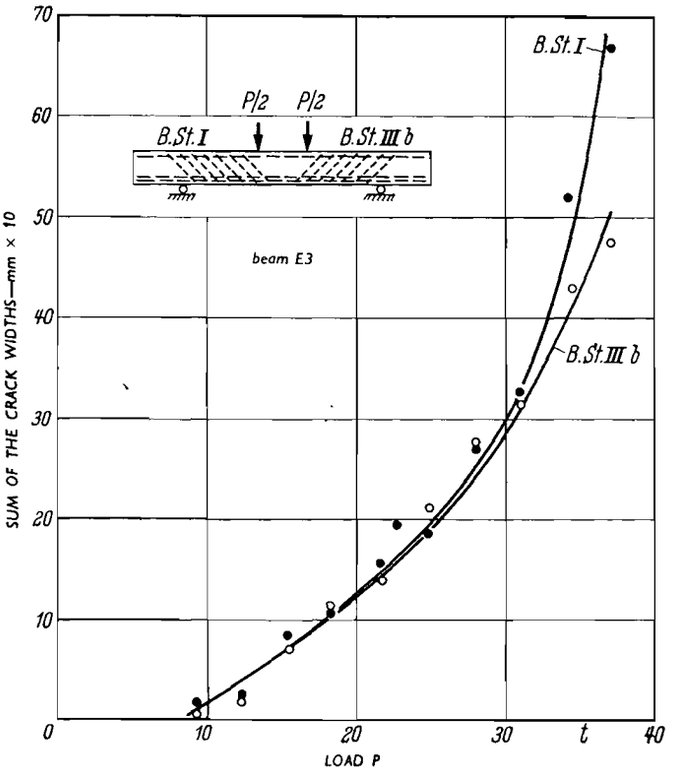

Figure 68: Comparison of the sum of the crack widths in the shear zone for stirrups of St I and of St IIIb in the case of beam E3 (measured at level of tensile reinforcement).

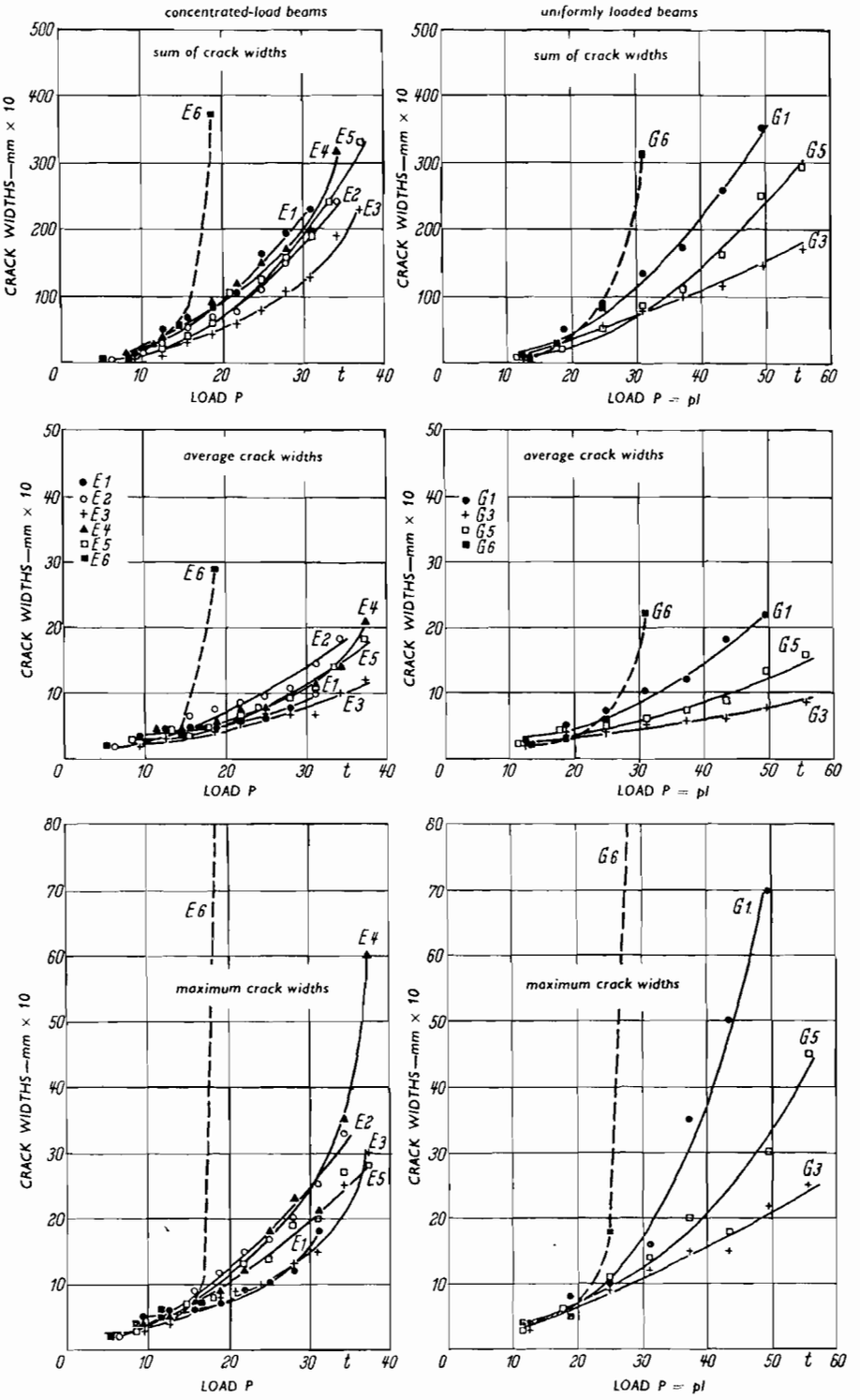

Figure 69: Crack widths (measured at level of longitudinal reinforcement). Total average values of the left-hand and right-hand shear regions, including those cases where different grades of stirrup were used on either side.

With uniformly distributed loading the differences in the crack widths between the various types of shear reinforcement were more pronounced than with uniformly distributed loads (Figure 69).

Under working load the maximum crack widths in all the beams were approx imately 0·04 to 0·08 mm and were therefore below 0·2 mm, which is considered to be the limiting permissible value.

The characteristics of the crack widths in different beams at mid-depth are hardly different from those at the level of the reinforcement: at the lower stages of loading, however, the cracks at the bottom of the beams were substantially wider than at h/2 (more than twice as wide on average). In this report these values are given in comparison with the bottom crack widths for beam E2 only (Figure 70). Whereas the crack widths on the side of the beam provided with stirrups of steel IIIb showed an approximately linear increase up to the upper stages of loading, in the case of stirrups of steel I they increased very rapidly from about P = 30 tons onwards, owing to the fact that the yield point of the steel was exceeded.

At high loads the crack widths at h/2 increased more rapidly than at the level of the tensile reinforcement in the beams with stirrups of steel IIIb also.

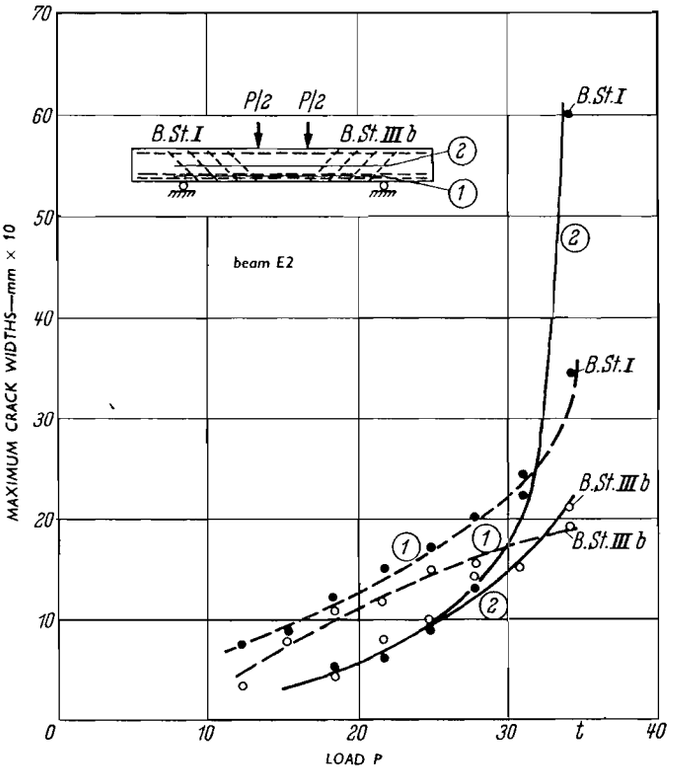

Figure 70: Comparison of the maximum crack widths for stirrups of St I and St IIIb, measured at the level of the tensile reinforcement (1) and at mid-depth of the beam (2).

6.43 Stirrup stresses and anchorage of the stirrups

Although the strains in the stirrups were not measured in this series of tests, the loads at which the yield point was reached in the stirrups of steel I provide a criterion for the stress in the stirrups. The stirrup stress was calculated for these loads (Table XIII, column 22). The ratio of this calculated value to the yield point shows that the stirrups of steel I were subjected to only about 1/3 of the calculated stress. Further indications as to the stirrup stresses will be obtained in Section 7 of this report.

The higher strength of the stirrups consisting of steel IIIb had a favourable effect.

The stirrups inclined at 45° exhibited no slip relative to the ribbed longitudinal reinforcing steel at their anchorages in the tensile zone of the beam. This observation is of some importance, the more so as there was, in these tests, no additional transverse reinforcement in the tensile zone, as distinct from the test beams referred to in Section II.1.

6.44 Deflexions

In the case of the concentrated-load beams the different kinds of shear reinforcement hardly affect the deflexion (Figure 71). At moderate shear stresses the effect of shear deformation on the deflexion of the beam is still only slight.

The deflexions of the beams with uniformly distributed loading are seen to be somewhat smaller with inclined stirrups than with vertical stirrups (Figure 72), while the beam with bent-up bars is clearly found to have the largest deflexion.

In the case of beams E6 and G6 the development of the shear crack was followed by rapidly increasing deflexions due to shear deformation, which at failure had attained about the same magnitude as the flexural deformation.

6.5 PROVISIONAL CONCLUSIONS

Although the tests in the present series are merely of a preliminary and tentative character, they indicate that the efficiency of the various types of shear reinforcement can be classified according to the following scale (in descending order of efficiency):

1. inclined stirrups, closely spaced
2. vertical stirrups, closely spaced
3. inclined stirrups, normal spacing
4. vertical stirrups, normal spacing
5. inclined bent-up bars

The first shear tests by C. Bach and O. Graf in 1909 already showed [20] that the greatest increase in the shear strength of a member is obtained with closely spaced thin stirrups. In beams having a depth of 40 cm, 1 kg of stirrup reinforcement consisting of 5 mm bars of steel I at 10 cm centres produced an increase of 3,431 kg in the ultimate load, whereas 1 kg of 10 mm stirrups produced an increase of only 1,343 kg. It must therefore once again be stated that close spacing of the stirrups is advantageous.

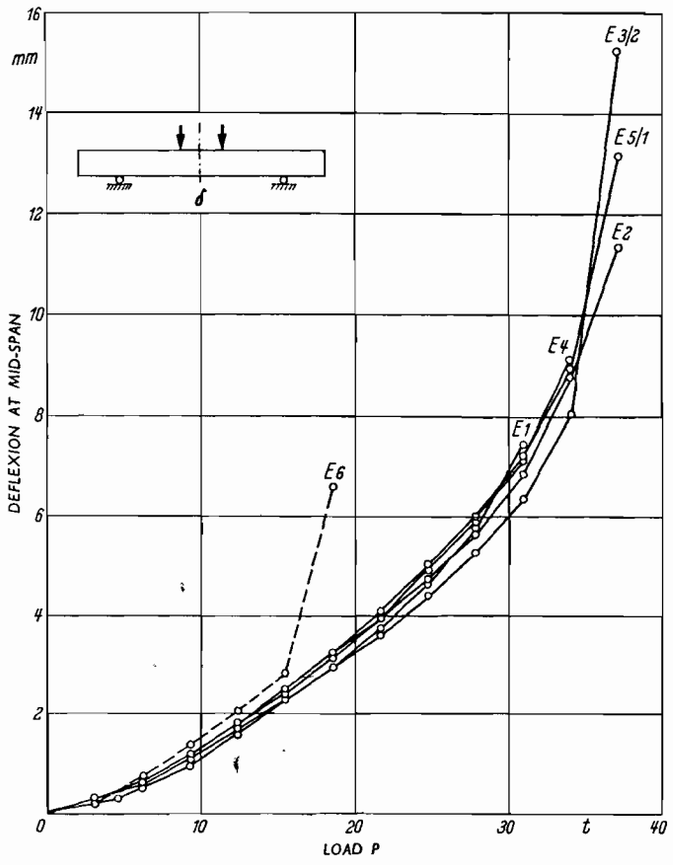

Figure 71: Load-deflexion diagram of concentrated-load beams with different shear reinforcement.

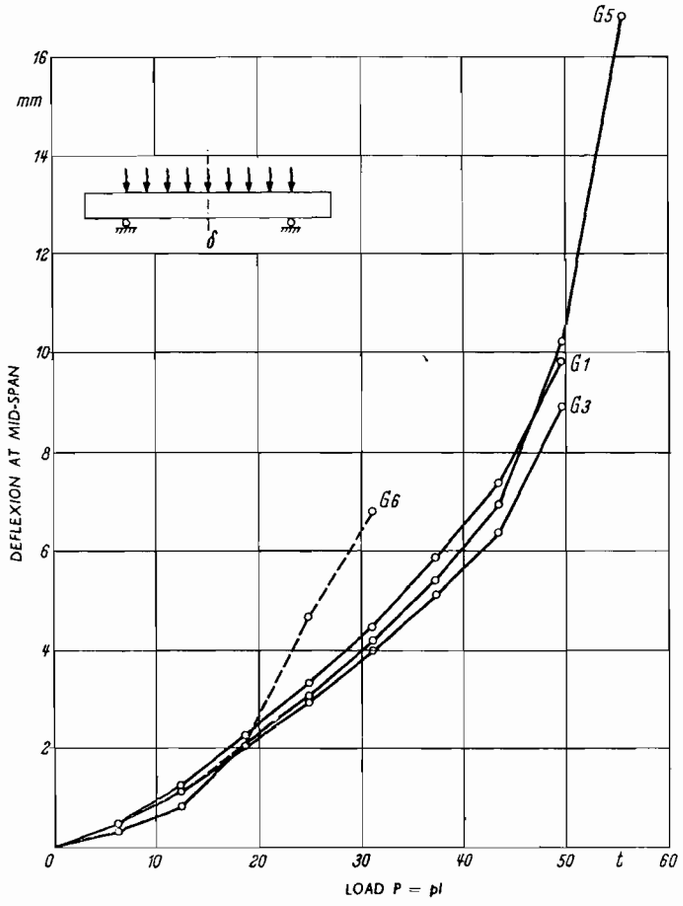

Figure 72: Load-deflexion diagram of uniformly loaded beams with different shear reinforcement.

With the fairly moderate shear stresses $\tau_o = 40 - 70$ kg/cm^2 for ultimate load in the tests under present consideration the difference between inclined and vertical stirrups is not so pronounced as in the case of the test beams (T-beams) discussed in Section II.1, so that for most practical purposes vertical stirrups can quite suitably continue to be used. Indeed, in so far as shear failure is caused by crushing of the compressive zone, vertical stirrups are preferable because they enclose and laterally restrain the compressive zone more effectively and because the thrust D at the critical spot remains smaller than with inclined stirrups (Figure 15). It is clearly established that even in the case of rectangular beams likely to fail in shear with $M/Qh \simeq 3$ or $l/h \simeq 7$, about half the amount of shear reinforcement required for ensuring full safeguard against failure in shear (i.e. stirrups designed for only half the shear force T) was sufficient to enable flexural failure to be attained.

The fact that the bent-up bars behaved less favourably than the stirrups is not difficult to understand in the light of present-day knowledge of the influencing factors affecting the widths and spacing of the cracks. With individual inclined bars in the middle of the section and, moreover, spaced far apart it was only to be expected that wider cracks would occur than with more closely spaced bars installed close to the two edges of the section. Large cracks are associated with more shear deformation, i.e. more shear rotation, more rapid upward spreading of the shear crack and therefore greater risk of shear failure.

The very small stirrup forces - as compared with the tensile forces calculated on the basis of the lattice analogy (only about 1/3 of these last-mentioned forces) - indicate that, despite the provision of full shear reinforcement, a large proportion of the shear force is transmitted by means of the "arch and tie-rod" action, i.e. the resultant thrust must be steeply sloped. This is possible only if the tensile force in the tensile zone of the beam does not decrease with the bending moments but is, instead, substantially larger close to the bearings than it would be according to the conventional beam theory. Serious weakening of the tensile region by bending up bars must therefore be recognized as being detrimental, inasmuch as the shear crack width will then be adversely affected by the steel strain occurring already at the beginning of the shear crack.

In addition, bent-up bars exercise a longitudinal splitting action upon the concrete at the bends; also, they do not enclose the concrete (so as to restrain it laterally), nor do they effectively help to connect a compression flange (if any) to the web of the beam. Hence, for T-beams - which are so extensively used in practice - the efficiency of bent-up bars for providing shear strength is even less than for rectangular beams.

This conclusion can, for that matter, also be drawn from earlier tests, as will be shown in the following.

6.6 REFERENCE TO EARLIER TESTS WITH MEMBERS SO REINFORCED AS TO PROVIDE ONLY HALF THE REQUISITE SHEAR SAFEGUARD

In the old shear tests of C. Bach, O. Graf and E. Mörsch, dating as far back as 1910, which are reported in the publications of the Deutscher Ausschuss fur Eisenbeton (German Committee on Reinforced Concrete), the problem of partial safeguard against shear failure was considered on a number of occasions. It is from these shear tests that Mörsch derived his general requirement as to "full shear safeguard". On examining those tests in the

light of present-day knowledge, we find that the cracking patterns and failure loads obtained were very significantly affected by the deficient bond of the thick plain round steel bars (26 - 40 mm diameter) employed. In a great many cases failure was not due to shear at all but to anchorage failure caused by splitting of the concrete in the longitudinal direction. Mörsch gave much attention to the consequences of slip of the longitudinal reinforcement, even only from the point of view of accounting for the so-called secondary shear cracks which appeared above the primary cracks towards the ends of the member (cf. reference 8, p.117). In the tests described in the present report, no such secondary cracks occurred. As has been shown, bond significantly affects the safety against shear failure. For this reason the results of the earlier tests must not be uncritically applied to present-day conditions. This was, in fact, one of the reasons why the present authors undertook fresh tests.

Amongst these earlier tests, however, there are cases where beams with only half the shear safeguard carried more load than beams with full shear safeguard, and it will be worth our while to consider these cases more particularly with reference to the efficiency of the different types of shear reinforcement. The beams in question are Nos. 1124 and 1132 of the oft-quoted supplementary tests to Communication 48, performed by the firm of Wayss & Freytag with test specimens made of so-called "structural concrete" (cf. reference 8, pp. 196 - 218).

Beam No. 1124 (Figure 73) was fully reinforced with regard to shear ("full safeguard against shear failure") with bent-up bars of 26 mm diameter and stirrups of 8 mm diameter spaced at 18 cm centres. No stirrups were provided in the region between the two concentrated loads.

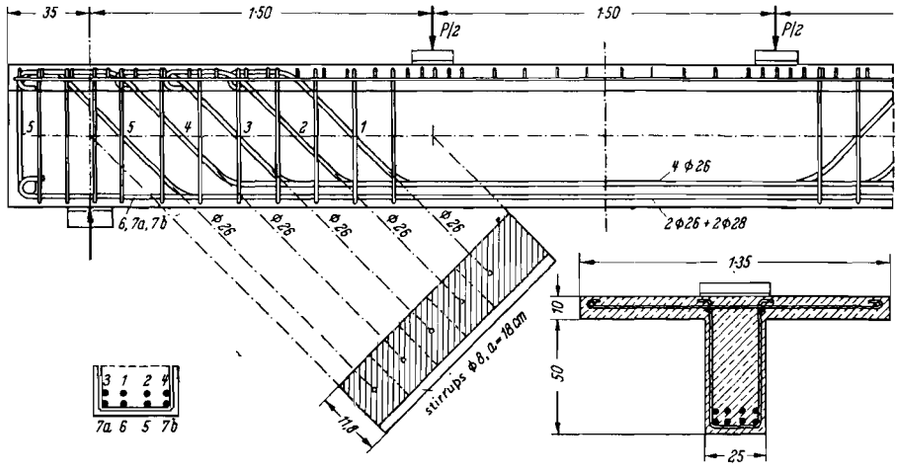

Figure 73: Test beam 1124 of the supplementary tests for Communication No. 48 of the German Committee on Reinforced Concrete (full safeguard against shear failure).

Beam No. 1132 (Figure 74) was only half safeguarded with regard to shear failure, being reinforced only with stirrups of 12 mm diameter at 15 cm centres; here again there were no stirrups in the region between the loads. The stirrups, which consisted of plain round bars, were provided just with short right-angled hooks (L-hooks), i.e. they were not, by present-day standards, properly anchored into the top flange.

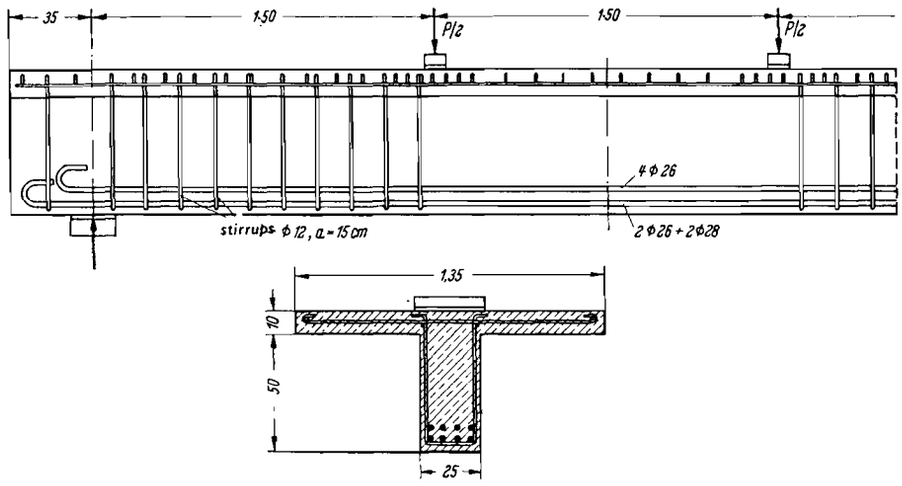

Figure 74: Test beam 1132 of the supplementary tests for Communication No. 48 of the German Committee on Reinforced Concrete (half safeguard against shear failure).

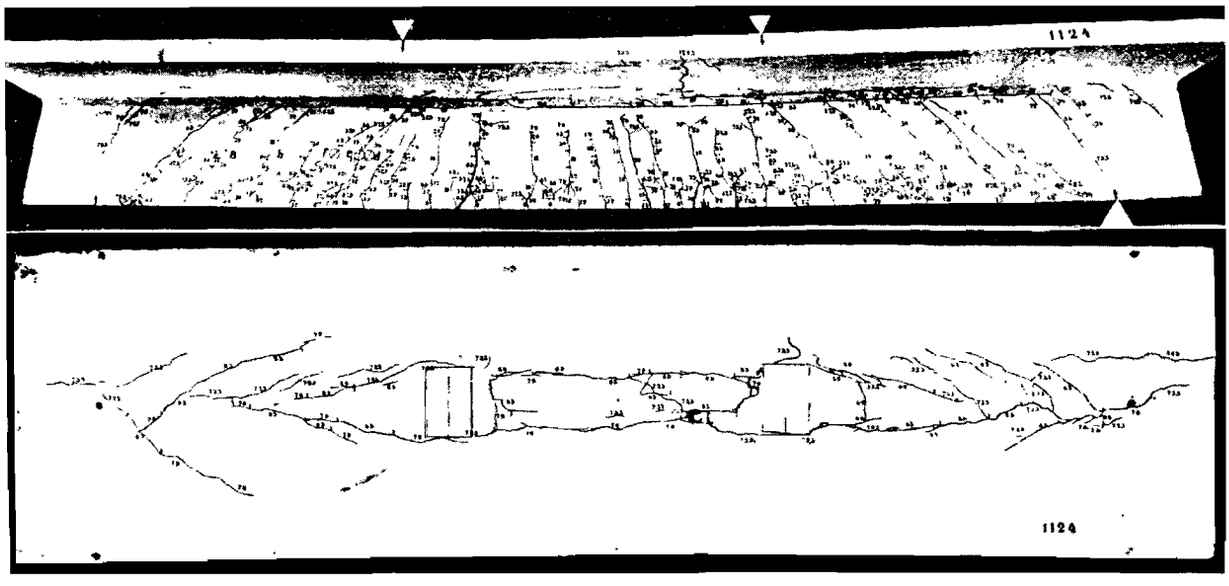

Figure 75: Cracking patterns obtained with beam 1124.

The quality of the concrete was practically identical for the two beams, the cube strengths being 117 and 116 kg/cm^2 respectively.

Beam No. 1132 was able to carry a load P = 75 tons, whereas beam No. 1124, despite its full shear safeguard, was only able to carry a load of 73·5 tons. Mörsch attributed the difference, in the main, to a somewhat higher yield point of the longitudinal reinforcement in beam No. 1132 as compared with that in beam No. 1124 (yield point for 26 mm bars: 2,720 kg/cm^2 as against 2,320 kg/cm^2; for 28 mm bars: 2,835 kg/cm^2 as against 2,510 kg/cm^2).

However, on considering the failure patterns and the phenomena associated with failure (see Figures 75 and 76), we see that beam No. 1124 developed flexural failure and that this occurred without full co-operation of the compression flange. Mörsch reported that the coherence between web and slab

was progressively destroyed; and indeed the horizontal cracks between web and slab are clearly visible along nearly the whole length of the beam. The top view of the slab shows cracks which indicate that the anchorages of the bent-up bars produced splitting cracks in the slab. In the region between the two loads it is apparent that only the middle portion between the longitudinal cracks over the web was destroyed by crushing. At flexural failure the slab was therefore only inefficiently co-operating in carrying the load, with the result that the internal lever arm z was reduced.

This adversely affected the flexural failure moment. At this ultimate moment M_U = 56·7 tm the yield point of the longitudinal reinforcement had to be exceeded, however.

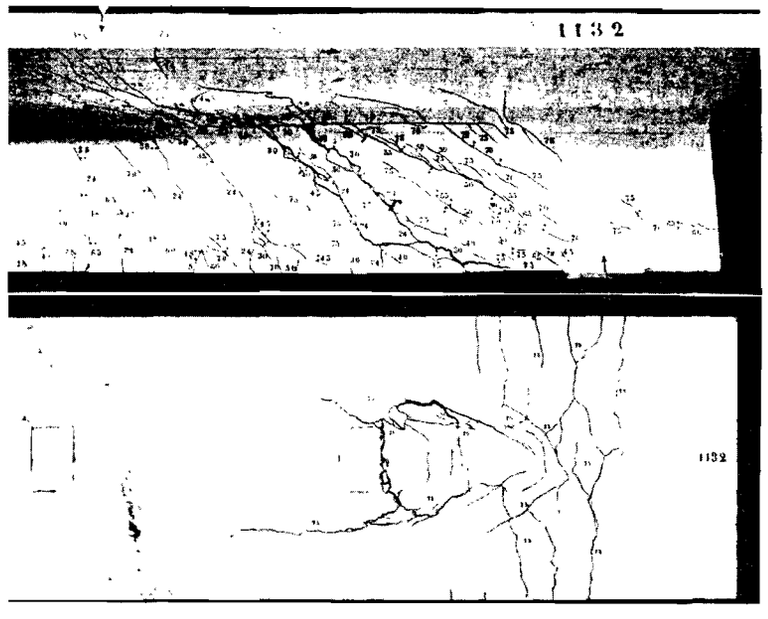

Figure 76: Cracking patterns obtained with beam 1132.

On the other hand, the failure patterns of beam No. 1132 (Figure 76) show a clear case of shear failure. In the right-hand portion, over the shear crack r (in the centre of the photograph), the flexural compressive zone is seen to have effected an upward "break-through" directly beside the load. In the higher stages of loading, the secondary shear cracks in the upper part of the web occurred over the primary main shear cracks. The secondary cracks occur only if the main reinforcement slips, i.e. in the event of bond failure. Already at 35 tons "slip cracks" appeared beside the tensile bars. The congestion of the anchorage hooks then moreover gave rise to cracks which indicated that anchorage failure had developed. The slip of the main reinforcement in the concrete was, however, an important factor in causing the shear crack to open out, thus resulting in premature shear failure (which would not happen with the deformed bars nowadays employed).

There was yet no danger of flexural failure, since the slab was properly connected to the web (thanks to the more substantial stirrups) and therefore fully continued to co-operate in the region between the loads until shear failure occurred, even though the stirrups which should essentially have been provided in that region were lacking. At the ultimate moment of 57·8 tm the main reinforcement had not yet reached its yield point (this would have been reached only at a moment equal to about 59·3 tm). The difference in yield point of the main reinforcements increased the flexural failure to such an extent that in this case shear failure occurred, though this does not necessarily constitute proof that "full safeguard against shear failure" is necessary.

7. Effect of the web width on the shear strength of T-beams with light stirrup reinforcement

7.1 PRELIMINARY REMARK

According to the present regulations, which limit the permissible shear stress conditions solely in terms of the permissible shear stress τ_0, it might be supposed that the shear strength (load-carrying capacity in shear) of T-beams would, for otherwise equal conditions, have to be proportional to the web width b_0 . The tests of Mörsch and Graf, as described in publication No. 10 of the Deutscher Ausschuss für Eisenbeton [20] (which tests were, in fact, one of the fundamental sources of data on which the Standard Specifications DIN 1045 were to be based), did indeed indicate an approximately linear relationship between failure load and web width (Figure 77). However, as demonstrated in reference 21, those were not actually cases of shear failure but of anchorage failure. The latter type of failure presents cracking and failure patterns which often are hardly different from those of shear failure.

The object of the following test series was to reveal the actual effect of the width b_0 of the web, to the exclusion of anchorage failures. The beams were reinforced only with vertical stirrups, which had been designed for about half the shear force. The load arrangement, slenderness and percentage of main reinforcement were so chosen that, according to present-day knowledge, the greatest possible likelihood of shear failure would be obtained.

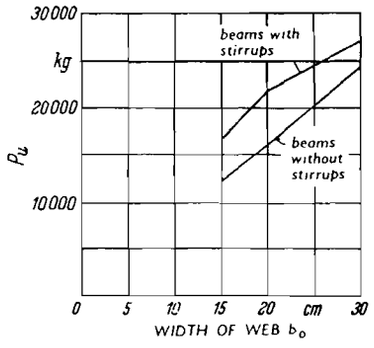

Figure 77: Failure load plotted against web width (tests by Mörsch and Graf, reported in Communication No. 10 of the German Committee on Reinforced Concrete).

7.2 TEST ARRANGEMENT AND DETAILS OF TEST BEAMS

Two series of tests were arranged:

Series ET:	concentrated loads	- four T-beams
Series GT:	uniformly distributed loads	- six T-beams

The dimensions, reinforcement details and loading are indicated in Figure 78.

Starting from a rectangular section having a width b = 30 cm and a depth d = 35 cm (beam No. 1), the web width was progressively reduced to 15, 10 and 5 cm, while the width of the compression flange (7·5 cm thick) was kept constant at 30 cm. The beams with 5 cm wide webs had to be provided with a 10 cm wide bottom flange in which to accommodate the longitudinal reinforcement.

In the beams of series "E" the two point loads were applied at a distance a = 1·05 m from the respective bearings, which corresponds to a situation that is still unfavourable with regard to shear, viz. $M/Qh = a/h = 105/30 = 3{\cdot}5$. The slenderness of the beams - a deciding factor in connexion with uniformly distributed loading - was $l/h = 10$.

In all the beams the tensile reinforcement consisted of four straight 20 mm diameter ribbed Tor steel bars (steel IIIb). The degree of reinforcement (percentage of steel) was $\mu = 100\, F_e/bh = 1{\cdot}36$ %. The anchorage length provided was 20 cm and was therefore greater than the required six bar diameters = 6 x 2·0 = 12 cm for deformed reinforcing steel. To rule out any possibility of anchorage failure, the projecting ends of the beams were also provided with four 6 mm diameter stirrups of steel IIIb.

The shear reinforcement in all cases consisted of vertical two-leg stirrups formed of 6 mm plain round bars (steel I) which enclosed the longitudinal bars and were bent round at right angles or provided with hooks at the top. For the concentrated-load beams a constant spacing of the stirrups (distance a = 11 cm) was adopted in the shear region. In the case of the uniformly-loaded beams the stirrups in the one half of the beam were given a distribution corresponding to the shear force diagram, whereas in the other half the same number of stirrups was installed, but with constant spacing a = 15 cm, in order to check the efficiency of this simple stirrup arrangement frequently adopted in practice (Figure 78). The cross-sectional area of stirrup reinforcement corresponds to only about 45 % of the shear safeguard required by DIN 1045 for the permissible working load. As the beams GT3 and GT4 failed prematurely in shear in the halves with stirrups at constant spacing, two additional test beams were subsequently made (GT3/2 and GT4/2) in which the stirrups in both halves were spaced according to the shear force diagram.

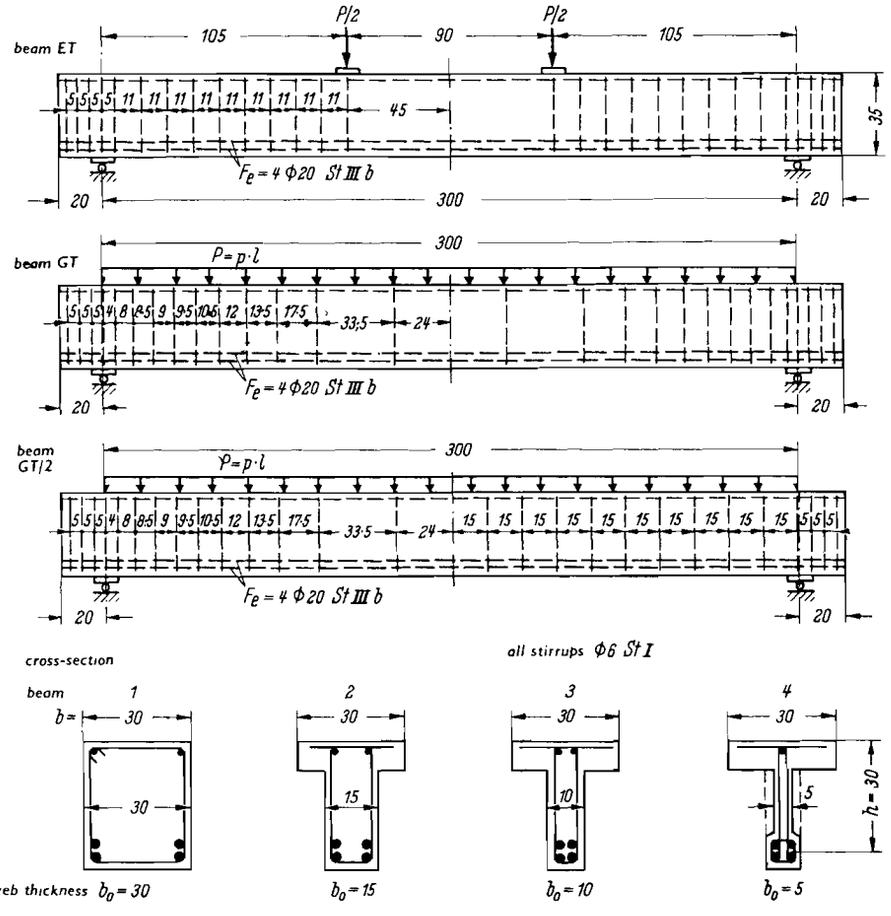

Figure 78: Dimensions and reinforcement of the test beams with varying web widths.

7.21 Calculated stresses under working load

The working load adopted in the tests was the permissible load g+p in bending according to the conventional theory of reinforced concrete design (modular ratio n = 15) as laid down in DIN 1045.

The determining value is the permissible concrete stress (permiss. σ_b), which was obtained for the actual concrete strength by linear interpolation between the values laid down for concretes B 225 and B 300 respectively (see column 7 of Table XV). The working-load moments M_{g+p} calculated from the values thus determined are given in column 8. As the neutral axis calculated for state II (cracked section) is located below the compression flange, the working-load moments decrease with reduction of the web width, for constant concrete strength.

Under working load the stress in the main reinforcement was σ_e = 1,400 kg/cm^2, i.e. only 60 % of the permissible value of 2,400 kg/cm^2. This over-designing of the longitudinal reinforcement increased the strength of the beam in bending more than the strength in shear and thus increased the likelihood of shear failure (as intended). The shear stresses τ_o (column 11) for the two rectangular beams were 6·3 kg/cm^2 (ET1) and 8·0 kg/cm^2 (GT1), substantially below the upper shear stress limit of 20 kg/cm^2 (for B 300) according to DIN 1045. On the other hand, for the beams with very thin webs these shear stresses τ_o were a good deal higher than that limit (viz. 33·0 kg/cm^2 for ET4 and 46·1 kg/cm^2 for GT4). The calculated stresses in the stirrups (columns 12 and 13) were little affected by the web width and were approximately 3,000 kg/cm^2, i.e. intentionally far above the permissible stress of 1,400 kg/cm^2 for steel I. In the case of the beams subjected to uniformly distributed loading the calculated steel stresses $\sigma_{e(stirrups)}$ in the beam with constant stirrup spacing were indeed over 5,000 kg/cm^2 in the vicinity of the bearing.

7.22 Manufacture of the test beams

The same procedure as described in Section 6.23 was employed.

7.23 Materials

Steel

The characteristic values and the stress-strain diagrams of the steels (in each case the values are the averages of two tensile tests) are indicated in Figure 79. Half the tensile test-pieces for steel I were provided with two small holes similar to those made in the actual stirrups for receiving the demountable strain gauges. For the same cross-sectional steel area F_e = 30 mm^2 the test-pieces with holes gave lower values of yield point (β_S) and tensile strength (β_Z).

Concrete

The aggregates - washed Rhine gravel - were separated into four size fractions and combined in accordance with the grading curve in Figure 80. In the range of very fine particle sizes the cement was supplemented by the addition of quartz powder (0 - 0·02 mm size). The characteristic values and strengths of the concrete are summarized in Table XVI. The cylinder strength β_c was determined on cylinders of 15 cm diameter and 30 cm height. The average values were obtained from three to twelve individual values.

TABLE XV: Summary of the results of the shear tests on T-beams with webs of varying width.

Dimenaions: l = 3·00 m; b = 30 cm; d_o = 7·5 cm
l' = 0·20 m; d = 35 cm; h = 30 cm

Tensile reinforcement: 4 x 20 mm Grade IIIb with F_e = 12·24 cm^2, μ = 1·36%(1)

Compressive reinforcement: 2 x 8 mm Grade IIIb with F'_e = 1·22 cm^2, μ' = 0·14%(1)

1	2	3	4	5	6	7	8	9	10	11	12	13	14	15	16	17	18	19	20	21	22	23	24
						Calculated values for permiss. σ_b according to DIN 1045, with n = 15									Test results								
Designation	Loading	b_o	Shear reinforcement Left	Right	β_w	Permiss. σ_b (interpolated)	M_{g+p}	P_{g+p}	σ_e(2) calculated under M_{g+p}	τ_o	Calculated σ_e stirrups under g + p Left	Right	Permiss. σ_e stirrups(3) / calculated σ_e stirrups Left	Right	M_{crack} (bending)	σ_{bz} (beam)	P_U	Q_U(4)	τ_o(4) at failure $\frac{Q}{b_o z}$	M_U or M_{SU}	Calculated σ_e stirrups failure on right	$S = \frac{M_U}{M_{g+p}}$	Type of failure
		(cm)			(kg/cm^2)	(kg/cm^2)	(tm)	(t)	(kg/cm^2)	(kg/cm^2)	(kg/cm^2)				(tm)	(kg/cm^2)	(t)	(t)	(kg/cm^2)	(tm)	(kg/cm^2)		
ET 1	Concentrated load a/l = 3·5	30	6 mm Grade I e = 11 cm		285	96	5·08	9·68	1630	6·3	3460		0·40	0·40	2·15	30·0	28·0	14·45	18·7	14·96	10200	2·95	Flexural failure
ET 2		15			285	96	4·80	9·14	1510	11·8	3240		0·43	0·43	1·79	36·0	26·3	13·45	34·6	14·02	9500	2·93	Shear failure; destruction of compressive zone beside load application area
ET 3		10			285	96	4·67	8·90	1470	17·2	3160		0·44	0·44	1·63	40·0	25·5	13·00	50·0	13·55	9160	2·90	Shear failure; yielding of the stirrups, then destruction of the web concrete and compressive zone
ET 4		5			285	96	4·50	8·58	1400	33·0	3030		0·46	0·46	1·05	30·6	19·8	10·10	77·0	10·50	7050	2·33	Shear failure; destruction of the web subsequent to yielding of the stirrups
GT 1	Uniformly distributed load l/h = 10	30	The same number of stirrups provided on the left, distributed according to the shear force diagram		251	87	4·60	12·28	1480	8·0	5400(5)	3000	0·26(5)	0·46	2·55	35·5	48·0	24·60	32·3	18·45	12000	4·01	Flexural failure
GT 2		15			251	87	4·35	11·60	1370	14·9	5040	2800	0·28	0·50	2·21	44·5	46·0	23·45	60·4	17·59	11300	4·04	Flexural failure
GT 3/1		10	6 mm Grade I e = 15 cm		251	87	4·22	11·28	1330	21·7	4880	2710	0·29	0·51	1·50	36·8	34·4	17·60	67·7	13·20	8450	3·12	Shear failure; destruction of the web subsequent to yielding of the stirrups
GT 4/1		5			251	87	4·08	10·90	1270	41·5	4660	2590	0·30	0·54	1·16	33·8	29·4	15·05	110·8(6)	11·29	7150	2·76	Shear failure; destruction of the web subsequent to yielding of the stirrups
GT 3/2		10	The same number of stirrups as in GT1 - 4 right and left, distributed according to shear force diagram		287	97	4·67	12·45	1470	24·0	3000	3000	0·46	0·46	1·35	33·1	47·2	24·00	92·3	18·00	11500	3·85	Flexural failure
GT 4/2		5			287	97	4·53	12·08	1420	46·1	2890	2890	0·48	0·48	0·71	20·6	36·0	18·35	135·2(6)	13·76	8780	3·04	Shear failure; sudden destruction of the web due to oblique compression

(1) referred to b

(2) permiss. σ_e = 2,400 kg/cm^2

(3) permiss. $\sigma_{e(stirrups)}$ = 1,400 kg/cm^2

(4) self-weight taken into account

(5) at distance h/2 from bearing

(6) beside the local thickening at the bearing

The stress-strain diagrams of the concrete were determined from two 10 x 10 x 53 cm prisms subjected to axial compression (Figure 81).

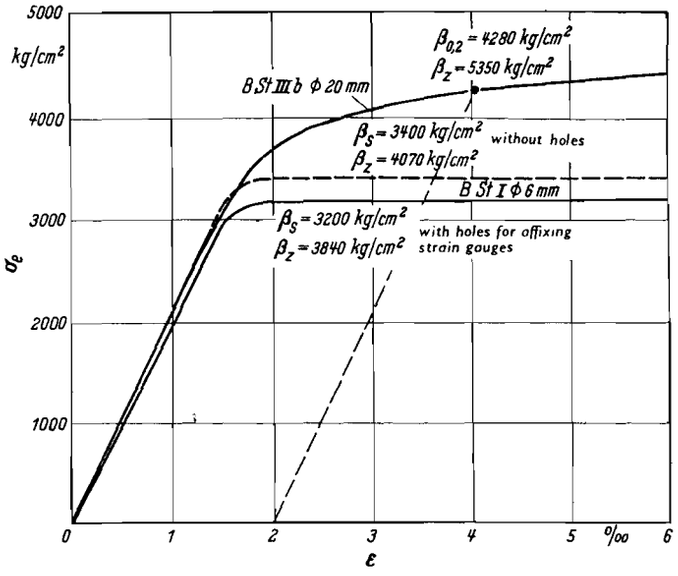

Figure 79: Stress-strain diagrams of the steels employed.

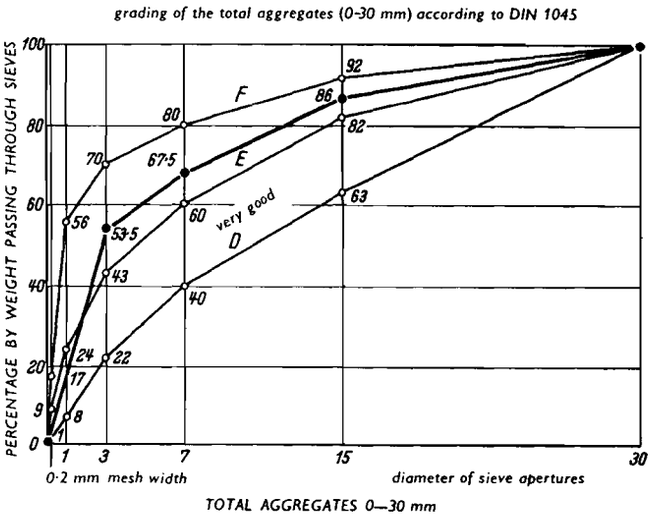

Figure 80: Grading curve for the aggregates employed.

TABLE XVI: Composition and strength of the concrete.

Cement, grade PZ 475	226 kg/m³
Fine quartz	120 kg/m³
Water	199 kg/m³
Water/cement ratio (referred to cement and quartz)	0·58
Spread (German flow-table test)	35 cm
Air voids content	2·3 %
Bulk density of the compacted concrete	2270 kg/m³

Compressive strength (kg/cm²)	ET beams average values	GT beams average values	GT/2 beams average values
β_w	285	251	287
β_p	230	207	227
β_{bz}	41·9	37·9	45·4
β_c	262	-	267
β_c/β_w	0·92	-	0·93
β_p/β_w	0·81	0·80	0·79

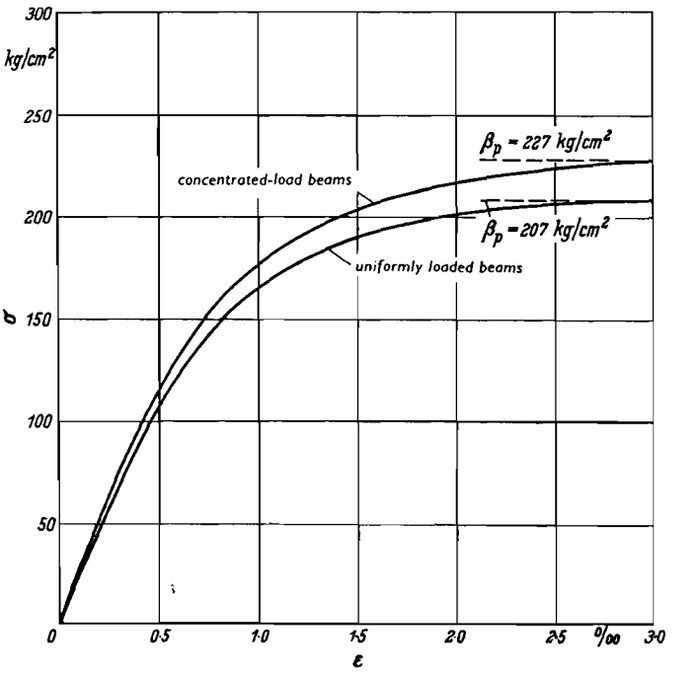

Figure 81: Stress-strain diagram of the concrete.

7.3 TESTING PROCEDURE

7.31 Measurements

The following measurements were carried out:

cracking loads and failure loads;

strain of the stirrups - by means of demountable strain gauges (gauge length 10 cm);

shortening of the compressive zone at the beam surface - with demountable strain gauges (gauge lengths 5 cm and 10 cm);

shortening of the concrete in the web in the direction of the oblique compression at 45° - with demountable strain gauges (gauge length 10 cm);

slip of the longitudinal reinforcement at the ends of the beams - with dial gauges (accuracy 0·01 mm);

deflexions of the beams at the eighth-span points - with dial gauges (accuracy 0·01 mm);

cracking pattern and crack widths (accuracy 0·01 mm) at the level of the tensile reinforcement and half-way up the web.

The location and designation of the points of measurement are indicated in Figures 82 and 83.

The stirrups were provided with small drilled holes for the locating pins of the strain gauges and were accessible from the exterior of the beam through small tubes provided for the purpose.

In order to determine the oblique compressive stresses in the middle of the "struts" in the web, the locating plates for the strain gauges were affixed (to the unloaded beam) only after the shear cracks had formed.

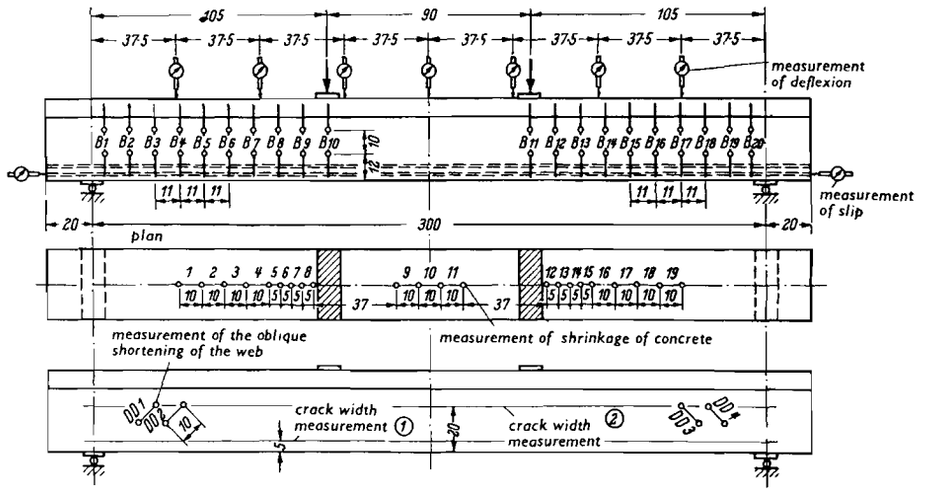

Figure 82: Arrangement of the points of measurement on concentrated-load beams with varying web widths.

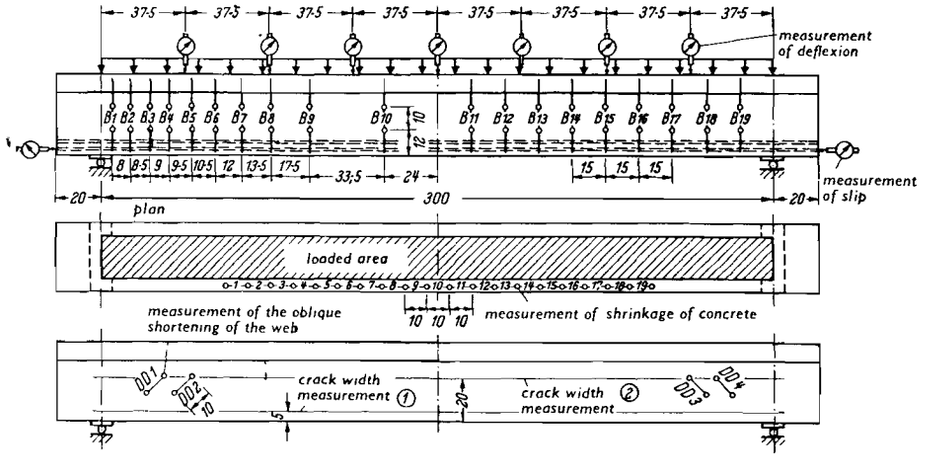

Figure 83: Arrangement of the points of measurement on uniformly loaded beams with varying web widths.

7.32 Load arrangement

The concentrated loads were transmitted into the beams through 4 cm thick steel plates (dimensions 12 x 30 cm) laid on a thin mortar bed and extending over the full width of the flange. The uniformly distributed load was applied over the length l = 3·00 m through two water-filled lengths of fire hose, as illustrated in Figure 28 (page 35). This load was spread over a width of 19 cm.

The bearings at each end were provided with rollers allowing freedom of rotation and longitudinal movement.

The loading was applied in incremental stages of about 1/8 of the flexural failure load, with removal of the load in between successive increments (about 30 min load duration per stage).

7.4 TEST RESULTS

7.4.1 General considerations regarding cracking and failure

Three kinds of failure were observed:

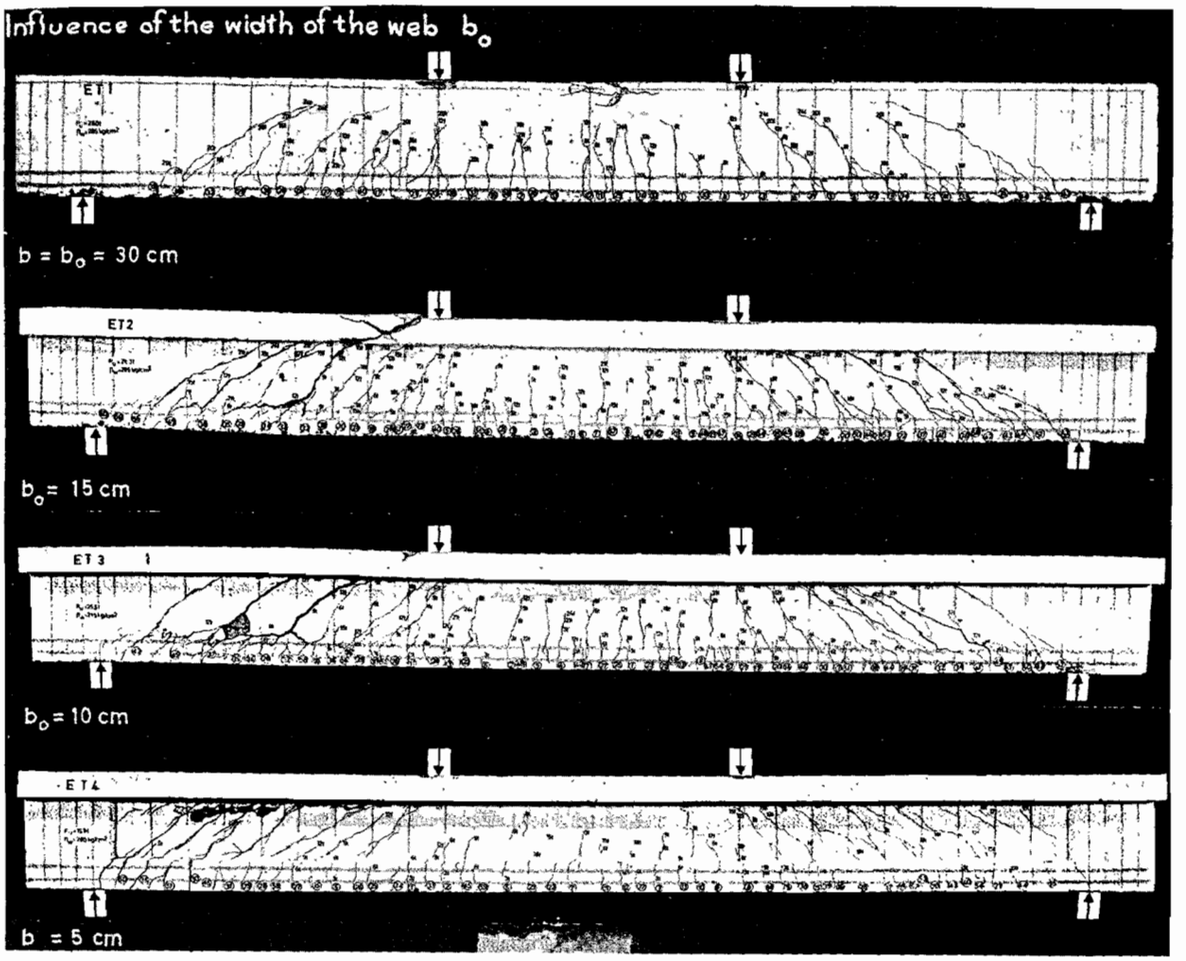

Figure 84: Concentrated-load beams with varying web widths, after failure. (Encircled figures denote order of occurrence of cracks; the other figures denote the load at which a crack had penetrated as far as the point indicated.)

1. Flexural failure: crushing of the concrete in bending in the region of maximum bending moment.

2. Shearing flexural failure: crushing of the flexural compressive zone at the end of the main shear crack.

3. Web failure:
   (a) due to oblique compression: the oblique principal compressive stresses $\sigma_{II} = 2\tau_o$ attain the compressive strength of the concrete;
   (b) as a result of yielding of the stirrups the web zone becomes considerably deformed, so that the oblique concrete "struts" are additionally stressed in bending and are therefore destroyed at $\sigma_{II} < \beta_p$.

The cracking and failure patterns of the test beams are shown in Figures 84 and 85.

With both types of loading, the rectangular beams failed in bending, although the shear cracks had extended very far upwards and the shear reinforcement had been greatly under-designed by present rules of design. Flexural failure also occurred in the case of two of the beams subjected to uniformly distributed loading, viz. GT2 with b_o = 15 cm and GT3/2 with b_o = 10 cm.

In the case of beam GT3/1 - identical with GT/2 in everything except the stirrup arrangement - the web on the side with constant stirrup spacing was destroyed as a result of yielding of the stirrups. All the beams with 5 cm wide webs (viz. GT4/1, GT4/2 and ET4) failed in consequence of oblique compression in the web. The beam ET2 with concentrated loads (b_o = 15 cm) developed shearing flexural failure. A borderline case between the failure types 2 and 3 occurred in the case of beam ET3 with b_o = 10 cm: the load-

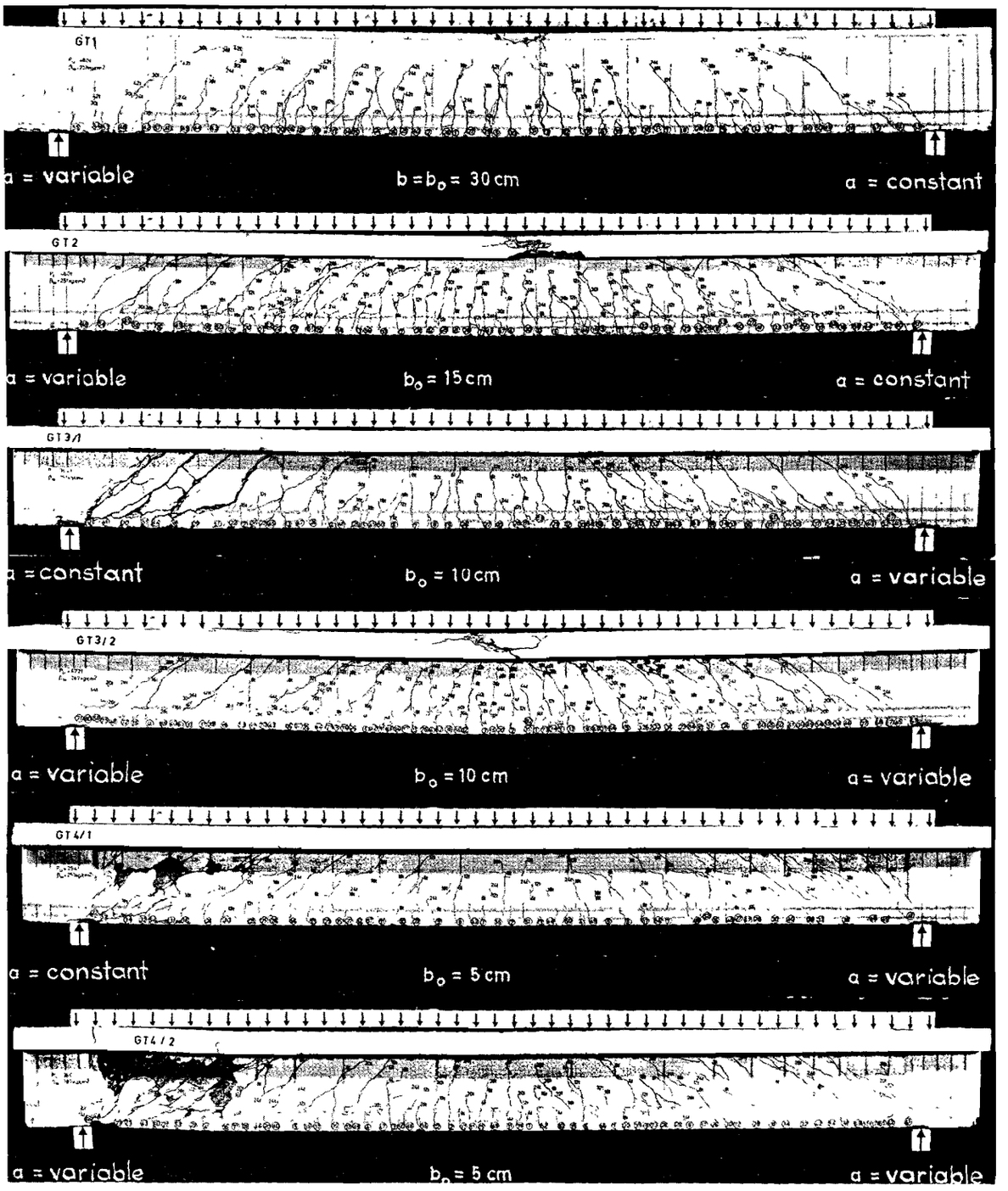

Figure 85: Uniformly loaded beams with varying web widths, after failure. (Encircled figures denote order of occurrence of cracks; the other figures denote the load at which a crack had penetrated as far as the point indicated.)

carrying capacity of the compressive zone was exhausted (the ultimate compressive strain of the concrete directly beside the load-spreading plate was exceeded, i.e. $\varepsilon_b > 0{\cdot}3$ %); at the same time, destruction of the bottom part of the web in the left-hand half of the beam occurred.

The pattern and spacing of the shear and flexural cracks varied little with the web width and type of loading. As was to be expected, however, a larger number of flexural and shear cracks were formed in the thin-webbed beams than in the rectangular beams.

7.4.2 The load-carrying capacity of the beams (depending on the web width)

In order to be better able to compare the load-carrying capacity of the beams investigated, the results of the tests to failure in Table XVII were converted to the reference strength $\beta_w = 270$ kg/cm^2 by linear interpolation.

In Figure 86 the failure loads (ultimate loads) have been plotted against the width b_o of the web. On reduction of the web width, the failure loads at first do not decrease appreciably but, instead, remain approximately constant down to $b_o = 15$ cm for uniformly distributed loading and even down to $b_o = 10$ cm for concentrated loads. It is not until the web fails due to oblique compression (i.e. when failure type 3 occurs) that a marked decrease in failure load is exhibited. Hence, as long as the compressive stresses in the web do not become the deciding factor, the web width has only a slight effect, even if - as in the present case - it is reduced to 1/2 or indeed 1/3 of the full rectangular width of the section.

TABLE XVII: Failure load values converted to reference strength $\beta_w = 270$ kg/cm^2; dead load taken into account.

1	2	3	4	5	6	7
Designation of beam	Width of web (cm)	P_U (t)	M_U or M_{SU}(3) (tm)	$\tau_{o,u} = Q/b_o z$ (kg/cm^2)	σ_{II}(2) = $2\tau_o$ (kg/cm^2)	Type of failure(1)
ET 1	30	26·5	14·16	17·7	35·4	Bending (or flexural) 1
ET 2	15	25·9	13·30	32·8	65·6	Shear 2
ET 3	10	24·1	12·83	47·5	95·0	Shears 2 and 3 b
ET 4	5	18·8	9·95	73·0	146·0	Shear 3 b
GT 1	30	51·6	19·83	34·8	69·6	Bending (or flexural) 1
GT 2	15	49·5	18·90	65·0	130·0	Bending (or flexural) 1
GT 3/1	10	37·0	14·30	73·0	146·0	Shear 3 b
GT 4/1	5	31·6	12·12	119·1	238·2	Shear 3 a
GT 3/2	10	44·5	16·97	87·0	174·0	Bending (or flexural) 1
GT 4/2	5	33·9	12·96	127·6	255·2	Shear 3 a

(1) For definition see Section 7.41

(2) Approximate "oblique" compressive stress according to Section II.1, Figure 15

(3) Maximum moment at mid-span at failure, independent of location of fracture section.

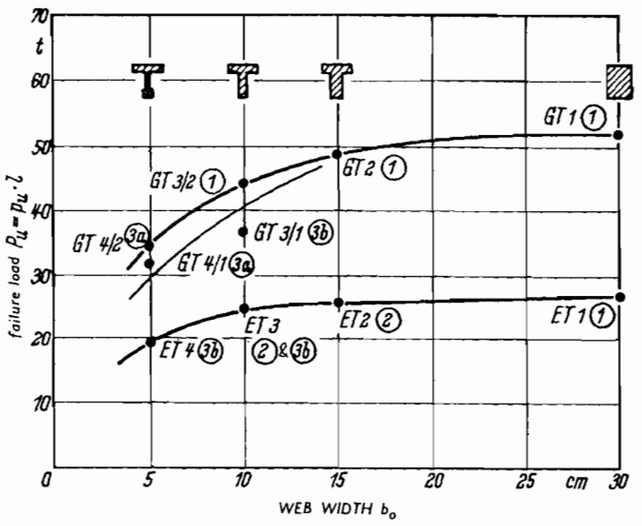

Figure 86: Relationship between the failure loads (referred to cube strength β_W = 270 kg/cm^2) and web width. The encircled figures after the beam designations indicate the type of failure (see Section 7.41).

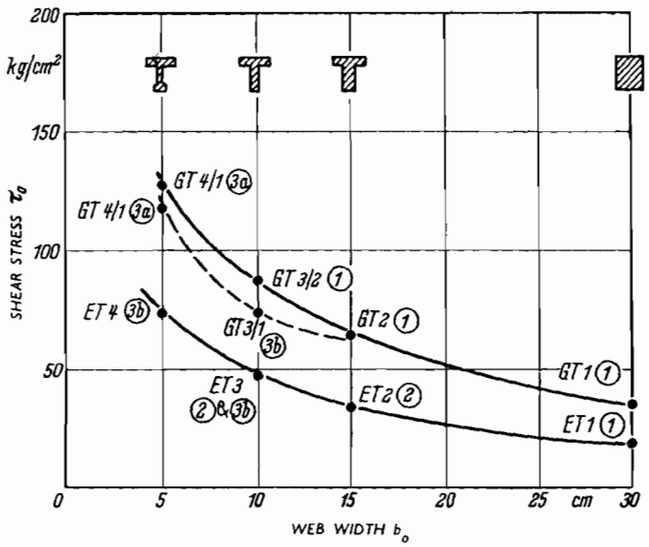

Figure 87: Calculated shear stresses at failure plotted against the web width of the beams (referred to β_W = 270 kg/cm^2). The figures in circles indicate the type of failure (see Section 7.41).

These results are clearly different from those obtained by C. Bach and O. Graf in 1911 (Figure 77), as reported in publication No. 10 of the Deutscher Ausschuss fur Eisenbeton (German Committee on Reinforced Concrete).

The maximum shear stresses $\tau_{o,U}$ attained at failure (Figure 87) steadily decrease with increasing web width, viz. for shear failure they decrease from 127 kg/cm^2 (beam GT4/1) to 33 kg/cm^2 (beam ET3). In the case of beam GT3/2 with b_o = 10 cm flexural failure occurred, although $\tau_{o,U}$ was 87 kg/cm^2.

The failure moments (ultimate moments) for uniformly distributed loading are again significantly larger than for concentrated loads (Table XVII, column 4): for flexural failure they are 40 % larger. This is again probably due to the strengthening effect of the distributed load on the compressive zone and to the undisturbed transmission of the load into the beam.

Let us compare the failure moments of the uniformly loaded beams which failed in bending. They were:

GT1	b_o = 30 cm;	M_U = 19·83 tm	(flexural failure moments)
GT2	b_o = 15 cm;	M_U = 18·90 tm	
GT3/2	b_o = 10 cm;	M_U = 16·97 tm	

We see that the flexural failure load depends upon the web width because, for one thing, the neutral axis is located in the web even at failure, and because, on the other hand, the shear deformation has a marked effect, which is apparent from the deflexions which, in the case of GT3/2 for P = 40 tons, were 50 % greater than for GT1 anyway (see Figure 99). For this reason the flexural cracks in GT3/2 spread distinctly higher up into the beam than in GT1 and GT2.

7.4.3 Safety against failure

Table XV, column 23, gives the quotients s = failure load divided by permissible working load for bending, in accordance with DIN 1045. For the purpose of design based on permissible stresses these quotients may be taken as being the factor of safety against failure.

For both types of loading the factor of safety is remarkably high, which is chiefly due to the considerable under-estimation of the flexural compressive zone in designing with permiss. σ_b for linear distribution of the concrete stresses σ_b.

Another notable feature is that the factors of safety against failure for the first three concentrated-load beams hardly differ from one another, although ET1 failed in bending, whereas ET2 and ET3 developed shear failure. Hence, despite the small amount of stirrup reinforcement provided, the load-carrying capacity in shear was only little less than the flexural load-carrying capacity. Only in the case of the 5 cm wide web was there a marked reduction in the safety factor (s = 2·33) because the web failed in oblique compression. The safety factor s = 3·04 for beam GT4/2 with b_o = 5 cm must in any case be regarded as very high, the more so as max. τ_o under working load was 46·1 kg/cm^2.

7.4.4 Oblique compressive stresses in the web

With the aid of the stress-strain diagram of Figure 81 the compressive stresses were calculated from the shortening strains (measured at 45°) of the "struts" bounded by the shear cracks. These values may be affected by errors, inasmuch as the gauge length does not reliably give the average of the oblique compressive stress in the case of the irregularly shaped cracks. Nevertheless, for the concentrated loads (Figure 88) these values exhibit good agreement with the theoretical values, which - according to Figure 15 - must be $\sigma_{II} = 2\,\tau_o$ for vertical stirrups. In the case of beam ET4 the maximum oblique compressive stresses at failure of the stirrups was found to be 150 kg/cm^2, corresponding to 0·65 β_p.

In the uniformly loaded beams, too, the oblique compressive stresses in the thin webs are close to the theoretical values of σ_{II}, whereas in the

thick webs they remain considerably below the theoretical values (see Figure 89). The maximum value in the web of beam GT4/2 was 220 kg/cm , i.e. $0{\cdot}9\beta_p$. The fact that such high compressive stresses were attained is surprising if it is borne in mind that there was only very light shear reinforcement in the destroyed zone of the beam GT4/2 (roughly 40 % of the amount of stirrup steel required by DIN 1045).

In the beams subjected to uniformly distributed loading the places at which shear failure developed were situated in the vicinity of the bearing, i.e. in a zone where large shear forces and small bending moments occurred.

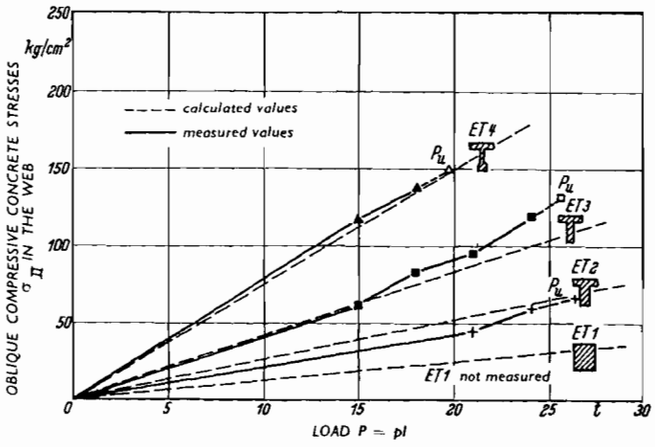

Figure 88: Comparison of the measured oblique compressive stresses σ_{II} in the web with the theoretical values ($\sigma_{II} = 2\tau_o$) for concentrated-load beams with varying web widths.

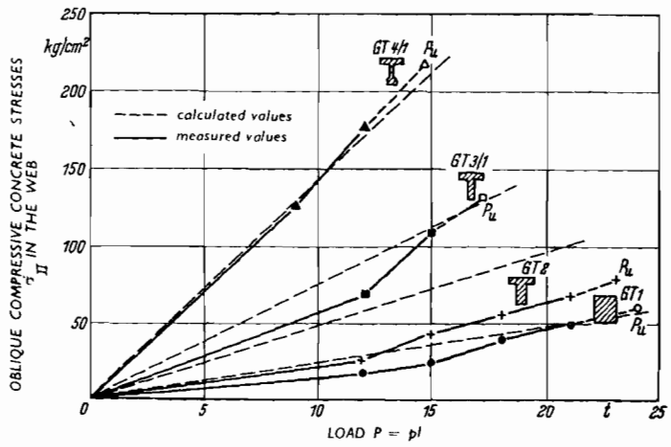

Figure 89: Comparison of the measured oblique compressive stresses σ_{II} in the web with the theoretical values ($\sigma_{II} = 2\tau_o$) at distance h/2 from the bearings, for uniformly loaded beams with varying web widths.

In the beams with concentrated loads the failure places were farther towards the middle of the beam and upwards, i.e. in a zone where fairly large moments still occur in addition to the shear forces, which to some extent explains why the stresses $\sigma_{II,U}$ remained substantially below the prism strength. Probably as a result of the considerable shear deformation and, more particularly, as a result of strain of the stirrups, the "struts" were additionally stressed in bending at their upper ends.

7.4.5 Stresses in the stirrups

The measured stirrup stresses have been plotted against the loading in Figures 90 and 91. In the case of the beams with concentrated loads the four stirrups numbered B 4 - B 7 (Figure 82) on each side were averaged; in the case of the uniformly loaded beams, on the other hand, the average values were determined only from the four stirrups B 3 - B 6 (Figure 83) on the side where the stirrups were spaced at varying distances.

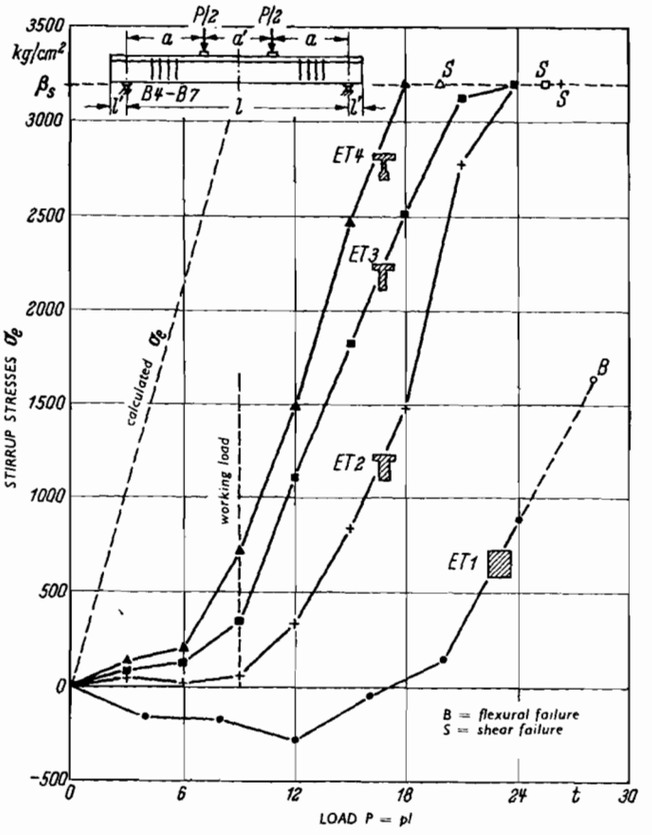

Figure 90: Average stresses in stirrups in concentrated-load beams with varying web widths, plotted against load.

For both types of loading the stress in the stirrups is therefore to a considerable extent dependent upon the web width. In thick webs the stirrups do not take up load until fairly high loads are reached, because the formation

of shear cracks - determined by τ_o - commences later than it does in thin webs. But even after the occurrence of the shear cracks the stirrup stresses in thick webs remained - contrary to what the lattice analogy would lead us to expect - substantially lower than in thin webs. The stress curves become in the long run approximately parallel.

It is evident that, even under fairly high loads, the greater stiffness of the compression members, including the oblique struts between the shear cracks, in conjunction with the "tie-rod", prevent the weak tension members (i.e. the stirrups) from taking more than a small share of load. This means to say that the "truss and tie-rod" action predominates and that the "lattice system" is operative only with thin webs, in which the struts are not so stiff. A large proportion of the shear force is therefore carried by the "arch" or "truss". This load-bearing action is more fully developed under uniformly distributed loading than under concentrated loads, this being apparent from the regular spacing of the stress curves $\sigma_{e(stirrups)}$ in Figure 91.

A most significant point is that the stirrup stresses remain far below the calculated $\sigma_{e(stirrups)}$ even in the beams with very thin webs (b_o = 5 cm, i.e. b/b_o = 6), attaining only 24 % of the calculated value under working load in the case of concentrated loads, and only 40 % in the case of uniformly distributed loading (diminishing towards failure). In the case of the large

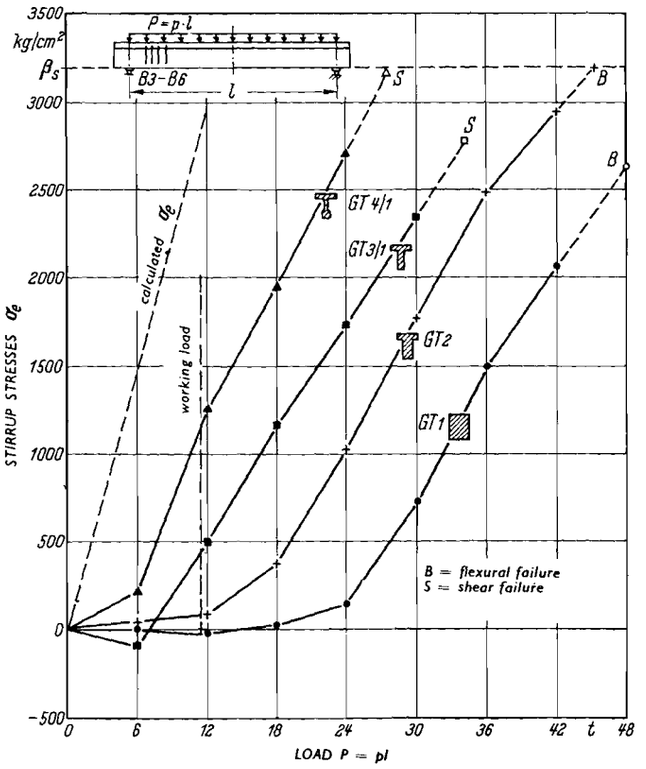

Figure 91: Average stresses in stirrups in uniformly loaded beams with varying web widths, plotted against load. The 4 stirrups used in arriving at the averages are indicated in the beam diagram (on the side of the beam with variable stirrup spacing).

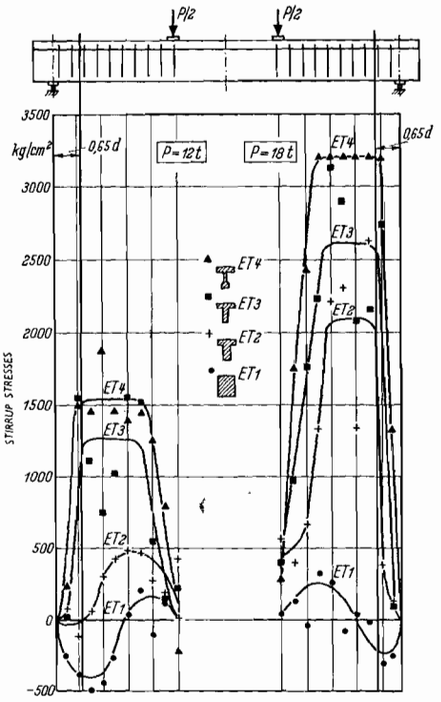

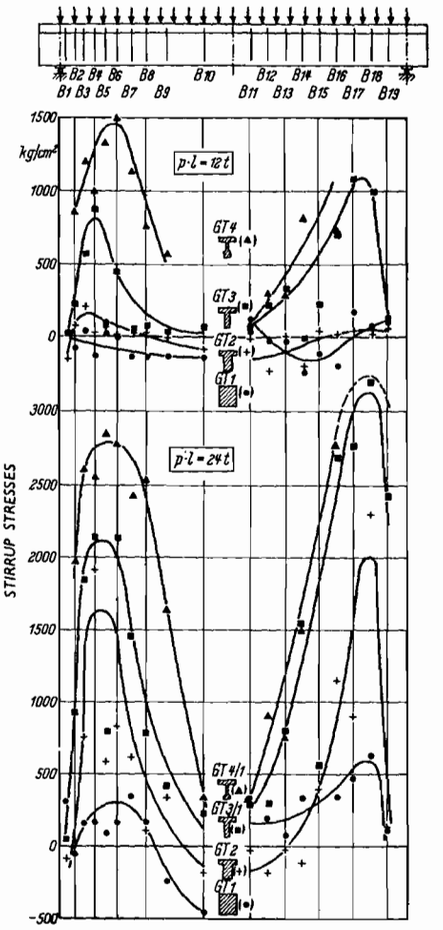

Figure 92 (left): Stresses in the stirrups at various sections along the beams with concentrated loads, for load P = 12 tons and P = 18 tons. For convenience, the stress curves have been idealized (average of adjacent measurements).

Figure 93 (right): Stresses in the stirrups at various sections along the beams with uniformly distributed loading, for pl = 12 tons and pl = 18 tons. For convenience, the stress curves have been idealized. The symbols relating to the measured values obtained for individual beams are shown in parentheses beside the relevant cross-sections.

beam T1 referred to in Section II.1, stirrup stresses of 72 % of the calculated value were found for concentrated loads and b/b_o = 15. Hence there is clearly seen to be a relationship between the stirrup stress and b/b_o.

The yield point of the stirrup steel was reached only in the beams ET2, ET3, ET4 and GT2. With concentrated loads the slope of the stirrup stress lines corresponds approximately to the calculated increase of stress; with uniformly distributed loading, however, the slope is always smaller, which is attributable to the effect of σ_y, which is dependent upon the loading.

Figures 92 and 93 show how the stress in the consecutive stirrups varies along the beam. The values for neighbouring stirrups in some cases exhibit considerable variations, depending upon the position and length of the shear cracks. If average curves are drawn through the points corresponding to the measured values, it here again becomes clearly apparent that the stresses in

the stirrups undergo a considerable increase with decreasing width of the web. In the vicinity of the bearings and of the points of load application they are small, and sometimes even negative, because in those regions the oblique principal tensile stresses are reduced by the vertical stresses σ_y due to the transmission of the load into the concrete. In the case of uniformly distributed loading it appears that the stirrup stresses for stirrups spaced in accordance with the shear force diagram (Figure 93, left) remain lower than those stirrups spaced equal distances apart (Figure 93, right).

For beam GT3 the differences between stirrups spaced at progressively varying distances and stirrups at constant spacing are shown in Figure 94. In this diagram the average stirrup stresses for the undisturbed shear range c have been plotted against the load. The difference is 50 %, which must, of course, affect the shear strength of the beam.

If the stirrups are given constant spacing, it is obvious that their spacing in the vicinity of the bearing - and not the absolute quantity of stirrup steel - is the determining factor with regard to the strength of the beam in shear.

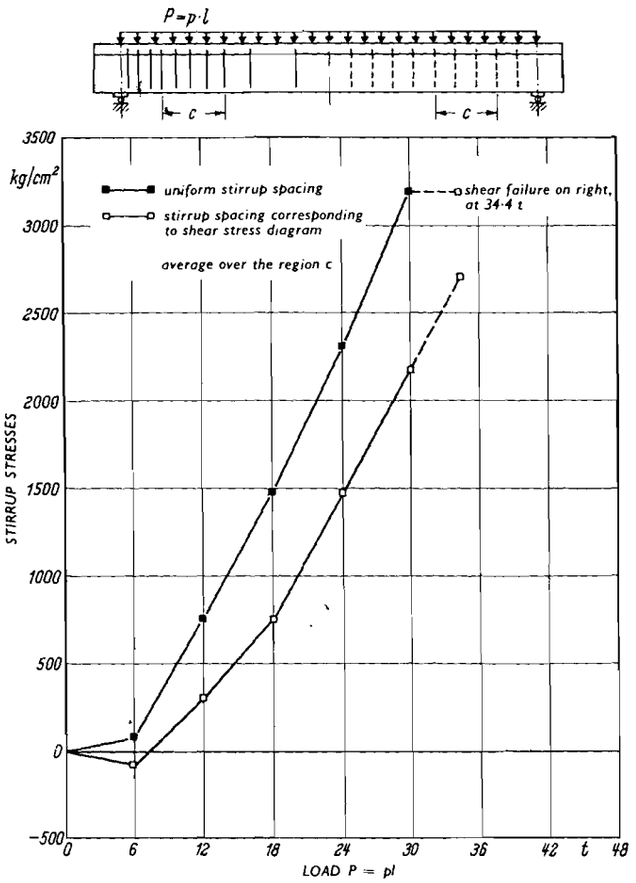

Figure 94: Average values of measured stirrup stresses in the region c for varying arrangement of stirrups in the uniformly loaded beam GT3.

For uniformly distributed loading, Figure 93 shows that in the left-hand half of the beam the stress in the stirrups undergoes a greater decrease towards the centre of the beam than it does in the right-hand half, although the stirrup spacing on the left in the mid-span region is larger (spacing a = 18 to 33 cm) than it is on the right (where a = constant = 15 cm). Hence

it follows that the stirrups in the mid-span region of the beam are less severely stressed according as the stirrups are more closely spaced near the ends of the beam and, therefore, according as the shear deformations in the main shear region are smaller. Spacing the stirrups a constant distance apart is therefore not an efficient arrangement.

7.4.6 Stirrup arrangement close to the bearings

The great difference between the failure loads of beams GT3/1 and GT3/2, which differ only in the stirrup spacing employed, must be particularly emphasized, inasmuch as it yields an important piece of information. The failure loads (referred to cube strength β_w = 270 kg/cm^2) are as follows:

Beam	GT3/1	GT3/2
stirrup spacing near left-hand bearing	wide spacing	close spacing
failure load (tons)	37·0	44·5

The marked difference in cracking behaviour is shown in Figure 95. In the case of beam GT3/1 the small number of stirrups near the bearing were inadequate for resisting the oblique compressive forces (developed by the concrete struts between the shear cracks and thrusting against the bottom flange) and, as it were, suspending them from the upper part of the beam; the main reinforcement was forced downwards and this resulted in shear failure. In the case of beam GT3/2, on the other hand, the more closely spaced stirrups in that region secured the struts, so that flexural failure occurred instead.

We see, therefore, that it is important to have stirrups spaced close together particularly at the bearings, so as to ensure that each of the narrow struts is duly supported. The stirrups may be relatively thin. This close stirrup spacing is particularly important in the case of partial safeguard against shear failure, because this is practicable only if the web thickness is such that an efficient "truss" action can still be developed. At the

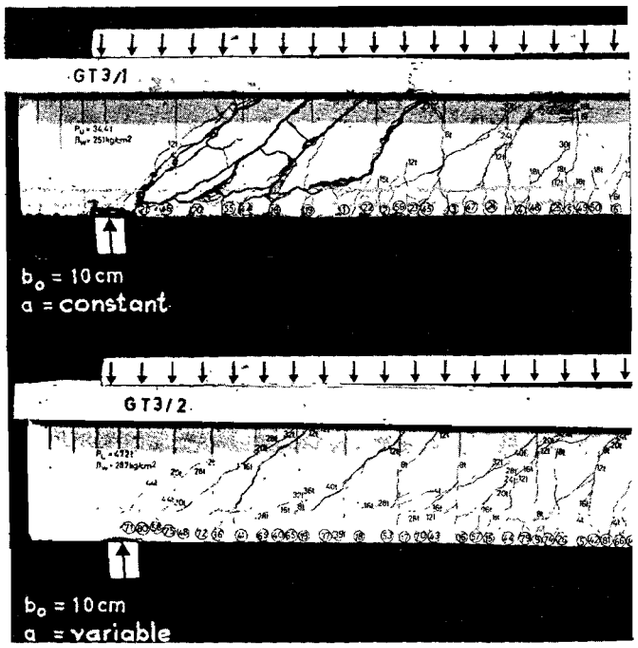

Figure 95: Cracking and fracture patterns for different stirrup spacing (same width of web and number of stirrups).

end of the beam the "truss" comprises a number of struts, however. Bent-up reinforcing bars are unsuitable in this region, since they do not enclose the struts, which thrust down against, and have to be supported by, the main tensile reinforcement. The close stirrup spacing in the vicinity of the bearings also provides a safeguard against anchorage failures.

For these test results it must be inferred that the proposal [23] to reduce the area of the shear diagram (by "slicing" it off obliquely) near the bearings because of the stresses σ_y due to the transmission of force into the beam, i.e. to reduce the amount of shear reinforcement in that region, would result in a lowering of the safety against shear failure and is therefore to be deprecated.

7.4.7 Shear cracking

The loads and shear stresses giving rise to shear cracking* can be determined from the stirrup stress curves (Figures 90 and 91) by finding the intersection of the straight portion of the stress-load curve with the horizontal axis of co-ordinates. This yields the following result, on the assumption of state II (cracked sections) for determining τ_o.

TABLE XVIII

	$2Q_{sr}$ (t)	$\tau_{o\,sr} = Q_{sr}/b_o z$ (kg/cm²)	
ET 1	19·1	19·1	
ET 2	9·8	12·9	average - 14 kg/cm²
ET 3	7·8	16·4	
ET 4	4·0	15·5	
GT 1	24·6	16·1	
GT 2	12·6	16·2	average - 16 kg/cm²
GT 3/1	6·8	13·1	
GT 4/1	4·6	17·9	

Because of σ_y, and despite the lower strength of the concrete, the values are somewhat higher for the uniformly loaded beams than for beams with concentrated loads. It would be more correct in this case to calculate the principal tensile stresses for the uncracked state. However, depending on the web width, they are only 5 - 10 % higher than those calculated on the assumption of state II. The principal tensile stresses causing shear cracking therefore again do not attain the tensile strength of the concrete, which in the present case can be taken as 25 - 28 kg/cm².

Note

The stirrup stress curves (Figures 90 and 91) can be approximately represented by the following formulae:

* The shear stress τ_o which produces cracking is designated as τ_{oSR}. (Translator's note.)

for concentrated loads: $\sigma_{e(\text{stirrups})} = \dfrac{\tau_o - \tau_{oSR}}{\mu\,(\text{stirrups})}$

for uniformly distributed load: $\sigma_{e(\text{stirrups})} = \dfrac{\tau_o - \tau_{oSR} - \sigma_y}{\mu\,(\text{stirrups})}$

The first formula corresponds approximately to the American Standard Specifications for reinforced concrete and prestressed concrete beams, according to which only a portion of the shear force (or of the principal tensile stresses) has to be catered for by shear reinforcement. American designers are permitted to deduct a strip of constant width from the shear force diagram. In the early days of reinforced concrete design this was also allowed by the Prussian Standard Specifications, but was rightly deprecated by Mörsch. Formulae of this sort create the false impression that the concrete is still able to resist tensile stress after it has cracked. Actually, however, the stirrup stresses are reduced not because the web assists in resisting oblique tension but because of the greater stiffness of the inclined struts, which is approximately proportional to b_o.

If the stirrups are designed on the basis of the difference $\tau_o - \tau_o$ crack the amount of stirrup reinforcement would be too much governed by the web width. On this basis, in the case of the tests under present consideration, the beams with webs about 15 cm wide and upwards would not have needed any shear reinforcement at all, whereas beam GT4/2 would have had to be provided with 50 % more stirrup reinforcement than it actually contained. The tests show clearly, however, that this method of design would not be a sensible one for thin webs and would be dangerous in the case of the thick webs.

We shall therefore have to derive other factors for justifying a possible reduction of the shear reinforcement from the test results.

7.4.8 Stresses in the compression flange

The compressive stresses which occurred at the top surfaces of the beams will be reported in the publication of the Deutscher Ausschuss für Stahlbeton containing the full test results obtained.

7.4.9 The cracking behaviour of the beams

The cracking pattern is shown in Figures 84 and 85. The thinner the web, the greater is the number of shear cracks inclined at 45°. Approximately vertical flexural cracks occurred only between the two concentrated loads and in a region equal to about 1/5 of the span length in the case of the beams with uniformly distributed loading.

Although the reinforcement comprising four 20 mm bars was not particularly well distributed, only very fine flexural cracks at an average spacing of 6 - 8 cm occurred. Under working load the maximum widths of the flexural cracks were 0·06 mm. No differences in the widths of the cracks associated with different types of loading were observed. The cracking load, of course, decreased with the web thickness (see Table XV, column 18).

On the other hand, the shear cracks are found to be considerably affected by the web width. A comparison of the flexural and shear cracks

of the ET series (Figure 96) shows that in the case of the rectangular section (beam ET 1) the sum of the shear crack widths measured half-way up the web is significantly smaller than that measured at the level of the reinforcement. In the case of beam ET2 these sums of the crack widths are approximately equal in the higher stages of loading. With beam ET3 and, even more so, with beam ET4 the sum of the shear crack widths is a multiple of the sum of the flexural crack widths.

The steel stress behaviour in the stirrups (Figures 90 and 91) is in close agreement with the increase of the crack widths: as soon as the stirrup stresses increase, the cracks open out; if yielding of the stirrups occurs, very wide shear cracks are formed.

The beams subjected to uniformly distributed loading present the same picture (Figure 97). As the beams of the GT series did, indeed, have the same numbers of stirrups to the right and left of mid-span, but not the same stirrup arrangement, the sums of the crack widths on each side are compared in Figure 97. In the case of beam GT1 there is found to be no difference in the sums of the crack widths, since the stirrups were subjected only to low stresses. In all the other beams, however, the crack width on the side with constant stirrup spacing is significantly larger, which corresponds to the higher stress in the steel (cf. Figure 91). Under working load nevertheless even the widest shear cracks remained below 0·10 mm (with the exception of 0·13 mm in the case of GT4/1), i.e. the stirrup reinforcement was adequate to prevent excessively wide shear cracks even in thin webs.

7.4.10 Deflexions

The deflexions (Figures 98 and 99) are clearly related to the web width and stirrup arrangement; this can be attributed to the shear deformations. In particular, the difference in deflexions of beams GT3/1 and 3/2 and of GT4/1 and 4/2 should be noted: here again the favourable effect of stirrups closely spaced at the supports is confirmed. The effect of the shear deformation becomes very clearly apparent if the deflexion curves for a certain stage of loading are plotted upwards, starting from the middle ordinate, as in Figures 100 and 101. The beams of the E-series exhibit a 50 % increase of deflexion, and those of the G-series an 80 % increase, owing to the shear deformation due to the smaller web thickness, or alternatively, in the case of the G-series, owing to unfavourable stirrup arrangement. These shear deformations, of course, have a substantial share in reducing the shear strength of the beam with decreasing web thickness.

7.4.11 Anchorage of longitudinal reinforcement

In view of the stirruped anchorage length of 20 cm, no anchorage failure was anticipated. No slip of the reinforcing bars was found to occur. Only in the case of beam GT3/1 were a displacement of 0·01 mm under a load of 30 tons, and a displacement of 0·07 mm after failure, measured. The partial failure of the anchorage in this case is attributable to the horizontal cracks over the reinforcement in the region of the large shear cracks which formed on the side with constant stirrup spacing as a result of yielding of the stirrups (cf. Figure 95).

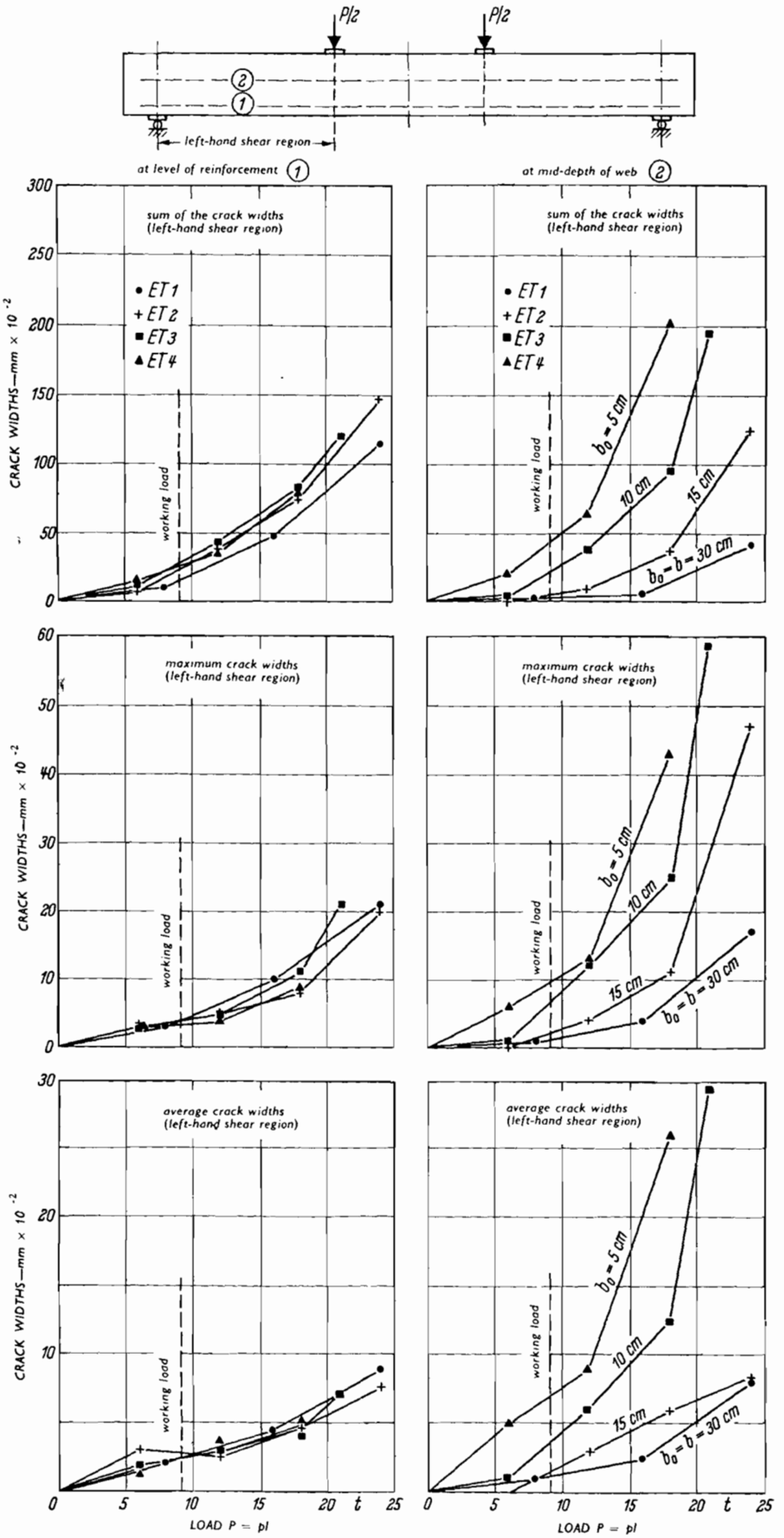

Figure 96: Comparison of crack widths for concentrated-load beams with varying web widths.

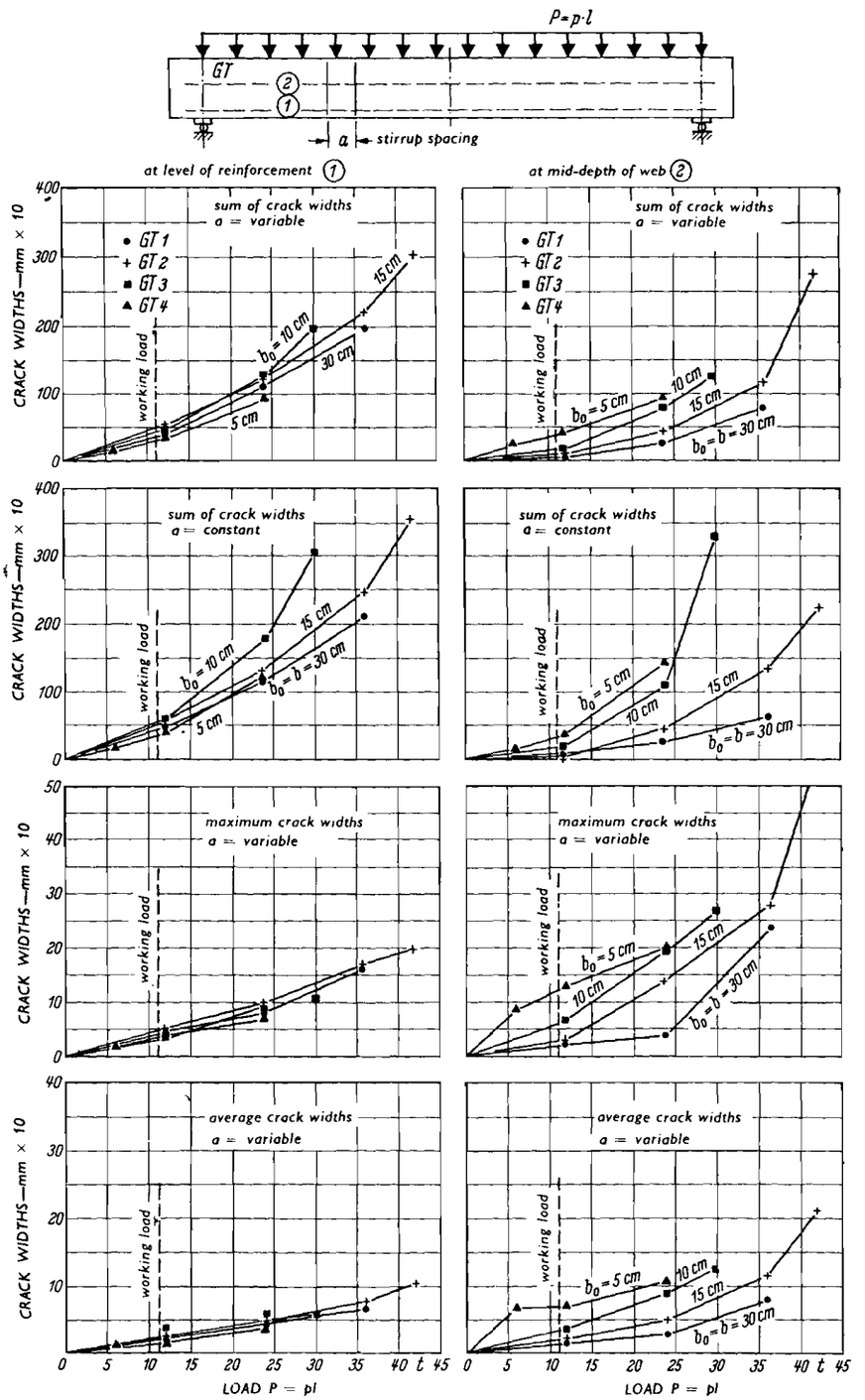

Figure 97: Comparison of crack widths for uniformly loaded beams with varying web widths.

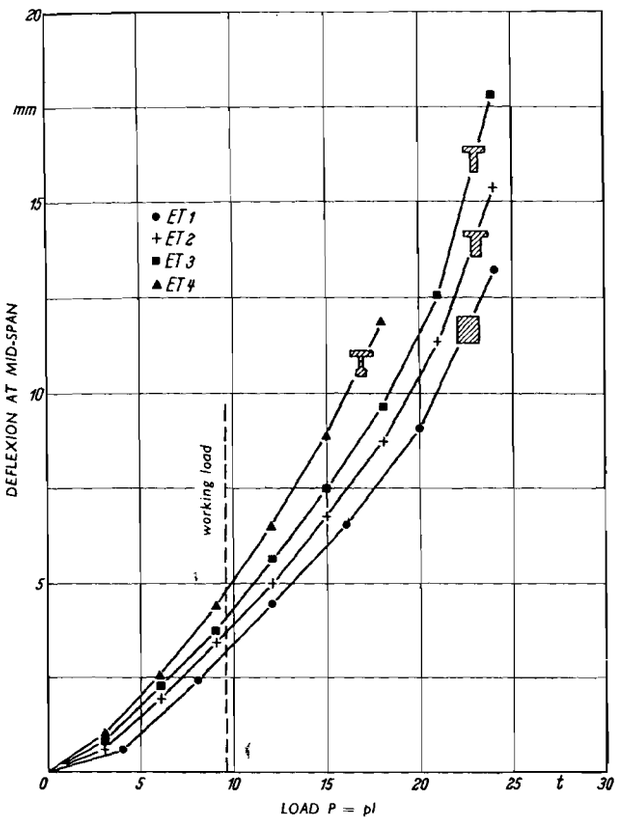

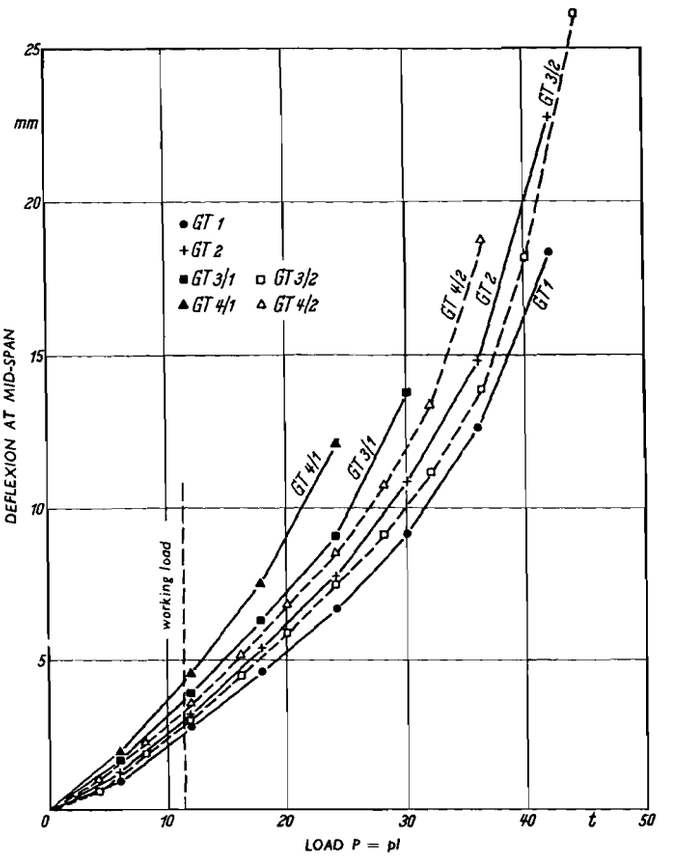

Figure 98 (left): Comparison of the deflexion at mid-span for varying web widths (beams with concentrated loads).

Figure 99 (right): Comparison of the deflexions at mid-span for varying web widths (beams with uniformly distributed loading).

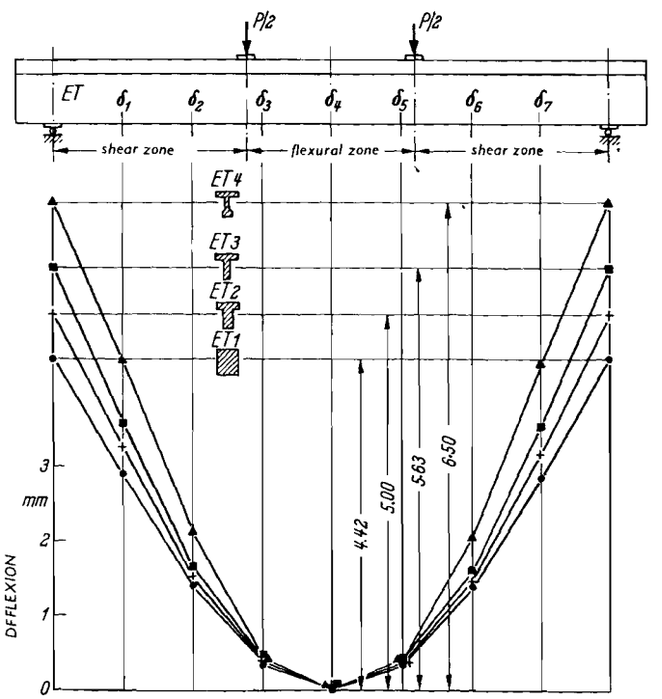

Figure 100: Deflexion curves for P = 12 tons on concentrated-load beams with varying web widths.

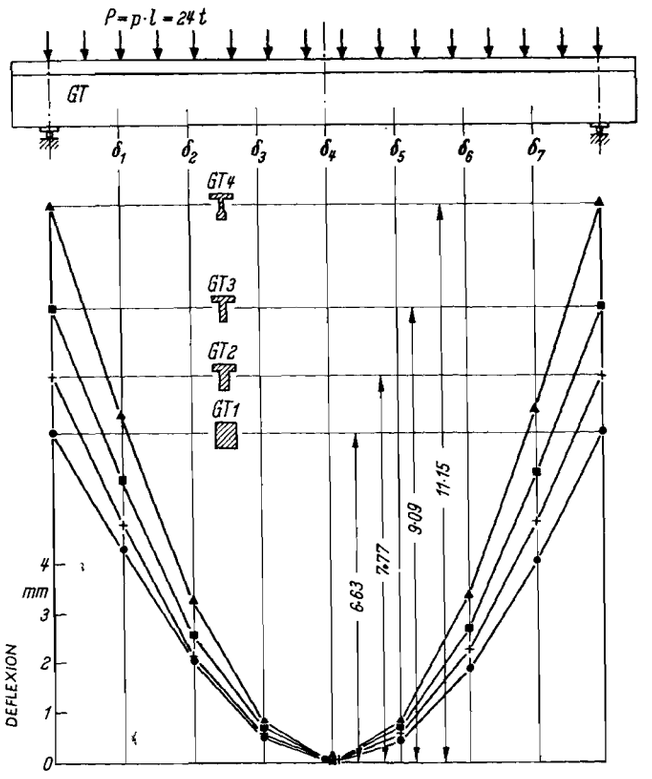

Figure 101: Deflexion curves for pl = 24 tons on uniformly loaded beams with varying web widths.

8. Final remark to Section II - Test reports

The tests described in Sections II.2 - II.7 were carried out by a team under the leadership of Dr-Ing. R. Walther in Prof. Dr-Ing. G. Weil's departments of the Otto Graf Institute (Technological University of Stuttgart). The testing programmes were drawn up by the authors of this article. Co-workers of the Institute and of Prof. Dr-Ing. F. Leonhardt participated in the execution and evaluation of the tests. The authors acknowledge their indebtedness to all those who were associated with this work.

The considerable funds nowadays involved in the execution of such tests were very kindly made available by the Ministry of Economic Affairs of Baden-Wurtemberg, the Fachverband Zement (Cement Federation), and the Federation of the Baden-Wurtemberg Building Industry. The various materials were made available free of charge: the steel reinforcement by Betonstahl-Gemeinschaft Deutscher Hüttenwerke, and the cement by Messrs C.Schwenck, Ulm, and Portlandzementwerke Heidelberg. The authors trust that they have used the available means in the best interests of building owners and the building industry and that the test results will soon lead to advantageous modifications of the official regulations and thus make for simpler design methods and help to effect savings.

III. SUMMARY AND PROVISIONAL CONCLUSIONS

1. Types of shear failure

The following types of shear failure can be distinguished:

1.1 Shear flexural failure: The shear cracks rise so high that eventually

the compressive zone fails; it occurs more particularly in beams which are not or only partially reinforced against shear failure, but it may also occur over the intermediate supports of continuous beams which are so reinforced as to have "full safeguard against shear failure ".

1.2 Web failure:

(a) in oblique compression for large values of τ_o, the determining oblique compressive stress being largely dependent upon the direction of the web reinforcement;

(b) as a result of overstressing of the shear reinforcement (occurs only in the case of reduced safeguard against shear failure); in certain circumstances the compression flange may also be destroyed.

1.3 Failure of the anchorage of the main reinforcement: causes the web or the compression flange to be destroyed before actual shear failure occurs.

Splitting of the web concrete at the curves of bent-up inclined bars.

2. Factors affecting the shear strength

The shear strength (ultimate load-carrying capacity in shear)* of reinforced concrete beams is governed by the following quantities and influencing factors:

2.1 The quality of the concrete. In the case of shear flexural failure the shear strength - like the purely flexural ultimate strength - increases approximately in proportion to $\sqrt[3]{\beta_p}$ (Figure 102). On the other hand, in the case of failure in oblique compression (1.2a) a more linear relationship can be expected.

2.2 The degree of reinforcement (percentage of steel) μ of the flexural reinforcement, i.e. the shear strength is affected by the tensile strain of the bars at cracks in the shearing region (Figure 103).

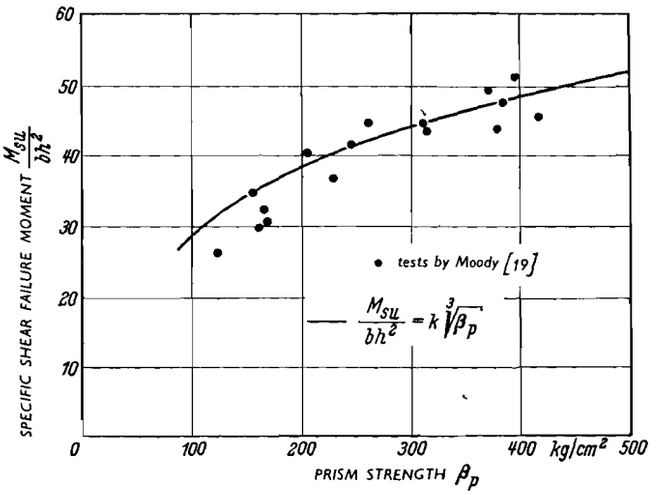

Figure 102: Relationship between shear strength (load capacity in respect of shear) and concrete quality.

* In the following diagrams the shear strength is generally indicated as the "specific" shear failure moment M_{SU}/bh^2 or $M_{SU}/\sqrt[3]{\beta_p}bh^2$

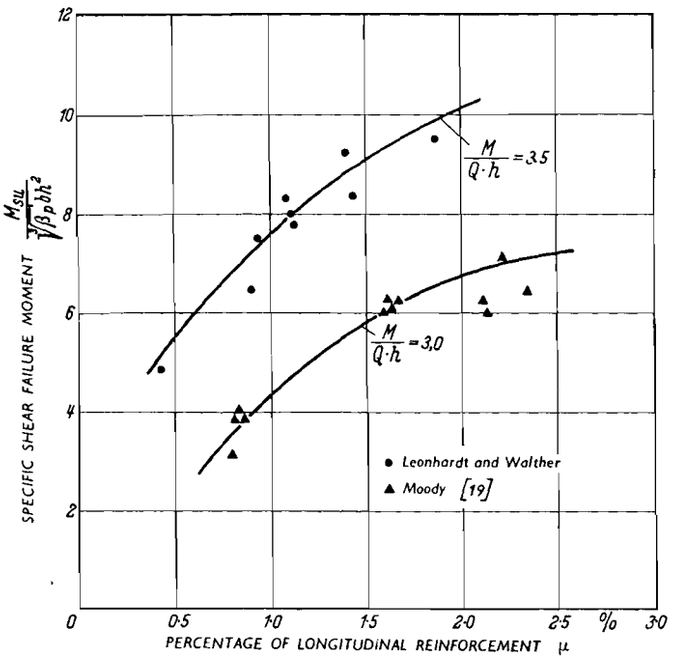

Figure 103: Relationship between shear strength and percentage of longitudinal reinforcement.

2.3 The quality of the bond between the reinforcement and the concrete, even if none but deformed bars are used. Distributing the reinforcement over a larger number of thinner bars - e.g. 16 mm instead of 26 mm - produced increases in shear strength of 15 - 28 %. The distribution of the reinforcement in the form of closely spaced thin bars is, in the case of high-tensile steel, favourable not only because of the reduced crack widths but also from the viewpoint of shear strength (Figure 104).

2.4 The curtailment of the flexural reinforcement. The effect of the tensile strain (2.2) shows that curtailment of the reinforcement so as to follow the outline of the bending moment diagram in beams which are not or only partially reinforced against shear failure will result in reduced shear strength as compared with such beams in which the bars are continued beyond the supports (test results relating to this will follow in due course).

2.5 The quality of the anchorage of the reinforcing bars. In the tests described in the present report, anchorage failures were deliberately prevented.

The need for good anchorage must not be overlocked, however, because the steel stresses do not decrease proportionally to the bending moments towards the bearings. Even a slight amount of slip will result in premature shear-like failure. It appears that the anchorage length for ribbed deformed bars, as laid down in the provisional regulations (October 1954), viz. 6 times the bar diameter, is not adequate for closely spaced bars in the absence of transverse reinforcement. It is essential that this anchorage length also be appropriately varied according to the quality (i.e., the strength) of the concrete employed.

2.6 The cross-sectional shape. Beams with thin webs (high τ_o) have lower shear failure loads than beams with thick webs, as the shear reinforcement is more and more highly stressed according as the stiffness of the oblique compressive members ("struts") decreases. The effect is not a linear one, however (Figure 105).

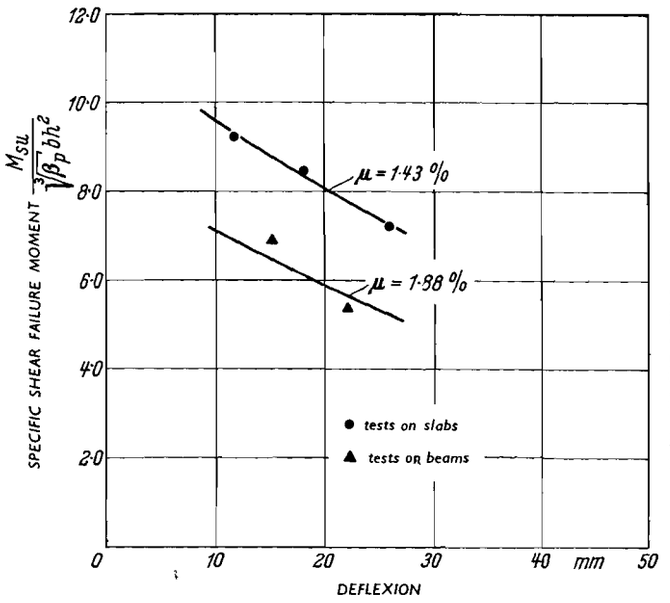

Figure 104: Relationship between shear strength and bar diameter for a given percentage of reinforcing steel.

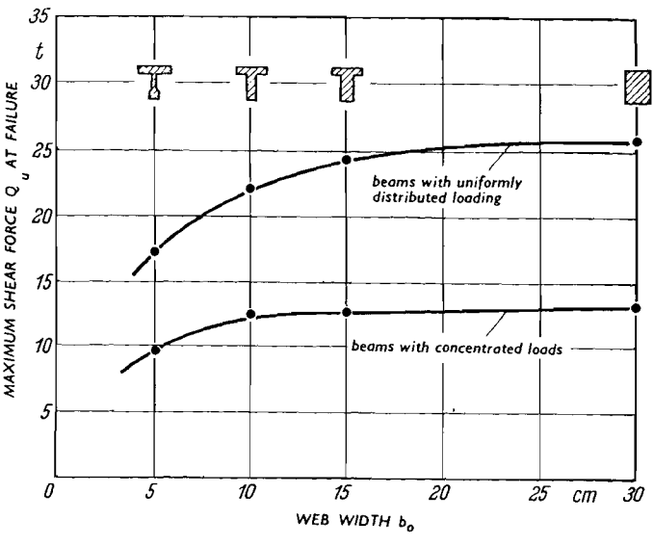

Figure 105: Relationship between shear strength and web width b_o for constant width b of compression flange.

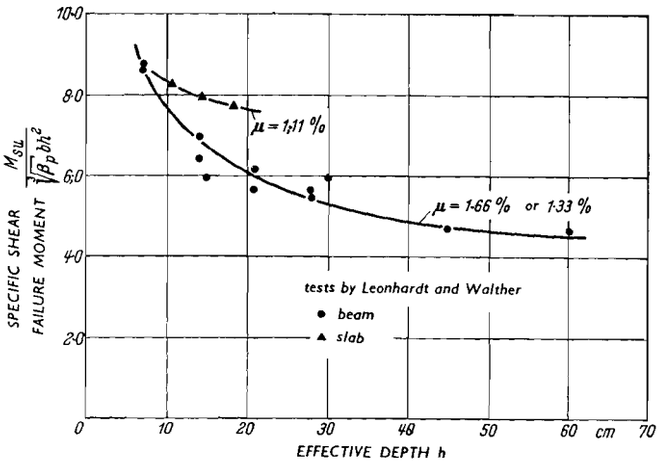

Figure 106: Relationship between shear strength and absolute value of beam depth h.

2.7 The absolute depth d of the cross-section (or the effective depth h). Shallower sections have relatively greater shear strength than deeper ones (Figure 106). The limit of this effect is approximately at d = 40 cm. For h = 7 cm the relative shear strength was about 50 % higher than for h = 28 cm. Hence it is wrong to use too small test specimens for tests aimed at determining absolute values of the shear strength which are required to be valid for larger members as well.

2.8 The type of loading is of considerable importance. In all the tests, uniformly distributed loading was associated with 20 - 40 % higher shear strength, if the largest shear force Q is adopted as the criterion. This is due to the effect of the bending moment (which with concentrated loads is larger at the shear failure section than with uniformly distributed loading) and to the pressure exerted by the loading, which strengthens the compressive zone. However, actual live loads usually do not consist of distri-

buted loading exerting a uniform pressure. It is therefore not possible to take general advantage of the favourable results obtained with this kind of loading. Instead, the results obtained with concentrated loads must be taken into account for design purposes. No test results with distributed loading applied only to parts of the total span length are available.

2.9 The moment-shear ratio M/Qh, which is determined by the loading and support conditions.

With shear flexural failure the shear crack spreads upwards at the section where M/Qh is large, until the flexural compressive zone crushes: in this process the deciding factor is not Q alone, but always Q in combination with M. For a given Q, shear failure will occur earlier according as the moment which acts at the same time is larger. The determining value of M/Qh is that which occurs at the section corresponding to the upper end of the shear fracture. The shear force attained at failure decreases with increasing M/Qh: the relevant curves (Figure 107) slope steeply up to about M/Qh = 3 and then flatten out, attaining their minimum at M/Qh = 7 - 8, provided that the reinforcement is sufficient to ensure that flexural failure does not occur first. We can thus distinguish two ranges: in the first range the moment-shear ratio M/Qh has a considerable effect (up to a value M/Qh = 3); in the second range the effect of M is smaller, for approximately constant max.Q_u.

With uniformly distributed loading, the borderline between the two ranges is determined more by the slenderness ratio l/h: in the tests performed, the borderline was determined by $l/h = 12$ (Figure 108).

The increased shear strength for small values of M/Qh is undoubtedly because a larger proportion of the shear force is then resisted by the "arch and tie-rod" or "truss" action (large depth/span ratio, steep slope of the thrust resultants). Hence it follows that loads close to the bearings are less dangerous from the viewpoint of shear failure than are loads for which $x \geq 3h$.

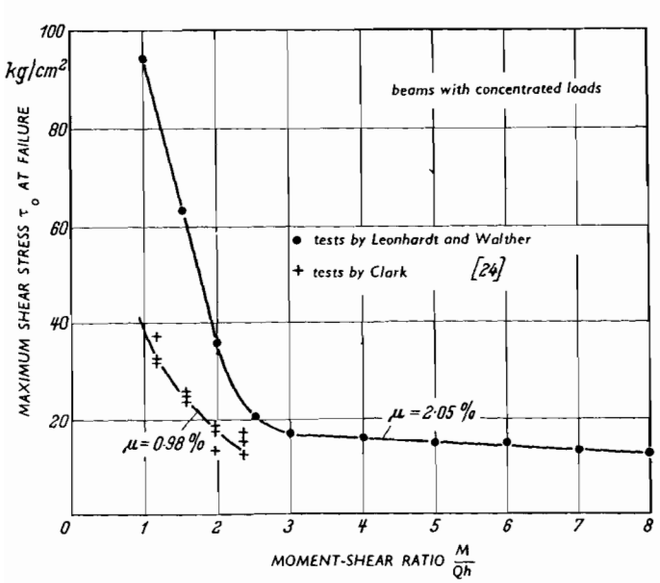

Figure 107: Relationship between shear strength and moment-shear ratio M/Qh.

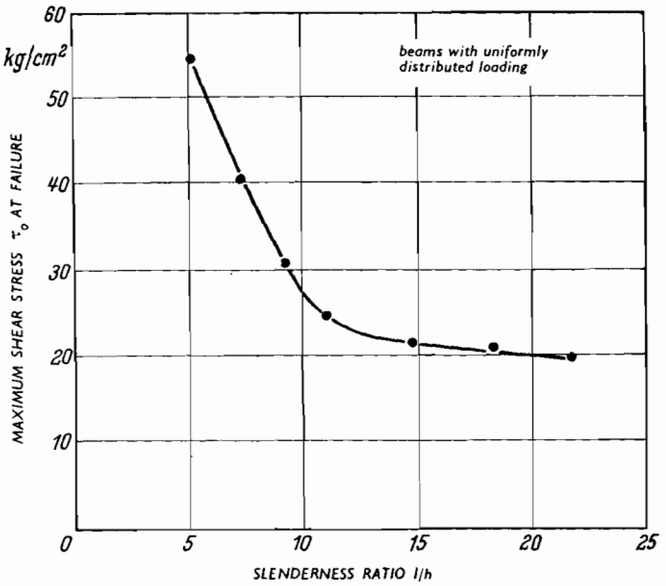

Figure 108: Relationship between shear strength and slenderness of the beam under uniformly distributed loading.

It is tempting to define the limit of this range in terms of slenderness, i.e. to state that short beams or girder walls without shear reinforcement can permissibly be more highly loaded in shear than slender beams. This would, however, be erroneous for concentrated loads or distributed loads acting on parts of the span only: for such loads the enhanced shear strength is obtained also in slender beams, if the load is applied close to the bearing. The criterion M/Qh cannot therefore be replaced by the slenderness ratio of the structure.

As long as the safety against shear failure is verified with the aid of permiss. τ_o, the effect of the moment-shear ratio M/Qh can be taken into account by laying down a diminishing value for permiss. τ_o for values of M/Qh increasing from 0 to 3, and a constant value for permiss. τ_o for M/Qh > 3.

For the shear failure of beams with $l/h > 4$ it is never the section directly beside the bearing which is critical, but in the case of uniformly distributed loading always a section at a distance of 2·0 h to 3·5 h from the bearing, and in the case of concentrated loads the section besides the concentrated load which produces the unfavourable M/Qh.

3. The requisite degree of safeguard against shear failure

The shear reinforcement necessary for ensuring the desired safety against shear failure depends not only on the quantities M and Q, but to a considerable extent also on the stiffness conditions of the structure or its components. If we make use of the lattice analogy, we must adopt not the statically determinate lattice system, but the internally multi-redundant lattice system with varying stiffnesses of the tension and compression members - i.e. the compression chord, the many oblique struts, the stirrups, and the main tensile reinforcement. Depending on these stiffness conditions, a transition from arch action to lattice action is developed. Quite often the arch action only has to be slightly assisted by the lattice action in order to avoid a shear failure.

Obviously, in most cases encountered in practice, namely, full rectangular sections of T-beams with web thicknesses designed on the basis of permiss. τ_o in accordance with the existing rules, a lower degree of safeguard against shear failure is adequate. If the condition where the entire τ_o diagram is catered for by means of stirrups and inclined bars (according to E. Morsch's concepts) is rated as 100 % shear safeguard, then in many cases a 30 - 50 % shear safeguard will suffice.

The loads are carried primarily by the "arch and tie-rod" action, which constitutes a stiffer load-carrying system than the lattice structure with highly extensible tensile members. The shear reinforcement does not come into operation until the "arch and tie-rod" action is disturbed by shear cracks. But even then the oblique struts (compression members) of the lattice system are stiffer than the tension members formed by the shear reinforcement, so that part of the arch action continues to exist and the shear force therefore does not have to be resisted by the "web members" alone: instead, part of the shear force is taken up by the compression flange (and, in the case of I-section beams, also by the tension flange).

The predominance of the "arch and tie-rod" action in the normally encountered cases requires that the main reinforcement (i.e., the "tie-rod") should largely be continued up to the bearings of the beam. In cases where reduced safeguard against shear failure is to be applied, stirrups are accordingly more suitable than bent-up inclined bars.

Now the requisite degree of safeguard against shear failure is dependent not only upon Q (or τ_o) alone, but also upon the bending moment; it will therefore be no simple matter to determine it reliably. Further tests in this connexion are in progress. For shear flexural failure a method based on Walther's shear failure theory will be indicated. As long as design is based on permissible stresses under working-load conditions, the requisite degree of shear safeguard can be approximately related to τ_o if at the same time we consider the stress σ_e in the flexural reinforcement which expresses the effect of the moment M acting at the critical section. It will still have to be investigated, however, from which value of τ_o onwards it will be necessary to provide full shear safeguard.

The tests described in Sections II.1 and II.7 have given sufficient information as to the upper τ_o limit which, in view of the type of failure considered in point 1.2a, must not be exceeded. For high shear load and full shear safeguard the lattice action predominates, so that the oblique compressive stresses can be adequately calculated by means of the simple lattice theory with appropriate allowances to take account of the stiffness conditions. It must be remembered, however, that in the oblique struts the full compressive strength of the concrete can develop only if the struts are rigidly supported and firmly held at the top and bottom, as was ensured by the transversely reinforced webs and narrow stirrups in tests II.1. With wide stirrups, complete utilization of the compressive strength in the oblique struts will not be possible, as will be further explained in Section 4.

Even under very high shear load the tensile stresses in the shear reinforcement remain about 20 % below the values calculated on the basis of the lattice theory, so that the reinforcement designed for full safeguard against shear failure is always adequate.

Even if full shear safeguard under high shear load is provided, the curtailment of the flexural reinforcement (the main bars in the bottom of the beam) in accordance with the bending moment diagram must not be overdone, since even in this case a portion of the shear force is resisted by the "arch and tie-rod" action. For this reason the "tie-rod" must not be too greatly weakened in the vicinity of the bearings. Besides, with vertical stirrups, the tensile force Z is larger then the compressive force D (see Figure 15) in a vertical section.

4. The efficient use of the various types of shear reinforcement

The tests and the interpretation thereof show that closely spaced thin stirrups are far superior to - usually thick - bent-up bars as shear reinforcement * in that they are associated with narrower cracks and smaller shear deformations and thus result in higher shear strength of the beam. Bent-up bars are associated with wide shear cracks. This does not mean to say that bent-up inclined bars should no longer be used; they will certainly continue to be employed as a means of resisting the negative bending moments in continuous structures.

However, as soon as less than full safeguard against shear failure is adopted, stirrups are preferable, as they are better suited for "suspending" the oblique struts than inclined bars are, because they enclose the main reinforcement which primarily has to support the concrete struts. Strictly

---

* The favourable effect of very thin closely spaced stirrups was ascertained by C. Bach and O. Graf as far back as 1909 [20].

speaking, a stirrup as a means of suspension should be available for each strut, especially in the vicinity of the bearings of the beam. In T-beams the stirrups are also necessary for ensuring the shear connexion between the compression flange and the web. The desirable close spacing of the stirrups can be conveniently obtained by means of welded reinforcement cages (e.g. bent-up mesh reinforcement mats), though in small beams it may be preferable to use spirally wound stirrups.

For normal beams, for which it will be permissible to reduce the degree of safeguard against shear failure, it is sufficient to provide stirrups only, i.e. without bent-up bars. Thanks to the web reinforcement, a proportion of the flange members (1/3 to 1/2, depending on the degree of shear safeguard provided) can terminate with sufficient anchorage length in the tensile zone. Hence it will often be possible to reinforce a beam with straight bars and stirrups only, thus obviating the bending-up of bars, without having to use more steel. This simplification of the reinforcement is economically advantageous, having regard to the present high level of wages.

Stirrups sloped at 45° or - in more general terms - sloped in the direction of the principal tensile stresses at the level of the centroidal axis for state I (uncracked) have the most favourable effect and are associated with the narrowest shear cracks. As long as the oblique compressive stresses do not become the determining factor, however, there appears to be no significant difference in shear strength as compared with vertical stirrup arrangement, which is more convenient for practical purposes. Up to a certain value of τ_o it is therefore permissible to use vertical stirrups. But if τ_o exceeds that value, then oblique stirrups should be provided, whereby the oblique compressive stresses in the web are reduced. For webs subjected to high shear loads or for diaphragms (girder walls) it is in any case preferable to install oblique stirrups because of the reduced crack widths obtained with them. The constructional advantages are indicated in Figure 26 (Beton-und Stahlbetonbau. Vol. 56, No. 12. December 1961.)

The tests showed that stirrups inclined at 45° need not have any special structural connexion to the ribbed flange bars, provided that they enclose these bars.

The effect of the stirrups which enclose and restrain the concrete is favourable both in the tensile flange for transmitting the oblique compressive forces into the reinforcement and also in the compressive flange for increasing the load-carrying capacity. On the other hand, bent-up bars exert a splitting, i.e. unfavourable, action.

More attention will in future have to be paid to the width of the stirrups. The tests were concerned only with fairly narrow webs (up to b_o = 30 cm). With substantially wider webs the stirrups can be expected to exercise the same favourable effect, because in such cases the oblique struts are, as it were, supported only laterally at the edges, where the stirrup forces are acting (Figure 109). They can be regarded as amall "girder walls" (diaphragm type deep beams), and their load-carrying capacity will be exhausted when the concrete fails near the bearings in consequence of local pressure, possibly influenced by splitting action. These considerations suggest that the maximum stirrup width b_B must be related to the oblique compressive stress σ_{II} , i.e. to the stress τ_o. If it is desired to make full use of a high τ_o, then the stirrup legs will have to be closely spaced in the direction transverse to the centre-line of the beam, e.g. at 20 cm centres, and thick webs will have to be reinforced with three- or four-leg

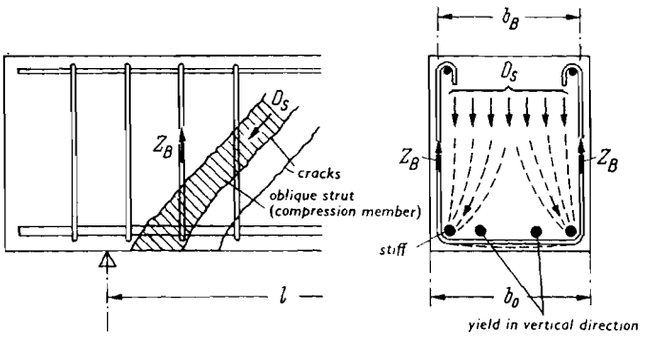

Figure 109: The oblique "strut" suspended from stirrups is somewhat like a deep beam supported on the longitudinal bars at the bottom corners of the section; the longitudinal bars between the corner bars are yielding.

stirrups, as has hitherto already been normal practice for wide beams. If τ_0 and therefore σ_{II} is small, the transverse spacing of the stirrup legs can be made 40 cm or more, though the spacing should not exceed the effective depth h of the beam. For supporting the oblique struts, it is necessary also to provide longitudinal bars at the corners of the stirrups, and these bars should continue as far as the bearings of the beam, i.e. they should never be bent up.

The stirrups should always be properly anchored at top and bottom. Stirrups which are open at the top and have no hooks must be regarded as unsatisfactory, even if ribbed bars are used. They should at least be provided with L-hooks or preferably U-hooks. In cases where mesh mats are used for forming the stirrup reinforcement it is still advisable to bend them over at the top, and at least one longitudinal bar close to the upper end of the stirrups should be welded on to ensure proper anchorage.

The tests revealed only minor differences between ribbed and plain stirrups if the ends were duly anchored.

Class III and IV steels can, in terms of their permissible stress, be fully utilized for stirrups if they are closely spaced (10 - 20 cm).

5. Proposal for permissible shear stresses and the degrees of shear safeguard associated with them

As long as ultimate-load analysis in respect of shear failure is not introduced into the Code of Practice, the safeguard against this type of failure will continue to be catered for on the basis of permissible shear stresses τ_0. The test results indicate that the permissible values of τ_0 should conform to a more closely graded scale than hitherto, so as to take account of the effect of M/Qh and avoid the unnecessary jump from no shear safeguard to full shear safeguard on exceeding the lower limit for τ_0. To achieve this, it is necessary to relate permiss. τ_0 to M/Qh or to l/h, as was apparent from the tests. In actual practice, however, this relationship will have to be taken into account only if τ_0 exceeds the limiting values that have hitherto been applicable.

Four ranges can be introduced with regard to permiss. τ_0, the degree and the nature of the safeguard against shear failure:

1. Lower range, with low τ_0 (depending upon $\sqrt{\beta_p}$): no shear reinforcement in slabs; beams should be provided with thin "nominal" stirrups (i.e. not checked by calculation) with spacing $\leq d < 40$ cm, where d denotes over-all depth of beam.

2. Middle range, approximately up to the upper limit of τ_o as hitherto applied, with a degree of shear safeguard increasing from 20 - 100 % linearly with τ_o: shear reinforcement should consist preferably of vertical stirrups with spacing $\leq \frac{1}{2}d < 30$ cm; longitudinal bars should not be curtailed or be curtailed only to a small extent.

3. Upper range, approximately up to $\tau_o = 0{\cdot}14\ \beta_p$, with full shear safeguard provided by stirrups or stirrups in conjunction with bent-up inclined bars: stirrup spacing same as in middle range.

4. Top range, approximately up to $\tau_o = 0{\cdot}18\ \beta_p$, with full shear safeguard provided by closely spaced stirrups inclined approximately in the direction of the principal tensile stress at the level of the centroidal axis of the beam in state (uncracked): permissible deviation of direction $\pm$ 15° to $\pm$ 20°.

The permissible shear stresses and the degrees of shear safeguard associated with them are represented for B 300 concrete in Figure 110. For other classes of concrete the limiting values are indicated in the scales to the left of the diagram. A diagram of this kind should preferably be prepared for each class of concrete. It shows directly the requisite degree of shear safeguard for the actual τ_o due to max. Q.

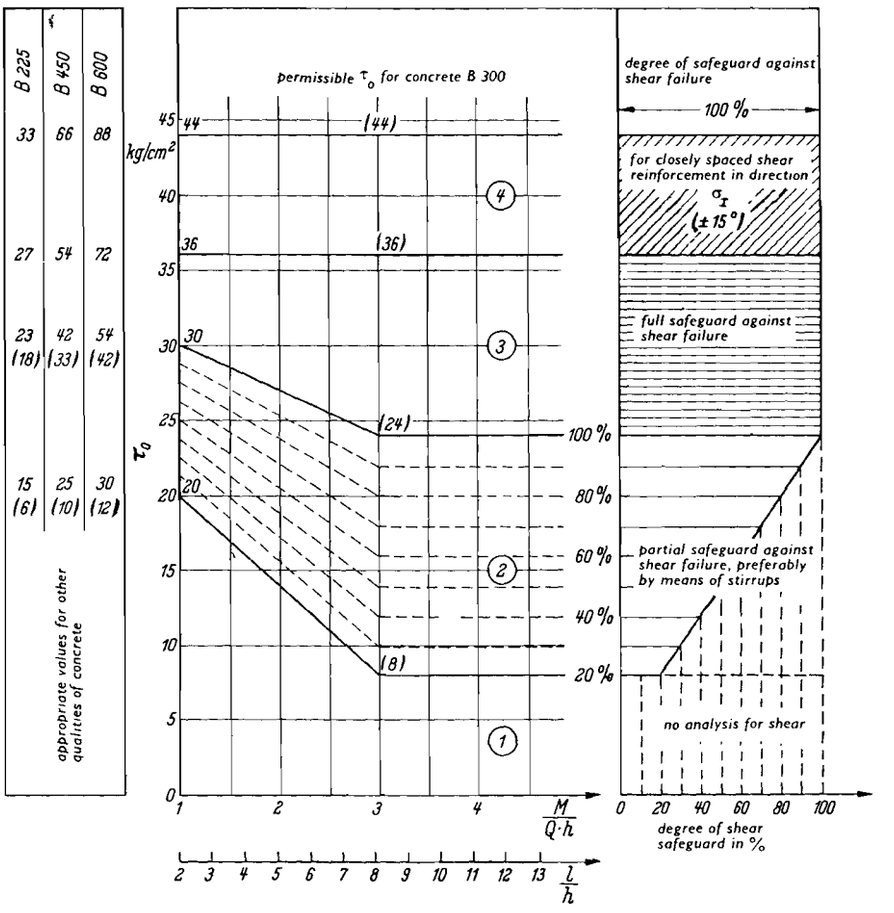

Figure 110: Proposal for permissible τ_o due to maximum Q and associated degree of safeguard against shear failure for concrete B 300 and ribbed longitudinal reinforcement. For other concrete qualities, appropriate diagrams of this kind should be drawn.

If τ_o exceeds the limiting value for $M/Qh > 3$ or $l/h > 8$ of any particular range, it should be checked whether M/Qh at the critical shear section or l/h is such that higher values are permissible. The requisite degree of shear safeguard should then be established for the point in the diagram (Figure 110) determined by M/Qh or l/h and τ_o. This proposal takes no account of various influencing factors ascertained in the tests, e.g. percentage of reinforcing steel and quality of bond, in order to obtain a set of rules which is as simple as possible for practical purpose and yet safe.

In comparison with the test results, the limiting values for the lower range are somewhat too high, if a factor of safety of 2·1 for failure without warning is taken as the basis. The favourable experience that has hitherto been gained at even higher values, in the absence of shear reinforcement, justifies this. For all other values a safety factor of at least 3 can be expected.

The flange reinforcement * should consist of ribbed or deformed steel. With plain round reinforcing bars it is permissible to use only the ranges 1 and 2, in conjunction with values of permiss. τ_o reduced by 20 %.

This proposal is presented as a basis for discussion; comments, particularly from practising engineers, will be welcomed.

The test results have yielded knowledge which permits considerable savings and constructional simplification in shear reinforcement and which this proposal seeks to utilize.

---

* The term "Gurtbewehrung" presumably refers more particularly to the main reinforcement at the bottom of the beam (which need not actually have a bottom flange). (Translator's note.)

REFERENCES

1. WALTHER, R. Über die Beanspruchung der Schubarmierung von Eisenbetonbalken. Schweizerische Bauzeitung. Vol. 74. No. 1. 7 January 1956. pp. 8 - 12. No. 2. 14 January 1956. pp. 13 - 17. No. 3. 21 January 1956. pp. 34 - 37.

2. LAUPA, A., SIESS, C.P. and NEWMARK, N.M. Strength in shear of reinforced concrete beams. University of Illinois Engineering Experiment Station Bulletin No. 428. March 1955. pp. 73.

3. MOODY, K.G., VIEST, I.M., ELSTNER, R.C. and HOGNESTAD, E. Shear strength of reinforced concrete beams. Part 1. Tests of simple beams. Journal of the American Concrete Institute. Vol. 26. No. 4. December 1954. pp. 317 - 332. No. 5. January 1955. pp. 417 - 434. No. 6. February 1955. pp. 525 - 539. No. 7. March 1955. pp. 697 - 730.

4. GURALNICK, S.A. Shear strength of reinforced concrete beams. Proceedings of the American Society of Civil Engineers. Vol. 85, No. ST 1. January 1959. pp. 1 - 63.

5. SOZEN, M.A., ZWOYER, E.M. and SIESS, C.P. Investigation of prestressed concrete for highway bridges. Part 1. Strength in shear of beams without web reinforcement. University of Illinois Engineering Experiment Station Bulletin No. 452. 1959. pp. 69.

6. RÜSCH, H. and VIGERUST, G. Schubsicherung bei Spannbeton ohne Schubbewehrung. Berlin, Deutscher Auschuss für Stahlbeton, 1960. pp. 1 - 18. No. 137.

7. WALTHER, R. The ultimate strength of prestressed and conventionally reinforced concrete under the combined action of moment and shear. Thesis submitted to Lehigh University for the degree of Ph.D., October 1957. pp. 145. Fritz Laboratory Report 223.17.

8. MÖRSCH, E. Der Eisenbetonbau, seine Theorie und Anwendung, Vol. 1, Part 2. 6th Edition. Stuttgart, Konrad Wittwer, 1929. pp. 541.

9. GYENGÖ, T. and EGRESI, M. Über die Biegeschubfestigkeit der Stahlbeton-Plattenbalken. Die Bautechnik. Vol. 37, No. 11. November 1960. pp. 436 - 437.

10. LEONHARDT, F. and ANDRÄ, W. Fächerverankerung grosser Vorspannkabel. 1. Teil Versuche. Beton- und Stahlbetonbau. Vol. 53, No. 5. May 1958. pp. 121 - 130.

11. RAUSCH, E. Drillung (Torsion), Schub und Scheren im Stahlbetonbau. 3rd edition. Dusseldorf, Deutscher Ingenieur Verlag, 1953. pp. 168.

12. ROBINSON, J.R. Essais à l'effort tranchant de poutres à âme mince en béton armé. Annales des Ponts et Chaussées. Vol. 131, No. 2. March - April 1961. pp. 225 - 255.

13. LEONHARDT, F. Anfängliche und nachträgliche Durchbiegungen von Stahlbetonbalken im Zustand II. Vorschläge für Begranzungen und vereinfachte Nachweise. Beton- und Stahlbetonbau. Vol. 54, No. 10. October 1959. pp. 240 - 247.

14. WALTHER, R. Zum Problem der Schubsicherheit im Spannbeton. Schweizer Archiv. Vol. 25, No. 9. September 1959. pp. 329 - 337.

15. RÜSCH, H. and REHM, G. Notes on crack spacing in members subjected to bending. RILEM Symposium on bond and crack formation in reinforced concrete, Stockholm 1957. Stockholm, Teckniska Högskolans Rotaprint-tryckeri, 1957. Volume 2. pp. 525 - 531.

16. BROCK, G. Effect of shear on ultimate strength of rectangular beams with tensile reinforcement. Journal of the American Concrete Institute. Vol. 31, No. 1. January 1960. pp. 619 - 637.

17. MÖRSCH, E. Die Ermittlung des Bruchmomentes von Spannbetonbalken. Beton- und Stahlbetonbau. Vol. 45, No. 7. July 1950. pp. 149 - 157.

18. RÜSCH, H. Versuche zur Festigkeit der Biegedruckzone. Berlin, Deutscher Auschuss für Stahlbeton, 1955. pp. 94. No. 120.

19. MOODY, K.G. An investigation of reinforced concrete beams failing in shear. Thesis submitted to the University of Illinois for the degree of Ph.D., 1953.

20. BACH, C. and GRAF, O. Versuche mit Eisenbeton-Balken zur Ermittlung der Widerstandsfähigkeit verschiedener Bewehrung gegen Schubkräfte. Berlin, Deutscher Auschuss für Eisenbeton, 1911. pp. 132. No. 10.

21. LEONHARDT, F. and WALTHER, R. Versuche an Plattenbalken mit hoher Schubbeanspruchung. Berlin, Deutscher Auschuss für Stahlbeton, 1962. pp. 71. No. 152.

22. BAY, H. Schubbewehrung und Bruchsicherheit beim Stahlbetonbalken. Beton- und Stahlbetonbau. Vol. 52, No. 7. July 1957. pp. 156 - 162.

23. BAY, H. Die Schubkraftfläche und ihre Verminderung durch die lotrechten Balkenpressungen. Beton- und Stahlbetonbau. Vol. 50, No. 3. March 1955. pp. 79 - 81.

24. CLARK, A.P. Diagonal tension in reinforced concrete beams. Journal of the American Concrete Institute. Vol. 23, No. 2. October 1951. pp. 145 - 156.